

# **Atmospheric Aerosol Properties and Climate Impacts**

**U.S. Climate Change Science Program  
Synthesis and Assessment Product 2.3**

**January 2009**

## **FEDERAL EXECUTIVE TEAM**

Director, Climate Change Science Program: William J. Brennan

Director, Climate Change Science Program Office: Peter A. Schultz

Associate Director for Research, Earth Science Division,  
National Aeronautics and Space Administration: Jack Kaye

Product Lead, Laboratory for Atmospheres,  
Earth Science Division, Goddard Space Flight Center,  
National Aeronautics and Space Administration: Mian Chin

Chair, Synthesis and Assessment Product Advisory Group  
Associate Director, National Center for Environmental  
Assessment, U.S. Environmental Protection Agency: Michael W. Slimak

Synthesis and Assessment Product Coordinator,  
Climate Change Science Program Office: Fabien J.G. Laurier

## **EDITORIAL AND PRODUCTION TEAM**

Editors: Mian Chin, NASA  
Ralph A. Kahn, NASA  
Stephen E. Schwartz, DOE

This document, part of the Synthesis and Assessment Products described in the U.S. Climate Change Science Program (CCSP) Strategic Plan, was prepared in accordance with Section 515 of the Treasury and General Government Appropriations Act for Fiscal Year 2001 (Public Law 106-554) and the information quality act guidelines issued by the National Aeronautics and Space Administration pursuant to Section 515. The CCSP Interagency Committee relies on National Aeronautics and Space Administration certifications regarding compliance with Section 515 and Agency guidelines as the basis for determining that this product conforms with Section 515. For purposes of compliance with Section 515, this CCSP Synthesis and Assessment Product is an “interpreted product” as that term is used in National Aeronautics and Space Administration guidelines and is classified as “highly influential”. This document does not express any regulatory policies of the United States or any of its agencies, or provides recommendations for regulatory action.

# Atmospheric Aerosol Properties and Climate Impacts

## Synthesis and Assessment Product 2.3

Report by the U.S. Climate Change Science Program  
And the Subcommittee on Global Change Research

### **Coordinating Lead Author:**

Mian Chin, NASA Goddard Space Flight Center

### **Lead and Contributing Authors:**

Ralph A. Kahn, Lorraine A. Remer, Hongbin Yu, NASA GSFC;  
David Rind, NASA GISS;  
Graham Feingold, NOAA ESRL; Patricia K. Quinn, NOAA PMEL;  
Stephen E. Schwartz, DOE BNL; David G. Streets, DOE ANL;  
Philip DeCola, Rangasayi Halthore, NASA HQ



January 2009,

Members of Congress:

On behalf of the National Science and Technology Council, the U.S. Climate Change Science Program (CCSP) is pleased to transmit to the President and the Congress this Synthesis and Assessment Product (SAP) *Aerosol Properties and their Impacts on Climate*. This is part of a series of 21 SAPs produced by the CCSP aimed at providing current assessments of climate change science to inform public debate, policy, and operational decisions. These reports are also intended to help the CCSP develop future program research priorities.

The CCSP's guiding vision is to provide the Nation and the global community with the science-based knowledge needed to manage the risks and capture the opportunities associated with climate and related environmental changes. The SAPs are important steps toward achieving that vision and help to translate the CCSP's extensive observational and research database into informational tools that directly address key questions being asked of the research community.

This SAP reviews current knowledge about global distributions and properties of atmospheric aerosols, as they relate to aerosol impacts on climate. It was developed in accordance with the Guidelines for Producing CCSP SAPs, the Information Quality Act (Section 515 of the Treasury and General Government Appropriations Act for Fiscal Year 2001 (Public Law 106-554)), and the guidelines issued by the National Aeronautics and Space Administration pursuant to Section 515.

We commend the report's authors for both the thorough nature of their work and their adherence to an inclusive review process.

Sincerely,

Handwritten signature of Carlos M. Gutierrez in black ink.

Carlos M. Gutierrez  
Secretary of Commerce  
Chair, Committee on  
Climate Change Science  
and Technology Integration

Handwritten signature of Samuel W. Bodman in black ink.

Samuel W. Bodman  
Secretary of Energy  
Vice Chair, Committee on  
Climate Change Science  
and Technology Integration

Handwritten signature of John H. Marburger III in black ink.

John H. Marburger III  
Director, Office of Science  
and Technology Policy  
Executive Director, Committee  
on Climate Change Science and  
Technology Integration

## AUTHOR TEAM FOR THIS REPORT

### Executive Summary

Lorraine A. Remer, NASA GSFC; Mian Chin, NASA GSFC; Philip DeCola, NASA HQ; Graham Feingold, NOAA ERSL; Rangasayi Halthore, NASA HQ/NRL; Ralph A. Kahn, NASA GSFC; Patricia K. Quinn, NOAA PMEL; David Rind, NASA GISS; Stephen E. Schwartz, DOE BNL; David G. Streets, DOE ANL; Hongbin Yu, NASA GSFC/UMBC

### Chapter 1

**Lead authors:** Ralph A. Kahn, NASA GSFC; Hongbin Yu, NASA GSFC/UMBC

**Contributing authors:** Stephen E. Schwartz, DOE BNL; Mian Chin, NASA GSFC; Graham Feingold, NOAA ESRL; Lorraine Remer, NASA GSFC; David Rind, NASA GISS; Rangasayi Halthore, NASA HQ/NRL; Philip DeCola, NASA HQ

### Chapter 2

**Lead Authors:** Hongbin Yu, NASA GSFC/UMBC; Patricia K. Quinn, NOAA PMEL; Graham Feingold, NOAA ESRL; Lorraine A. Remer, NASA GSFC; Ralph A. Kahn, NASA GSFC

**Contributing Authors:** Mian Chin, NASA GSFC; Stephen E. Schwartz, DOE BNL

### Chapter 3

**Lead authors:** David Rind, NASA GISS; Mian Chin, NASA GSFC; Graham Feingold, NOAA ESRL; David G. Streets, DOE ANL

**Contributing authors:** Ralph A. Kahn, NASA GSFC; Stephen E. Schwartz, DOE BNL; Hongbin Yu, NASA GSFC/UMBC

### Chapter 4

David Rind, NASA GISS; Ralph A. Kahn, NASA GSFC; Mian Chin, NASA GSFC; Stephen E. Schwartz, DOE BNL; Lorraine A. Remer, NASA GSFC; Graham Feingold, NOAA ESRL; Hongbin Yu, NASA GSFC; Patricia Quinn, NOAA PMEL; Rangasayi Halthore, NASA HQ/NRL

## **Acknowledgments**

This Climate Change Science Program Synthesis and Assessment Product (CCSP SAP) 2.3 has been reviewed by a group of experts, the public, and Federal Agencies. The purpose of these independent reviews was to assure the quality of this product.

We wish to thank the following individuals for their expert review of this report: Sundar Christopher (University of Alabama Huntsville), Daniel Jacob (Harvard University), Steven Ghan (Pacific Northwest National Laboratory), John Ogren (NOAA Earth System Research Laboratory), and Susan Solomon (NOAA Earth System Research Laboratory).

We also wish to thank the following individuals for their public/federal agency review of this report: Joel D. Scheraga (EPA), Samuel P. Williamson (NOAA/OFCM), Alan Carlin, David L. Hagen, Douglas Hoyt, Forrest M. Mims III (Geronimo Creek observatory), John Pittman, Nathan Taylor (Texas A&M University), and Werner Weber (Technische University Dortmund, Germany), and the NOAA Research Council.

## Recommended citations

### For the Report as a Whole:

CCSP 2009: *Atmospheric Aerosol Properties and Impacts on Climate*, A Report by the U.S. Climate Change Science Program and the Subcommittee on Global Change Research. [Mian Chin, Ralph A. Kahn, and Stephen E. Schwartz (eds.)]. National Aeronautics and Space Administration, Washington, D.C., USA, xxx pp.

### For the Executive Summary:

Remer, L. A., M. Chin, P. DeCola, G. Feingold, R. Halthore, R. A. Kahn, P. K. Quinn, D. Rind, S. E. Schwartz, D. Streets, and H. Yu, 2009: Executive Summary, in *Atmospheric Aerosol Properties and Impacts on Climate*, A Report by the U.S. Climate Change Science Program and the Subcommittee on Global Change Research. [Mian Chin, Ralph A. Kahn, and Stephen E. Schwartz (eds.)]. National Aeronautics and Space Administration, Washington, D.C., USA.

### For Chapter 1:

Kahn, R. A., H. Yu, S. E. Schwartz, M. Chin, G. Feingold, L. A. Remer, D. Rind, R. Halthore, and P. DeCola, 2009: Introduction, in *Atmospheric Aerosol Properties and Impacts on Climate*, A Report by the U.S. Climate Change Science Program and the Subcommittee on Global Change Research. [Mian Chin, Ralph A. Kahn, and Stephen E. Schwartz (eds.)]. National Aeronautics and Space Administration, Washington, D.C., USA.

### For Chapter 2:

Yu, H., P. K. Quinn, G. Feingold, L. A. Remer, R. A. Kahn, M. Chin, and S. E. Schwartz, 2009: Remote Sensing and *In Situ* Measurements of Aerosol Properties, Burdens, and Radiative Forcing, in *Atmospheric Aerosol Properties and Impacts on Climate*, A Report by the U.S. Climate Change Science Program and the Subcommittee on Global Change Research. [Mian Chin, Ralph A. Kahn, and Stephen E. Schwartz (eds.)]. National Aeronautics and Space Administration, Washington, D.C., USA.

### For Chapter 3:

Rind, D., M. Chin, G. Feingold, D. Streets, R. A. Kahn, S. E. Schwartz, and H. Yu, 2009: Modeling the Effects of Aerosols on Climate, in *Atmospheric Aerosol Properties and Impacts on Climate*, A Report by the U.S. Climate Change Science Program and the Subcommittee on Global Change Research. [Mian Chin, Ralph A. Kahn, and Stephen E. Schwartz (eds.)]. National Aeronautics and Space Administration, Washington, D.C., USA.

### For Chapter 4:

Rind, D., R. A. Kahn, M. Chin, S. E. Schwartz, L. A. Remer, G. Feingold, H. Yu, P. K. Quinn, and R. Halthorne, 2009: The Way Forward, in *Atmospheric Aerosol Properties and Impacts on Climate*, A Report by the U.S. Climate Change Science Program and the Subcommittee on Global Change Research. [Mian Chin, Ralph A. Kahn, and Stephen E. Schwartz (eds.)]. National Aeronautics and Space Administration, Washington, D.C., USA.



To the memory of Dr. Yoram J. Kaufman (1948 – 2006), who led the effort towards understanding the role of aerosols in climate



# Table of Contents

<b>Executive Summary</b> .....	1
ES 1. Aerosols and Their Climate Effects .....	1
ES 1.1. Atmospheric Aerosols .....	1
ES 1.2. Radiative Forcing of Aerosols .....	1
ES 1.3. Reducing Uncertainties in Aerosol Radiative Forcing Estimates .....	2
ES 2. Measurement-Based Assessment of Aerosol Radiative Forcing .....	3
ES 2.1. Assessments of Aerosol Direct Radiative Forcing .....	3
ES 2.2. Assessments of Aerosol Indirect Radiative Forcing .....	4
ES 3. Model Estimated Aerosol Radiative Forcing and Its Climate Impact .....	4
ES 3.1. The Importance of Aerosol Radiative Forcing in Climate Models .....	5
ES 3.2. Modeling Atmospheric Aerosols .....	5
ES 3.3. Aerosol Effects on Clouds .....	6
ES 3.4. Impacts of Aerosols on Climate Model Simulations .....	6
ES 4. The Way Forward .....	6
<b>CHAPTER 1</b>	
<b>Introduction</b> .....	9
1.1 Description of Atmospheric Aerosols .....	9
1.2 The Climate Effects of Aerosols .....	12
1.3. Reducing Uncertainties in Aerosol-Climate Forcing Estimates .....	19
1.4 Contents of This Report .....	22
<b>CHAPTER 2</b>	
<b>Remote Sensing and <i>In Situ</i> Measurements of Aerosol Properties, Burdens, and Radiative Forcing</b> .....	24
2.1. Introduction .....	24
2.2. Overview of Aerosol Measurement Capabilities .....	25
2.2.1. Satellite Remote Sensing .....	25
2.2.2. Focused Field Campaigns .....	33
2.2.3. Ground-based In situ Measurement Networks .....	33
2.2.4. In situ Aerosol Profiling Programs .....	36
2.2.5. Ground-based Remote Sensing Measurement Networks .....	36
2.2.6. Synergy of Measurements and Model Simulations .....	38
2.3. Assessments of Aerosol Characterization and Climate Forcing .....	40
2.3.1. The Use of Measured Aerosol Properties to Improve Models .....	40
2.3.2. Intercomparisons of Satellite Measurements and Model Simulation of Aerosol Optical Depth .....	44
2.3.3. Satellite Based Estimates of Aerosol Direct Radiative Forcing .....	46
2.3.4. Satellite Based Estimates of Anthropogenic Component of Aerosol Direct Radiative Forcing .....	50
2.3.5. Aerosol-Cloud Interactions and Indirect Forcing .....	53

2.4. Outstanding Issues .....	59
2.5. Concluding Remarks.....	62

### **CHAPTER 3**

<b>Modeling the Effects of Aerosols on Climate Forcing .....</b>	<b>64</b>
3.1. Introduction .....	64
3.2. Modeling of Atmospheric Aerosols .....	65
3.2.1. Estimates of Emissions .....	66
3.2.2. Aerosol Mass Loading and Optical Depth .....	68
3.3. Calculating Aerosol Direct Radiative Forcing.....	72
3.4. Calculating Aerosol Indirect Forcing .....	77
3.4.1. Aerosol Effects on Clouds .....	77
3.4.2. Model Experiments.....	79
3.4.3. Additional Aerosol Influences .....	81
3.4.4. High Resolution Modeling.....	82
3.5. Aerosol in the Climate Models .....	84
3.5.1. Aerosol in the IPCC AR4 Climate Model Simulations .....	84
3.5.2. Additional considerations.....	91
3.6. Impacts of Aerosols on Climate Model Simulations.....	92
3.6.1. Surface Temperature Change .....	92
3.6.2. Implications for Climate Model Simulations.....	94
3.7. Outstanding Issues .....	95
3.8 Conclusions .....	96

### **CHAPTER 4**

<b>The Way Forward .....</b>	<b>98</b>
4.1. Major Research Needs .....	98
4.2. Priorities .....	100
4.2.1. Measurements.....	100
4.2.2. Modeling .....	102
4.2.3. Emissions .....	103
4.3. Concluding Remarks.....	104
<b>References.....</b>	<b>105</b>
<b>Glossary.....</b>	<b>129</b>
<b>Acronyms and Symbols .....</b>	<b>136</b>

# Executive Summary

**Authors:** Lorraine A. Remer, NASA GSFC; Mian Chin, NASA GSFC; Philip DeCola, NASA HQ; Graham Feingold, NOAA ERSL; Rangasayi Halthore, NASA HQ/NRL; Ralph A. Kahn, NASA GSFC; Patricia K. Quinn, NOAA PMEL; David Rind, NASA GISS; Stephen E. Schwartz, DOE BNL; David G. Streets, DOE ANL; Hongbin Yu, NASA GSFC/UMBC

This report critically reviews current knowledge about global distributions and properties of atmospheric aerosols, as they relate to aerosol impacts on climate. It assesses possible next steps aimed at substantially reducing uncertainties in aerosol radiative forcing estimates. Current measurement techniques and modeling approaches are summarized, providing context. As a part of the Synthesis and Assessment Product in the Climate Change Science Program, this assessment builds upon recent related assessments, including the Fourth Assessment Report of the Intergovernmental Panel on Climate Change (IPCC AR4, 2007) and other Climate Change Science Program reports. The objectives of this report are (1) to promote a consensus about the knowledge base for climate change decision support, and (2) to provide a synthesis and integration of the current knowledge of the climate-relevant impacts of anthropogenic aerosols for policy makers, policy analysts, and general public, both within and outside the U.S government and worldwide.

## ES 1. Aerosols and Their Climate Effects

### ES 1.1. Atmospheric Aerosols

Atmospheric aerosols are suspensions of solid and/or liquid particles in air. Aerosols are ubiquitous in air and are often observable as dust, smoke, and haze. Both natural and human processes contribute to aerosol concentrations. On a global basis, aerosol mass derives predominantly from natural sources, mainly sea salt and dust. However, anthropogenic (manmade) aerosols, arising primarily from a variety of combustion sources, can dominate in and downwind of highly populated and industrialized regions, and in areas of intense agricultural burning.

The term “atmospheric aerosol” encompasses a wide range of particle types having different compositions, sizes, shapes, and optical properties. Aerosol loading, or amount in the atmosphere, is usually quantified by mass concentration or by an optical measure, aerosol optical depth (AOD). AOD is the vertical integral through the entire height of the atmosphere of the fraction of incident light either scattered or absorbed by airborne particles per unit length. Usually numerical models and *in situ* observations use mass concentration as the primary measure of aerosol loading, whereas most remote sensing methods retrieve AOD.

### ES 1.2. Radiative Forcing of Aerosols

Aerosols affect Earth's energy budget by scattering and absorbing radiation (the “direct effect”) and by modifying amounts and microphysical and radiative properties of clouds (the “indirect effects”). Aerosols influence cloud properties through their role as cloud condensation nuclei

1 (CCN) and/or ice nuclei. Increases in aerosol particle concentrations may increase the ambient  
2 concentration of CCN and ice nuclei, affecting cloud properties. A CCN increase can lead to  
3 more cloud droplets so that, for fixed cloud liquid water content, the cloud droplet size will  
4 decrease. This effect leads to brighter clouds (the “cloud albedo effect”). Aerosols can also affect  
5 clouds by absorbing solar energy and altering the environment in which the cloud develops, thus  
6 changing cloud properties without actually serving as CCN. Such effects can change  
7 precipitation patterns as well as cloud extent and optical properties.

8 The addition of aerosols to the atmosphere alters the intensity of sunlight scattered back to space,  
9 absorbed in the atmosphere, and arriving at the surface. Such a perturbation of sunlight by  
10 aerosols is designated *aerosol radiative forcing* (RF). Note that RF must be defined as a  
11 perturbation from an initial state, whether that state be the complete absence of aerosols, the  
12 estimate of aerosol loading from pre-industrial times, or an estimate of aerosol loading for  
13 today’s natural aerosols. The RF calculated from the difference between today’s total aerosol  
14 loading (natural plus anthropogenic) and each of the three initial states mentioned above will  
15 result in different values. Also, the aerosol RF calculated at the top of the atmosphere, the bottom  
16 of the atmosphere, or any altitude in between, will result in different values. Other quantities that  
17 need to be specified when reporting aerosol RF include the wavelength range, the temporal  
18 averaging, the cloud conditions considered for direct effects, and the aerosol-cloud interactions  
19 that are being considered for the broad classifications of indirect and semi-direct effects.  
20 Regardless of the exact definition of aerosol RF, it is characterized by large spatial and temporal  
21 heterogeneity due to the wide variety of aerosol sources and types, the spatial non-uniformity  
22 and intermittency of these sources, the short atmospheric lifetime of aerosols, and the chemical  
23 and microphysical processing that occurs in the atmosphere.

24 On a global average basis, the sum of direct and indirect forcing by anthropogenic aerosols at the  
25 top of the atmosphere is almost certainly negative (a cooling influence), and thus almost  
26 certainly offsets a fraction of the positive (warming) forcing due to anthropogenic greenhouse  
27 gases. However, because of the spatial and temporal non-uniformity of the aerosol RF, and likely  
28 differences in the effects of shortwave and longwave forcings, the net effect on Earth’s climate is  
29 not simply a fractional offset to the effects of forcing by anthropogenic greenhouse gases.

### 30 ***ES 1.3. Reducing Uncertainties in Aerosol Radiative Forcing Estimates***

31 The need to represent aerosol influences on climate is rooted in the larger, policy related  
32 requirement to predict the climate changes that would result from different future emission  
33 strategies. This requires that confidence in climate models be based on their ability to accurately  
34 represent not just present climate, but also the changes that have occurred over roughly the past  
35 century. Achieving such confidence depends upon adequately understanding the forcings that  
36 have occurred over this period. Although the forcing by long-lived greenhouse gases is known  
37 relatively accurately for this period, the history of total forcing is not, due mainly to the uncertain  
38 contribution of aerosols.

39 Present-day aerosol radiative forcing relative to preindustrial is estimated primarily using  
40 numerical models that simulate the emissions of aerosol particles and gaseous precursors and the  
41 aerosol and cloud processes in the atmosphere. The accuracy of the models is assessed primarily  
42 by comparison with observations. The key to reducing aerosol RF uncertainty estimates is to  
43 understand the contributing processes well enough to accurately reproduce them in models. This  
44 report assesses present ability to represent in models the distribution, properties and forcings of

1 present-day aerosols, and examines the limitations of currently available models and  
2 measurements. The report identifies three specific areas where continued, focused effort would  
3 likely result in substantial reduction in present-day aerosol forcing uncertainty estimates: (1)  
4 improving quality and coverage of aerosol measurements, (2) achieving more effective use of  
5 these measurements to constrain model simulation/assimilation and to test model  
6 parameterizations, and (3) producing more accurate representation of aerosols and clouds in  
7 models.

## 8 **ES 2. Measurement-Based Assessment of Aerosol Radiative** 9 **Forcing**

10 Over the past decade, measurements of aerosol amount, geographical distribution, and physical  
11 and chemical properties have substantially improved, and understanding of the controlling  
12 processes and the direct and indirect radiative effects of aerosols has increased. Key research  
13 activities have been:

- 14 • Development and implementation of new and enhanced *satellite-borne sensors* capable  
15 of observing the spatial and temporal characteristics of aerosol properties and examine  
16 aerosol effects on atmospheric radiation.
- 17 • Execution of *focused field experiments* examining aerosol processes and properties in  
18 various aerosol regimes around the globe;
- 19 • Establishment and enhancement of *ground-based networks* measuring aerosol properties  
20 and radiative effects;
- 21 • Development and deployment of *new and enhanced instrumentation* including devices  
22 to determine size dependent particle composition on fast timescales, and methods for  
23 determining aerosol light absorption coefficients and single scattering albedo.

### 24 **ES 2.1. Assessments of Aerosol Direct Radiative Forcing**

25 Over the past 15 years, focused field campaigns have provided detailed characterizations of  
26 regional aerosol, chemical, microphysical and radiative properties, along with relevant surface  
27 and atmospheric conditions. Studies from these campaigns provide highly reliable  
28 characterization of submicrometer spherical particles such as sulfate and carbonaceous aerosol.  
29 *In situ* characterization of larger particles such as dust are much less reliable.

30 For all their advantages, field campaigns are inherently limited by their relatively short duration  
31 and small spatial coverage. Surface networks and satellites provide a needed long-term view, and  
32 satellites provide additional extensive spatial coverage. Surface networks, such as the Aerosol  
33 Robotic Network (AERONET), provide observations of AOD at mid-visible wavelengths with  
34 an accuracy of 0.01 to 0.02, nearly three to five times more accurate than satellite retrievals.  
35 These same remote sensing ground networks also typically retrieve column integrated aerosol  
36 microphysical properties, but with uncertainties that are much larger than *in situ* measurements.

37 The satellite remote sensing capability developed over the past decades has enabled the estimate  
38 of aerosol radiative forcing on a global scale. Current satellite sensors such as the MODerate  
39 resolution Imaging Spectroradiometer (MODIS) and Multi-angle Imaging SpectroRadiometer  
40 (MISR) can retrieve AOD ( $\tau$ ) under cloud free conditions with an accuracy of  $\pm 0.05 \pm 0.20\tau$  over  
41 land and better than  $\pm 0.04 \pm 0.1\tau$  over ocean. In addition, these and other satellite sensors can  
42 qualitatively retrieve particle properties (size, shape and absorption), a major advance over the  
43 previous generation of satellite instruments. Much effort has gone into comparing different

1 observational methods to estimate global oceanic cloud-free aerosol direct radiative forcing for  
2 solar wavelengths at the top of the atmosphere (TOA). Applying various methods using MODIS,  
3 MISR and the Clouds and Earth's Radiant Energy System (CERES), the aerosol direct RF at  
4 TOA derived above ocean converges to  $-5.5 \pm 0.2 \text{ W m}^{-2}$ , where the initial state of the forcing  
5 perturbation is a completely aerosol-free atmosphere. Here, the uncertainty is the standard  
6 deviation of the various methods, indicating close agreement between the different satellite data  
7 sets. However, regional comparisons of the various methods show greater spread than the global  
8 mean. Estimates of direct radiative forcing at the ocean surface, and at top and bottom of the  
9 atmosphere over land, are also reported, but are much less certain. All these measurement-based  
10 estimates are calculated for cloud-free conditions using an initial state of an aerosol-free  
11 atmosphere.

12 Although no proven methods exist for measuring the anthropogenic component of the observed  
13 aerosol over broad geographic regions, satellite retrievals are able to qualitatively determine  
14 aerosol type under some conditions. From observations of aerosol type, the best estimates  
15 indicate approximately 20% of the AOD over the global oceans is a result of human activities.  
16 Following from these estimates of anthropogenic fraction, the cloud-free anthropogenic direct  
17 radiative forcing at TOA is approximated to be  $-1.1 \pm 0.4 \text{ W m}^{-2}$  over the global ocean,  
18 representing the anthropogenic perturbation to today's natural aerosol.

## 19 **ES 2.2. Assessments of Aerosol Indirect Radiative Forcing**

20 Remote sensing estimates of aerosol indirect forcing are still very uncertain. Even on small  
21 spatial scales, remote sensing of aerosol effects on cloud albedo do not match *in situ*  
22 observations, due to a variety of difficulties with the remote sensing of cloud properties at fine  
23 scales, the inability of satellites to observe aerosol properties beneath cloud base, and the  
24 difficulty of making aerosol retrievals in cloud fields. Key quantities such as liquid water path,  
25 cloud updraft velocity and detailed aerosol size distributions are rarely constrained by coincident  
26 observations.

27 Most remote sensing observations of aerosol-cloud interactions and aerosol indirect forcing are  
28 based on simple correlations among variables, which do not establish cause-and-effect  
29 relationships. Inferring aerosol effects on clouds from the observed relationships is complicated  
30 further because aerosol loading and meteorology are often correlated, making it difficult to  
31 distinguish aerosol from meteorological effects. As in the case of direct forcing, the regional  
32 nature of indirect forcing is especially important for understanding actual climate impact.

## 33 **ES 3. Model Estimated Aerosol Radiative Forcing and Its** 34 **Climate Impact**

35 Just as different types of aerosol observations serve similar purposes, diverse types of models  
36 provide a variety of approaches to understanding aerosol forcing of climate. Large-scale  
37 Chemistry and Transport Models (CTMs) are used to test current understanding of the processes  
38 controlling aerosol spatial and temporal distributions, including aerosol and precursor emissions,  
39 chemical and microphysical transformations, transport, and removal. CTMs are used to describe  
40 the global aerosol system and to make estimates of direct aerosol radiative forcing. In general,  
41 CTMs do not explore the climate response to this forcing. General Circulation Models (GCMs),  
42 sometimes called Global Climate Models, have the capability of including aerosol processes as a  
43 part of the climate system to estimate aerosol climate forcing, including aerosol-cloud

1 interactions, and the climate response to this forcing. Another type of model represents  
2 atmospheric processes on much smaller scales, such as cloud resolving and large eddy simulation  
3 models. These small-scale models are the primary tools for improving understanding of aerosol-  
4 cloud processes, although they are not used to make estimates of aerosol-cloud radiative forcing  
5 on regional or global scales.

### 6 ***ES 3.1. The Importance of Aerosol Radiative Forcing in Climate Models***

7 Calculated change of surface temperature due to forcing by anthropogenic greenhouse gases and  
8 aerosols was reported in IPCC AR4 based on results from more than 20 participating global  
9 climate modeling groups. Despite a wide range of climate sensitivity (i.e. the amount of surface  
10 temperature increase due to a change in radiative forcing, such as an increase of CO<sub>2</sub>) exhibited  
11 by the models, they all yield a global average temperature change very similar to that observed  
12 over the past century. This agreement across models appears to be a consequence of the use of  
13 very different aerosol forcing values, which compensates for the range of climate sensitivity. For  
14 example, the direct cooling effect of sulfate aerosol varied by a factor of six among the models.  
15 An even greater disparity was seen in the model treatment of black carbon and organic carbon.  
16 Some models ignored aerosol indirect effects whereas others included large indirect effects. In  
17 addition, for those models that included the indirect effect, the aerosol effect on cloud brightness  
18 (reflectivity) varied by up to a factor of nine. Therefore, the fact that models had reproduced the  
19 global temperature change in the past does not imply that their future forecasts are accurate. This  
20 state of affairs will remain until a firmer estimate of radiative forcing by aerosols, as well as  
21 climate sensitivity, is available.

### 22 ***ES 3.2. Modeling Atmospheric Aerosols***

23 Simulations of the global aerosol distribution by different models show good agreement in their  
24 representation of the global mean AOD, which in general also agrees with satellite-observed  
25 values. However, large differences exist in model simulations of regional and seasonal  
26 distributions of AOD, and in the proportion of aerosol mass attributed to individual species. Each  
27 model uses its own estimates of aerosol and precursor emissions and configurations for chemical  
28 transformations, microphysical properties, transport, and deposition. Multi-model experiments  
29 indicate that differences in the models' atmospheric processes play a more important role than  
30 differences in emissions in creating the diversity among model results. Although aerosol mass  
31 concentration is the basic measure of aerosol loading in the models, this quantity is translated to  
32 AOD via mass extinction efficiency in order to compare with observations and then to estimate  
33 aerosol direct RF. Each model employs its own mass extinction efficiency based on assumed  
34 optical and physical properties of each aerosol type. Thus, it is possible for the models to  
35 produce different distributions of aerosol loading as mass concentrations but agree in their  
36 distributions of AOD, and vice-versa.

37 Model calculated total global mean direct anthropogenic aerosol RF at TOA, based on the  
38 difference between pre-industrial and current aerosol fields, is  $-0.22 \text{ W m}^{-2}$ , with a range from  $-$   
39  $0.63$  to  $+0.04 \text{ W m}^{-2}$ . This estimate does not include man-made contributions of nitrate and dust,  
40 which could add another  $-0.2 \text{ W m}^{-2}$  estimated by IPCC AR4. The mean value is much smaller  
41 than the estimates of total greenhouse gas forcing of  $+2.9 \text{ W m}^{-2}$ , but the comparison of global  
42 average values does not take into account immense regional variability. Over the major sources  
43 and their downwind regions, the model-calculated negative forcing from aerosols can be  
44 comparable to or even larger than the positive forcing by greenhouse gases.

### 1 **ES 3.3. Aerosol Effects on Clouds**

2 Large-scale models are increasingly incorporating aerosol indirect effects into their calculations.  
3 Published large-scale model studies report calculated global cloud albedo effect RF at top-of-  
4 atmosphere, based on the perturbation from pre-industrial aerosol fields, ranging from -0.22 to  
5  $-1.85 \text{ W m}^{-2}$  with a central value of  $-0.7 \text{ W m}^{-2}$ . Numerical experiments have shown that the  
6 cloud albedo effect is not a strong function of a model's cloud or radiation scheme, and that  
7 although model representations of cloud physics are important, the differences in modeled  
8 aerosol concentrations play a strong role in inducing differences in the indirect as well as the  
9 direct effect. Although small-scale models, such as cloud-resolving or large eddy simulation  
10 models, do not attempt to estimate global aerosol RF, they are essential for understanding the  
11 fundamental processes occurring in clouds, which then leads to better representation of these  
12 processes in larger-scale models.

### 13 **ES 3.4. Impacts of Aerosols on Climate Model Simulations**

14 The current aerosol modeling capability demonstrated by chemical transport models has not been  
15 fully incorporated into GCM simulations. Of the 20+ models used in the IPCC AR4 assessment,  
16 most included sulfate direct RF, but only a fraction considered other aerosol types, and only less  
17 than a third included aerosol indirect effects. The lack of a comprehensive presentation of  
18 aerosols in climate models makes it difficult to determine climate sensitivity, and thus to make  
19 climate change predictions.

20 Although the nature and geographical distribution of forcings by greenhouse gases and aerosols  
21 are quite different, it is often assumed that to first approximation the effects of these forcings on  
22 global mean surface temperature are additive, so that the negative forcing by anthropogenic  
23 aerosols has partially offset the positive forcing by incremental greenhouse gas increases over  
24 the industrial period. The IPCC AR4 estimates the total global average TOA forcing by  
25 incremental greenhouse gases to be  $2.9 \pm 0.3 \text{ W m}^{-2}$ , where the uncertainty range is meant to  
26 encompass the 90% probability that the actual value will be within the indicated range. The  
27 corresponding value for aerosol forcing at TOA (direct plus enhanced cloud albedo effects),  
28 defined as the perturbation from pre-industrial conditions, is  $-1.3 (-2.2 \text{ to } -1.5) \text{ W m}^{-2}$ . The total  
29 forcing,  $1.6 (0.6 \text{ to } 2.4) \text{ W m}^{-2}$ , reflects the offset of greenhouse gas forcing by aerosols, where  
30 the uncertainty in total anthropogenic RF is dominated by the uncertainty in aerosol RF.

31 However, since aerosol forcing is much more pronounced on regional scales than on the global  
32 scale because of the highly variable aerosol distributions, it would be insufficient or even  
33 misleading to place too much emphasis on the global average. Also, aerosol RF at the surface is  
34 stronger than that at TOA, exerting large impacts within the atmosphere to alter the atmospheric  
35 circulation patterns and water cycle. Therefore, impacts of aerosols on climate should be  
36 assessed beyond the limitation of considering only global average radiative forcing at TOA.

## 37 **ES 4. The Way Forward**

38 The uncertainty in assessing total anthropogenic greenhouse gas and aerosol impacts on climate  
39 must be much reduced from its current level to allow meaningful predictions of future climate.  
40 This uncertainty is currently dominated by the aerosol component. In addition, evaluation of  
41 aerosol effects on climate must take into account high spatial and temporal variation of aerosol  
42 amounts and properties as well as the aerosol interactions with clouds and precipitation. Thus,



1 the way forward requires more certain estimates of aerosol radiative forcing, which in turn  
2 requires better observations, improved models and a synergistic approach.

3 From the observational perspective, the high priority tasks are:

- 4 • **Maintain current and enhance future satellite capabilities** for measuring geographical  
5 and vertical distribution of aerosol amount and optical properties, suitable for estimating  
6 aerosol forcing over multi-decadal time scales and for evaluating global models.
- 7 • **Maintain, enhance, and expand the surface observation networks** measuring aerosol  
8 optical properties for satellite retrieval validation, model evaluation, and climate change  
9 assessments. Observation should be augmented with routine measurements of other key  
10 parameters with state-of-art techniques.
- 11 • **Execute a continuing series of coordinated field campaigns** aiming to study the  
12 atmospheric processes, to broaden the database of detailed aerosol chemical, physical,  
13 and optical/radiative characteristics, to validate remote-sensing retrieval products, and to  
14 evaluate chemistry transport models.
- 15 • **Initiate and carry out a systematic program of simultaneous measurement of**  
16 **aerosol** composition and size distribution, **cloud** microphysical properties, and  
17 **precipitation** variables.
- 18 • **Fully exploit the existing information in satellite observations of AOD and particle**  
19 **type** by refining retrieval algorithms, quantifying data quality, extracting greater aerosol  
20 information from joint multi-sensor products, and generating uniform, climate-quality  
21 data records.
- 22 • **Measure the formation, evolution, and properties of aerosols under controlled**  
23 **laboratory conditions** to develop mechanistic and quantitative understanding of aerosol  
24 formation, chemistry, and dynamics.
- 25 • **Improve measurement-based techniques for distinguishing anthropogenic from**  
26 **natural aerosols** by combining satellite data analysis with in situ measurements and  
27 modeling methods.

28 Individual sensors or instruments have both strengths and limitations, and no single strategy is  
29 adequate for characterizing the complex aerosol system. The best approach is to make synergistic  
30 use of measurements from multiple platforms, sensors and instruments having complementary  
31 capabilities. The wealth of information coming from the variety of today's sensors has not yet  
32 been fully exploited. Advances in measurement-based estimates of aerosol radiative forcing are  
33 expected in the near future, as existing data sets are more fully explored. Even so, the long-term  
34 success in reducing climate-change prediction uncertainties rests with improving modeling  
35 capabilities, and today's suite of observations can only go so far towards that goal.

36 From the modeling perspective, the high priority tasks are:

- 37 • **Improve the accuracy and capability of model simulation of aerosols** (including  
38 components and atmospheric processes) and aerosol direct radiative forcing.  
39 Observational strategies described above must be developed to constrain and validate the  
40 key parameters in the model.
- 41 • **Advance the ability to model aerosol-cloud-precipitation interaction in climate**  
42 **models, particularly the simulation of clouds**, in order to reduce the largest uncertainty  
43 in the climate forcing/feedback processes.

- 1 • **Incorporate improved representation of aerosol processes in coupled aerosol-climate**  
2 **system models** and evaluate the ability of these models to simulate present climate and  
3 past (twentieth century) climate change.
- 4 • **Apply coupled aerosol-climate system models to assess the climate change** that would  
5 result from alternative scenarios of prospective future emissions of greenhouse gases and  
6 aerosols and aerosol precursors.

7 In addition to the above priorities in measurements and modeling, there is a critical need to:

- 8 • **Develop and evaluate emission inventories of aerosol particles and precursor gases.**  
9 Continuous development and improvement of current emissions, better estimates of past  
10 emissions, and projection of future emissions should be maintained.

11 Progress in improving modeling capabilities requires effort on the observational side, to reduce  
12 uncertainties and disagreements among observational data sets. The way forward will require  
13 integration of satellite and *in situ* measurements into global models. However, understanding the  
14 strengths and weaknesses of each observational data set must be clear in order for the constraints  
15 they provide to improve confidence in the models, and for efforts at data assimilation to succeed.

16 Narrowing the gap between the current understanding of long-lived greenhouse gas and that of  
17 anthropogenic aerosol contributions to RF will require progress in all aspects of aerosol-climate  
18 science. Development of new space-based, field and laboratory instruments will be needed, and  
19 in parallel, more realistic simulations of aerosol, cloud and atmospheric processes must be  
20 incorporated into models. Most importantly, greater synergy among different types of  
21 measurements, among different types of models, and especially between measurements and  
22 models is critical. Aerosol-climate science will naturally expand to encompass not only radiative  
23 effects on climate, but also aerosol effects on cloud processes, precipitation, and weather. New  
24 initiatives will strive to more effectively include experimentalists, remote sensing scientists and  
25 modelers as equal partners, and the traditionally defined communities in different atmospheric  
26 science disciplines will increasingly find common ground in addressing the challenges ahead.

27

1  
2  
3  
4  
5  
6  
7  
8  
9  
10  
11  
12  
13  
14  
15  
16  
17  
18  
19  
20  
21  
22  
23  
24  
25  
26  
27  
28  
29  
30  
31  
32  
33  
34  
35  
36  
37

# CHAPTER 1

## Introduction

**Lead authors:** Ralph A. Kahn, NASA GSFC; Hongbin Yu, NASA GSFC/UMBC

**Contributing authors:** Stephen E. Schwartz, DOE BNL; Mian Chin, NASA GSFC; Graham Feingold, NOAA ESRL; Lorraine Remer, NASA GSFC; David Rind, NASA GISS; Rangasayi Halthore, NASA HQ/NRL; Philip DeCola, NASA HQ

This report highlights key aspects of current knowledge about the global distribution of aerosols and their properties, as they relate to climate change. Leading measurement techniques and modeling approaches are briefly summarized, providing context for an assessment of the next steps needed to significantly reduce uncertainties in this component of the climate change picture. The present assessment builds upon the recent Inter-governmental Panel on Climate Change Fourth Assessment Report (IPCC AR4, 2007) and other sources.

### 1.1 Description of Atmospheric Aerosols

Although Earth’s atmosphere consists primarily of gases, aerosols and clouds play significant roles in shaping conditions at the surface and in the lower atmosphere. Aerosols are liquid or solid particles suspended in the air, whose typical diameters range over four orders of magnitude, from a few nanometers to a few tens of micrometers. They exhibit a wide range of compositions and shapes, that depend on their origins and subsequent atmospheric processing. For many applications, aerosols from about 0.05 to 10 micrometers in diameter are of greatest interest, as particles in this size range dominate aerosol direct interaction with sunlight, and also make up the majority of the aerosol mass. Particles at the small end of this size range play a significant role in interactions with clouds, whereas particles at the large end, though much less numerous, can contribute significantly near dust and volcanic sources. Over the ocean, giant salt particles may also play a role in cloud development.

Large fraction of aerosols are natural in origin, including desert and soil dust, wildfire smoke, sea salt particles produced mainly by breaking bubbles in the spray of ocean whitecaps, and volcanic ash. Volcanoes are also sources of sulfur dioxide, which, along with sulfur-containing gases produced by ocean biology and the decomposition of organic matter, as well as hydrocarbons such as terpenes and isoprene emitted by vegetation, are examples of gases that can be converted to so-called “secondary” aerosols by chemical processes in the atmosphere. **Figure 1.1** gives a summary of aerosol processes most relevant to their influence on climate.

**Table 1.1** reports estimated source strengths, lifetimes, and amounts for major aerosol types, based on an aggregate of emissions estimates and global model simulations; the ranges provided represent model diversity only, as the global measurements required to validate these quantities are currently lacking.

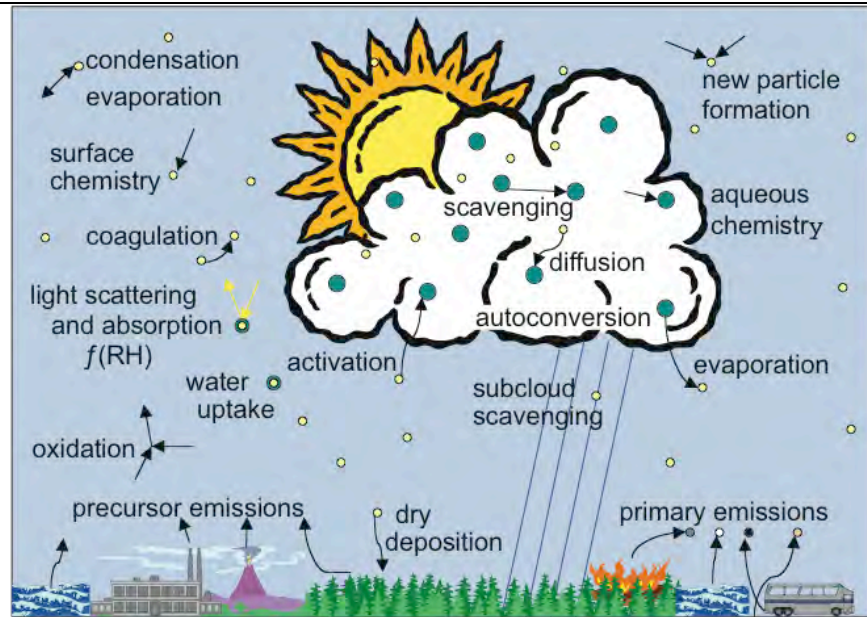


**Figure 1.1 Major aerosol processes relevant to their impact on climate.** Aerosols can be directly emitted as primary particles and can form secondarily by the oxidation of emitted gaseous precursors. Changes in relative humidity (RH) can cause particle growth or evaporation, and can alter particle properties. Physical processes within clouds can further alter particle properties, and conversely, aerosols can affect the properties of clouds, serving as condensation nuclei for new cloud droplet formation. Aqueous-phase chemical reactions in cloud drops or in clear air can also affect aerosol properties. Particles are ultimately removed from the atmosphere, scavenged by falling raindrops or settling by dry deposition. Modified from Ghan and Schwartz (2007).

1

**Table 1.1.** Estimated source strengths, lifetimes, mass loadings, and optical depths of major aerosol types. Statistics are based on results from 16 models examined by the Aerosol Comparisons between Observations and Models (AeroCom) project (Textor et al., 2006; Kinne et al., 2006). BC = black carbon; POM = particulate organic matter.

	Total source <sup>1</sup> (Tg yr <sup>-1</sup> )	Lifetime (day)	Mass loading <sup>1</sup> (Tg)	Optical depth @ 550 nm
	Median (Range)	Median (Range)	Median (Range)	Median (Range)
Sulfate <sup>2</sup>	186 (100 – 233)	4.1 (2.5 – 5.4)	2.0 (0.92 – 2.7)	0.034 (0.015 – 0.051)
BC	11.3 (7.8 – 19.5)	6.5 (5.3 – 15)	0.21 (0.046 – 0.51)	0.004 (0.002 – 0.009)
POM <sup>2</sup>	96.0 (53 – 138)	6.2 (4 – 11)	1.8 (0.46 – 2.56)	0.019 (0.006 – 0.030)
Dust	1640 (700 – 4000)	4.0 (1.3 – 7)	20.5 (4.5 – 29.5)	0.032 (0.012 – 0.054)
Sea-salt	6280 (2000 – 120000)	0.4 (0.03 – 1.1)	6.4 (2.5 – 13.2)	0.030 (0.020 – 0.067)
Total				0.127 (0.065 – 0.15)

<sup>1</sup>Tg (teragram) = 10<sup>12</sup> g, or million metric tons.

<sup>2</sup>The sulfate aerosol source is mainly SO<sub>2</sub> oxidation, plus a small fraction of direct emission. The organic matter source includes direct emission and hydrocarbon oxidation.

2

3 *Aerosol optical depth (AOD)* (also called aerosol optical thickness, AOT, in the literature) is a  
 4 measure of the amount of incident light either scattered or absorbed by airborne particles.  
 5 Formally, aerosol optical depth is a dimensionless quantity, the integral of the product of particle  
 6 number concentration and particle extinction cross-section (which accounts for individual

1 particle scattering + absorption), along a path length through the atmosphere, usually measured  
2 vertically. In addition to AOD, particle size, composition, and structure, which are mediated both  
3 by source type and subsequent atmospheric processing, determine how particles interact with  
4 radiant energy and influence the heat balance of the planet. Size and composition also determine  
5 the ability of particles to serve as nuclei upon which cloud droplets form. This provides an  
6 indirect means for aerosol to interact with radiant energy by modifying cloud properties.

7 Among the main aerosol properties required to evaluate their effect on radiation is the *single-*  
8 *scattering albedo* (SSA), which describes the fraction of light interacting with the particle that is  
9 scattered, compared to the total that is scattered and absorbed. Values range from 0 for totally  
10 absorbing (dark) particles to 1 for purely scattering ones; in nature, SSA is rarely lower than  
11 about 0.75. Another quantity, the *asymmetry parameter* (*g*), reports the first moment of the  
12 cosine of the scattered radiation angular distribution. The parameter *g* ranges from -1 for entirely  
13 back-scattering particles, to 0 for isotropic (uniform) scattering, to +1 for entirely forward-  
14 scattering. One further quantity that must be considered in the energy balance is the *surface*  
15 *albedo* (*A*), a measure of reflectivity at the ground, which, like SSA, ranges from 0 for purely  
16 absorbing to 1 for purely reflecting. In practice, *A* can be near 0 for dark surfaces, and can reach  
17 values above 0.9 for visible light over snow. AOD, SSA, *g*, and *A* are all dimensionless  
18 quantities, and are in general wavelength-dependent. In this report, AOD, SSA, and *g* are given  
19 at mid-visible wavelengths, near the peak of the solar spectrum around 550 nanometers, and *A* is  
20 given as an average over the solar spectrum, unless specified otherwise.

21 About 10% of global atmospheric aerosol mass is generated by human activity, but it is  
22 concentrated in the immediate vicinity, and downwind of sources (e.g., Textor et al., 2006).  
23 These anthropogenic aerosols include primary (directly emitted) particles and secondary particles  
24 that are formed in the atmosphere. Anthropogenic aerosols originate from urban and industrial  
25 emissions, domestic fire and other combustion products, smoke from agricultural burning, and  
26 soil dust created by overgrazing, deforestation, draining of inland water bodies, some farming  
27 practices, and generally, land management activities that destabilize the surface regolith to wind  
28 erosion. The amount of aerosol in the atmosphere has greatly increased in some parts of the  
29 world during the industrial period, and the nature of this particulate matter has substantially  
30 changed as a consequence of the evolving nature of emissions from industrial, commercial,  
31 agricultural, and residential activities, mainly combustion-related.

32 One of the greatest challenges in studying aerosol impacts on climate is the immense diversity,  
33 not only in particle size, composition, and origin, but also in spatial and temporal distribution.  
34 For most aerosols, whose primary source is emissions near the surface, concentrations are  
35 greatest in the atmospheric boundary layer, decreasing with altitude in the free troposphere.  
36 However, smoke from wildfires and volcanic effluent can be injected above the boundary layer;  
37 after injection, any type of aerosol can be lofted to higher elevations; this can extend their  
38 atmospheric lifetimes, increasing their impact spatially and climatically.

39 Aerosols are removed from the atmosphere primarily through cloud processing and wet  
40 deposition in precipitation, a mechanism that establishes average tropospheric aerosol  
41 atmospheric lifetimes at a week or less (Table 1.1). The efficiency of removal therefore depends  
42 on the proximity of aerosols to clouds. For example, explosive volcanoes occasionally inject  
43 large amounts of aerosol precursors into the stratosphere, above most clouds; sulfuric acid  
44 aerosols formed by the 1991 Pinatubo eruption exerted a measurable effect on the atmospheric

1 heat budget for several years thereafter (e.g., Minnis et al., 1993; McCormick et al., 1995;  
2 Robock, 2000, 2002). Aerosols are also removed by dry deposition processes: gravitational  
3 settling tends to eliminate larger particles, impaction typically favors intermediate-sized  
4 particles, and coagulation is one way smaller particles can aggregate with larger ones, leading to  
5 their eventual deposition by wet or dry processes. Particle injection height, subsequent air mass  
6 advection, and other factors also affect the rate at which dry deposition operates.

7 Despite relatively short average residence times, aerosols regularly travel long distances. For  
8 example, particles moving at mean velocity of  $5 \text{ m s}^{-1}$  and remaining in the atmosphere for a  
9 week will travel 3000 km. Global aerosol observations from satellites provide ample evidence of  
10 this— Saharan dust reaches the Caribbean and Amazon basin, Asian desert dust and  
11 anthropogenic aerosol is found over the central Pacific and sometimes as far away as North  
12 America, and Siberian smoke can be deposited in the Arctic. This transport, which varies both  
13 seasonally and inter-annually, demonstrates the global scope of aerosol influences.

14 As a result of the non-uniform distribution of aerosol sources and sinks, the short atmospheric  
15 lifetimes and intermittent removal processes compared to many atmospheric greenhouse trace  
16 gases, the spatial distribution of aerosol particles is quite non-uniform. The amount and nature of  
17 aerosols vary substantially with location and from year to year, and in many cases exhibit strong  
18 seasonal variations.

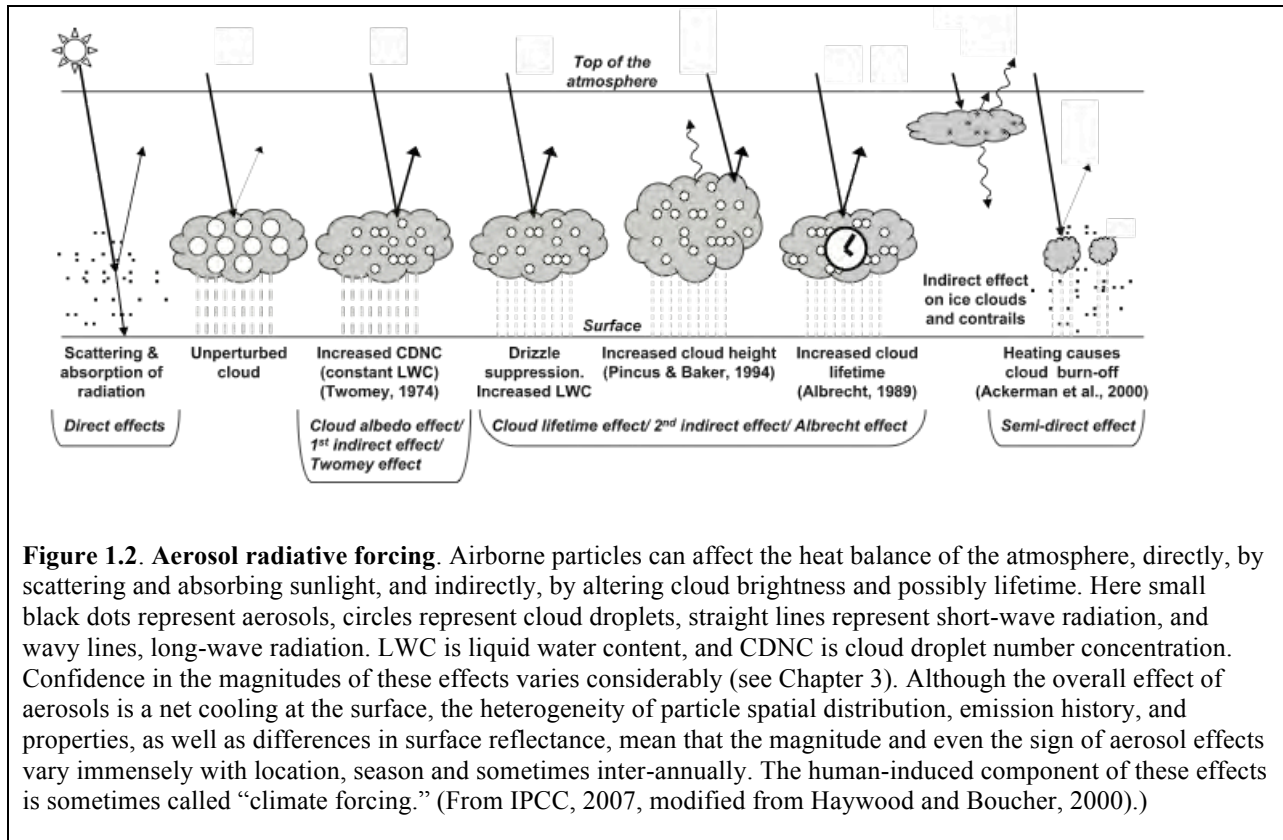
19 One consequence of this heterogeneity is that the impact of aerosols on climate must be  
20 understood and quantified on a *regional* rather than just a global-average basis. AOD trends  
21 observed in the satellite and surface-based data records suggest that since the mid-1990s, the  
22 amount of anthropogenic aerosol has decreased over North America and Europe, but has  
23 increased over parts of east and south Asia; on average, the atmospheric concentration of low-  
24 latitude smoke particles has increased (Mishchenko and Geogdzhayev, 2007). The observed  
25 AOD trends in the northern hemisphere are qualitatively consistent with changes in  
26 anthropogenic emissions (e.g. Streets et al., 2006a), and with observed trends in surface solar  
27 radiation flux (“solar brightening” or “dimming”), though other factors could be involved (e.g.,  
28 Wild et al., 2005). Similarly, the increase in smoke parallels is associated with changing biomass  
29 burning patterns (e.g., Koren et al., 2007a).

## 30 **1.2 The Climate Effects of Aerosols**

31 Aerosols exert a variety of impacts on the environment. Aerosols (sometimes referred to  
32 particulate matter or “PM,” especially in air quality applications), when concentrated near the  
33 surface, have long been recognized as affecting pulmonary function and other aspects of human  
34 health. Sulfate and nitrate aerosols play a role in acidifying the surface downwind of gaseous  
35 sulfur and odd nitrogen sources. Particles deposited far downwind might fertilize iron-poor  
36 waters in remote oceans, and Saharan dust reaching the Amazon Basin is thought to contribute  
37 nutrients to the rainforest soil.

38 Aerosols also interact strongly with solar and terrestrial radiation in several ways. **Figure 1.2**  
39 offers a schematic overview. First, they scatter and absorb sunlight (McCormick and Ludwig,  
40 1967; Charlson and Pilat, 1969; Atwater, 1970; Mitchell, Jr., 1971; Coakley et al., 1983); these  
41 are described as “direct effects” on shortwave (solar) radiation. Second, aerosols act as sites at  
42 which water vapor can accumulate during cloud droplet formation, serving as cloud  
43 condensation nuclei or CCN. Any change in number concentration or hygroscopic properties of

1 such particles has the potential to modify the physical and radiative properties of clouds, altering  
 2 cloud brightness (Twomey, 1977) and the likelihood and intensity with which a cloud will  
 3 precipitate (e.g., Gunn and Phillips, 1957; Liou and Ou 1989; Albrecht, 1989). Collectively  
 4 changes in cloud processes due to anthropogenic aerosols are referred to as *aerosol indirect*  
 5 *effects*. Finally, absorption of solar radiation by particles is thought to contribute to a reduction in  
 6 cloudiness, a phenomenon referred to as the *semi-direct effect*. This occurs because absorbing  
 7 aerosol warms the atmosphere, which changes the atmospheric stability, and reduces surface flux



8  
 9 The primary direct effect of aerosols is a brightening of the atmosphere when viewed from space,  
 10 as much of Earth’s surface is dark ocean, and most aerosols scatter more than 90% of the visible  
 11 light reaching them. The primary indirect effects of aerosol on clouds include an increase in  
 12 cloud brightness, a reduction in precipitation (at least for ice-free clouds) and possibly an  
 13 increase in lifetime; thus the overall net impact of aerosols is an enhancement of Earth’s  
 14 reflectance (shortwave albedo). This reduces the sunlight reaching Earth’s surface, producing a  
 15 net climatic cooling, as well as a redistribution of the radiant and latent heat energy deposited in  
 16 the atmosphere. These effects can alter atmospheric circulation and the water cycle, including  
 17 precipitation patterns, on a variety of length and time scales (e.g., Ramanathan et al., 2001a;  
 18 Zhang et al., 2006).

19 Several variables are used to quantify the impact aerosols have on Earth’s energy balance; these  
 20 are helpful in describing current understanding, and in assessing possible future steps.

21 For the purposes of this report, *aerosol radiative forcing* (RF) is defined as the net energy flux  
 22 (down-welling minus upwelling) difference between an initial and a perturbed aerosol loading

1 state, at a specified level in the atmosphere. (Other quantities, such as solar radiation, are  
2 assumed to be the same for both states.) This difference is defined such that a negative aerosol  
3 forcing implies that the change in aerosols relative to the initial state exerts a cooling influence,  
4 whereas a positive forcing would mean the change in aerosols exerts a warming influence.

5 There are a number of subtleties associated with this definition:

6 (1) The initial state against which aerosol forcing is assessed must be specified. For direct  
7 aerosol radiative forcing, it is sometimes taken as the complete absence of aerosols. IPCC AR4  
8 (2007) uses as the initial state their estimate of aerosol loading in 1750. That year is taken as the  
9 approximate beginning of the era when humans exerted accelerated influence on the  
10 environment.

11 (2) A distinction must be made between aerosol RF and the *anthropogenic contribution to*  
12 *aerosol RF*. Much effort has been made to distinguishing these contributions by modeling and  
13 with the help of space-based, airborne, and surface-based remote sensing, as well as *in-situ*  
14 measurements. These efforts are described in subsequent chapters.

15 (3) In general, aerosol RF and anthropogenic aerosol RF include energy associated with both the  
16 shortwave (solar) and the long-wave (primarily planetary thermal infrared) components of  
17 Earth's radiation budget. However, the solar component typically dominates, so in this document,  
18 these terms are used to refer to the solar component only, unless specified otherwise. The  
19 wavelength separation between the short- and long-wave components is usually set at around  
20 three or four micrometers.

21 (4) The IPCC AR4 (2007) defines radiative forcing as the net downward minus upward  
22 irradiance at the tropopause due to an external driver of climate change. This definition excludes  
23 stratospheric contributions to the overall forcing. Under typical conditions, most aerosols are  
24 located within the troposphere, so aerosol forcing at TOA and at the tropopause are expected to  
25 be very similar. Major volcanic eruptions or conflagrations can alter this picture regionally, and  
26 even globally.

27 (5) Aerosol radiative forcing can be evaluated at the surface, within the atmosphere, or at top-of-  
28 atmosphere (TOA). In this document, unless specified otherwise, aerosol radiative forcing is  
29 assessed at TOA.

30 (6) As discussed subsequently, aerosol radiative forcing can be greater at the surface than at  
31 TOA if the aerosols absorb solar radiation. TOA forcing affects the radiation budget of planet.  
32 Differences between TOA forcing and surface forcing represent heating within the atmosphere  
33 that can affect vertical stability, circulation on many scales, cloud formation, and precipitation,  
34 all of which are climate effects of aerosols. In this document, unless specified otherwise, these  
35 additional climate effects are not included in aerosol radiative forcing.

36 (7) Aerosol direct radiative forcing can be evaluated under cloud-free conditions or under natural  
37 conditions, sometimes termed "all-sky" conditions, which include clouds. Cloud-free direct  
38 aerosol forcing is more easily and more accurately calculated; it is generally greater than all-sky  
39 forcing because clouds can mask the aerosol contribution to the scattered light. Indirect forcing,  
40 of course, must be evaluated for cloudy or all-sky conditions. In this document, unless specified  
41 otherwise, aerosol radiative forcing is assessed for all-sky conditions.



1 (8) Aerosol radiative forcing can be evaluated instantaneously, daily (24-hour) averaged, or  
2 assessed over some other time period. Many measurements, such as those from polar-orbiting  
3 satellites, provide instantaneous values, whereas models usually consider aerosol RF as a daily  
4 average quantity. In this document, unless specified otherwise, daily averaged aerosol radiative  
5 forcing is reported.

6 (9) Another subtlety is the distinction between a “forcing” and a “feedback.” As different parts  
7 of the climate system interact, it is often unclear which elements are “causes” of climate change  
8 (forcings among them), which are responses to these causes, and which might be some of each.  
9 So, for example, the concept of aerosol effects on clouds is complicated by the impact clouds  
10 have on aerosols; the aggregate is often called aerosol-cloud interactions. This distinction  
11 sometimes matters, as it is more natural to attribute responsibility for causes than for responses.  
12 However, practical environmental considerations usually depend on the net result of all  
13 influences. In this report, “feedbacks” are taken as the consequences of changes in surface or  
14 atmospheric temperature, with the understanding that for some applications, the accounting may  
15 be done differently.

16 In summary, aerosol radiative forcing, the fundamental quantity about which this report is  
17 written, must be qualified by specifying the initial and perturbed aerosol states for which the  
18 radiative flux difference is calculated, the altitude at which the quantity is assessed, the  
19 wavelength regime considered, the temporal averaging, the cloud conditions, and whether total  
20 or only human-induced contributions are considered. The definition given here, qualified as  
21 needed, is used throughout the report.

22 Although the possibility that aerosols affect climate was recognized more than 40 years ago, the  
23 measurements needed to establish the magnitude of such effects, or even whether specific  
24 aerosol types warm or cool the surface, were lacking. Satellite instruments capable of at least  
25 crudely monitoring aerosol amount globally were first deployed in the late 1970s. But scientific  
26 focus on this subject grew substantially in the 1990s (e.g. Charlson et al., 1990; 1991; 1992;  
27 Penner et al., 1992), in part because it was recognized that to reproduce with climate models the  
28 observed temperature trends over the industrial period, net global cooling by aerosols must be  
29 included in the calculation (IPCC, 1995; 1996), along with the warming influence of enhanced  
30 atmospheric greenhouse gas (*GHG*) concentrations – mainly carbon dioxide, methane, nitrous  
31 oxide, chlorofluorocarbons, and ozone.

32 Improved satellite instruments, ground- and ship-based surface monitoring, more sophisticated  
33 chemical transport and climate models, and field campaigns that brought all these elements  
34 together with aircraft remote sensing and *in situ* sampling for focused, coordinated study, began  
35 to fill in some of the knowledge gaps. By the Fourth IPCC Assessment Report, the scientific  
36 community consensus held that in global average, the sum of direct and indirect top-of-  
37 atmosphere (TOA) forcing by anthropogenic aerosols is negative (cooling) of about  $-1.3 \text{ W m}^{-2}$   
38 ( $-2.2$  to  $-0.5 \text{ W m}^{-2}$ ). This is significant compared to the positive forcing by anthropogenic GHGs  
39 (including ozone), about  $2.9 \pm 0.3 \text{ W m}^{-2}$  (IPCC, 2007). However, the spatial distribution of the  
40 gases and aerosols are very different, and they do not simply exert compensating influences on  
41 climate.

42 The IPCC aerosol forcing assessments are based largely on model calculations, constrained as  
43 much as possible by observations. At present, aerosol influences are not yet quantified

1 adequately, according to **Figure 1.3**, as scientific understanding is designated as “Medium -  
 2 Low” and “Low” for the direct and indirect climate forcing, respectively. The IPCC AR4 (2007)  
 3 concluded that uncertainties associated with changes in Earth’s radiation budget due to  
 4 anthropogenic aerosols make the largest contribution to the overall uncertainty in radiative  
 5 forcing of climate change among the factors assessed over the industrial period.

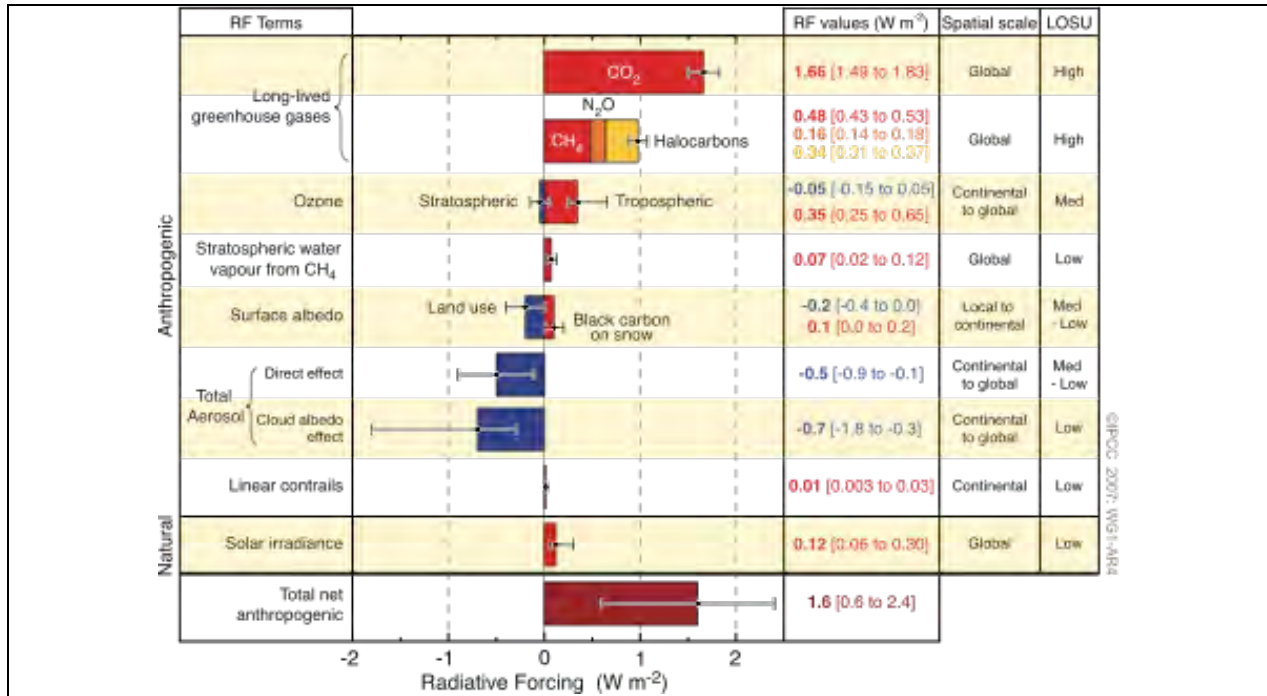


**Figure 1.3a.** (Above) Global average radiative forcing (RF) estimates and uncertainty ranges in 2005, relative to the pre-industrial climate. Anthropogenic carbon dioxide (CO<sub>2</sub>), methane (CH<sub>4</sub>), nitrous oxide (N<sub>2</sub>O), ozone, and aerosols as well as the natural solar irradiance variations are included. Typical geographical extent of the forcing (spatial scale) and the assessed level of scientific understanding (LOSU) are also given. Forcing is expressed in units of watts per square meter ( $W m^{-2}$ ). The total anthropogenic radiative forcing and its associated uncertainty are also given. Figure from IPCC (2007).

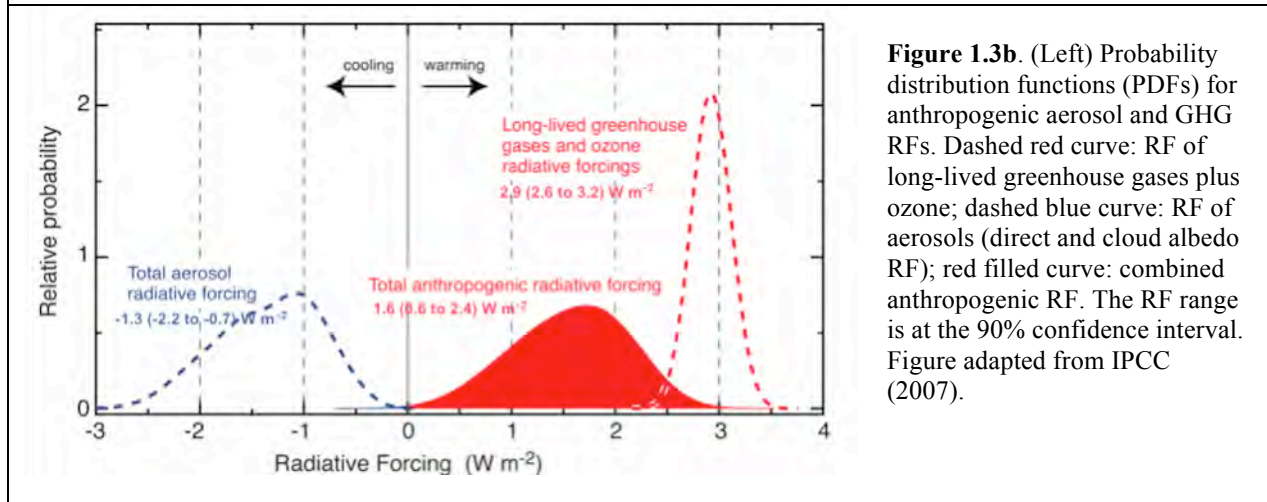


**Figure 1.3b.** (Left) Probability distribution functions (PDFs) for anthropogenic aerosol and GHG RFs. Dashed red curve: RF of long-lived greenhouse gases plus ozone; dashed blue curve: RF of aerosols (direct and cloud albedo RF); red filled curve: combined anthropogenic RF. The RF range is at the 90% confidence interval. Figure adapted from IPCC (2007).

6

1 Although AOD, aerosol properties, aerosol vertical distribution, and surface reflectivity all  
 2 contribute to aerosol radiative forcing, AOD usually varies on regional scales more than the  
 3 other aerosol quantities involved. *Forcing efficiency* ( $E_r$ ), defined as a ratio of direct aerosol  
 4 radiative forcing to AOD at 550 nm, reports the sensitivity of aerosol radiative forcing to AOD,  
 5 and is useful for isolating the influences of particle properties and other factors from that of  
 6 AOD.  $E_r$  is expected to exhibit a range of values globally, because it is governed mainly by  
 7 aerosol size distribution and chemical composition (which determine aerosol single-scattering  
 8 albedo and phase function), surface reflectivity, and solar irradiance, each of which exhibit  
 9 pronounced spatial and temporal variations. To assess aerosol RF,  $E_r$  is multiplied by the  
 10 ambient AOD.

11 **Figure 1.4** shows a range of  $E_r$  derived from AERONET surface sun photometer network  
 12 measurements of aerosol loading and particle properties, representing different aerosol and  
 13 surface types, and geographic locations. It demonstrates how aerosol direct solar radiative  
 14 forcing (with initial state takes as the absence of aerosol) is determined by a combination of  
 15 aerosol and surface properties. For example,  $E_r$  due to southern African biomass burning smoke  
 16 is greater at the surface and smaller at TOA than South American smoke because the southern  
 17 African smoke absorbs sunlight more strongly, and the magnitude of  $E_r$  for mineral dust for  
 18 several locations varies depending on the underlying surface reflectance. Figure 1.4 illustrates  
 19 one further point, that the radiative forcing by aerosols on surface energy balance can be much  
 20 greater than that at TOA. This is especially true when the particles have SSA substantially less  
 21 than 1, which can create differences between surface and TOA forcing as large as a factor of five  
 22 (e.g., Zhou et al., 2005).

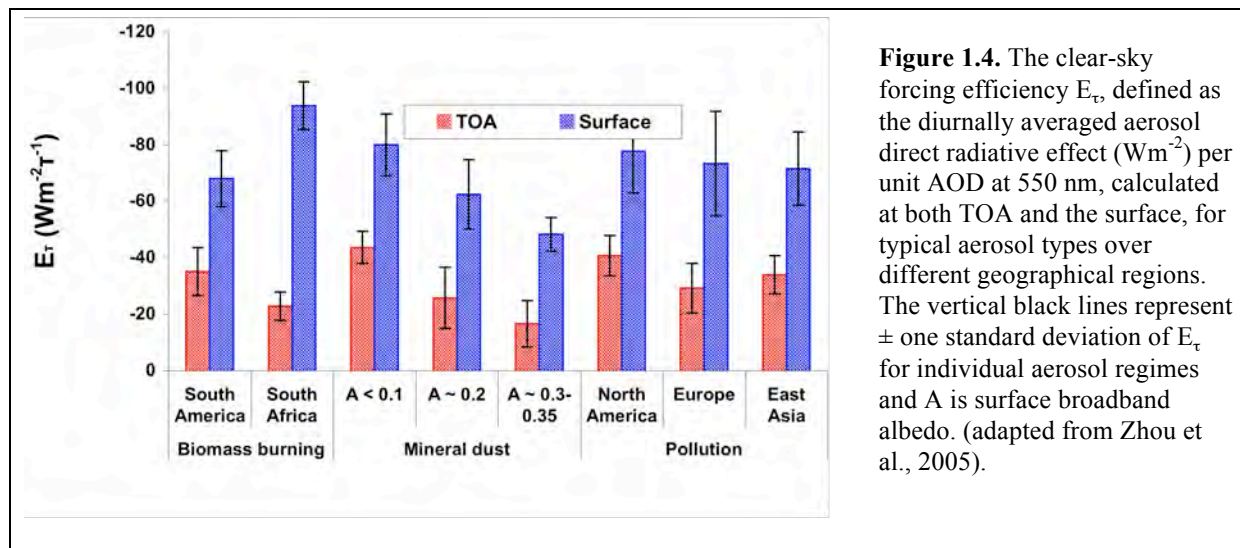


**Figure 1.4.** The clear-sky forcing efficiency  $E_r$ , defined as the diurnally averaged aerosol direct radiative effect (Wm<sup>-2</sup>) per unit AOD at 550 nm, calculated at both TOA and the surface, for typical aerosol types over different geographical regions. The vertical black lines represent  $\pm$  one standard deviation of  $E_r$  for individual aerosol regimes and A is surface broadband albedo. (adapted from Zhou et al., 2005).

23  
 24 **Table 1.2** presents estimates of cloud-free, instantaneous, aerosol direct RF dependence on  
 25 AOD, and on aerosol and surface properties, calculated for three sites maintained by the US  
 26 Department of Energy's Atmospheric Radiation Measurement (ARM) program, where surface  
 27 and atmospheric conditions span a significant range of natural environments (McComiskey et al.,  
 28 2008a). Here aerosol RF is evaluated relative to an initial state that is the complete absence of  
 29 aerosols. Note that aerosol direct RF dependence on individual parameters varies considerably,  
 30 depending on the values of the other parameters, and in particular, that aerosol RF dependence

1 on AOD actually changes sign, from net cooling to net warming, when aerosols reside over an  
 2 exceedingly bright surface. Sensitivity values are given for snapshots at fixed solar zenith angles,  
 3 relevant to measurements made, for example, by polar-orbiting satellites.

4 The lower portion of **Table 1.2**  
 5 presents upper bounds on  
 6 instantaneous measurement  
 7 uncertainty, assessed individually  
 8 for each of AOD, SSA,  $g$ , and  $A$ , to  
 9 produce a  $1 \text{ W m}^{-2}$  top-of-  
 10 atmosphere, cloud-free aerosol RF  
 11 accuracy. The values are derived  
 12 from the upper portion of the table,  
 13 and reflect the diversity of  
 14 conditions captured by the three  
 15 ARM sites. Aerosol RF sensitivity  
 16 of  $1 \text{ W m}^{-2}$  is used as an example;  
 17 uncertainty upper bounds are  
 18 obtained from the partial derivative  
 19 for each parameter by neglecting the  
 20 uncertainties for all other  
 21 parameters. These estimates  
 22 produce an instantaneous AOD  
 23 measurement uncertainty upper  
 24 bound between about 0.01 and 0.02,  
 25 and SSA constrained to about 0.02  
 26 over surfaces as bright or brighter  
 27 than the ARM Southern Great  
 28 Plains site, typical of mid-latitude,  
 29 vegetated land. Other researchers,  
 30 using independent data sets, have  
 31 derived ranges of  $E_r$  and aerosol RF  
 32 sensitivity similar to those presented  
 33 here, for a variety of conditions  
 34 (e.g., Christopher and Jones, 2008;  
 35 Yu et al., 2006; Zhou et al., 2005).

<b>Table 1.2.</b> Top-of-atmosphere, cloud-free, instantaneous direct aerosol radiative forcing dependence on aerosol and surface properties. Here TWP, SGP, and NSA are the Tropical West Pacific island, Southern Great Plains, and North Slope Alaska observation stations maintained by the DOE ARM program, respectively. Instantaneous values are given at specific solar zenith angle. Upper and middle parts are from McComiskey et al. (2008a). Representative, parameter-specific measurement uncertainty upper bounds for producing $1 \text{ W m}^{-2}$ instantaneous TOA forcing accuracy are given in the lower part, based on sensitivities at three sites from the middle part of the table.			
<b>Parameters</b>	<b>TWP</b>	<b>SGP</b>	<b>NSA</b>
<i>Aerosol properties (AOD, SSA, <math>g</math>), solar zenith angle (SZA), surface albedo (<math>A</math>), and aerosol direct RF at TOA (<math>F</math>):</i>			
<b>AOD</b>	0.05	0.1	0.05
<b>SSA</b>	0.97	0.95	0.95
<b><math>g</math></b>	0.8	0.6	0.7
<b><math>A</math></b>	0.05	0.1	0.9
<b>SZA</b>	30	45	70
<b><math>F \text{ (W m}^{-2}\text{)}</math></b>	-2.2	-6.3	2.6
<i>Sensitivity of cloud-free, instantaneous, TOA direct aerosol radiative forcing to aerosol and surface properties:</i>			
$\partial F/\partial(\text{AOD})$	-45	-64	51
$\partial F/\partial(\text{SSA})$	-11	-50	-60
$\partial F/\partial g$	13	23	2
$\partial F/\partial A$	8	24	6
<i>Representative measurement uncertainty upper bounds for producing <math>1 \text{ W m}^{-2}</math> accuracy of aerosol RF:</i>			
<b>AOD</b>	0.022	0.016	0.020
<b>SSA</b>	0.091	0.020	0.017
<b><math>g</math></b>	0.077	0.043	--
<b><math>A</math></b>	0.125	0.042	0.167

36 These uncertainty bounds provide a baseline against which current and expected near-future  
 37 instantaneous measurement capabilities are assessed in Chapter 2. Model sensitivity is usually  
 38 evaluated for larger-scale (even global) and longer-term averages. When instantaneous measured  
 39 values from a randomly sampled population are averaged, the uncertainty component associated  
 40 with random error diminishes as something like the inverse square root of the number of  
 41 samples. As a result, the accuracy limits used for assessing more broadly averaged model results  
 42 corresponding to those used for assessing instantaneous measurements, would have to be tighter,  
 43 as discussed in Chapter 4.

44 In summary, much of the challenge in quantifying aerosol influences arises from large spatial  
 45 and temporal heterogeneity, caused by the wide variety of aerosol sources, sizes and

1 compositions, the spatial non-uniformity and intermittency of these sources, the short  
2 atmospheric lifetime of most aerosols, and the spatially and temporally non-uniform chemical  
3 and microphysical processing that occurs in the atmosphere. In regions having high  
4 concentrations of anthropogenic aerosol, for example, aerosol forcing is much stronger than the  
5 global average, and can exceed the magnitude of GHG warming, locally reversing the sign of the  
6 net forcing. It is also important to recognize that the global-scale aerosol TOA forcing alone is  
7 not an adequate metric for climate change (NRC, 2005). Due to aerosol absorption, mainly by  
8 soot, smoke, and some desert dust particles, the aerosol direct radiative forcing at the surface can  
9 be much greater than the TOA forcing, and in addition, the radiative heating of the atmosphere  
10 by absorbing particles can change the atmospheric temperature structure, affecting vertical  
11 mixing, cloud formation and evolution, and possibly large-scale dynamical systems such as the  
12 monsoons (Kim et al., 2006; Lau et al., 2008). By realizing aerosol's climate significance and the  
13 challenge of charactering highly variable aerosol amount and properties, the US Climate Change  
14 Research Initiative (*CCRI*) identified research on atmospheric concentrations and effects of  
15 aerosols specifically as a top priority (NRC, 2001).

### 16 **1.3. Reducing Uncertainties in Aerosol-Climate Forcing** 17 **Estimates**

18 Regional as well as global aerosol radiative effects on climate are estimated primarily through  
19 the use of climate models (e.g., Penner et al., 1994; Schulz et al., 2006). These numerical models  
20 are evaluated based on their ability to simulate the aerosol- and cloud-related processes that  
21 affect climate for current and past conditions. The derived accuracy serves as a measure of the  
22 accuracy with which the models might be expected to predict the dependence of future climate  
23 conditions on prospective human activities. To generate such predictions, the models must  
24 simulate the physical, chemical, and dynamical mechanisms that govern aerosol formation and  
25 evolution in the atmosphere (**Figure 1.1**), as well as the radiative processes that govern their  
26 direct and indirect climate impact (**Figure 1.2**), on all the relevant space and time scales.

27 Some models simulate aerosol emissions, transports, chemical processing, and sinks, using  
28 atmospheric and possibly also ocean dynamics generated off-line by separate numerical systems.  
29 These are often called Aerosol Models or Chemistry and Transport Models (CTMs). In contrast,  
30 General Circulation Models or Global Climate Models (GCMs) can couple aerosol behavior and  
31 dynamics as part of the same calculation, and are capable of representing interactions between  
32 aerosols and dynamical aspects of the climate system, although currently many of them still use  
33 prescribed aerosols to study climate sensitivity.

34 The IPCC AR4 total anthropogenic radiative forcing estimate, shown in **Figure 1.3**, is  $1.6 \text{ W m}^{-2}$   
35 from preindustrial times to the present, with a likely range of  $0.6$  to  $2.4 \text{ W m}^{-2}$ . This estimate  
36 includes long-lived GHGs, ozone, and aerosols. The increase in global mean surface temperature  
37 of  $0.7^\circ\text{C}$ , from the transient climate simulations in response to this forcing, yields a transient  
38 climate sensitivity (defined as the surface temperature change per unit RF) over the industrial  
39 period of  $0.3$  to  $1.1^\circ\text{C}/(\text{W m}^{-2})$ .

40 Under most emission scenarios,  $\text{CO}_2$  is expected to double by the latter part of the 21st century.  
41 A climate sensitivity range of  $0.3$  to  $1.1^\circ\text{C}/(\text{W m}^{-2})$  translates into a future surface temperature  
42 increase attributable to  $\text{CO}_2$  forcing at the time of doubled  $\text{CO}_2$  of  $1.2$  to  $4.7^\circ\text{C}$ . Such a range is  
43 too wide to meaningfully predict the climate response to increased greenhouse gases. As **Figure**

1 **1.3** shows, the largest contribution to overall uncertainty in estimating the climate response is  
2 from aerosol RF.

3 The key to reducing uncertainty in the role of aerosols in climate is to understand the processes  
4 that contribute to these effects well enough to reproduce them in models. This report highlights  
5 three specific areas for continued, focused effort: (1) improving measurement quality and  
6 coverage, (2) achieving more effective use of measurements to constrain model simulations and  
7 to test model parameterizations, and (3) producing more accurate representation of aerosols and  
8 clouds in models. This section provides a brief introduction to the current state of aerosol  
9 measurements and model representations of aerosol processes, as they relate to assessing aerosol  
10 impacts on climate. More complete discussion of these topics and assessment of possible next  
11 steps are given in Chapters 2, 3, and 4.

12 *Improving measurement quality and coverage.* Aerosol mass concentration, size and composition  
13 distributions, and absorption properties, as functions of location and time, are the main aerosol-  
14 specific elements of CTMs. They depend on primary particle and precursor gas emissions, on  
15 gas-to-particle conversion processes, on transport, humidification and cloud processing, and  
16 removal mechanisms. Satellite instruments, surface-based networks (*in situ* and remote), and  
17 research aircraft all contribute quantitative measurements of aerosol properties and/or  
18 distributions that can be used to help constrain models, as well as to test and refine the model  
19 representations of processes that govern aerosol life cycles. As described in Chapter 2, the  
20 current situation reflects the significant progress that has been made over the past decade in  
21 satellite, airborne, ground-based and laboratory instrumentation, actual measurements available  
22 from each of these sources, remote sensing retrieval methods, and data validation techniques.

23 However, each type of measurement is limited in terms of the accuracy, and spatial and temporal  
24 sampling of measured quantities. At present, satellite passive imagers monitor AOD globally up  
25 to once per day, with accuracies under cloud-free, good but not necessarily ideal viewing  
26 conditions of about 0.05 or (0.1 to 0.2)  $\times$  AOD, whichever is larger, for vegetated land,  
27 somewhat better over dark water, and less well over bright desert (e.g., Kahn et al., 2005a;  
28 Remer et al., 2005). Reliable AOD retrieval over snow and ice from passive remote sensing  
29 imagers has not yet been achieved. From space, aerosol vertical distribution is provided mainly  
30 by lidars that offer sensitivity to multiple layers, even in the presence of thin cloud, but they  
31 require several weeks to observe just a fraction of a percent of the planet.

32 From the expansive vantage point of space, there is enough information to identify column-  
33 average ratios of coarse to fine AOD, or even aerosol air mass types in some circumstances, but  
34 not sufficient to deduce chemical composition and vertical distribution of type, nor to constrain  
35 light absorption approaching the  $\sim 0.02$  SSA sensitivity suggested in Section 1.2.

36 As a result, it is difficult to separate anthropogenic from natural aerosols using currently  
37 available satellite data alone, though attempts at this have been made based on retrieved particle  
38 size and shape information (see Chapter 2). At present, better quantification of anthropogenic  
39 aerosol depends upon integrating satellite measurements with other observations and models.  
40 Aircraft and ground-based *in situ* sampling can help fill in missing physical and chemical detail,  
41 although coverage is very limited in both space and time. Models can contribute by connecting  
42 observed aerosol distributions with likely sources and associated aerosol types. Surface remote-  
43 sensing monitoring networks offer temporal resolution of minutes to hours, and greater column

1 AOD accuracy than satellite observations, but height-resolved particle property information has  
2 been demonstrated by only a few cutting-edge technologies such as high-spectral-resolution lidar  
3 (HSRL), and again, spatial coverage is extremely limited.

4 Even for satellite observations, sampling is an issue. From the passive imagers that provide the  
5 greatest coverage, AOD retrievals can only be done under cloud-free conditions, leading to a  
6 “clear-sky bias,” and there are questions about retrieval accuracy in the vicinity of clouds. And  
7 retrievals of aerosol type from these instruments as well as from surface-based passive remote  
8 sensing require at least a certain minimum column AOD to be effective; the thresholds depend in  
9 part on aerosol type itself and on surface reflectivity, leading to an “AOD bias” in these data sets.

10 Other measurement-related issues include obtaining sufficiently extensive aerosol vertical  
11 distributions outside the narrow sampling beam of space-based, airborne, or ground-based lidars,  
12 retrieving layer-resolved aerosol properties, which is especially important in the many regions  
13 where multiple layers of different types are common, obtaining representative *in situ* samples of  
14 large particles, since they tend to be under-sampled when collected by most aircraft inlets, and  
15 acquiring better surface measurement coverage over oceans.

16 *Achieving more effective use of measurements to constrain models.* Due to the limitations  
17 associated with each type of observational data record, reducing aerosol-forcing uncertainties  
18 requires coordinated efforts at integrating data from multiple platforms and techniques (Seinfeld  
19 et al., 1996; Kaufman et al., 2002a; Diner et al., 2004; Anderson et al., 2005a). Initial steps have  
20 been taken to acquire complementary observations from multiple platforms, especially through  
21 intensive field campaigns, and to merge data sets, exploiting the strengths of each to provide  
22 better constraints on models (e.g., Bates et al., 2006; Yu et al., 2006; Kinne et al., 2006; see  
23 Chapter 2, Section 2.2.6). Advanced instrument concepts, coordinated measurement strategies,  
24 and retrieval techniques, if implemented, promise to further improve the contributions  
25 observations make to reducing aerosol forcing uncertainties.

26 *Producing more accurate representation of aerosols in models.* As discussed in Chapter 3,  
27 models, in turn, have developed increasingly sophisticated representations of aerosol types and  
28 processes, have improved the spatial resolution at which simulations are performed, and through  
29 controlled experiments and inter-comparisons of results from many models, have characterized  
30 model diversity and areas of greatest uncertainty (e.g., Textor et al 2006; Kinne et al., 2006).

31 A brief chronology of aerosol modeling used for the IPCC reports illustrates these developments.  
32 In the IPCC First Assessment Report (1990), the few transient climate change simulations that  
33 were discussed used only increases in greenhouse gases. By IPCC Second Assessment Report  
34 (1995), although most GCMs still considered only greenhouse gases, several simulations  
35 included the direct effect of sulfate aerosols. The primary purpose was to establish whether the  
36 pattern of warming was altered by including aerosol-induced cooling in regions of high  
37 emissions such as the Eastern U.S. and eastern Asia. In these models, the sulfate aerosol  
38 distribution was derived from a sulfur cycle model constrained by estimated past aerosol  
39 emissions and an assumed future sulfur emission scenario. The aerosol forcing contribution was  
40 mimicked by increasing the surface albedo, which improved model agreement with the observed  
41 global mean temperature record for the final few decades of the twentieth century, but not for the  
42 correct reasons (see Chapter 3).

1 The IPCC Third Assessment Report (TAR, 2001) report cited numerous groups that included  
2 aerosols in both 20<sup>th</sup> and 21<sup>st</sup> century simulations. The direct effect of sulfate aerosols was  
3 required to reproduce the observed global temperature change, given the models' climate  
4 sensitivity and ocean heat uptake. Although most models still represented aerosol forcing by  
5 increasing the surface albedo, several groups explicitly represented sulfate aerosols in their  
6 atmospheric scattering calculations, with geographical distributions determined by off-line CTM  
7 calculations. The first model calculations that included any indirect effects of aerosols on clouds  
8 were also presented.

9 The most recent IPCC assessment report (AR4; 2007) summarized the climate change  
10 experiments from more than 20 modeling groups that this time incorporated representations of  
11 multiple aerosol species, including black and organic carbon, mineral dust, sea salt and in some  
12 cases nitrates (see Chapter 3). In addition, many attempts were made to simulate indirect effects,  
13 in part because the better understood direct effect appeared to be insufficient to properly simulate  
14 observed temperature changes, given model sensitivity. As in previous assessments, the AR4  
15 aerosol distributions responsible for both the direct and indirect effect were produced off-line, as  
16 opposed to being run in a coupled mode that would allow simulated climate changes to feed back  
17 on the aerosol distributions.

18 The fact that models now use multiple aerosol types and often calculate both direct and indirect  
19 aerosol effects does not imply that the requisite aerosol amounts and optical characteristics, or  
20 the mechanisms of aerosol-cloud interactions, are well represented. For example, models tend to  
21 have lower AOD relative to measurements, and are poorly constrained with regard to speciation  
22 (see **Table 3.2** and **Figure 3.1** in Chapter 3). To bridge the gap between measurements and  
23 models in this area, robust relationships need to be established for different aerosol types,  
24 connecting the AOD and types retrieved from spacecraft, aircraft, and surface remote sensing  
25 observations, with the aerosol mass concentrations that are the fundamental aerosol quantities  
26 tracked in CTMs and GCMs.

27 As detailed below, continued progress with measurement, modeling, and at the interfaces  
28 between the two, promises to improve estimates of aerosol contributions to climate change, and  
29 to reduce the uncertainties in these quantities reflected in **Figure 1.3**.

## 30 **1.4 Contents of This Report**

31 This report assesses current understanding of aerosol radiative effects on climate, focusing on  
32 developments of aerosol measurement and modeling subsequent to IPCC TAR (2001). It reviews  
33 the present state of understanding of aerosol influences on Earth's climate system, and in  
34 particular, the consequences for climate change of their direct and indirect effects. This report  
35 does not deal with several natural forcings that involve aerosols. Stratospheric aerosols produced  
36 by large volcanic eruptions exert large, short-term effects which are particularly important for  
37 characterizing climate system response to forcing, and the effects of recent eruptions (e.g.  
38 Pinatubo) are well documented (e.g., Minnis et al., 1993; McCormick et al., 1995; Robock et al.,  
39 2002). However these effects are intermittent and have only short-term environmental impacts  
40 (ca. 1 year). Galactic cosmic rays, modulated by the 11-year solar cycle, have been reported to  
41 correlate with the total cloud cover (e.g., Svensmark and Friis-Christensen, 1997), possibly by  
42 aiding the nucleation of new particles that grow into cloud condensation nuclei (e.g., Turco et al.,  
43 1998). However, the present mainstream consensus is that these phenomena exert little to no



1 effect on cloud cover or other cloud properties (e.g., Lockwood and Fröhlich, 2008; Kristjánsson  
2 et al., 2008).

3 The Executive Summary reviews the key concepts involved in the study of aerosol effects on  
4 climate, and provides a chapter-by-chapter summary of conclusions from this assessment.  
5 Chapter 1 provided basic definitions, radiative forcing accuracy requirements, and background  
6 material on critical issues needed to motivate the more detailed discussion and assessment given  
7 in subsequent chapters.

8 Chapter 2 assesses the aerosol contributions to radiative forcing based on remote sensing and *in*  
9 *situ* measurements of aerosol amounts and properties. Current measurement capabilities and  
10 limitations are discussed, as well as synergy with models, in the context of the needed aerosol  
11 radiative forcing accuracy.

12 Model simulation of aerosol and their direct and indirect effects are examined in Chapter 3.  
13 Representations of aerosols used for IPCC AR4 (2007) climate simulations are discussed,  
14 providing an overview of near-term modeling option strengths and limitations for assessing  
15 aerosol forcing of climate.

16 Finally, Chapter 4 provides an assessment of how current capabilities, and those within reach for  
17 the near future, can be brought together to reduce the aerosol forcing uncertainties reported in  
18 IPCC AR4 (2007).

# CHAPTER 2

## Remote Sensing and *In Situ* Measurements of Aerosol Properties, Burdens, and Radiative Forcing

**Lead Authors:** Hongbin Yu, NASA GSFC/UMBC; Patricia K. Quinn, NOAA PMEL; Graham Feingold, NOAA ESRL; Lorraine A. Remer, NASA GSFC; Ralph A. Kahn, NASA GSFC

**Contributing Authors:** Mian Chin, NASA GSFC; Stephen E. Schwartz, DOE BNL

### 2.1. Introduction

As discussed in Chapter 1, much of the challenge in quantifying aerosol direct radiative forcing (*DRF*) and aerosol-cloud interactions arises from large spatial and temporal heterogeneity of aerosol concentrations, compositions, and sizes, which requires an integrated approach that effectively combines measurements and model simulations. Measurements, both *in situ* and remote sensing, play essential roles in this approach by providing data with sufficient accuracy for validating and effectively constraining model simulations. For example, to achieve an accuracy of  $1 \text{ Wm}^{-2}$  for the instantaneous, top-of-atmosphere (TOA) aerosol DRF under cloud free conditions, the accuracy for measuring aerosol optical depth (AOD) should be within 0.01 and 0.02 for mid-visible wavelength, and that for single-scattering albedo (SSA) should be constrained to about 0.02 over land (Chapter 1, Table 1.2). The measurement requirements would be much tighter in order to achieve the same forcing accuracy at the surface. Quantifying anthropogenic component of DRF and aerosol indirect radiative forcing would impose additional accuracy requirements on measurements of aerosol chemical composition and microphysical properties (e.g., size distribution) that are needed to attribute material to sources or source type.

Over the past decade and since the Intergovernmental Panel on Climate Change (IPCC) Third Assessment Report (TAR) (IPCC 2001) in particular, a great deal of effort has gone into improving measurement data sets (as summarized in Yu et al., 2006; Bates et al., 2006; Kahn et al., 2004). Principal efforts have been:

- Development and implementation of new and enhanced satellite-borne sensors examining aerosol effects on atmospheric radiation;
- Execution of focused field experiments examining aerosol processes and properties in various aerosol regimes around the globe;
- Establishment and enhancement of ground-based networks measuring aerosol properties and radiative forcing; and
- Development and deployment of new and enhanced instrumentation, importantly aerosol mass spectrometers examining size dependent composition and several methods for measuring aerosol SSA.

These efforts have made it feasible to shift the estimates of aerosol radiative forcing increasingly

1 from largely model-based as in IPCC TAR to measurement-based as in the IPCC Fourth  
2 Assessment Report (AR4) (IPCC 2007). Satellite measurements that are evaluated,  
3 supplemented, and constrained by ground-based remote sensing measurements and *in situ*  
4 measurements from focused field campaigns, provide the basis for the regional- to global-scale  
5 assessments. Chemistry and transport models (CTMs) are used to interpolate and supplement the  
6 data in regions and under conditions where observational data are not available or to assimilate  
7 high-quality data from various observations to constrain and thereby improve model simulations  
8 of aerosol impacts. These developments have played an important role in advancing the scientific  
9 understanding of aerosol direct and indirect radiative forcing as documented in the IPCC AR4  
10 (IPCC, 2007).

11 The goals of this chapter are to:

- 12 • provide an overview of current aerosol measurement capabilities and limitations;
- 13 • describe the concept of synergies between different types of measurements and  
14 models;
- 15 • assess estimates of aerosol direct and indirect radiative forcing from different  
16 observational approaches; and
- 17 • discuss outstanding issues to which measurements can contribute.

18  
19 The synthesis and assessment in this chapter lays groundwork needed to develop a future  
20 research strategy for understanding and quantifying aerosol-climate interactions.

## 21 **2.2. Overview of Aerosol Measurement Capabilities**

### 22 **2.2.1. Satellite Remote Sensing**

23 A measurement-based characterization of aerosols on a global scale can be realized only through  
24 satellite remote sensing, which is the only means of characterizing the large spatial and temporal  
25 heterogeneities of aerosol distributions. Monitoring aerosols from space has been performed for  
26 over two decades and is planned for the coming decade with enhanced capabilities (King et al.,  
27 1999; Foster et al., 2007; Lee et al., 2006; Mishchenko et al., 2007b). **Table 2.1** summarizes  
28 major satellite measurements currently available for the tropospheric aerosol characterization and  
29 radiative forcing research.

30 Early aerosol monitoring from space relied on sensors that were designed for other purposes. The  
31 Advanced Very High Resolution Radiometer (*AVHRR*), intended as a cloud and surface  
32 monitoring instrument, provides radiance observations in the visible and near infrared  
33 wavelengths that are sensitive to aerosol properties over the ocean (Husar et al., 1997;  
34 Mishchenko et al., 1999). Originally intended for ozone monitoring, the ultraviolet (UV)  
35 channels used for the Total Ozone Mapping Spectrometer (*TOMS*) are sensitive to aerosol UV  
36 absorption with little surface interferences, even over land (Torres et al., 1998). This UV-  
37 technique makes TOMS suitable for monitoring biomass burning smoke and dust, though with  
38 limited sensitivity near the surface (Herman et al., 1997) and for retrieving aerosol single-  
39 scattering albedo from space (Torres et al., 2005). (A new sensor, the Ozone Monitoring  
40 Instrument (*OMI*) aboard Aura, has improved on such UV-technique advantages, providing  
41 higher spatial resolution and more spectral channels, see Veihelmann et al., 2007). Such  
42 historical sensors have provided multi-decadal climatology of aerosol optical depth that has  
43 significantly advanced the understanding of aerosol distributions and long-term variability (e.g.,

1 Geogdzhayev et al., 2002; Torres et al., 2002; Massie et al., 2004; Mishchenko et al., 2007a;  
 2 Mishchenko and Geogdzhayev, 2007; Zhao et al., 2008a).

3

**Table 2.1.** Summary of major satellite measurements currently available for the tropospheric aerosol characterization and radiative forcing research.

Category	Properties	Sensor/platform	Parameters	Spatial coverage	Temporal coverage
Column-integrated	Loading	AVHRR/NOAA-series	optical depth	~daily coverage of global ocean	1981-present
		TOMS/Nimbus, ADEOS1, EP		~daily coverage of global land and ocean	1979-2001
		POLDER-1, -2, PARASOL			1997-present
		MODIS/Terra, Aqua			2000-present (Terra) 2002-present (Aqua)
		MISR/Terra		~weekly coverage of global land and ocean, including bright desert and nadir sun-glint	2000-present
		OMI/Aura		~daily coverage of global land and ocean	2005-present
	Size, shape	AVHRR/NOAA-series	Angstrom exponent	global ocean	1981-present
		POLDER-1, -2, PARASOL	fine-mode fraction, Angstrom exponent, non-spherical fraction	global land+ocean	1997-present
		MODIS/Terra, Aqua	fine-mode fraction	global land+ocean (better quality over ocean)	2000-present (Terra) 2002-present (Aqua)
			Angstrom exponent		
			effective radius	global ocean	
			asymmetry factor		
	MISR/Terra	Angstrom exponent, small, medium, large fractions, non-spherical fraction	global land+ocean	2000-present	
	Absorption	TOMS/Nimbus, ADEOS1, EP	absorbing aerosol index, single-scattering albedo, absorbing optical depth	global land+ocean	1979-2001
		OMI/Aura			2005-present
MISR/Terra		2000-present			
Vertical-resolved	Loading, size, and shape	GLAS/ICESat	extinction/backscatter	global land+ocean, 16-day repeating cycle, single-nadir measurement	2003-present (~3months/year)
		CALIOP/CALIPSO	extinction/backscatter, color ratio, depolarization ratio		2006-present

4

5 Over the past decade, satellite aerosol retrievals have become increasingly sophisticated. Now,  
 6 satellites measure the angular dependence of radiance and polarization at multiple wavelengths  
 7 from UV through the infrared (IR) at fine spatial resolution. From these observations, retrieved  
 8 aerosol products include not only optical depth at one wavelength, but also spectral optical depth  
 9 and some information about particle size over both ocean and land, as well as more direct  
 10 measurements of polarization and phase function. In addition, cloud screening is much more  
 11 robust than before and onboard calibration is now widely available. Examples of such new and

1 enhanced sensors include the MODerate resolution Imaging Spectroradiometer (*MODIS*, see  
2 **Box 2.1**), the Multi-angle Imaging SpectroRadiometer (*MISR*, see **Box 2.2**), Polarization and  
3 Directionality of the Earth's Reflectance (*POLDER*, see **Box 2.3**), and OMI, among others. The  
4 accuracy for AOD measurement from these sensors is about 0.05 or 20% of AOD (Remer et al.,  
5 2005; Kahn et al., 2005a) and somewhat better over dark water, but that for aerosol  
6 microphysical properties, which is useful for distinguishing aerosol air mass types, is generally  
7 low. The Clouds and the Earth's Radiant Energy System (*CERES*, see **Box 2.4**) measures  
8 broadband solar and terrestrial radiances. The CERES radiation measurements in combination  
9 with satellite retrievals of aerosol optical depth can be used to determine aerosol direct radiative  
10 forcing.

11 Complementary to these passive sensors, active remote sensing from space is also now possible  
12 and ongoing (see **Box 2.5**). Both the Geoscience Laser Altimeter System (*GLAS*) and the Cloud  
13 and Aerosol Lidar with Orthogonal Polarization (*CALIOP*) are collecting essential information  
14 about aerosol vertical distributions. Furthermore, the constellation of six afternoon-overpass  
15 spacecrafts (as illustrated in **Figure 2.5**), the so-called *A-Train* (Stephens et al., 2002) makes it  
16 possible for the first time to conduct near simultaneous (within 15-minutes) measurements of  
17 aerosols, clouds, and radiative fluxes in multiple dimensions with sensors in complementary  
18 capabilities.

19 The improved accuracy of aerosol products (mainly AOD) from these new-generation sensors,  
20 together with improvements in characterizing the earth's surface and clouds, can help reduce the  
21 uncertainties associated with estimating the aerosol direct radiative forcing (Yu et al., 2006; and  
22 references therein). The retrieved aerosol microphysical properties, such as size, absorption, and  
23 non-spherical fraction can help distinguish anthropogenic aerosols from natural aerosols and  
24 hence help assess the anthropogenic component of aerosol direct radiative forcing (Kaufman et  
25 al., 2005a; Bellouin et al., 2005, 2008; Christopher et al., 2006; Yu et al., 2006, 2008). However,  
26 to infer aerosol number concentrations and examine indirect aerosol radiative effects from space,  
27 significant efforts are needed to measure aerosol size distribution with much improved accuracy,  
28 characterize aerosol type, account for impacts of water uptake on aerosol optical depth, and  
29 determine the fraction of aerosols that is at the level of the clouds (Kapustin et al., 2006;  
30 Rosenfeld, 2006). In addition, satellite remote sensing is not sensitive to particles much smaller  
31 than 0.1 micrometer in diameter, which comprise of a significant fraction of those that serve as  
32 cloud condensation nuclei.

33 Finally, algorithms are being developed to retrieve aerosol absorption or SSA from satellite  
34 observations (e.g., Kaufman et al., 2002b; Torres et al., 2005). The NASA Glory mission,  
35 scheduled to launch in 2009 and to be added to the A-Train, will deploy a multi-angle, multi-  
36 spectral polarimeter to determine the global distribution of aerosol and clouds. It will also be able  
37 to infer microphysical property information, from which aerosol type (e.g., marine, dust,  
38 pollution, etc.) can be inferred for improving quantification of the aerosol direct and indirect  
39 forcing on climate (Mishchenko et al., 2007b).

40

### Box 2.1: MODerate resolution Imaging Spectroradiometer

MODIS performs near global daily observations of atmospheric aerosols. Seven of 36 channels (between 0.47 and 2.13  $\mu\text{m}$ ) are used to retrieve aerosol properties over cloud and surface-screened areas (Martins et al., 2002; Li et al., 2004). Over vegetated land, MODIS retrieves aerosol optical depth at three visible channels with high accuracy of  $\pm 0.05 \pm 0.2\tau$  (Kaufman et al., 1997; Chu et al., 2002; Remer et al., 2005; Levy et al., 2007b). Most recently a deep-blue algorithm (Hsu et al., 2004) has been implemented to retrieve aerosols over bright deserts on an operational basis, with an estimated accuracy of 20-30%. Because of the greater simplicity of the ocean surface, MODIS has the unique capability of retrieving not only aerosol optical depth with greater accuracy, i.e.,  $\pm 0.03 \pm 0.05\tau$  (Tanré et al., 1997; Remer et al., 2002; 2005; 2008), but also quantitative aerosol size parameters (e.g., effective radius, fine-mode fraction of AOD) (Kaufman et al., 2002a; Remer et al., 2005; Kleidman et al., 2005). The fine-mode fraction has been used as a tool for separating anthropogenic aerosol from natural ones and estimating the anthropogenic aerosol direct climate forcing (Kaufman et al., 2005a). **Figure 2.1** shows composites of MODIS AOD and fine-mode fraction that illustrate seasonal and geographical variations of aerosol types. Clearly seen from the figure is heavy pollution over East Asia in both months, biomass burning smoke over South Africa, South America, and Southeast Asia in September, heavy dust storms over North Africa and North Atlantic in both months and over northern China in March, and a mixture of dust and pollution plume swept across North Pacific in March.

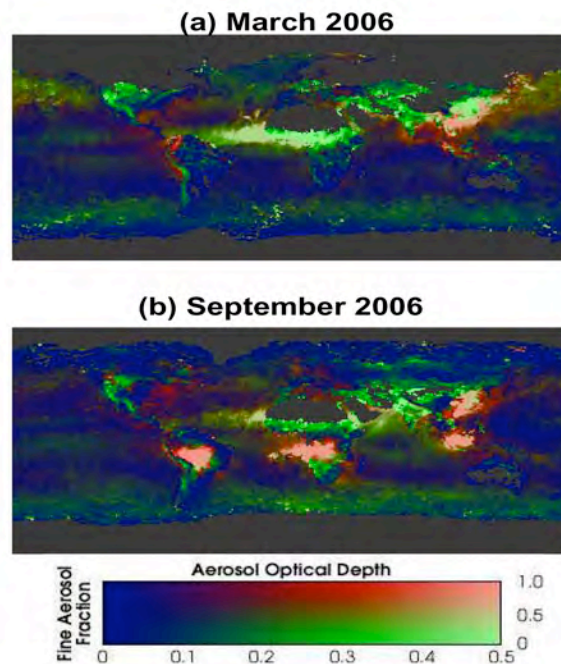


**Figure 2.1:** A composite of MODIS observed aerosol optical depth (at 550 nm, green light near the peak of human vision) and fine-mode fraction that shows spatial and seasonal variations of aerosol types. Industrial pollution and biomass burning aerosols are predominated by small particles (shown as red), while mineral dust consists of a large fraction of large particles (shown as green). Bright red and bright green indicate heavy pollution and dust plumes, respectively. The plots were generated from MODIS/Terra Collection 5 data by H. Yu.

### Box 2.2: Multi-angle Imaging SpectroRadiometer

MISR, aboard the sun-synchronous polar orbiting satellite Terra, measures upwelling solar radiance in four visible-near-IR spectral bands and at nine view angles spread out in the forward and aft directions along the flight path (Diner et al., 2002). It acquires global coverage about once per week. A wide range of along-track view angles makes it feasible to more accurately evaluate the surface contribution to the TOA radiances and hence retrieve aerosols over both ocean and land surfaces, including bright desert and sunglint regions (Diner et al., 1998; Martonchik et al., 1998a; 2002; Kahn et al., 2005a). MISR AODs are within 20% or  $\pm 0.05$  of coincident AERONET measurements (Kahn et al., 2005a; Abdou et al., 2005). The MISR multi-angle data also sample scattering angles ranging from about  $60^\circ$  to  $160^\circ$  in midlatitudes, yielding information about particle size (Kahn et al., 1998; 2001; 2005a; Chen et al., 2008) and shape (Kalashnikova and Kahn, 2006). The aggregate of aerosol microphysical properties can be used to aerosol air mass type, a more robust characterization of MISR-retrieved particle property information than individual attributes. MISR also retrieves plume height in the vicinity of wildfire, volcano, and mineral dust aerosol sources, where the plumes have discernable spatial contrast in the multi-angle imagery (Kahn et al., 2007a). **Figure 2.2** is an example that illustrates MISR's capability of characterizing the load, optical properties, and stereo height of near-source fire plumes.

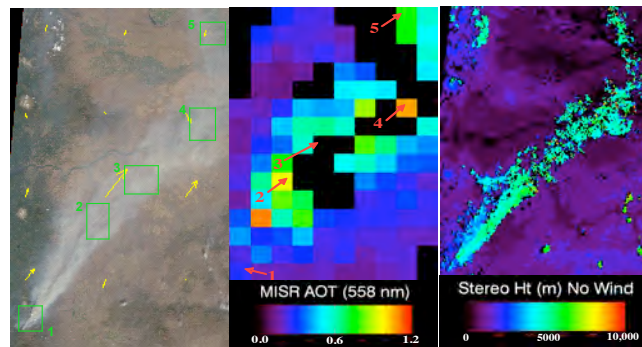


**Figure 2.2:** Oregon fire on September 4, 2003 as observed by MISR: (a) MISR nadir view of the fire plume, with five patch locations numbered and wind-vectors superposed in yellow; (b) MISR aerosol optical depth at 558 nm; and (c) MISR stereo height without wind correction for the same region (taken from Kahn et al., 2007a).

**Box 2.3: POLarization and Directionality of the Earth's Reflectance**

POLDER is a unique aerosol sensor that consists of wide field-of-view imaging spectro-radiometer capable of measuring multi-spectral, multi-directional, and polarized radiances (Deuzé et al., 2001). The observed radiances can be exploited to better separate the atmospheric contribution from the surface contribution over both land and ocean. POLDER -1 and -2 flew onboard the ADEOS (Advanced Earth Observing Satellite) from November 1996 to June 1997 and April to October of 2003, respectively. A similar POLDER instrument flies on the PARASOL satellite that was launched in December 2004.

**Figure 2.3** shows global horizontal patterns of AOD and Ångström exponent over the oceans derived from the POLDER instrument for June 1997. The oceanic AOD map (Figure 2.5.a) reveals near coastal plumes of high AOD, which decrease with distance from the coast. This pattern arises from aerosol emissions from the continents, followed by atmospheric dispersion, transformation, and removal in the downwind direction. In large-scale flow fields, such as the trade winds, these continental plumes persist over several thousand kilometers. The Ångström exponent shown in Figure 2.5.b exhibits a very different pattern from that of the aerosol optical depth; specifically, it exhibits high values downwind of industrialized regions and regions of biomass burning, indicative of small particles arising from direct emissions from combustion sources and/or gas-to-particle conversion, and low values associated with large particles in plumes of soil dust from deserts and in sea salt aerosols.

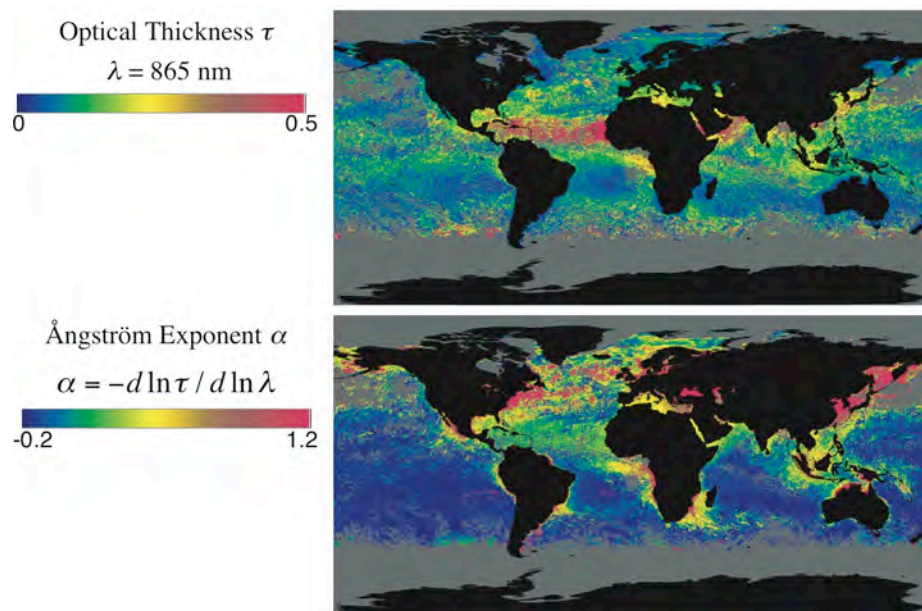


**Figure 2.3:** Global maps at 18 km resolution showing monthly average (a) AOD at 865 nm and (b) Ångström exponent of AOD over water surfaces only for June, 1997, derived from radiance measurements by the POLDER. Reproduced with permission of Laboratoire d'Optique Atmosphérique (LOA), Lille, FR; Laboratoire des Sciences du Climat et de l'Environnement (LSCE), Gif sur Yvette, FR; Centre National d'études Spatiales (CNES), Toulouse, FR; and National Space Development Agency (NASDA), Japan.



**Box 2.4: Clouds and the Earth’s Radiant Energy System**

CERES measures broadband solar and terrestrial radiances at three channels with a large footprint (e.g., 20 km for CERES/Terra) (Wielicki et al., 1996). It is collocated with MODIS and MISR aboard Terra and with MODIS on Aqua. The observed radiances are converted to the TOA irradiances or fluxes using the Angular Distribution Models (ADMs) as a function of viewing angle, sun angle, and scene type (Loeb and Kato, 2002; Zhang et al., 2005a; Loeb et al., 2005). Such estimates of TOA solar flux in clear-sky conditions can be compared to the expected flux for an aerosol-free atmosphere, in conjunction with measurements of aerosol optical depth from other sensors (e.g., MODIS, and MISR) to derive the aerosol direct radiative forcing (Loeb and Manalo-Smith, 2005; Zhang and Christopher, 2003; Zhang et al., 2005b; Christopher et al., 2006; Patadia et al., 2008). The derived instantaneous value is then scaled to obtain a daily average. A direct use of the coarse spatial resolution CERES measurements would exclude aerosol distributions in partly cloudy CERES scenes. Several approaches that incorporate coincident, high spatial and spectral resolution measurements (e.g., MODIS) have been employed to overcome this limitation (Loeb and Manalo-Smith, 2005; Zhang et al., 2005b).

1  
2 In summary, major advances have been made in both passive and active aerosol remote sensing  
3 from space in the past decade, providing better coverage, spatial resolution, retrieved AOD  
4 accuracy, and particle property information. However, AOD accuracy is still much poorer than  
5 that from surface-based sun photometers (0.01 to 0.02), even over vegetated land and dark water  
6 where retrievals are most reliable. Although there is some hope of approaching this level of  
7 uncertainty with a new generation of satellite instruments, the satellite retrievals entail additional  
8 sensitivities to aerosol and surface scattering properties. It seems unlikely that satellite remote  
9 sensing could exceed the sun photometer accuracy without introducing some as-yet-unspecified  
10 new technology. Space-based lidars are for the first time providing global constraints on aerosol  
11 vertical distribution, and multi-angle imaging is supplementing this with maps of plume injection  
12 height in aerosol source regions. Major advances have also been made during the past decade in  
13 distinguishing aerosol types from space, and the data are now useful for validating aerosol  
14 transport model simulations of aerosol air mass type distributions and transports, particularly  
15 over dark water. But particle size, shape, and especially SSA information has large uncertainty;  
16 improvements will be needed to better distinguish anthropogenic from natural aerosols using  
17 space-based retrievals. The particle microphysical property detail required to assess aerosol  
18 radiative forcing will come largely from targeted *in situ* and surface remote sensing  
19 measurements, at least for the near-future, although estimates of measurement-based aerosol RF  
20 can be made from judicious use of the satellite data with relaxed requirements for characterizing  
21 aerosol microphysical properties.  
22

### Box 2.5: Active Remote Sensing of Aerosols

Following a demonstration of lidar system aboard the U.S. Space Shuttle mission in 1994, i.e., Lidar In-space Technology Experiment (LITE) (Winker et al., 1996), the Geoscience Laser Altimeter System (GLAS) was launched in early 2003 to become the first polar orbiting satellite lidar. It provides global aerosol and cloud profiling for a one-month period out of every three-to-six months. It has been demonstrated that GLAS is capable of detecting and discriminating multiple layer clouds, atmospheric boundary layer aerosols, and elevated aerosol layers (e.g., Spinhirne et al., 2005). The Cloud-Aerosol Lidar and Infrared Pathfinder Satellite Observations (CALIPSO), launched on April 28, 2006, is carrying a lidar instrument (Cloud and Aerosol Lidar with Orthogonal Polarization - CALIOP) that has been collecting profiles of the attenuated backscatter at visible and near-infrared wavelengths along with polarized backscatter in the visible channel (Winker et al., 2003). CALIOP measurements have been used to derive the above-cloud fraction of aerosol extinction optical depth (Chand et al., 2008), one of the important factors determining aerosol direct radiative forcing in cloudy conditions. **Figure 2.4** shows an event of trans-Atlantic transport of Saharan dust captured by CALIPSO. Flying in formation with the Aqua, AURA, POLDER, and CloudSat satellites, the vertically resolved information is expected to greatly improve passive aerosol and cloud retrievals as well as allow the retrieval of vertical distributions of aerosol extinction, fine- and coarse-mode separately (Kaufman et al., 2003; Leon et al., 2003; Huneus and Boucher, 2007).

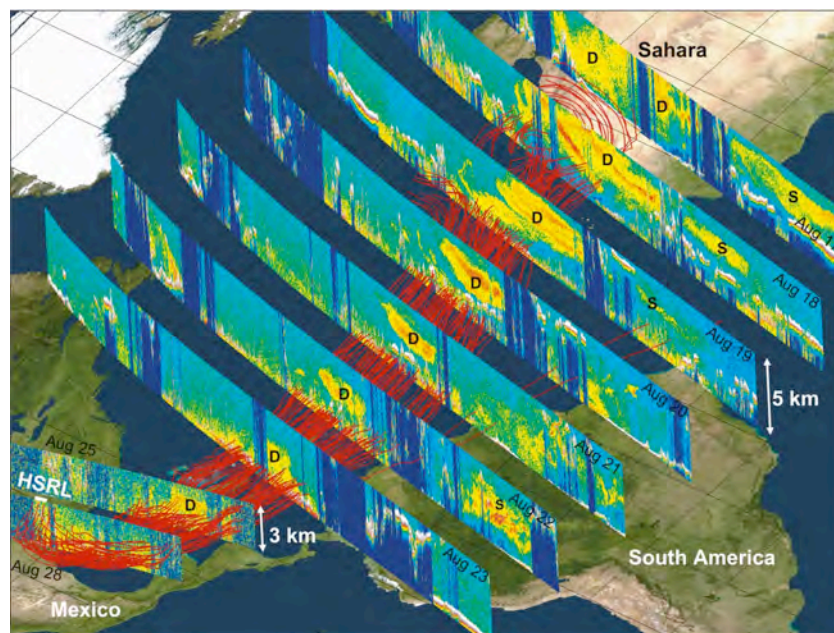
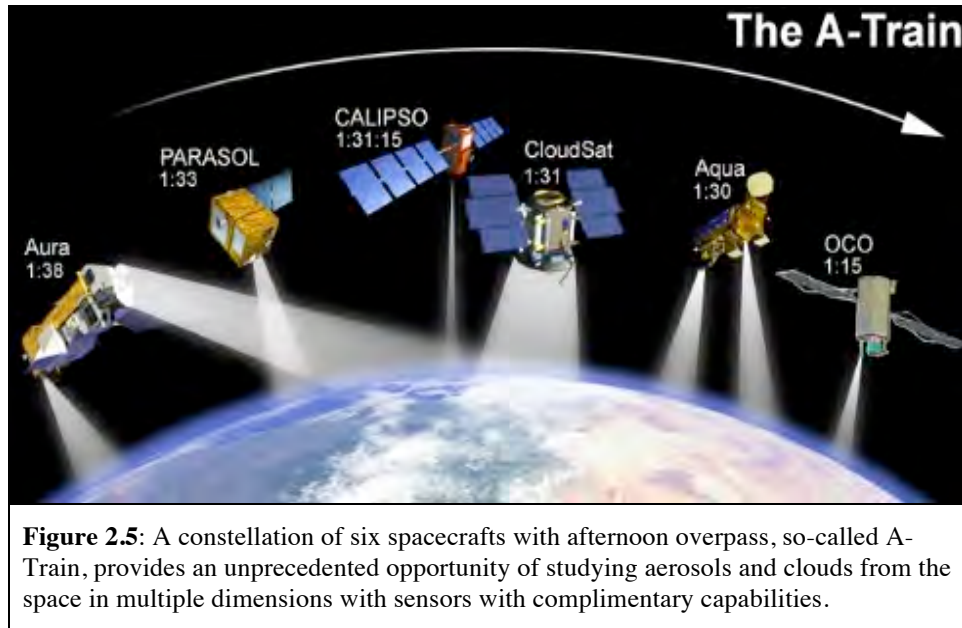


**Figure 2.4:** A dust event that originated in the Sahara desert on 17 August 2007 and was transported to the Gulf of Mexico. Red lines represent back trajectories indicating the transport track of the dust event. Vertical images are 532 nm attenuated backscatter coefficients measured by CALIOP when passing over the dust transport track. The letter “D” designates the dust layer, and “S” represents smoke layers from biomass burning in Africa (17–19 August) and South America (22 August). The track of the HSRL measurement is indicated by the white line superimposed on the 28 August CALIPSO image. The HSRL track is coincident with the track of the 28 August CALIPSO measurement off the coast of Texas between 28.75°N and 29.08°N (taken from Liu et al., 2008).

1  
2  
3  
4  
5



1

2 **2.2.2. Focused Field Campaigns**

3 Over the past two decades, numerous focused field campaigns have examined the physical,  
 4 chemical, and optical properties and radiative forcing of aerosols in a variety of aerosol regimes  
 5 around the world, as listed in **Table 2.2**. These campaigns, which have been designed with  
 6 aerosol characterization as the main goal or as one of the major themes in more interdisciplinary  
 7 studies, were conducted mainly over or downwind of known continental aerosol source regions,  
 8 but in some instances in low-aerosol regimes, for contrast. During each of these comprehensive  
 9 campaigns, aerosols were studied in great detail, using combinations of *in situ* and remote  
 10 sensing observations of physical and chemical properties from various platforms (e.g., aircraft,  
 11 ships, satellites, and ground-based stations) and numerical modeling. In spite of their relatively  
 12 short duration, these field studies have acquired comprehensive data sets of regional aerosol  
 13 properties that have been used to understand the properties and evolution of aerosols within the  
 14 atmosphere and to improve the climatology of aerosol microphysical properties used in satellite  
 15 retrieval algorithms and CTMs.

16 **2.2.3. Ground-based *In situ* Measurement Networks**

17 Major US-operated surface *in situ* and remote sensing networks for tropospheric aerosol  
 18 characterization and climate forcing research are listed in **Table 2.3**. These surface *in situ*  
 19 stations provide information about long-term changes and trends in aerosol concentrations and  
 20 properties, the influence of regional sources on aerosol properties, climatologies of aerosol  
 21 radiative properties, and data for testing models (e.g., Quinn et al., 2000; Quinn et al., 2002;  
 22 Delene and Ogren, 2002; Sheridan and Ogren, 1999; Fiebig and Ogren, 2006; Bates et al., 2006;  
 23 Quinn et al., 2007) and satellite aerosol retrievals. The NOAA Earth System Research  
 24 Laboratory (ESRL) aerosol monitoring network consists of baseline, regional, and mobile  
 25 stations. These near-surface measurements include submicrometer and sub-10 micrometer  
 26 scattering and absorption coefficients from which the extinction coefficient and single-scattering  
 27 albedo can be derived. Additional measurements include particle concentration and, at selected  
 28 sites, CCN concentration, the hygroscopic growth factor, and chemical composition.

**Table 2.2.** List of major intensive field experiments that are relevant to aerosol research in a variety of aerosol regimes around the globe conducted in the past two decades (updated from Yu et al., 2006).

Aerosol Regimes	Intensive Field Experiments			Major References
	Name	Location	Time Period	
Anthropogenic aerosol and boreal forest from North America and West Europe	TARFOX	North Atlantic	July, 1996	Russell et al., 1999
	NEAQS	North Atlantic	July – August, 2002	Quinn and Bates, 2003
	SCAR-A	North America	1993	Remer et al., 1997
	CLAMS	East Coast of U.S.	July-August, 2001	Smith et al., 2005
	INTEX-NA, ICARTT	North America	Summer 2004	Fehsenfeld et al., 2006
	DOE AIOP	northern Oklahoma	May 2003	Ferrare et al., 2006
	MILAGRO	Mexico city, Mexico	March 2006	Molina et al., 2008
	TexAQS/GoM ACCS	Texas and Gulf of Mexico	August-September 2006	Jiang et al., 2008; Lu et al., 2008
	ARCTAS	North-central Alaska to Greenland (Arctic haze)	March-April 2008	<a href="http://www.espo.nasa.gov/arctas/">http://www.espo.nasa.gov/arctas/</a>
	ARCTAS	Northern Canada (smoke)	June-July 2008	
	ACE-2	North Atlantic	June – July, 1997	Raes et al., 2000
	MINOS	Mediterranean region	July - August, 2001	Lelieveld et al., 2002
	LACE98	Lindberg, Germany	July-August, 1998	Ansmann et al., 2002
	Aerosols99	Atlantic	January - February, 1999	Bates et al., 2001
Brown Haze in South Asia	INDOEX	Indian subcontinent and Indian Ocean	January - April, 1998 and 1999	Ramanathan et al., 2001b
	ABC	South and East Asia	ongoing	Ramanathan and Crutzen, 2003
Anthropogenic aerosol and desert dust mixture from East Asia	EAST-AIRE	China	March-April, 2005	Li et al., 2007
	INTEX-B	northeastern Pacific	April 2006	Singh et al., 2008
	ACE-Asia	East Asia and Northwest Pacific	April, 2001	Huebert et al., 2003; Seinfeld et al., 2004
	TRACE-P		March - April, 2001	Jacob et al., 2003
	PEM-West A & B	Western Pacific off East Asia	September-October, 1991 February-March, 1994	Hoell et al., 1996; 1997
Biomass burning smoke in the tropics	BASE-A	Brazil	1989	Kaufman et al., 1992
	SCAR-B	Brazil	August - September, 1995	Kaufman et al., 1998
	LBA-SMOCC	Amazon basin	September-November 2002	Andreae et al., 2004
	SAFARI2000	South Africa and South Atlantic	August - September, 2000	King et al., 2003
	SAFARI92		September – October, 1992	Lindesay et al., 1996
	TRACE-A	South Atlantic	September-October, 1992	Fishman et al., 1996
	DABEX	West Africa	Januray-February, 2006	Haywood et al., 2008
Mineral dusts from North Africa and Arabian Peninsula	SAMUM	Southern Morocco	May-June, 2006	Heintzenberg et al., 2009
	SHADE	West coast of North Africa	September, 2000	Tanré et al., 2003
	PRIDE	Puerto Rico	June – July, 2000	Reid et al., 2003
	UAE <sup>2</sup>	Arabian Peninsula	August - September, 2004	Reid et al., 2008
Remote Oceanic Aerosol	ACE-1	Southern Oceans	December, 1995	Bates et al., 1998; Quinn and Coffman, 1998

1 Several of the stations, which are located across North America and world-wide, are in regions  
 2 where recent focused field campaigns have been conducted. The measurement protocols at the  
 3 stations are similar to those used during the field campaigns. Hence, the station data are directly  
 4 comparable to the field campaign data so that they provide a longer-term measure of mean  
 5 aerosol properties and their variability, as well as a context for the shorter-duration  
 6 measurements of the field campaigns.

**Table 2.3:** Summary of major US surface *in situ* and remote sensing networks for the tropospheric aerosol characterization and radiative forcing research. All the reported quantities are column-integrated or column-effective, except as indicated.

Surface Network		Measured/derived parameters				Spatial coverage	Temporal coverage
		Loading	Size, shape	Absorption	Chemistry		
<i>In Situ</i>	NOAA ESRL aerosol monitoring ( <a href="http://www.esrl.noaa.gov/gmd/aero/">http://www.esrl.noaa.gov/gmd/aero/</a> )	near-surface extinction coefficient, optical depth, CN/CCN number concentrations	Angstrom exponent, hemispheric backscatter fraction, asymmetry factor, hygroscopic growth	single-scattering albedo, absorption coefficient	chemical composition in selected sites and periods	5 baseline stations, several regional stations, aircraft and mobile platforms	1976 onward
	NPS/EPA IMPROVE ( <a href="http://vista.cira.colostate.edu/improve/">http://vista.cira.colostate.edu/improve/</a> )	near-surface mass concentrations and derived extinction coefficients by species	fine and coarse separately	single-scattering albedo, absorption coefficient	ions, ammonium sulfate, ammonium nitrate, organics, elemental carbon, fine soil	156 national parks and wilderness areas in the U.S.	1988 onward
Remote Sensing	NASA AERONET ( <a href="http://aeronet.gsfc.nasa.gov">http://aeronet.gsfc.nasa.gov</a> )	optical depth	fine-mode fraction, Angstrom exponents, asymmetry factor, phase function, non-spherical fraction	single-scattering albedo, absorption optical depth, refractive indices	N/A	~200 sites over global land and islands	1993 onward
	DOE ARM ( <a href="http://www.arm.gov">http://www.arm.gov</a> )					6 sites and 1 mobile facility in North America, Europe, and Asia	1989 onward
	NOAA SURFRAD ( <a href="http://www.srrb.noaa.gov/surfrad/">http://www.srrb.noaa.gov/surfrad/</a> )		N/A	N/A	N/A	7 sites in the US	1995 onward
	AERONET- MAN ( <a href="http://aeronet.gsfc.nasa.gov/maritime_aerosol_network.html">http://aeronet.gsfc.nasa.gov/maritime_aerosol_network.html</a> )		N/A	N/A	N/A	global ocean	2004-present (periodically)
	NASA MPLNET ( <a href="http://mplnet.gsfc.nasa.gov/">http://mplnet.gsfc.nasa.gov/</a> )	vertical profiles of backscatter /extinction coefficient	N/A	N/A	N/A	~30 sites in major continents, usually collocated with AERONET and ARM sites	2000 onward

1 The Interagency Monitoring of Protected Visual Environment (*IMPROVE*), which is operated by  
2 the National Park Service Air Resources Division, has stations across the US located within  
3 national parks (Malm et al., 1994). Although the primary focus of the network is air pollution,  
4 the measurements are also relevant to climate forcing research. Measurements include fine and  
5 coarse mode (PM<sub>2.5</sub> and PM<sub>10</sub>) aerosol mass concentration; concentrations of elements, sulfate,  
6 nitrate, organic carbon, and elemental carbon; and scattering coefficients.

7 In addition, to these US-operated networks, there are other national and international surface  
8 networks that provide measurements of aerosol properties including, but not limited to, the  
9 World Meteorological Organization (WMO) Global Atmospheric Watch (GAW) network  
10 (<http://www.wmo.int/pages/prog/arep/gaw/monitoring.html>), the European Monitoring and  
11 Evaluation Programme (EMEP) (<http://www.emep.int/>), the Canadian Air and Precipitation  
12 Monitoring Network (CAPMoN) ([http://www.msc-smc.ec.gc.ca/capmon/index\\_e.cfm](http://www.msc-smc.ec.gc.ca/capmon/index_e.cfm)), and the  
13 Acid Deposition Monitoring Network in East Asia (EANET) (<http://www.eanet.cc/eanet.html>).

#### 14 **2.2.4. In situ Aerosol Profiling Programs**

15 In addition to long-term ground based measurements, regular long-term aircraft *in situ*  
16 measurements recently have been implemented at several locations. These programs provide a  
17 statistically significant data set of the vertical distribution of aerosol properties to determine  
18 spatial and temporal variability through the vertical column and the influence of regional sources  
19 on that variability. In addition, the measurements provide data for satellite and model validation.  
20 As part of its long-term ground measurements, NOAA has conducted regular flights over  
21 Bondville, Illinois since 2006. Measurements include light scattering and absorption coefficients,  
22 the relative humidity dependence of light scattering, aerosol number concentration and size  
23 distribution, and chemical composition. The same measurements with the exception of number  
24 concentration, size distribution, and chemical composition were made by NOAA during regular  
25 overflights of DOE ARM's Southern Great Plains (SGP) site from 2000 to 2007 (Andrews et al.,  
26 2004) (<http://www.esrl.noaa.gov/gmd/aero/net/index.html>).

27 In summary of sections 2.2.2, 2.2.3, and 2.2.4, *in situ* measurements of aerosol properties have  
28 greatly expanded over the past two decades as evidenced by the number of focused field  
29 campaigns in or downwind of aerosol source regions all over the globe, the continuation of  
30 existing and implementation of new sampling networks worldwide, and the implementation of  
31 regular aerosol profiling measurements from fixed locations. In addition, *in situ* measurement  
32 capabilities have undergone major advancements during this same time period. These  
33 advancements include the ability to measure aerosol chemical composition as a function of size  
34 at a time resolution of seconds to minutes (e.g., Jayne et al., 2000), the development of  
35 instruments able to measure aerosol absorption and extinction coefficients at high sensitivity and  
36 time resolution and as a function of relative humidity (e.g., Baynard et al., 2007; Lack et al.,  
37 2006), and the deployment of these instruments across the globe on ships, at ground-based sites,  
38 and on aircraft. However, further advances are needed to make this newly developed  
39 instrumentation more affordable and turn-key so that it can be deployed more widely to  
40 characterize aerosol properties at a variety of sites world-wide.

#### 41 **2.2.5. Ground-based Remote Sensing Measurement Networks**

42 The Aerosol Robotic Network (*AERONET*) program is a federated ground-based remote sensing  
43 network of well-calibrated sun photometers and radiometers (<http://aeronet.gsfc.nasa.gov>).

1 AERONET includes about 200 sites around the world, covering all major tropospheric aerosol  
2 regimes (Holben et al., 1998; 2001), as illustrated in **Figure 2.6**. Spectral measurements of sun  
3 and sky radiance are calibrated and screened for cloud-free conditions (Smirnov et al., 2000).  
4 AERONET stations provide direct, calibrated measurements of spectral *AOD* (normally at  
5 wavelengths of 440, 670, 870, and 1020 nm) with an accuracy of  $\pm 0.015$  (Eck et al. 1999). In  
6 addition, inversion-based retrievals of a variety of effective, column-mean properties have been  
7 developed, including aerosol single-scattering albedo, size distributions, fine-mode fraction,  
8 degree of non-sphericity, phase function, and asymmetry factor (Dubovik et al., 2000; Dubovik  
9 and King, 2000; Dubovik et al., 2002; O'Neill, et al., 2004). The SSA can be retrieved with an  
10 accuracy of  $\pm 0.03$ , but only for *AOD*  $> 0.4$  (Dubovik et al., 2002), which precludes much of the  
11 planet. These retrieved parameters have been validated or are undergoing validation by  
12 comparison to *in situ* measurements (e.g., Haywood et al., 2003; Magi et al., 2005; Leahy et al.,  
13 2007).

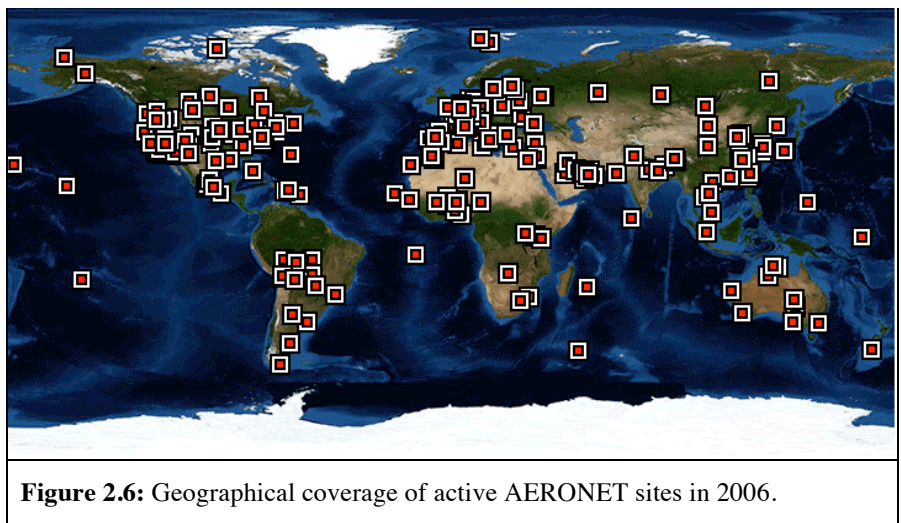


**Figure 2.6:** Geographical coverage of active AERONET sites in 2006.

- 14  
15 Recent developments associated with AERONET algorithms and data products include:
- 16 • simultaneous retrieval of aerosol and surface properties using combined AERONET and  
17 satellite measurements (Sinyuk et al., 2007) with surface reflectance taken into account  
18 (which significantly improves AERONET SSA retrieval accuracy) (Eck et al., 2008);
  - 19 • the addition of ocean color and high frequency solar flux measurements; and
  - 20 • the establishment of the Maritime Aerosol Network (MAN) component to monitor  
21 aerosols over the World oceans from ships-of-opportunity (Smirnov et al., 2006).

22 Because of consistent calibration, cloud-screening, and retrieval methods, uniformly acquired  
23 and processed data are available from all stations, some of which have operated for over 10  
24 years. These data constitute a high-quality, ground-based aerosol climatology and, as such, have  
25 been widely used for aerosol process studies as well as for evaluation and validation of model  
26 simulation and satellite remote sensing applications (e.g., Chin et al., 2002; Yu et al., 2003,  
27 2006; Remer et al., 2005; Kahn et al., 2005a). In addition, AERONET retrievals of aerosol size  
28 distribution and refractive indices have been used in algorithm development for satellite sensors  
29 (Remer et al., 2005; Levy et al., 2007a). A set of aerosol optical properties provided by  
30 AERONET has been used to calculate the aerosol direct radiative forcing (Procopio et al., 2004;

1 Zhou et al., 2005), which can be used to evaluate both satellite remote sensing measurements and  
2 model simulations.

3 AERONET measurements are complemented by other ground-based aerosol networks having  
4 less geographical or temporal coverage, such as the Atmospheric Radiation Measurement (ARM)  
5 network (Ackerman and Stokes, 2003), NOAA's national surface radiation budget network  
6 (SURFRAD) (Augustine et al., 2008) and other networks with multifilter rotating shadowband  
7 radiometer (*MFRSR*) (Harrison et al., 1994; Michalsky et al., 2001), and several lidar networks  
8 including

- 9 • NASA Micro Pulse Lidar Network (*MPLNET*) (Welton et al., 2001; 2002);
- 10 • Regional East Atmospheric Lidar Mesonet (*REALM*) in North America (Hoff et al., 2002;  
11 2004);
- 12 • European Aerosol Research Lidar Network (*EARLINET*) (Matthias et al., 2004); and
- 13 • Asian Dust Network (*AD-Net*) (e.g., Murayama et al., 2001).

14 Obtaining accurate aerosol extinction profile observations is pivotal to improving aerosol  
15 radiative forcing and atmospheric response calculations. The values derived from these lidar  
16 networks with state-of-the-art techniques (Schmid et al., 2006) are helping to fill this need.

### 17 **2.2.6. Synergy of Measurements and Model Simulations**

18 Individual approaches discussed above have their own strengths and limitations, and are usually  
19 complementary. None of these approaches alone is adequate to characterize large spatial and  
20 temporal variations of aerosol physical and chemical properties and to address complex aerosol-  
21 climate interactions. The best strategy for characterizing aerosols and estimating their radiative  
22 forcing is to integrate measurements from different satellite sensors with complementary  
23 capabilities from *in situ* and surface-based measurements. Similarly, while models are essential  
24 tools for estimating regional and global distributions and radiative forcing of aerosols at present  
25 as well as in the past and the future, observations are required to provide constraints and  
26 validation of the models. In the following, several synergistic approaches to studying aerosols  
27 and their radiative forcing are discussed.

28 **Closure experiments:** During intensive field studies, multiple platforms and instruments are  
29 deployed to sample regional aerosol properties through a well-coordinated experimental design.  
30 Often, several independent methods are used to measure or derive a single aerosol property or  
31 radiative forcing. This combination of methods can be used to identify inconsistencies in the  
32 methods and to quantify uncertainties in measured, derived, and calculated aerosol properties and  
33 radiative forcings. This approach, often referred to as a closure experiment, has been widely  
34 employed on both individual measurement platforms (local closure) and in studies involving  
35 vertical measurements through the atmospheric column by one or more platforms (column  
36 closure) (Quinn et al., 1996; Russell et al., 1997).

37 Past closure studies have revealed that the best agreement between methods occurs for  
38 submicrometer, spherical particles such that different measures of aerosol optical properties and  
39 optical depth agree within 10 to 15% and often better (e.g., Clarke et al., 1996; Collins et al.,  
40 2000; Schmid et al., 2000; Quinn et al., 2004). Larger particle sizes (e.g., sea salt and dust)  
41 present inlet collection efficiency issues and non-spherical particles (e.g., dust) lead to  
42 differences in instrumental responses. In these cases, differences between methods for



1 determining aerosol optical depth can be as great as 35% (e.g., Wang et al., 2003; Doherty et al.,  
2 2005). Closure studies on aerosol clear-sky DRF reveal uncertainties of about 25% for  
3 sulfate/carbonaceous aerosol and 60% for dust-containing aerosol (Bates et al., 2006). Future  
4 closure studies could integrate surface- and satellite-based radiometric measurements of AOD  
5 with *in situ* optical, microphysical, and aircraft radiometric measurements for a wide range of  
6 situations. There is also a need to maintain consistency in comparing results and expressing  
7 uncertainties (Bates et al., 2006).

8 **Constraining models with *in situ* measurements:** *In situ* measurements of aerosol chemical,  
9 microphysical, and optical properties with known accuracy, based in part on closure studies, can  
10 be used to constrain regional CTM simulations of aerosol direct forcing, as described by Bates et  
11 al. (2006). A key step in the approach is assigning empirically derived optical properties to the  
12 individual chemical components generated by the CTM for use in a Radiative Transfer Model  
13 (RTM). Specifically, regional data from focused, short-duration field programs can be segregated  
14 according to aerosol type (sea salt, dust, or sulfate/carbonaceous) based on measured chemical  
15 composition and particle size. Corresponding measured optical properties can be carried along in  
16 the sorting process so that they, too, are segregated by aerosol type. The empirically derived  
17 aerosol properties for individual aerosol types, including mass scattering efficiency, single-  
18 scattering albedo, and asymmetry factor, and their dependences on relative humidity, can be used  
19 in place of assumed values in CTMs.

20 Short-term, focused measurements of aerosol properties (e.g., aerosol concentration and AOD)  
21 also can be used to evaluate CTM parameterizations on a regional basis, to suggest  
22 improvements to such uncertain model parameters, such as emission factors and scavenging  
23 coefficients (e.g., Koch et al., 2007). Improvements in these parameterizations using  
24 observations yield increasing confidence in simulations covering regions and periods where and  
25 when measurements are not available. To evaluate the aerosol properties generated by CTMs on  
26 broader scales in space and time, satellite observations and long-term *in situ* measurements are  
27 required.

28 **Improving model simulations with satellite measurements:** Global measurements of aerosols  
29 from satellites (mainly AOD) with well-defined accuracies offer an opportunity to evaluate  
30 model simulations at large spatial and temporal scales. The satellite measurements can also be  
31 used to constrain aerosol model simulations and hence the assessment of aerosol DRF through  
32 data assimilation or objective analysis process (e.g., Collins et al., 2001; Yu et al., 2003; 2004,  
33 2006; Liu et al., 2005; Zhang et al., 2008). Both satellite retrievals and model simulations have  
34 uncertainties. The goal of data integration is to minimize the discrepancies between them, and to  
35 form an optimal estimate of aerosol distributions by combining them, typically with weights  
36 inversely proportional to the square of the errors of individual descriptions. Such integration can  
37 fill gaps in satellite retrievals and generate global distributions of aerosols that are consistent  
38 with ground-based measurements (Collins et al., 2001; Yu et al., 2003, 2006; Liu et al., 2005).  
39 Recent efforts have also focused on retrieving global sources of aerosol from satellite  
40 observations using inverse modeling, which may be valuable for reducing large aerosol  
41 simulation uncertainties (Dubovik et al., 2007). Model refinements guided by model evaluation  
42 and integration practices with satellite retrievals can then be used to improve aerosol simulations  
43 of the pre- and post-satellite eras.

1 Current measurement-based understanding of aerosol characterization and radiative forcing is  
2 assessed in Section 2.3 through inter-comparisons of a variety of measurement-based estimates  
3 and model simulations published in literature. This is followed by a detailed discussion of major  
4 outstanding issues in section 2.4.

## 5 **2.3. Assessments of Aerosol Characterization and Climate** 6 **Forcing**

7 This section focuses on the assessment of measurement-based aerosol characterization and its  
8 use in improving estimates of the direct radiative forcing on regional and global scales. *In situ*  
9 measurements provide highly accurate aerosol chemical, microphysical, and optical properties on  
10 a regional basis and for the particular time period of a given field campaign. Remote sensing  
11 from satellites and ground-based networks provide spatial and temporal coverage that intensive  
12 field campaigns lack. Both *in situ* measurements and remote sensing have been used to  
13 determine key parameters for estimating aerosol direct radiative forcing including aerosol single  
14 scattering albedo, asymmetry factor, optical depth. Remote sensing has also been providing  
15 simultaneous measurements of aerosol optical depth and radiative fluxes that can be combined to  
16 derive aerosol direct radiative forcing at the TOA with relaxed requirement for characterizing  
17 aerosol properties. Progress in using both satellite and surface-based measurements to study  
18 aerosol-cloud interactions and aerosol indirect forcing is also discussed.

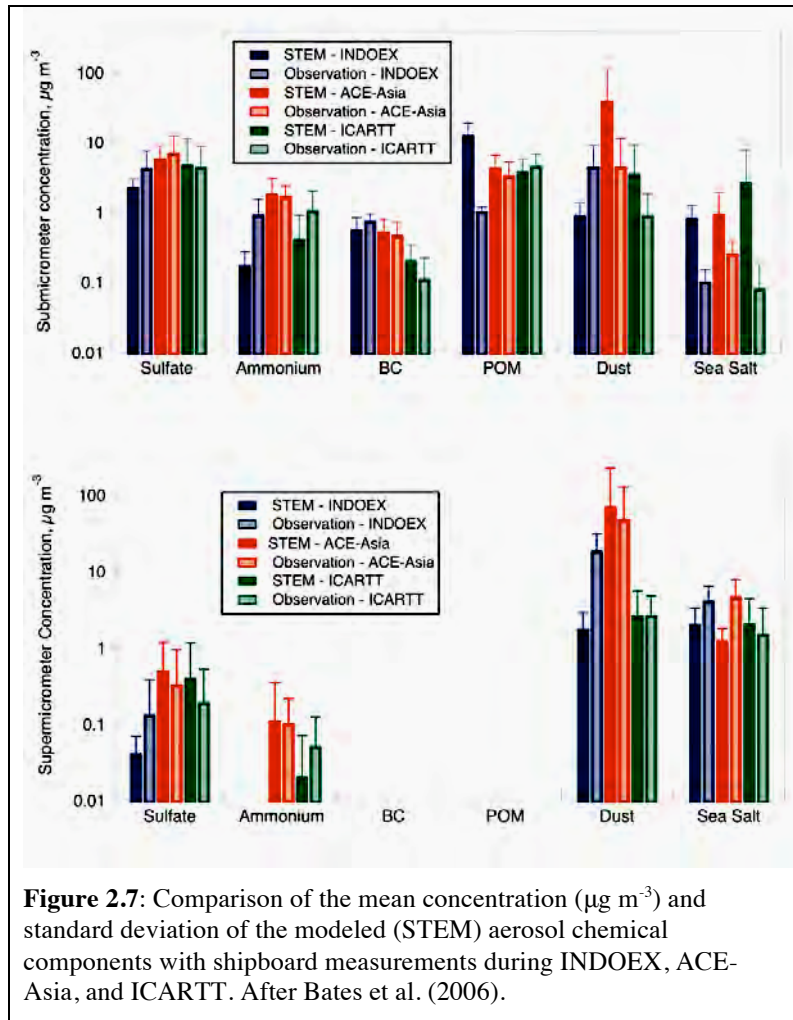
### 19 **2.3.1. The Use of Measured Aerosol Properties to Improve Models**

20 The wide variety of aerosol data sets from intensive field campaigns provides a rigorous  
21 “testbed” for model simulations of aerosol properties and distributions and estimates of DRF. As  
22 described in Section 2.2.6, *in situ* measurements can be used to constrain regional CTM  
23 simulations of aerosol properties, DRF, anthropogenic component of DRF, and to evaluate CTM  
24 parameterizations. In addition, *in situ* measurements can be used to develop simplifying  
25 parameterizations for use by CTMs.

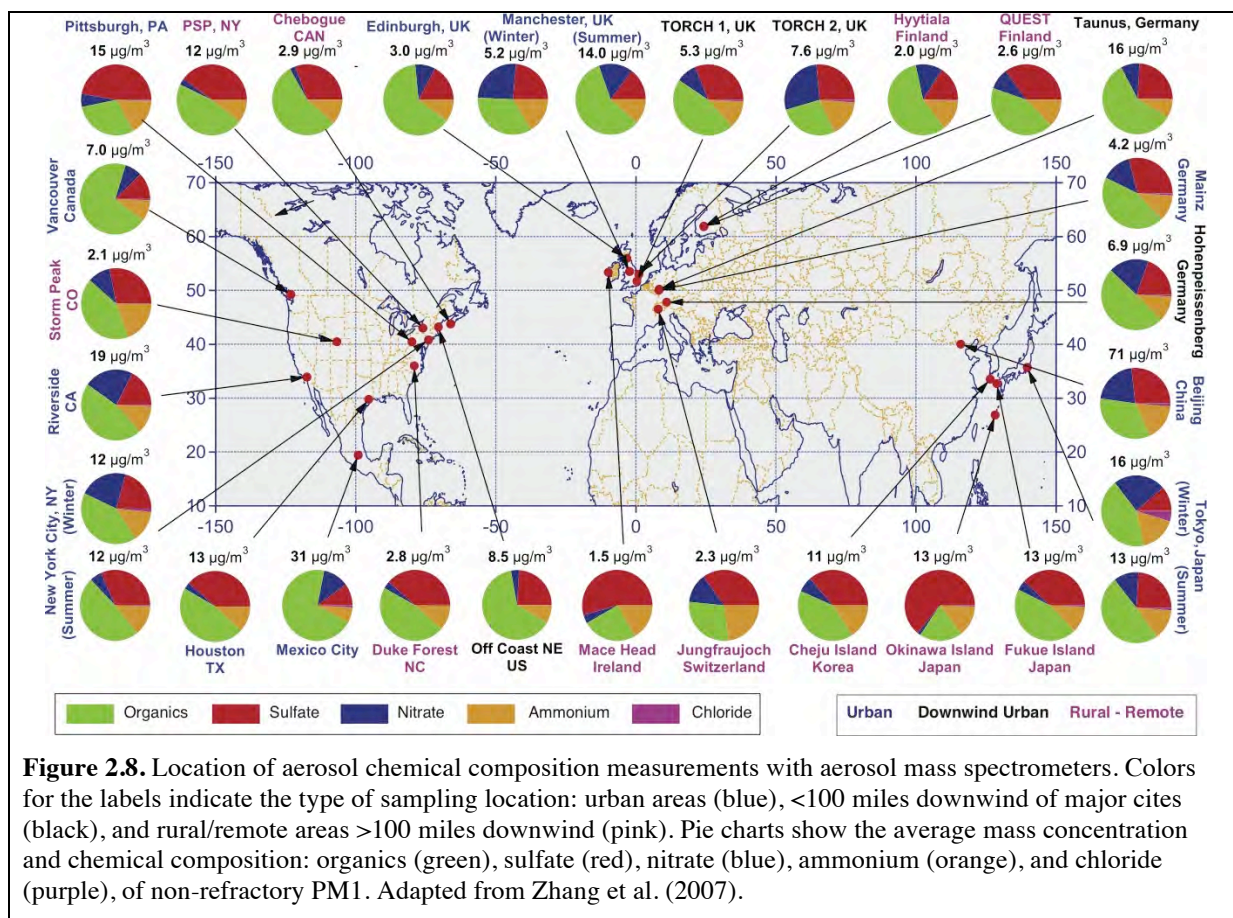
26 Several factors contribute to the uncertainty of CTM calculations of size-distributed aerosol  
27 composition including emissions, aerosol removal by wet deposition, processes involved in the  
28 formation of secondary aerosols and the chemical and microphysical evolution of aerosols,  
29 vertical transport, and meteorological fields including the timing and amount of precipitation,  
30 formation of clouds, and relative humidity. *In situ* measurements made during focused field  
31 campaigns provide a point of comparison for the CTM-generated aerosol distributions at the  
32 surface and at discrete points above the surface. Such comparisons are essential for identifying  
33 areas where the models need improvement.

34 **Figure 2.7** shows a comparison of submicrometer and supermicrometer aerosol chemical  
35 components measured during INDOEX, ACE-Asia, and ICARTT onboard a ship and the same  
36 values calculated with the Sulfate Transport and dEposition Model (*STEM*) (e.g., Carmichael et  
37 al., 2002, 2003; Tang et al., 2003, 2004; Bates et al., 2004; Streets et al., 2006b). To permit direct  
38 comparison of the measured and modeled values, the model was driven by analyzed  
39 meteorological data and sampled at the times and locations of the shipboard measurements every  
40 30 min along the cruise track. The best agreement was found for submicrometer sulfate and BC.  
41 The agreement was best for sulfate; this is attributed to greater accuracy in emissions, chemical  
42 conversion, and removal for this component. Underestimation of dust and sea salt is most likely

1 due to errors in model-calculated emissions. Large discrepancies between the modeled and  
 2 measured values occurred for submicrometer particulate organic matter (POM) (INDOEX), and  
 3 for particles in the supermicrometer size range such as dust (ACE-Asia), and sea salt (all  
 4 regions). The model underestimated the total mass of the supermicrometer aerosol by about a  
 5 factor of 3.

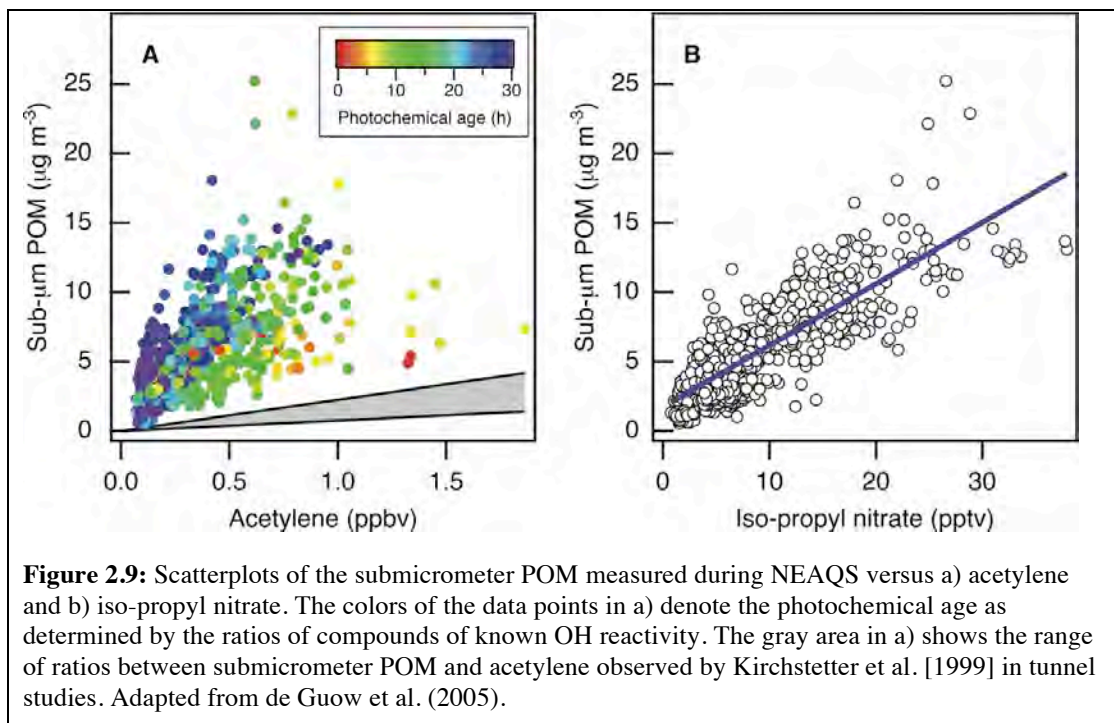


6  
 7  
 8 POM makes up a large and variable fraction of aerosol mass throughout the anthropogenically  
 9 influenced northern hemisphere, and yet models have severe problems in properly representing  
 10 this type of aerosol. Much of this discrepancy follows from the models inability to represent the  
 11 formation of secondary organic aerosols (SOA) from the precursor volatile organic compounds  
 12 (VOC). **Figure 2.8** shows a summary of the results from aerosol mass spectrometer  
 13 measurements at 30 sites over North America, Europe, and Asia Based on aircraft measurements  
 14 of urban-influenced air over New England, de Gouw et al. (2005) found that POM was highly  
 15 correlated with secondary anthropogenic gas phase species suggesting that the POM was derived  
 16 from secondary anthropogenic sources and that the formation took one day or more.



1

2 **Figure 2.9** shows scatterplots of submicrometer POM versus acetylene (a gas phase primary  
3 emitted VOC species) and isopropyl nitrate (a secondary gas phase organic species formed by  
4 atmospheric reactions). The increase in submicrometer POM with increasing photochemical age  
5 could not be explained by the removal of VOC alone, which are its traditionally recognized  
6 precursors. This result suggests that other species must have contributed and/or that the  
7 mechanism for POM formation is more efficient than assumed by models. Similar results were  
8 obtained from the 2006 MILAGRO field campaign conducted in Mexico City (Kleinman et al.,  
9 2008), and comparisons of GCM results with several long-term monitoring stations also showed  
10 that the model underestimated organic aerosol concentrations (Koch et al., 2007). Recent  
11 laboratory work suggests that isoprene may be a major SOA source missing from previous  
12 atmospheric models (Kroll et al., 2006; Henze and Seinfeld, 2006), but underestimating sources  
13 from certain economic sectors may also play a role (Koch et al., 2007). Models also have  
14 difficulty in representing the vertical distribution of organic aerosols, underpredicting their  
15 occurrence in the free troposphere (FT) (Heald et al., 2005). While organic aerosol presents  
16 models with some of their greatest challenges, even the distribution of well-characterized sulfate  
17 aerosol is not always estimated correctly in models (Shindell et al., 2008a).



1  
2 Comparisons of DRF and its anthropogenic component calculated with assumed optical  
3 properties and values constrained by *in situ* measurements can help identify areas of uncertainty  
4 in model parameterizations. In a study described by Bates et al. (2006), two different CTMs  
5 (MOZART and STEM) were used to calculate dry mass concentrations of the dominant aerosol  
6 species (sulfate, organic carbon, black carbon, sea salt, and dust). *In situ* measurements were  
7 used to calculate the corresponding optical properties for each aerosol type for use in a radiative  
8 transfer model. Aerosol DRF and its anthropogenic component estimated using the empirically  
9 derived and a priori optical properties were then compared. The DRF and its anthropogenic  
10 component were calculated as the net downward solar flux difference between the model state  
11 with aerosol and of the model state with no aerosol. It was found that the constrained optical  
12 properties derived from measurements increased the calculated AOD ( $34 \pm 8\%$ ), TOA DRF ( $32$   
13  $\pm 12\%$ ), and anthropogenic component of TOA DRF ( $37 \pm 7\%$ ) relative to runs using the *a priori*  
14 values. These increases were due to larger values of the constrained mass extinction efficiencies  
15 relative to the *a priori* values. In addition, differences in AOD due to using the aerosol loadings  
16 from MOZART versus those from STEM were much greater than differences resulting from the  
17 *a priori* vs. constrained RTM runs.

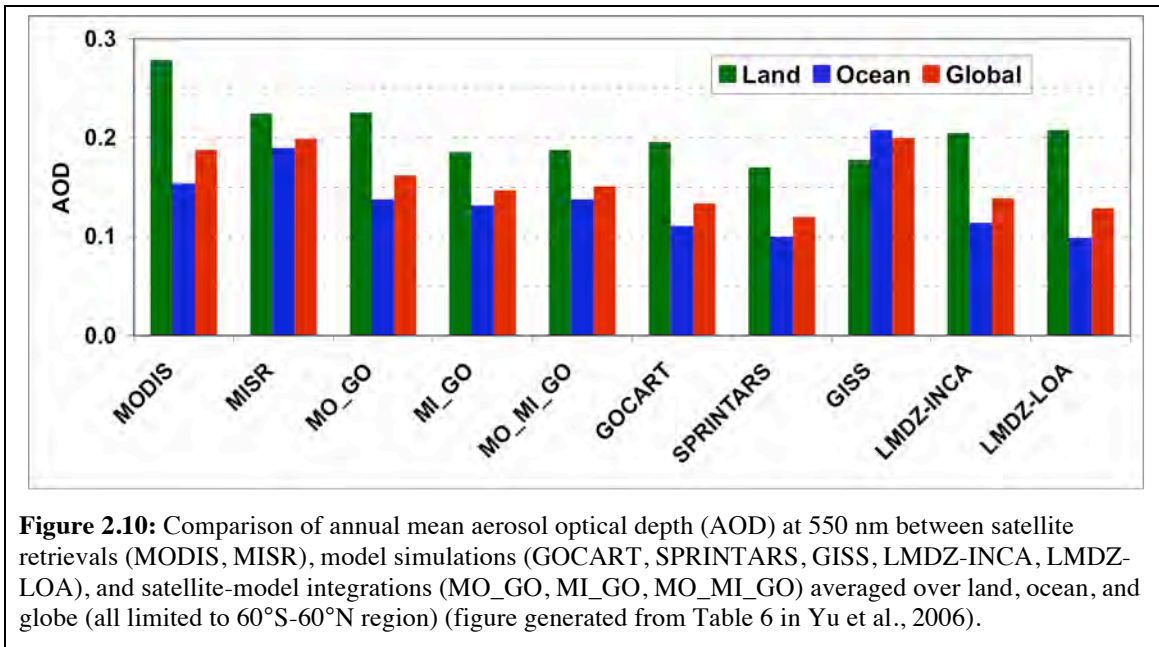
18 *In situ* observations also can be used to generate simplified parameterizations for CTMs and  
19 RTMs thereby lending an empirical foundation to uncertain parameters currently in use by  
20 models. CTMs generate concentration fields of individual aerosol chemical components that are  
21 then used as input to radiative transfer models (RTMs) for the calculation of DRF. Currently,  
22 these calculations are performed with a variety of simplifying assumptions concerning the RH  
23 dependence of light scattering by the aerosol. Chemical components often are treated as  
24 externally mixed each with a unique RH dependence of light scattering. However, both model  
25 and measurement studies reveal that POM, internally mixed with water-soluble salts, can reduce  
26 the hygroscopic response of the aerosol, which decreases its water content and ability to scatter

1 light at elevated relative humidity (e.g., Saxena et al., 1995; Carrico et al., 2005). The complexity  
2 of the POM composition and its impact on aerosol optical properties requires the development of  
3 simplifying parameterizations that allow for the incorporation of information derived from field  
4 measurements into calculations of DRF (Quinn et al., 2005). Measurements made during  
5 INDOEX, ACE-Asia, and ICARTT revealed a substantial decrease in  $f_{\text{osp}}(RH)$  with increasing  
6 mass fraction of POM in the accumulation mode. Based on these data, a parameterization was  
7 developed that quantitatively describes the relationship between POM mass fraction and  $f_{\text{osp}}(RH)$   
8 for accumulation mode sulfate-POM mixtures (Quinn et al., 2005). This simplified  
9 parameterization may be used as input to RTMs to derive values of  $f_{\text{osp}}(RH)$  based on CTM  
10 estimates of the POM mass fraction. Alternatively, the relationship may be used to assess values  
11 of  $f_{\text{osp}}(RH)$  currently being used in RTMs.

### 12 **2.3.2. Intercomparisons of Satellite Measurements and Model Simulation of** 13 **Aerosol Optical Depth**

14 Given the fact that DRF is highly dependent on the amount of aerosol present, it is of first-order  
15 importance to improve the spatial characterization of AOD on a global scale. This requires an  
16 evaluation of the various remote sensing AOD data sets and comparison with model-based AOD  
17 estimates. The latter comparison is particularly important if models are to be used in projections  
18 of future climate states that would result from assumed future emissions. Both remote sensing  
19 and model simulation have uncertainties and satellite-model integration is needed to obtain an  
20 optimum description of aerosol distribution.

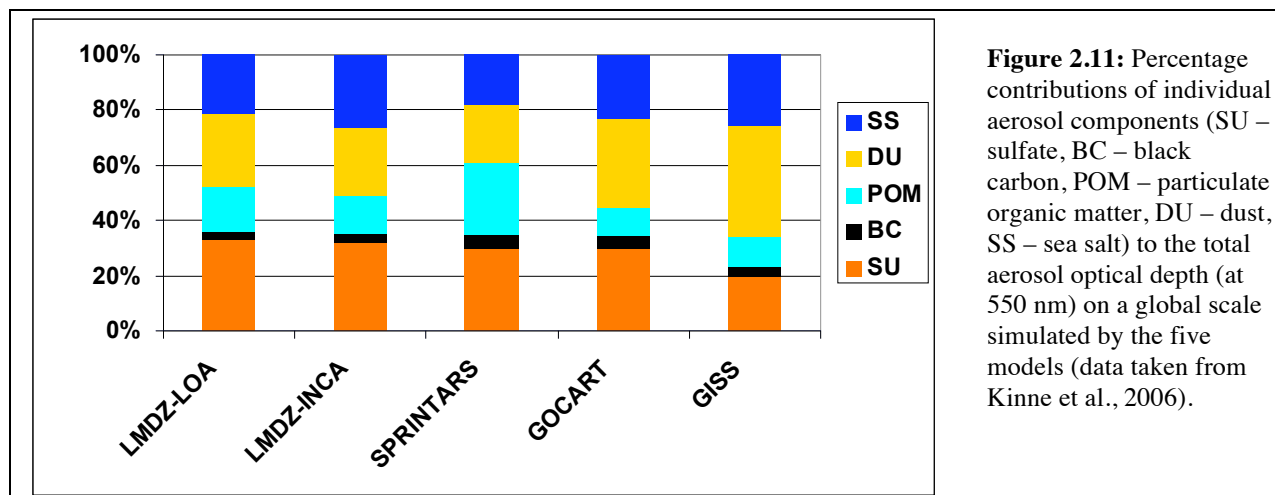
21 **Figure 2.10** shows an intercomparison of annual average AOD at 550 nm from two recent  
22 satellite aerosol sensors (MODIS and MISR), five model simulations (GOCART, GISS,  
23 SPRINTARS, LMDZ-LOA, LMDZ-INCA) and three satellite-model integrations (MO\_GO,  
24 MI\_GO, MO\_MI\_GO). These model-satellite integrations are conducted by using an optimum  
25 interpolation approach (Yu et al., 2003) to constrain GOCART simulated AOD with that from  
26 MODIS, MISR, or MODIS over ocean and MISR over land, denoted as MO\_GO, MI\_GO, and  
27 MO\_MI\_GO, respectively. MODIS values of AOD are from Terra Collection 4 retrievals and  
28 MISR AOD is based on early post launch retrievals. MODIS and MISR retrievals give a  
29 comparable average AOD on the global scale, with MISR greater than MODIS by 0.01~0.02  
30 depending on the season. However, differences between MODIS and MISR are much larger  
31 when land and ocean are examined separately: AOD from MODIS is 0.02-0.07 higher over land  
32 but 0.03-0.04 lower over ocean than the AOD from MISR. Several major causes for the  
33 systematic MODIS-MISR differences have been identified, including instrument calibration and  
34 sampling differences, different assumptions about ocean surface boundary conditions made in  
35 the individual retrieval algorithms, missing particle property or mixture options in the look-up  
36 tables, and cloud screening (Kahn et al., 2007b). The MODIS-MISR AOD differences are being  
37 reduced by continuous efforts on improving satellite retrieval algorithms and radiance  
38 calibration. The new MODIS aerosol retrieval algorithms in Collection 5 have resulted in a  
39 reduction of 0.07 for global land mean AOD (Levy et al., 2007b), and improved radiance  
40 calibration for MISR removed ~40% of AOD bias over dark water scenes (Kahn et al., 2005b).



1  
 2 The annual and global average AOD from the five models is  $0.19 \pm 0.02$  (mean  $\pm$  standard  
 3 deviation) over land and  $0.13 \pm 0.05$  over ocean, respectively. Clearly, the model-based mean  
 4 AOD is smaller than both MODIS- and MISR-derived values (except the GISS model). A  
 5 similar conclusion has been drawn from more extensive comparisons involving more models and  
 6 satellites (Kinne et al., 2006). On regional scales, satellite-model differences are much larger.  
 7 These differences could be attributed in part to cloud contamination (Kaufman et al., 2005b;  
 8 Zhang et al., 2005c) and 3D cloud effects in satellite retrievals (Kaufman et al., 2005b; Wen et  
 9 al., 2006) or to models missing important aerosol sources/sinks or physical processes (Koren et  
 10 al., 2007b). Integrated satellite-model products are generally in-between the satellite retrievals  
 11 and the model simulations, and agree better with AERONET measurements (e.g., Yu et al.,  
 12 2003).

13 As in comparisons between models and *in situ* measurements (Bates et al., 2006), there appears  
 14 to be a relationship between uncertainties in the representation of dust in models and the  
 15 uncertainty in AOD, and its global distribution. For example, the GISS model generates more  
 16 dust than the other models (Fig. 2.11), resulting in a closer agreement with MODIS and MISR in  
 17 the global mean (Fig. 2.10). However, the distribution of AOD between land and ocean is quite  
 18 different from MODIS- and MISR-derived values.

19 **Figure 2.11** shows larger model differences in the simulated percentage contributions of  
 20 individual components to the total aerosol optical depth on a global scale, and hence in the  
 21 simulated aerosol single-scattering properties (e.g., single-scattering albedo, and phase function),  
 22 as documented in Kinne et al. (2006). This, combined with the differences in aerosol loading (as  
 23 characterized by AOD) determines the model diversity in simulated aerosol direct radiative  
 24 forcing, as discussed later. However, current satellite remote sensing capability is not sufficient  
 25 to constrain model simulations of aerosol components.



1

### 2 2.3.3. Satellite Based Estimates of Aerosol Direct Radiative Forcing

3 **Table 2.4** summarizes approaches to estimating the aerosol direct radiative forcing, including a  
 4 brief description of methods, identifies major sources of uncertainty, and provides references.  
 5 These estimates fall into three broad categories, namely (A) satellite-based, (B) satellite-model  
 6 integrated, and (C) model-based. As satellite aerosol measurements are generally limited to  
 7 cloud-free conditions, the discussion here focuses on assessments of clear-sky aerosol direct  
 8 radiative forcing, a net (down-welling minus upwelling) solar flux difference between with  
 9 aerosol (natural + anthropogenic) and in the absence of aerosol.

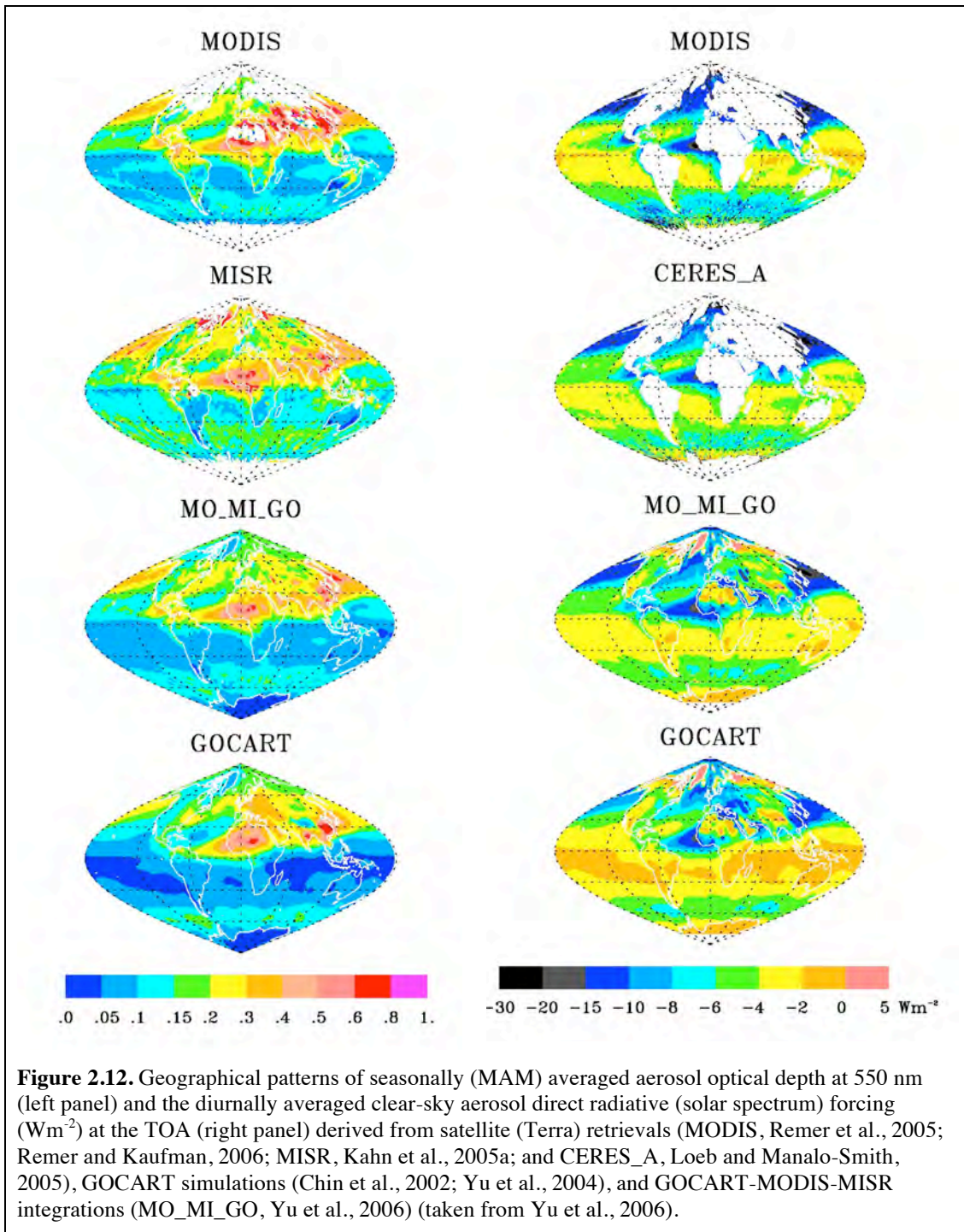
10

11 **Global distributions.** **Figure 2.12** shows global distributions of aerosol optical depth at 550 nm  
 12 (left panel) and diurnally averaged clear-sky TOA DRF (right panel) for March-April-May  
 13 (MAM) based on the different approaches. The DRF at the surface follows the same pattern as  
 14 that at the TOA but is significantly larger in magnitude because of aerosol absorption. It appears  
 15 that different approaches agree on large-scale patterns of aerosol optical depth and the direct  
 16 radiative forcing. In this season, the aerosol impacts in the Northern Hemisphere are much larger  
 17 than those in the Southern Hemisphere. Dust outbreaks and biomass burning elevate the optical  
 18 depth to more than 0.3 over large parts of North Africa and the tropical Atlantic. In the tropical  
 19 Atlantic, TOA cooling as large as  $-10 \text{ Wm}^{-2}$  extends westward to Central America. In eastern  
 20 China, the optical depth is as high as 0.6-0.8, resulting from the combined effects of industrial  
 21 activities and biomass burning in the south, and dust outbreaks in the north. The Asian impacts  
 22 also extend to the North Pacific, producing a TOA cooling of more than  $-10 \text{ Wm}^{-2}$ . Other areas  
 23 having large aerosol impacts include Western Europe, mid-latitude North Atlantic, and much of  
 24 South Asia and the Indian Ocean. Over the “roaring forties” in the Southern Hemisphere, high  
 25 winds generate a large amount of sea salt. Elevated optical depth, along with high solar zenith  
 26 angle and hence large backscattering to space, results in a band of TOA cooling of more than  $-4$   
 27  $\text{Wm}^{-2}$ . However, there is also some question as to whether thin cirrus (e.g., Zhang et al., 2005c)  
 28 and unaccounted-for whitecaps contribute to the apparent enhancement in AOD retrieved by  
 29 satellite. Some differences exist between different approaches. For example, the early post-  
 30 launch MISR retrieved optical depths over the southern hemisphere oceans are higher than  
 31 MODIS retrievals and GOCART simulations. Over the “roaring forties”, the MODIS derived  
 32 TOA solar flux perturbations are larger than the estimates from other approaches.



**Table 2.4:** Summary of approaches to estimating the aerosol direct radiative forcing in three categories: (A) satellite retrievals; (B) satellite-model integrations; and (C) model simulations. (adapted from Yu et al., 2006).

Category	Product	Brief Descriptions	Identified Sources of Uncertainty	Major References
<b>A. Satellite retrievals</b>	MODIS	Using MODIS retrievals of a linked set of AOD, $\omega_0$ , and phase function consistently in conjunction with a radiative transfer model (RTM) to calculate TOA fluxes that best match the observed radiances.	Radiance calibration, cloud-aerosol discrimination, instantaneous-to-diurnal scaling, RTM parameterizations	Remer and Kaufman, 2006
	MODIS_A	Splitting MODIS AOD over ocean into mineral dust, sea salt, and biomass-burning and pollution; using AERONET measurements to derive the size distribution and single-scattering albedo for individual components.	Satellite AOD and FMF retrievals, overestimate due to summing up the compositional direct forcing, use of a single AERONET site to characterize a large region	Bellouin et al., 2005
	CERES_A	Using CERES fluxes in combination with standard MODIS aerosol	Calibration of CERES radiances, large CERES footprint, satellite AOD retrieval, radiance-to-flux conversion (ADM), instantaneous-to-diurnal scaling, narrow-to-broadband conversion	Loeb and Manalo-Smith, 2005 ; Loeb and Kato, 2002
	CERES_B	Using CERES fluxes in combination with NOAA NESDIS aerosol from MODIS radiances		Zhang et al, 2005a,b ; Zhang and Christopher, 2003; Christopher et al., 2006; Patadia et al., 2008
	CERES_C	Using CERES fluxes in combination with MODIS (ocean) and MISR (non-desert land) aerosol with new angular models for aerosols		
	POLDER	Using POLDER AOD in combination with prescribed aerosol models (similar to MODIS)	Similar to MODIS	Boucher and Tanré, 2000 ; Bellouin et al., 2003
<b>B. Satellite-model integrations</b>	MODIS_G	Using GOCART simulations to fill AOD gaps in satellite retrievals	Propagation of uncertainties associated with both satellite retrievals and model simulations (but the model-satellite integration approach does result in improved AOD quality for MO_GO, and MO_MI_GO)	* Aerosol single-scattering albedo and asymmetry factor are taken from GOCART simulations; * Yu et al, 2003, 2004, 2006
	MISR_G			
	MO_GO	Integration of MODIS and GOCART AOD		
	MO_MI_GO	Integration of GOCART AOD with retrievals from MODIS (Ocean) and MISR (Land)		
SeaWiFS	Using SeaWiFS AOD and assumed aerosol models	Similar to MODIS_G and MISR_G, too weak aerosol absorption	Chou et al, 2002	
<b>C. Model simulations</b>	GOCART	Offline RT calculations using monthly average aerosols with a time step of 30 min (without the presence of clouds)	Emissions, parameterizations of a variety of sub-grid aerosol processes (e.g., wet and dry deposition, cloud convection, aqueous-phase oxidation), assumptions on aerosol size, absorption, mixture, and humidification of particles, meteorology fields, not fully evaluated surface albedo schemes, RT parameterizations	Chin et al., 2002; Yu et al., 2004
	SPRINTARS	Online RT calculations every 3 hrs (cloud fraction=0)		Takemura et al, 2002, 2005
	GISS	Online model simulations and weighted by clear-sky fraction		Koch and Hansen, 2005; Koch et al., 2006
	LMDZ-INCA	Online RT calculations every 2 hrs (cloud fraction = 0)		Balkanski et al., 2007; Schulz et al., 2006; Kinne et al., 2006
	LMDZ-LOA	Online RT calculations every 2 hrs (cloud fraction=0)		Reddy et al., 2005a,b



2

3 **Global mean.** Figure 2.13 summarizes the measurement- and model-based estimates of clear-  
 4 sky annual-averaged DRF at both the TOA and surface from  $60^{\circ}\text{S}$  to  $60^{\circ}\text{N}$ . Seasonal DRF values  
 5 for individual estimates are summarized in Table 2.5 and Table 2.6 for ocean and land,  
 6 respectively. Mean, median and standard error  $\epsilon$  ( $\epsilon = \sigma / (n-1)^{1/2}$ ), where  $\sigma$  is standard deviation and  
 7  $n$  is the number of methods) are calculated for measurement- and model-based estimates

1 separately. Note that although the standard deviation or standard error reported here is not a fully  
 2 rigorous measure of a true experimental uncertainty, it is indicative of the uncertainty because  
 3 independent approaches with independent sources of errors are used (see **Table 2.4**; in the  
 4 modeling community, this is called the “diversity”, see Chapter 3).

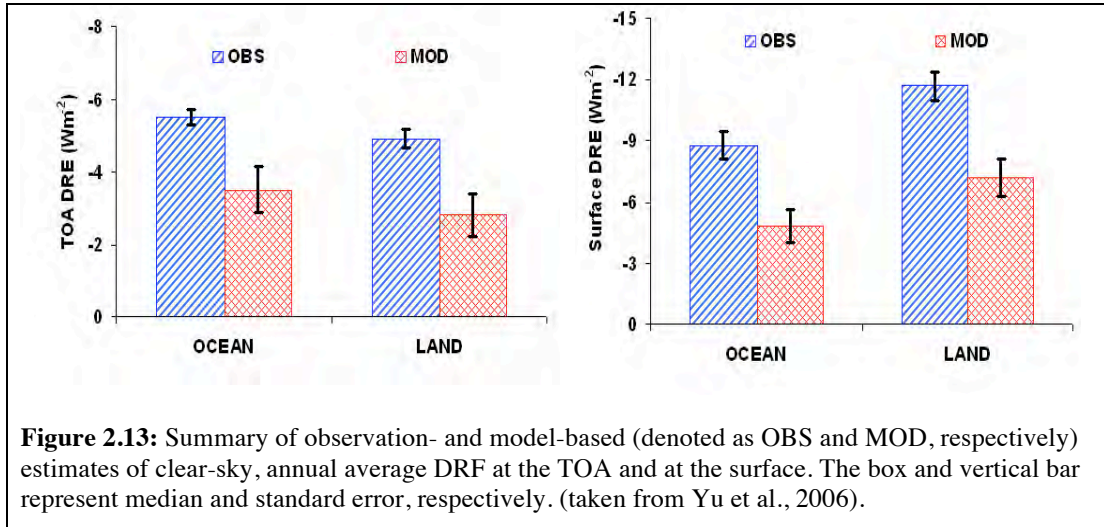


**Figure 2.13:** Summary of observation- and model-based (denoted as OBS and MOD, respectively) estimates of clear-sky, annual average DRF at the TOA and at the surface. The box and vertical bar represent median and standard error, respectively. (taken from Yu et al., 2006).

5

6 • **Ocean:** For the TOA DRF, a majority of measurement-based and satellite-model  
 7 integration-based estimates agree with each other within about 10%. On annual average,  
 8 the measurement-based estimates give the DRF of  $-5.5 \pm 0.2 \text{ Wm}^{-2}$  (mean  $\pm \epsilon$ ) at the TOA  
 9 and  $-8.7 \pm 0.7 \text{ Wm}^{-2}$  at the surface. This suggests that the ocean surface cooling is about  
 10 60% larger than the cooling at the TOA. Model simulations give wide ranges of DRF  
 11 estimates at both the TOA and surface. The ensemble of five models gives the annual  
 12 average DRF (mean  $\pm \epsilon$ ) of  $-3.2 \pm 0.6 \text{ Wm}^{-2}$  and  $-4.9 \pm 0.8 \text{ Wm}^{-2}$  at the TOA and surface,  
 13 respectively. On average, the surface cooling is about 37% larger than the TOA cooling,  
 14 smaller than the measurement-based estimate of surface and TOA difference of 60%.  
 15 However, the ‘measurement-based’ estimate of *surface* DRF is actually a calculated  
 16 value, using poorly constrained particle properties.

17 • **Land:** It remains challenging to use satellite measurements alone for characterizing  
 18 complex aerosol properties over land surfaces with high accuracy. As such, DRF  
 19 estimates over land have to rely largely on model simulations and satellite-model  
 20 integrations. On a global and annual average, the satellite-model integrated approaches  
 21 derive a mean DRF of  $-4.9 \text{ Wm}^{-2}$  at the TOA and  $-11.9 \text{ Wm}^{-2}$  at the surface respectively.  
 22 The surface cooling is more than a factor of 2 larger than the TOA cooling because of  
 23 aerosol absorption. Note that the TOA DRF of  $-4.9 \text{ Wm}^{-2}$  agrees quite well with the most  
 24 recent satellite-based estimate of  $-5.1 \pm 1.1 \text{ Wm}^{-2}$  over non-desert land based on coincident  
 25 measurements of MISR AOD and CERES solar flux (Patadia et al., 2008). For  
 26 comparisons, an ensemble of five model simulations derives a DRF (mean  $\pm \epsilon$ ) over land  
 27 of  $-3.0 \pm 0.6 \text{ Wm}^{-2}$  at the TOA and  $-7.6 \pm 0.9 \text{ Wm}^{-2}$  at the surface, respectively. Seasonal  
 28 variations of DRF over land, as derived from both measurements and models, are larger  
 29 than those over ocean.

1 The above analyses show that, on a global average, the measurement-based estimates of DRF are  
2 55-80% greater than the model-based estimates. The differences are even larger on regional  
3 scales. Such measurement-model differences are a combination of differences in aerosol amount  
4 (optical depth), single-scattering properties, surface albedo, and radiative transfer schemes (Yu et  
5 al., 2006). As discussed earlier, MODIS retrieved optical depths tend to be overestimated by  
6 about 10-15% due to the contamination of thin cirrus and clouds in general (Kaufman et al.,  
7 2005b). Such overestimation of optical depth would result in a comparable overestimate of the  
8 aerosol direct radiative forcing. Other satellite AOD data may have similar contamination, which  
9 however has not yet been quantified. On the other hand, the observations may be measuring  
10 enhanced AOD and DRF due to processes not well represented in the models including  
11 humidification and enhancement of aerosols in the vicinity of clouds (Koren et al., 2007b).

12 From the perspective of model simulations, uncertainties associated with parameterizations of  
13 various aerosol processes and meteorological fields, as documented under the AEROCOM and  
14 Global Modeling Initiative (GMI) frameworks (Kinne et al., 2006; Textor et al., 2006; Liu et al.,  
15 2007), contribute to the large measurement-model and model-model discrepancies. Factors  
16 determining the AOD should be major reasons for the DRF discrepancy and the constraint of  
17 model AOD with well evaluated and bias reduced satellite AOD through a data assimilation  
18 approach can reduce the DRF discrepancy significantly. Other factors (such as model  
19 parameterization of surface reflectance, and model-satellite differences in single-scattering  
20 albedo and asymmetry factor due to satellite sampling bias toward cloud-free conditions) should  
21 also contribute, as evidenced by the existence of a large discrepancy in the radiative efficiency  
22 (Yu et al., 2006). Significant effort will be needed in the future to conduct comprehensive  
23 assessments.

#### 24 **2.3.4. Satellite Based Estimates of Anthropogenic Component of Aerosol Direct** 25 **Radiative Forcing**

26 Satellite instruments do not measure the aerosol chemical composition needed to discriminate  
27 anthropogenic from natural aerosol components. Because anthropogenic aerosols are  
28 predominantly sub-micron, the fine-mode fraction derived from POLDER, MODIS, or MISR  
29 might be used as a tool for deriving anthropogenic aerosol optical depth. This could provide a  
30 feasible way to conduct measurement-based estimates of anthropogenic component of aerosol  
31 direct radiative forcing (Kaufman et al., 2002a). Such method derives anthropogenic AOD from  
32 satellite measurements by empirically correcting contributions of natural sources (dust and  
33 maritime aerosol) to the sub-micron AOD (Kaufman et al., 2005a). The MODIS-based estimate  
34 of anthropogenic AOD is about 0.033 over oceans, consistent with model assessments of  
35 0.030~0.036 even though the total AOD from MODIS is 25-40% higher than the models  
36 (Kaufman et al., 2005a). This accounts for  $21 \pm 7\%$  of the MODIS-observed total aerosol optical  
37 depth, compared with about 33% of anthropogenic contributions estimated by the models. The  
38 anthropogenic fraction of AOD should be much larger over land (i.e.,  $47 \pm 9\%$  from a composite  
39 of several models) (Bellouin et al., 2005), comparable to the 40% estimated by Yu et al. (2006).  
40 Similarly, the non-spherical fraction from MISR or POLDER can be used to separate dust from  
41 spherical aerosol (Kahn et al., 2001; Kalashnikova and Kahn, 2006), providing another constraint  
42 for distinguishing anthropogenic from natural aerosols.

**Table 2.5.** Summary of seasonal and annual average clear-sky DRF ( $\text{Wm}^{-2}$ ) at the TOA and the surface (SFC) over global OCEAN derived with different methods and data. Sources of data: MODIS (Remer & Kaufman, 2006), MODIS\_A (Bellouin et al., 2005), POLDER (Boucher and Tanré, 2000; Bellouin et al., 2003), CERES\_A and CERES\_B (Loeb and Manalo-Smith, 2005), CERES\_C (Zhang et al., 2005b), MODIS\_G, MISR\_G, MO\_GO, MO\_MI\_GO (Yu et al., 2004; 2006), SeaWiFS (Chou et al., 2002), GOCART (Chin et al., 2002; Yu et al., 2004), SPRINTARS (Takemura et al., 2002), GISS (Koch and Hansen, 2005; Koch et al., 2006), LMDZ-INCA (Kinne et al., 2006; Schulz et al., 2006), LMDZ-LOA (Reddy et al., 2005a, b). Mean, median, standard deviation ( $\sigma$ ), and standard error ( $\epsilon$ ) are calculated for observations (Obs) and model simulations (Mod) separately. The last row is the ratio of model median to observational median. (taken from Yu et al., 2006)

Products	DJF		MAM		JJA		SON		ANN	
	TOA	SFC	TOA	SFC	TOA	SFC	TOA	SFC	TOA	SFC
MODIS	-5.9	-	-5.8	-	-6.0	-	-5.8	-	-5.9	-
MODIS_A *	-6.0	-8.2	-6.4	-8.9	-6.5	-9.3	-6.4	-8.9	-6.4	-8.9
CERES_A	-5.2	-	-6.1	-	-5.4	-	-5.1	-	-5.5	-
CERES_B	-3.8	-	-4.3	-	-3.5	-	-3.6	-	-3.8	-
CERES_C	-5.3	-	-5.4	-	-5.2	-	-	-	-5.3	-
MODIS_G	-5.5	-9.1	-5.7	-10.4	-6.0	-10.6	-5.5	-9.8	-5.7	-10.0
MISR_G **	-6.4	-10.3	-6.5	-11.4	-7.0	-11.9	-6.3	-10.9	-6.5	-11.1
MO_GO	-4.9	-7.8	-5.1	-9.3	-5.4	-9.4	-5.0	-8.7	-5.1	-8.8
MO_MI_GO	-4.9	-7.9	-5.1	-9.2	-5.5	-9.5	-5.0	-8.6	-5.1	-8.7
POLDER	-5.7	-	-5.7	-	-5.8	-	-5.6	-	-5.7 -5.2***	-7.7***
SeaWiFS	-6.0	-6.6	-5.2	-5.8	-4.9	-5.6	-5.3	-5.7	-5.4	-5.9
Obs. Mean	-5.4	-8.3	-5.6	-9.2	-5.6	-9.4	-5.4	-8.8	-5.5	-8.7
Obs. Median	-5.5	-8.1	-5.7	-9.3	-5.5	-9.5	-5.4	-8.8	-5.5	-8.8
Obs. $\sigma$	0.72	1.26	0.64	1.89	0.91	2.10	0.79	1.74	0.70	1.65
Obs. $\epsilon$	0.23	0.56	0.20	0.85	0.29	0.94	0.26	0.78	0.21	0.67
GOCART	-3.6	-5.7	-4.0	-7.2	-4.7	-8.0	-4.0	-6.8	-4.1	-6.9
SPRINTARS	-1.5	-2.5	-1.5	-2.5	-1.9	-3.3	-1.5	-2.5	-1.6	-2.7
GISS	-3.3	-4.1	-3.5	-4.6	-3.5	-4.9	-3.8	-5.4	-3.5	-4.8
LMDZ-INCA	-4.6	-5.6	-4.7	-5.9	-5.0	-6.3	-4.8	-5.5	-4.7	-5.8
LMDZ-LOA	-2.2	-4.1	-2.2	-3.7	-2.5	-4.4	-2.2	-4.1	-2.3	-4.1
Mod. Mean	-3.0	-4.4	-3.2	-4.8	-3.5	-5.4	-3.3	-4.9	-3.2	-4.9
Mod. Median	-3.3	-4.1	-3.5	-4.6	-3.5	-4.9	-3.8	-5.4	-3.5	-4.8
Mod. $\sigma$	1.21	1.32	1.31	1.84	1.35	1.82	1.36	1.63	1.28	1.6
Mod. $\epsilon$	0.61	0.66	0.66	0.92	0.67	0.91	0.68	0.81	0.64	0.80
Mod./Obs.	0.60	0.51	0.61	0.50	0.64	0.52	0.70	0.61	0.64	0.55

\*High bias may result from adding the DRF of individual components to derive the total DRF (Bellouin et al., 2005).

\*\* High bias most likely results from an overall overestimate of 20% in early post-launch MISR optical depth retrievals (Kahn et al., 2005).

\*\*\* Bellouin et al. (2003) use AERONET retrieval of aerosol absorption as a constraint to the method in Boucher and Tanré (2000), deriving aerosol direct radiative forcing both at the TOA and the surface.

1  
2  
3  
4  
5  
6  
7  
8

**Table 2.6.** Summary of seasonal and annual average clear-sky DRF ( $\text{Wm}^{-2}$ ) at the TOA and the surface (SFC) over global LAND derived with different methods and data. Sources of data: MODIS\_G, MISR\_G, MO\_GO, MO\_MI\_GO (Yu et al., 2004, 2006), GOCART (Chin et al., 2002; Yu et al., 2004), SPRINTARS (Takemura et al., 2002), GISS (Koch and Hansen, 2005; Koch et al., 2006), LMDZ-INCA (Balkanski et al., 2007; Kinne et al., 2006; Schulz et al., 2006), LMDZ-LOA (Reddy et al., 2005a, b). Mean, median, standard deviation ( $\sigma$ ), and standard error ( $\epsilon$ ) are calculated for observations (Obs) and model simulations (Mod) separately. The last row is the ratio of model median to observational median. (taken from Yu et al., 2006)

Products	DJF		MAM		JJA		SON		ANN	
	TOA	SFC	TOA	SFC	TOA	SFC	TOA	SFC	TOA	SFC
MODIS_G	-4.1	-9.1	-5.8	-14.9	-6.6	-17.4	-5.4	-12.8	-5.5	-13.5
MISR_G	-3.9	-8.7	-5.1	-13.0	-5.8	-14.6	-4.6	-10.7	-4.9	-11.8
MO_GO	-3.5	-7.5	-5.1	-12.9	-5.8	-14.9	-4.8	-10.9	-4.8	-11.6
MO_MI_GO	-3.4	-7.4	-4.7	-11.8	-5.3	-13.5	-4.3	-9.7	-4.4	-10.6
Obs. Mean	-3.7	-8.2	-5.2	-13.2	-5.9	-15.1	-4.8	-11.0	-4.9	-11.9
Obs. Median	-3.7	-8.1	-5.1	-13.0	-5.8	-14.8	-4.7	-10.8	-4.9	-11.7
Obs. $\sigma$	0.33	0.85	0.46	1.29	0.54	1.65	0.46	1.29	0.45	1.20
Obs. $\epsilon$	0.17	0.49	0.26	0.74	0.31	0.85	0.27	0.75	0.26	0.70
GOCART	-2.9	-6.1	-4.4	-10.9	-4.8	-12.3	-4.3	-9.3	-4.1	-9.7
SPRINTARS	-1.4	-4.0	-1.5	-4.6	-2.0	-6.7	-1.7	-5.2	-1.7	-5.1
GISS	-1.6	-3.9	-3.2	-7.9	-3.6	-9.3	-2.5	-6.6	-2.8	-7.2
LMDZ-INCA	-3.0	-5.8	-4.0	-9.2	-6.0	-13.5	-4.3	-8.2	-4.3	-9.2
LMDZ-LOA	-1.3	-5.4	-1.8	-6.4	-2.7	-8.9	-2.1	-6.7	-2.0	-6.9
Mod. Mean	-2.0	-5.0	-3.0	-7.8	-3.8	-10.1	-3.0	-7.2	-3.0	-7.6
Mod. Median	-1.6	-5.4	-3.2	-7.9	-3.6	-9.3	-2.5	-6.7	-2.8	-7.2
Mod. $\sigma$	0.84	1.03	1.29	2.44	1.61	2.74	1.24	1.58	1.19	1.86
Mod. $\epsilon$	0.42	0.51	0.65	1.22	0.80	1.37	0.62	0.79	0.59	0.93
Mod./Obs.	0.43	0.67	0.63	0.61	0.62	0.63	0.53	0.62	0.58	0.62

1 There have been several estimates of anthropogenic component of DRF in recent years. **Table**  
2 **2.7** lists such estimates of anthropogenic component of TOA DRF that are from model  
3 simulations (Schulz et al., 2006) and constrained to some degree by satellite observations  
4 (Kaufman et al., 2005a; Bellouin et al., 2005, 2008; Chung et al., 2005; Christopher et al., 2006;  
5 Matsui and Pielke, 2006; Yu et al., 2006; Quaas et al., 2008; Zhao et al., 2008b). The satellite-  
6 based clear-sky DRF by anthropogenic aerosols is estimated to be  $-1.1 \pm 0.37 \text{ Wm}^{-2}$  over ocean,  
7 about a factor of 2 stronger than model simulated  $-0.6 \text{ Wm}^{-2}$ . Similar DRF estimates are rare over  
8 land, but a few studies do suggest that the anthropogenic DRF over land is much more negative  
9 than that over ocean (Yu et al., 2006; Bellouin et al., 2005, 2008). On global average, the  
10 measurement-based estimate of anthropogenic DRF ranges from  $-0.9 \sim -1.9 \text{ Wm}^{-2}$ , again stronger  
11 than the model-based estimate of  $-0.8 \text{ Wm}^{-2}$ . Similar to DRF estimates for total aerosols,  
12 satellite-based estimates of anthropogenic component of DRF are rare over land.

13  
14  
15  
16

1

**Table 2.7:** Estimates of anthropogenic components of aerosol optical depth ( $\tau_{\text{ant}}$ ) and clear-sky DRF at the TOA from model simulations (Schulz et al., 2006) and approaches constrained by satellite observations (Kaufman et al., 2005a; Bellouin et al., 2005, 2008; Chung et al., 2005; Yu et al., 2006; Christopher et al., 2006; Matsui and Pielke, 2006; Quaas et al., 2008; Zhao et al., 2008b).

Data Sources	Ocean		Land		Global		Estimated uncertainty or model diversity for DRF
	$\tau_{\text{ant}}$	DRF ( $\text{Wm}^{-2}$ )	$\tau_{\text{ant}}$	DRF ( $\text{Wm}^{-2}$ )	$\tau_{\text{ant}}$	DRF ( $\text{Wm}^{-2}$ )	
Kaufman et al. (2005a)	0.033	-1.4	-	-	-	-	30%
Bellouin et al. (2005)	0.028	-0.8	0.13	-	0.062	-1.9	15%
Chung et al. (2005)	-	-	-	-	-	-1.1	-
Yu et al. (2006)	0.031	-1.1	0.088	-1.8	0.048	-1.3	47% (ocean), 84% (land), and 62% (global)
Christopher et al. (2006)	-	-1.4	-	-	-	-	65%
Matsui and Pielke (2006)	-	-1.6	-	-	-	-	30°S-30°N oceans
Quaas et al. (2008)	-	-0.7	-	-1.8	-	-0.9	45%
Bellouin et al. (2008)	0.021	-0.6	0.107	-3.3	0.043	-1.3	Update to Bellouin et al. (2005) with MODIS Collection 5 data
Zhao et al. (2008b)	-	-1.25	-	-	-	-	35%
Schulz et al. (2006)	0.022	-0.59	0.065	-1.14	0.036	-0.77	30-40%; same emissions prescribed for all models

2

3 On global average, anthropogenic aerosols are generally more absorptive than natural aerosols.  
 4 As such the anthropogenic component of DRF is much more negative at the surface than at  
 5 TOA. Several observation-constrained studies estimate that the global average, clear-sky,  
 6 anthropogenic component of DRF at the surface ranges from  $-4.2$  to  $-5.1 \text{ Wm}^{-2}$  (Yu et al., 2004;  
 7 Bellouin et al., 2005; Chung et al., 2005; Matsui and Pielke, 2006), which is about a factor of 2  
 8 larger in magnitude than the model estimates (e.g., Reddy et al., 2005b).

9 Estimates of anthropogenic component of DRF have larger uncertainty than DRF estimates for  
 10 total aerosol, particularly over land. An uncertainty analysis (Yu et al., 2006) partitions the  
 11 uncertainty for the global average anthropogenic DRF between land and ocean more or less  
 12 evenly. Five parameters, namely fine-mode fraction ( $f_f$ ) and anthropogenic fraction of fine-mode  
 13 fraction ( $f_{\text{af}}$ ) over both land and ocean, and  $\tau$  over ocean, contribute nearly 80% of the overall  
 14 uncertainty in the anthropogenic DRF estimate, with individual shares ranging from 13-20% (Yu  
 15 et al., 2006). These uncertainties presumably represent a lower bound because the sources of  
 16 error are assumed to be independent. Uncertainties associated with several parameters are also  
 17 not well defined. Nevertheless, such uncertainty analysis is useful for guiding future research and  
 18 documenting advances in understanding.

### 19 **2.3.5. Aerosol-Cloud Interactions and Indirect Forcing**

20 Satellite views of the Earth show a planet whose albedo is dominated by dark oceans and  
 21 vegetated surfaces, white clouds, and bright deserts. The bright white clouds overlying darker  
 22 oceans or vegetated surface demonstrate the significant effect that clouds have on the Earth's  
 23 radiative balance. Low clouds reflect incoming sunlight back to space, acting to cool the planet,  
 24 whereas high clouds can trap outgoing terrestrial radiation and act to warm the planet. In the  
 25 Arctic, low clouds have also been shown to warm the surface (Garrett and Zhao, 2006). Changes

1 in cloud cover, in cloud vertical development, and cloud optical properties will have strong  
2 radiative and therefore, climatic impacts. Furthermore, factors that change cloud development  
3 will also change precipitation processes. These changes may alter amounts, locations and  
4 intensities of local and regional rain and snowfall, creating droughts, floods and severe weather.

5 Cloud droplets form on a subset of aerosol particles called cloud condensation nuclei (CCN). In  
6 general, an increase in aerosol leads to an increase in CCN and an increase in drop concentration.  
7 Thus, for the same amount of liquid water in a cloud, more available CCN will result in a greater  
8 number but smaller size of droplets (Twomey, 1977). A cloud with smaller but more numerous  
9 droplets will be brighter and reflect more sunlight to space, thus exerting a cooling effect. This is  
10 the first aerosol indirect radiative effect, or “albedo effect”. The effectiveness of a particle as a  
11 CCN depends on its size and composition so that the degree to which clouds become brighter for  
12 a given aerosol perturbation, and therefore the extent of cooling, depends on the aerosol size  
13 distribution and its size-dependent composition. In addition, aerosol perturbations to cloud  
14 microphysics may involve feedbacks; for example, smaller drops are less likely to collide and  
15 coalesce; this will inhibit growth, suppressing precipitation, and possibly increasing cloud  
16 lifetime (Albrecht et al. 1989). In this case clouds may exert an even stronger cooling effect.

17 A distinctly different aerosol effect on clouds exists in thin Arctic clouds ( $LWP < 25 \text{ g m}^{-2}$ )  
18 having low emissivity. Aerosol has been shown to increase the longwave emissivity in these  
19 clouds, thereby *warming* the surface (Lubin and Vogelmann, 2006; Garrett and Zhao, 2006).

20 Some aerosol particles, particularly black carbon and dust, also act as ice nuclei (IN) and in so  
21 doing, modify the microphysical properties of mixed-phase and ice-clouds. An increase in IN  
22 will generate more ice crystals, which grow at the expense of water droplets due to the difference  
23 in vapor pressure over ice and water surfaces. The efficient growth of ice particles may increase  
24 the precipitation efficiency. In deep convective, polluted clouds there is a delay in the onset of  
25 freezing because droplets are smaller. These clouds may eventually precipitate, but only after  
26 higher altitudes are reached that result in taller cloud tops, more lightning and greater chance of  
27 severe weather (Rosenfeld and Lensky, 1998; Andreae et al., 2004). The present state of  
28 knowledge of the nature and abundance of IN, and ice formation in clouds is extremely poor.  
29 There is some observational evidence of aerosol influences on ice processes, but a clear link  
30 between aerosol, IN concentrations, ice crystal concentrations and growth to precipitation has not  
31 been established. This report therefore only peripherally addresses ice processes. More  
32 information can be found in a review by the WMO/IUGG International Aerosol-Precipitation  
33 Scientific Assessment (Levin and Cotton, 2008).

34 In addition to their roles as CCN and IN, aerosols also absorb and scatter light, and therefore  
35 they can change atmospheric conditions (temperature, stability, and surface fluxes) that influence  
36 cloud development and properties (Hansen et al, 1997; Ackerman et al., 2000). Thus, aerosols  
37 affect clouds through changing cloud droplet size distributions, cloud particle phase, and by  
38 changing the atmospheric environment of the cloud.

### 39 ***2.3.5a. Remote Sensing of Aerosol-Cloud Interactions and Indirect Forcing***

40 The AVHRR satellite instruments have observed relationships between columnar aerosol  
41 loading, retrieved cloud microphysics, and cloud brightness over the Amazon Basin that are  
42 consistent with the theories explained above (Kaufman and Nakajima, 1993; Kaufman and



1 Fraser, 1997; Feingold et al., 2001), but do not necessarily prove a causal relationship. Other  
2 studies have linked cloud and aerosol microphysical parameters or cloud albedo and droplet size  
3 using satellite data applied over the entire global oceans (Wetzel and Stowe, 1999; Nakajima et  
4 al., 2001; Han et al., 1998). Using these correlations with estimates of aerosol increase from the  
5 pre-industrial era, estimates of anthropogenic aerosol indirect radiative forcing fall into the range  
6 of  $-0.7$  to  $-1.7 \text{ Wm}^{-2}$  (Nakajima et al., 2001).

7 Introduction of the more modern instruments (POLDER and MODIS) has allowed more detailed  
8 observations of relationships between aerosol and cloud parameters. Cloud cover can both  
9 decrease and increase with increasing aerosol loading (Koren et al., 2004; Kaufman et al., 2005c;  
10 Koren et al., 2005; Sekiguchi et al., 2003; Matheson et al., 2005; Yu et al., 2007). The same is  
11 true of LWP (Han et al., 2002; Matsui et al., 2006). Aerosol absorption appears to be an  
12 important factor in determining how cloud cover will respond to increased aerosol loading  
13 (Kaufman and Koren, 2006; Jiang and Feingold, 2006; Koren et al., 2008). Different responses  
14 of cloud cover to increased aerosol could also be correlated with atmospheric thermodynamic  
15 and moisture structure (Yu et al., 2007). Observations in the MODIS data show that aerosol  
16 loading correlates with enhanced convection and greater production of ice anvils in the summer  
17 Atlantic Ocean (Koren et al., 2005), which conflicts with previous results that used AVHRR and  
18 could not isolate convective systems from shallow clouds (Sekiguchi et al., 2003).

19 In recent years, surface-based remote sensing has also been applied to address aerosol effects on  
20 cloud microphysics. This method offers some interesting insights, and is complementary to the  
21 global satellite view. Surface remote sensing can only be applied at a limited number of  
22 locations, and therefore lacks the global satellite view. However, these surface stations yield high  
23 temporal resolution data and because they sample aerosol below, rather than adjacent to clouds  
24 they do not suffer from “cloud contamination”. With the appropriate instrumentation (lidar) they  
25 can measure the local aerosol entering the clouds, rather than a column-integrated aerosol optical  
26 depth. Under well-mixed conditions, surface *in situ* aerosol measurements can be used. Surface  
27 remote-sensing studies are discussed in more detail below, although the main science issues are  
28 common to satellite remote sensing.

29 Feingold et al. (2003) used data collected at the ARM Southern Great Plains (SGP) site to allow  
30 simultaneously retrieval of aerosol and cloud properties. A combination of a Doppler cloud radar  
31 and a microwave radiometer was used to retrieve cloud drop effective radius  $r_e$  profiles in non-  
32 precipitating (radar reflectivity  $Z < -17 \text{ dBZ}$ ), ice-free clouds. Simultaneously, sub-cloud aerosol  
33 extinction profiles were measured with a lidar to quantify the response of drop sizes to changes  
34 in aerosol properties. Cloud data were binned according to liquid water path (LWP) as measured  
35 with a microwave radiometer, consistent with Twomey’s (1977) conceptual view of the aerosol  
36 impact on cloud microphysics. With high temporal/spatial resolution data (on the order of 20’s or  
37 100’s of meters), realizations of aerosol-cloud interactions at the large eddy scale were obtained,  
38 and quantified in terms of the relative decrease in  $r_e$  in response to a relative increase in aerosol  
39 extinction ( $d \ln r_e / d \ln \text{extinction}$ ), as shown in **Figure 2.14**. Examining the dependence in this  
40 way reduces reliance on absolute measures of cloud and aerosol parameters and minimizes  
41 sensitivity to measurement error, provided errors are unbiased. This formulation permitted these  
42 responses to be related to cloud microphysical theory. Restricting the examination to updrafts  
43 only (as determined from the radar Doppler signal) permitted examination of the role of updraft  
44 in determining the response of  $r_e$  to changes in aerosol (via changes in drop number

1 concentration  $N_d$ ). Analysis of data from 7 days showed that turbulence intensifies the aerosol  
2 impact on cloud microphysics.

3 In addition to radar/microwave radiometer  
4 retrievals of aerosol and cloud properties,  
5 measurements of cloud optical depth by surface  
6 based radiometers such as the MFRSR (Michalsky  
7 et al., 2001) have been used in combination with  
8 measurements of cloud LWP by microwave  
9 radiometer to measure an average value of  $r_e$  during  
10 daylight when the solar elevation angle is  
11 sufficiently high (Min and Harrison, 1996). Using  
12 this retrieval, Kim et al. (2003) performed analyses  
13 of the  $r_e$  response to changes in aerosol at the same  
14 continental site, using a surface measurement of the  
15 aerosol light scattering coefficient instead of using  
16 extinction near cloud base as a proxy for CCN.

17 Variance in LWP was shown to explain most of the  
18 variance in cloud optical depth, exacerbating  
19 detection of an aerosol effect. Although a decrease  
20 in  $r_e$  was observed with increasing scattering  
21 coefficient, the relation was not strong, indicative  
22 of other influences on  $r_e$  and/or decoupling between  
23 the surface and cloud layer. A similar study was conducted by Garrett et al. (2004) at a location  
24 in the Arctic. They suggested that summertime Arctic clouds are more sensitive to aerosol  
25 perturbations than clouds at lower latitudes. The advantage of the MFRSR/microwave  
26 radiometer combination is that it derives  $r_e$  from cloud optical depth and LWP and it is not as  
27 sensitive to large drops as the radar is. A limitation is that it can be applied only to clouds with  
28 extensive horizontal cover during daylight hours.

29 More recent data analyses by Feingold et al. (2006), Kim et al. (2008) and McComiskey et al.  
30 (2008b) at a variety of locations, and modeling work (Feingold, 2003) have investigated (i) the  
31 use of different proxies for cloud condensation nuclei, such as the light scattering coefficient and  
32 aerosol index; (ii) sensitivity of cloud microphysical/optical properties to controlling factors such  
33 as aerosol size distribution, entrainment, LWP, and updraft velocity; (iii) the effect of optical- as  
34 opposed to radar-retrievals of drop size; and (iv) spatial heterogeneity. These studies have  
35 reinforced the importance of LWP and vertical velocity as controlling parameters. They have  
36 also begun to reconcile the reasons for the large discrepancies between various approaches, and  
37 platforms (satellite, aircraft *in situ*, and surface-based remote sensing). These investigations are  
38 important because satellite measurements that use a similar approach are being employed in  
39 GCMs to represent the albedo indirect effect (Quaas and Boucher, 2005). In fact the weakest  
40 albedo indirect effect in IPCC (2007) derives from satellite measurements that have very weak  
41 responses of  $r_e$  to changes in aerosol. The relationship between these aerosol-cloud  
42 microphysical responses and cloud radiative forcing has been examined by McComiskey and  
43 Feingold (2008). They showed that for plane-parallel clouds, a typical uncertainty in the  
44 logarithmic gradient of a  $r_e$ -aerosol relationship of 0.05 results in a local forcing error of -3 to -10  
45  $\text{Wm}^{-2}$ , depending on the aerosol perturbation. This sensitivity reinforces the importance of

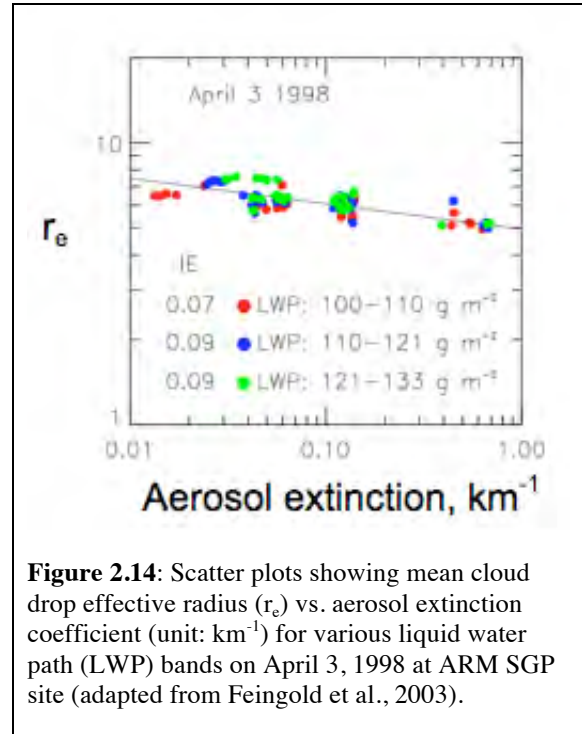


**Figure 2.14:** Scatter plots showing mean cloud drop effective radius ( $r_e$ ) vs. aerosol extinction coefficient (unit:  $\text{km}^{-1}$ ) for various liquid water path (LWP) bands on April 3, 1998 at ARM SGP site (adapted from Feingold et al., 2003).

1 adequate quantification of aerosol effects on cloud microphysics to assessment of the radiative  
2 forcing, i.e., the indirect effect. Quantification of these effects from remote sensors is  
3 exacerbated by measurement errors. For example, LWP is measured to an accuracy of  $25 \text{ gm}^{-2}$  at  
4 best, and since it is the thinnest clouds (i.e., low LWP) that are most susceptible (from a radiative  
5 forcing perspective) to changes in aerosol, this measurement uncertainty represents a significant  
6 uncertainty in whether the observed response is related to aerosol, or to differences in LWP. The  
7 accuracy and spatial resolution of satellite-based LWP measurements is much poorer and this  
8 represents a significant challenge. In some cases important measurements are simply absent, e.g.,  
9 updraft is not measured from satellite-based remote sensors.

10 Finally, cloud radar data from CloudSat, along with the A-train aerosol data, is providing great  
11 opportunity for inferring aerosol effects on precipitation (e.g., Stephens and Haynes, 2007). The  
12 aerosol-precipitation problem is far more complex than the albedo effect because the  
13 instantaneous view provided by satellites makes it difficult to establish causal relationships.

### 14 **2.3.5b. *In Situ Studies of Aerosol-Cloud Interactions***

15 *In situ* observations of aerosol effects on cloud microphysics date back to the 1950s and 1960s  
16 (Gunn and Phillips, 1957; Squires, 1958; Warner, 1968; Warner and Twomey, 1967; Radke et  
17 al., 1989; Leaitch et al., 1992; Brenguier et al., 2000; to name a few). These studies showed that  
18 high concentrations of CCN from anthropogenic sources, such as industrial pollution or the  
19 burning of sugarcane, can increase cloud droplet number concentration  $N_d$ , thus increasing cloud  
20 microphysical stability and potentially reducing precipitation efficiency. As in the case of remote  
21 sensing studies, the causal link between aerosol perturbations and cloud microphysical responses  
22 (e.g.  $r_e$  or  $N_d$ ) is much better established than the relationship between aerosol and changes in  
23 cloud fraction, LWC, and precipitation (see also Levin and Cotton, 2008).

24  
25 *In situ* cloud measurements are usually regarded as “ground truth” for satellite retrievals but in  
26 fact there is considerable uncertainty in measured parameters such liquid water content (LWC),  
27 and size distribution, which forms the basis of other calculations such as drop concentration,  $r_e$   
28 and extinction. It is not uncommon to see discrepancies in LWC on the order of 50% between  
29 different instruments, and cloud drop size distributions are difficult to measure, particularly for  
30 droplets  $< 10 \mu\text{m}$  where Mie scattering oscillations generate ambiguities in drop size.  
31 Measurement uncertainty in  $r_e$  from *in situ* probes is assessed, for horizontally homogeneous  
32 clouds, to be on the order of 15-20%, compared to 10% for MODIS and 15-20% for other  
33 spectral measurements (Feingold et al., 2006). As with remote measurements it is prudent to  
34 consider relative (as opposed to absolute) changes in cloud microphysics related to relative  
35 changes in aerosol. An added consideration is that *in situ* measurements typically represent a  
36 very small sample of the atmosphere akin to a thin pencil line through a large volume. For an  
37 aircraft flying at  $100 \text{ ms}^{-1}$  and sampling at 1 Hz, the sample volume is on the order of  $10 \text{ cm}^3$ .  
38 The larger spatial sampling of remote sensing has the advantage of being more representative but  
39 it removes small-scale (i.e., sub sampling-volume) variability, and therefore may obscure  
40 important cloud processes.

41 Measurements at a wide variety of locations around the world have shown that increases in  
42 aerosol concentration lead to increases in  $N_d$ . However the rate of this increase is highly variable  
43 and always sub-linear, as exemplified by the compilation of data in Ramanathan et al. (2001a).  
44 This is because, as discussed previously,  $N_d$  is a function of numerous parameters in addition to

1 aerosol number concentration, including size distribution, updraft velocity (Leaith et al., 1996),  
2 and composition. In stratocumulus clouds, characterized by relatively low vertical velocity (and  
3 low supersaturation) only a small fraction of particles can be activated whereas in vigorous  
4 cumulus clouds that have high updraft velocities, a much larger fraction of aerosol particles is  
5 activated. Thus the ratio of  $N_d$  to aerosol particle number concentration is highly variable.

6 In recent years there has been a concerted effort to reconcile measured  $N_d$  concentrations with  
7 those calculated based on observed aerosol size and composition, as well as updraft velocity.  
8 These so-called “closure experiments” have demonstrated that on average, agreement in  $N_d$   
9 between these approaches is on the order of 20% (e.g., Conant et al., 2004). This provides  
10 confidence in theoretical understanding of droplet activation, however, measurement accuracy is  
11 not high enough to constrain the aerosol composition effects that have magnitudes  $< 20\%$ .

12 One exception to the rule that more aerosol particles result in larger  $N_d$  is the case of giant CCN  
13 (sizes on the order of a few microns), which, in concentrations on the order of  $1 \text{ cm}^{-3}$  (i.e.,  $\sim 1\%$   
14 of the total concentration) can lead to significant suppression in cloud supersaturation and  
15 reductions in  $N_d$  (O’Dowd et al., 1999). The measurement of these large particles is difficult and  
16 hence the importance of this effect is hard to assess. These same giant CCN, at concentrations as  
17 low as 1/liter, can significantly affect the initiation of precipitation in moderately polluted clouds  
18 (Johnson, 1982) and in so doing alter cloud albedo (Feingold et al., 1999).

19 The most direct link between the remote sensing of aerosol-cloud interactions discussed in  
20 section 2.3.5.1 and *in situ* observations is via observations of relationships between drop  
21 concentration  $N_d$  and CCN concentration. Theory shows that if  $r_e$ -CCN relationships are  
22 calculated at constant LWP or LWC, their logarithmic slope is  $-1/3$  that of the  $N_d$ -CCN  
23 logarithmic slope (i.e.  $d \ln r_e / d \ln \text{CCN} = -1/3 d \ln N_d / d \ln \text{CCN}$ ). In general,  $N_d$ -CCN slopes  
24 measured *in situ* tend to be stronger than equivalent slopes obtained from remote sensing –  
25 particularly in the case of satellite remote sensing (McComiskey and Feingold 2008). There are a  
26 number of reasons for this: (i) *in situ* measurements focus on smaller spatial scales and are more  
27 likely to observe the droplet activation process as opposed to remote sensing that incorporates  
28 larger spatial scales and includes other processes such as drop coalescence that reduce  $N_d$ , and  
29 therefore the slope of the  $N_d$ -CCN relationship (McComiskey et al., 2008b). (ii) Satellite remote  
30 sensing studies typically do not sort their data by LWP, and this has been shown to reduce the  
31 magnitude of the  $r_e$ -CCN response (Feingold, 2003).

32 In conclusion, observational estimates of aerosol indirect radiative forcings are still in their  
33 infancy. Effects on cloud microphysics that result in cloud brightening have to be considered  
34 along with effects on cloud lifetime, cover, vertical development and ice production. For *in situ*  
35 measurements, aerosol effects on cloud microphysics are reasonably consistent (within  $\sim 20\%$ )  
36 with theory but measurement uncertainties in remote sensing of aerosol effects on clouds, as well  
37 as complexity associated with three-dimensional radiative transfer, result in significant  
38 uncertainty in radiative forcing. The higher order indirect effects are poorly understood and even  
39 the sign of the microphysical response and forcing may not always be the same. Aerosol type  
40 and specifically the absorption properties of the aerosol may cause different cloud responses.  
41 Early estimates of observationally based aerosol indirect forcing range from  $-0.7$  to  $-1.7 \text{ Wm}^{-2}$   
42 (Nakajima et al, 2001) and  $-0.6$  to  $-1.2 \text{ Wm}^{-2}$  (Sekiguchi et al., 2003), depending on the estimate  
43 for aerosol increase from pre-industrial times and whether aerosol effects on cloud fraction are  
44 also included in the estimate.

## 2.4. Outstanding Issues

Despite substantial progress, as summarized in section 2.2 and 2.3, most measurement-based studies so far have concentrated on influences produced by the sum of natural and anthropogenic aerosols on solar radiation under clear sky conditions. Important issues remain:

- Because accurate measurements of aerosol absorption are lacking and land surface reflection values are uncertain, DRF estimates over land and at the ocean surface are less well constrained than the estimate of TOA DRF over ocean.
- Current estimates of the anthropogenic component of aerosol direct radiative forcing have large uncertainties, especially over land.
- Because there are very few measurements of aerosol absorption vertical distribution, mainly from aircraft during field campaigns, estimates of direct radiative forcing of above-cloud aerosols and profiles of atmospheric radiative heating induced by aerosol absorption are poorly constrained.
- There is a need to quantify aerosol impacts on thermal infrared radiation, especially for dust.
- The diurnal cycle of aerosol direct radiative forcing cannot be adequately characterized with currently available, sun-synchronous, polar orbiting satellite measurements.
- Measuring aerosol, cloud, and ambient meteorology contributions to indirect radiative forcing remains a major challenge.
- Long-term aerosol trends and their relationship to observed surface solar radiation changes are not well understood.

The current status and prospects for these areas are briefly discussed below.

**Measuring aerosol absorption and single-scattering albedo:** Currently, the accuracy of both *in situ* and remote sensing aerosol SSA measurements is generally  $\pm 0.03$  at best, which implies that the inferred accuracy of clear sky aerosol DRF would be larger than  $1 \text{ W m}^{-2}$  (see Chapter 1). Recently developed photoacoustic (Arnott et al., 1997) and cavity ring down extinction cell (Strawa et al., 2002) techniques for measuring aerosol absorption produce SSA with improved accuracy over previous methods. However, these methods are still experimental, and must be deployed on aircraft. Aerosol absorption retrievals from satellites using the UV-technique have large uncertainties associated with its sensitivity to the height of the aerosol layer(s) (Torres et al., 2005), and it is unclear how the UV results can be extended to visible wavelengths. Views in and out of sunglint can be used to retrieve total aerosol extinction and scattering, respectively, thus constraining aerosol absorption over oceans (Kaufman et al., 2002b). However, this technique requires retrievals of aerosol scattering properties, including the real part of the refractive index, well beyond what has so far been demonstrated from space. In summary, there is a need to pursue a better understanding of the uncertainty of *in situ* measured and remote sensing retrieved SSA in a robust way and, with this knowledge, to synthesize different data sets to yield a characterization of aerosol absorption with well-defined uncertainty (Leahy et al., 2007). Laboratory studies of aerosol absorption of specific known composition are also needed to interpret *in situ* measurements and remote sensing retrievals and to provide updated database of particle absorbing properties for models.

**Estimating the aerosol direct radiative forcing over land:** Land surface reflection is large, heterogeneous, and anisotropic, which complicates aerosol retrievals and DRF determination

1 from satellites. Currently, the aerosol retrievals over land have relatively lower accuracy than  
2 those over ocean (Section 2.2.5) and satellite data are rarely used alone for estimating DRF over  
3 land (Section 2.3). Several issues need to be addressed, such as developing appropriate angular  
4 models for aerosols over land (Patadia et al., 2008) and improving land surface reflectance  
5 characterization. MODIS and MISR measure land surface reflection wavelength dependence and  
6 angular distribution at high resolution (Moody et al., 2005; Martonchik et al., 1998b; 2002). This  
7 offers a promising opportunity for inferring the aerosol direct radiative forcing over land from  
8 satellite measurements of radiative fluxes (e.g., CERES) and from critical reflectance techniques  
9 (Fraser and Kaufman, 1985; Kaufman, 1987). The aerosol direct radiative forcing over land  
10 depends strongly on aerosol absorption and improved measurements of aerosol absorption are  
11 required.

12 **Distinguishing anthropogenic from natural aerosols:** Current estimates of anthropogenic  
13 components of AOD and direct radiative forcing have larger uncertainties than total aerosol  
14 optical depth and direct radiative forcing, particularly over land (see Section 2.3.4), because of  
15 relatively large uncertainties in the retrieved aerosol microphysical properties (see Section 2.2).  
16 Future measurements should focus on improved retrievals of such aerosol properties as size  
17 distribution, particle shape, and absorption, along with algorithm refinement for better aerosol  
18 optical depth retrievals. Coordinated *in situ* measurements offer a promising avenue for  
19 validating and refining satellite identification of anthropogenic aerosols (Anderson et al., 2005a,  
20 2005b). For satellite-based aerosol type characterization, it is sometimes assumed that all  
21 biomass-burning aerosol is anthropogenic and all dust aerosol is natural (Kaufman et al., 2005a).  
22 The better determination of anthropogenic aerosols requires a quantification of biomass burning  
23 ignited by lightning (natural origin) and mineral dust due to human induced changes of land  
24 cover/land use and climate (anthropogenic origin). Improved emissions inventories and better  
25 integration of satellite observations with models seem likely to reduce the uncertainties in  
26 aerosol source attribution.

27 **Profiling the vertical distributions of aerosols:** Current aerosol profile data are far from  
28 adequate for quantifying the aerosol radiative forcing and atmospheric response to the forcing.  
29 The data have limited spatial and temporal coverage, even for current spaceborne lidar  
30 measurements. Retrieving aerosol extinction profile from lidar measured attenuated backscatter  
31 is subject to large uncertainties resulting from aerosol type characterization. Current space-borne  
32 Lidar measurements are also not sensitive to aerosol absorption. Because of lack of aerosol  
33 vertical distribution observations, the estimates of DRF in cloudy conditions and dust DRF in the  
34 thermal infrared remain highly uncertain (Schulz et al., 2006; Sokolik et al., 2001; Lubin et al.,  
35 2002). It also remains challenging to constrain the aerosol-induced atmospheric heating rate  
36 increment that is essential for assessing atmospheric responses to the aerosol radiative forcing  
37 (e.g., Yu et al., 2002; Feingold et al., 2005; Lau et al., 2006). Progress in the foreseeable future is  
38 likely to come from (1) better use of existing, global, space-based backscatter lidar data to  
39 constrain model simulations, and (2) deployment of new instruments, such as high-spectral-  
40 resolution lidar (HSRL), capable of retrieving both extinction and backscatter from space. The  
41 HSRL lidar system will be deployed on the EarthCARE satellite mission tentatively scheduled  
42 for 2013 ([http://asimov/esrin.esi.it/esaLP/ASESMYNW9SC\\_Lpearthcare\\_1.html](http://asimov/esrin.esi.it/esaLP/ASESMYNW9SC_Lpearthcare_1.html)).

43 **Characterizing the diurnal cycle of aerosol direct radiative forcing:** The diurnal variability of  
44 aerosol can be large, depending on location and aerosol type (Smirnov et al., 2002), especially in

1 wildfire situations, and in places where boundary layer aerosols hydrate or otherwise change  
2 significantly during the day. This cannot be captured by currently available, sun-synchronous,  
3 polar orbiting satellites. Geostationary satellites provide adequate time resolution (Christopher  
4 and Zhang, 2002; Wang et al., 2003), but lack the information required to characterize aerosol  
5 types. Aerosol type information from low earth orbit satellites can help improve accuracy of  
6 geostationary satellite aerosol retrievals (Costa et al., 2004a, 2004b). For estimating the diurnal  
7 cycle of aerosol DRF, additional efforts are needed to adequately characterize the anisotropy of  
8 surface reflection (Yu et al., 2004) and daytime variation of clouds.

9 **Studying aerosol-cloud interactions and indirect radiative forcing:** Remote sensing estimates  
10 of aerosol indirect forcing are still rare and uncertain. Improvements are needed for both aerosol  
11 characterization and measurements of cloud properties, precipitation, water vapor, and  
12 temperature profiles. Basic processes still need to be understood on regional and global scales.  
13 Remote sensing observations of aerosol-cloud interactions and aerosol indirect forcing are for the  
14 most part based on simple correlations among variables, from which cause-and-effects cannot be  
15 deduced. One difficulty in inferring aerosol effects on clouds from the observed relationships is  
16 separating aerosol from meteorological effects, as aerosol loading itself is often correlated with  
17 the meteorology. In addition, there are systematic errors and biases in satellite aerosol retrievals  
18 for partly cloud-filled scenes. Stratifying aerosol and cloud data by liquid water content, a key  
19 step in quantifying the albedo (or first) indirect effect, is usually missing. Future work will need  
20 to combine satellite observations with in situ validation and modeling interpretation. A  
21 methodology for integrating observations (in situ and remote) and models at the range of relevant  
22 temporal/spatial scales is crucial to improve understanding of aerosol indirect effects and  
23 aerosol-cloud interactions.

24 **Quantifying long-term trends of aerosols at regional scales:** Because secular changes are  
25 subtle, and are superposed on seasonal and other natural variability, this requires the construction  
26 of consistent, multi-decadal records of climate-quality data. To be meaningful, aerosol trend  
27 analysis must be performed on a regional basis. Long-term trends of aerosol optical depth have  
28 been studied using measurements from surface remote sensing stations (e.g., Hoyt and Frohlich,  
29 1983; Augustine et al., 2008; Luo et al., 2001) and historic satellite sensors (Massie et al., 2004;  
30 Mishchenko et al., 2007a; Mishchenko and Geogdzhayev, 2007; Zhao et al., 2008a). An  
31 emerging multi-year climatology of high quality AOD data from modern satellite sensors (e.g.,  
32 Remer et al., 2008; Kahn et al., 2005a) has been used to examine the inter-annual variations of  
33 aerosol (e.g., Koren et al., 2007a, Mishchenko and Geogdzhayev, 2007) and contribute  
34 significantly to the study of aerosol trends. Current observational capability needs to be  
35 continued to avoid any data gaps. A synergy of aerosol products from historical, modern and  
36 future sensors is needed to construct as long a record as possible. Such a data synergy can build  
37 upon understanding and reconciliation of AOD differences among different sensors or platforms  
38 (Jeong et al., 2005). This requires overlapping data records for multiple sensors. A close  
39 examination of relevant issues associated with individual sensors is urgently needed, including  
40 sensor calibration, algorithm assumptions, cloud screening, data sampling and aggregation,  
41 among others.

42 **Linking aerosol long-term trends with changes of surface solar radiation:** Analysis of the  
43 long-term surface solar radiation record suggests significant trends during past decades (e.g.,  
44 Stanhill and Cohen, 2001; Wild et al., 2005; Pinker et al., 2005; Alpert et al., 2005). Although a

1 significant and widespread decline in surface total solar radiation (the sum of direct and diffuse  
2 irradiance) occurred up to 1990 (so-called solar dimming), a sustained increase has been  
3 observed during the subsequent decade. Speculation suggests that such trends result from  
4 decadal changes of aerosols and the interplay of aerosol direct and indirect radiative forcing  
5 (Stanhill and Cohen, 2001; Wild et al., 2005; Streets et al., 2006a; Norris and Wild, 2007;  
6 Ruckstuhl et al., 2008). However, reliable observations of aerosol trends are required test these  
7 ideas. In addition to aerosol optical depth, changes in aerosol composition must also be  
8 quantified, to account for changing industrial practices, environmental regulations, and biomass  
9 burning emissions (Novakov et al., 2003; Streets et al., 2004; Streets and Aunan et al., 2005).  
10 Such compositional changes will affect the aerosol SSA and size distribution, which in turn will  
11 affect the surface solar radiation (e.g., Qian et al., 2007). However such data are currently rare  
12 and subject to large uncertainties. Finally, a better understanding of aerosol-radiation-cloud  
13 interactions and trends in cloudiness, cloud albedo, and surface albedo is badly needed to  
14 attribute the observed radiation changes to aerosol changes with less ambiguity.

## 15 **2.5. Concluding Remarks**

16 Since the concept of aerosol-radiation-climate interactions was first proposed around 1970,  
17 substantial progress has been made in determining the mechanisms and magnitudes of these  
18 interactions, particularly in the last ten years. Such progress has greatly benefited from  
19 significant improvements in aerosol measurements and increasing sophistication of model  
20 simulations. As a result, knowledge of aerosol properties and their interaction with solar  
21 radiation on regional and global scales is much improved. Such progress plays a unique role in  
22 the definitive assessment of the global anthropogenic radiative forcing, as “*virtually certainly*  
23 *positive*” in IPCC AR4 (Haywood and Schulz, 2007).

24 *In situ* measurements of aerosols: New *in situ* instruments such as aerosol mass spectrometers,  
25 photoacoustic techniques, and cavity ring down cells provide high accuracy and fast time  
26 resolution measurements of aerosol chemical and optical properties. Numerous focused field  
27 campaigns and the emerging ground-based aerosol networks are improving regional aerosol  
28 chemical, microphysical, and radiative property characterization. Aerosol closure studies of  
29 different measurements indicate that measurements of submicrometer, spherical sulfate and  
30 carbonaceous particles have a much better accuracy than that for dust-dominated aerosol. The  
31 accumulated comprehensive data sets of regional aerosol properties provide a rigorous “test bed”  
32 and strong constraint for satellite retrievals and model simulations of aerosols and their direct  
33 radiative forcing.

34 Remote sensing measurements of aerosols: Surface networks, covering various aerosol regimes  
35 around the globe, have been measuring aerosol optical depth with an accuracy of 0.01~0.02,  
36 which is adequate for achieving the accuracy of  $1 \text{ Wm}^{-2}$  for cloud-free TOA DRF. On the other  
37 hand, aerosol microphysical properties retrieved from these networks, especially SSA, have  
38 relatively large uncertainties and are only available in very limited conditions. Current satellite  
39 sensors can measure AOD with an accuracy of about 0.05 or 15 to 20% in most cases. The  
40 implementation of multi-wavelength, multi-angle, and polarization measuring capabilities has  
41 also made it possible to measure particle properties (size, shape, and absorption) that are  
42 essential for characterizing aerosol type and estimating anthropogenic component of aerosols.  
43 However, these microphysical measurements are more uncertain than AOD measurements.



1 Observational estimates of clear-sky aerosol direct radiative forcing: Closure studies based on  
2 focused field experiments reveal DRF uncertainties of about 25% for sulfate/carbonaceous  
3 aerosol and 60% for dust at regional scales. The high-accuracy of MODIS, MISR and POLDER  
4 aerosol products and broadband flux measurements from CERES make it feasible to obtain  
5 observational constraints for aerosol TOA DRF at a global scale, with relaxed requirements for  
6 measuring particle microphysical properties. Major conclusions from the assessment are:

- 7 • A number of satellite-based approaches consistently estimate the clear-sky diurnally  
8 averaged TOA DRF (on solar radiation) to be about  $-5.5 \pm 0.2 \text{ Wm}^{-2}$  (mean  $\pm$  standard  
9 error from various methods) over global ocean. At the ocean surface, the diurnally  
10 averaged DRF is estimated to be  $-8.7 \pm 0.7 \text{ Wm}^{-2}$ . These values are calculated for the  
11 difference between today's measured total aerosol (natural plus anthropogenic) and the  
12 absence of all aerosol.
- 13 • Overall, in comparison to that over ocean, the DRF estimates over land are more poorly  
14 constrained by observations and have larger uncertainties. A few satellite retrieval and  
15 satellite-model integration yield the over-land clear-sky diurnally averaged DRF of  
16  $-4.9 \pm 0.7 \text{ Wm}^{-2}$  and  $-11.8 \pm 1.9 \text{ Wm}^{-2}$  at the TOA and surface, respectively. These values  
17 over land are calculated for the difference between total aerosol and the complete absence  
18 of all aerosol.
- 19 • Use of satellite measurements of aerosol microphysical properties yields that on a global  
20 ocean average, about 20% of AOD is contributed by human activities and the clear-sky  
21 TOA DRF by anthropogenic aerosols is  $-1.1 \pm 0.4 \text{ Wm}^{-2}$ . Similar DRF estimates are rare  
22 over land, but a few measurement-model integrated studies do suggest much more  
23 negative DRF over land than over ocean.
- 24 • These satellite-based DRF estimates are much greater than the model-based estimates,  
25 with differences much larger at regional scales than at a global scale.

26 Measurements of aerosol-cloud interactions and indirect radiative forcing: *In situ* measurement  
27 of cloud properties and aerosol effects on cloud microphysics suggest that theoretical  
28 understanding of the activation process for water cloud is reasonably well-understood. Remote  
29 sensing of aerosol effects on droplet size associated with the albedo effect tends to underestimate  
30 the magnitude of the response compared to *in situ* measurements. Recent efforts trace this to a  
31 combination of lack of stratification of data by cloud water, the relatively large spatial scale over  
32 which measurements are averaged (which includes variability in cloud fields, and processes that  
33 obscure the aerosol-cloud processes), as well as measurement uncertainties (particularly in  
34 broken cloud fields). It remains a major challenge to infer aerosol number concentrations from  
35 satellite measurements. The present state of knowledge of the nature and abundance of IN, and  
36 ice formation in clouds is extremely poor.

37  
38 Despite the substantial progress in recent decades, several important issues remain, such as  
39 measurements of aerosol size distribution, particle shape, absorption, and vertical profiles, and  
40 the detection of aerosol long-term trend and establishment of its connection with the observed  
41 trends of solar radiation reaching the surface, as discussed in section 2.4. To further the  
42 understanding of aerosol impacts on climate, coordinated research strategy needs to be  
43 developed to improve the measurement accuracy and use the measurements to validate and  
44 effectively constrain model simulations. Concepts of future research in measurements are  
45 discussed in Chapter 4 "Way Forward".

# CHAPTER 3

## Modeling the Effects of Aerosols on Climate

**Lead authors:** David Rind, NASA GISS; Mian Chin, NASA GSFC; Graham Feingold, NOAA ESRL; David G. Streets, DOE ANL

**Contributing authors:** Ralph A. Kahn, NASA GSFC; Stephen E. Schwartz, DOE BNL; Hongbin Yu, NASA GSFC/UMBC

### 3.1. Introduction

The IPCC Fourth Assessment Report (AR4) (IPCC, 2007) concludes that man's influence on the warming climate is in the category of "very likely". This conclusion is based on, among other things, the ability of models to simulate the global and, to some extent, regional variations of temperature over the past 50 to 100 years. When anthropogenic effects are included, the simulations can reproduce the observed warming (primarily for the past 50 years); when they are not, the models do not get very much warming at all. In fact, all of the models runs for the IPCC AR4 assessment (more than 20 here) produce this distinctive result, driven by the greenhouse gas increases that have been observed to occur.

These results were produced in models whose global warming associated with a doubled CO<sub>2</sub> forcing of about 4 W m<sup>-2</sup> was on average of an order of 3°C, hence translating this into a climate sensitivity (surface temperature change in response to atmospheric CO<sub>2</sub> change) of 0.75°C/Wm<sup>-2</sup>. The determination of this value is crucial to predicting the future impact of increased greenhouse gases, and the credibility of this predicted value relies on the ability of these models to simulate the observed temperature changes over the past century. However, in producing the observed temperature trend in the past, the models made use of very uncertain aerosol forcing. The greenhouse gas change by itself produces warming in models that exceeds that observed by some 40% on average (IPCC, 2007). Cooling associated with aerosols reduces this warming to the observed level. Different climate models use differing aerosol forcings, both direct (aerosol scattering and absorption of short and longwave radiation) and indirect (aerosol effect on cloud cover reflectivity and lifetime), whose magnitudes vary markedly from one model to the next. Kiehl (2007) using nine of the IPCC (2007) AR4 climate models found that they had a factor of three forcing differences in the aerosol contribution for the 20th century. The differing aerosol forcing is the prime reason why models whose climate sensitivity varies by almost a factor of three can produce the observed trend. It was thus concluded that the uncertainty in IPCC (2007) anthropogenic climate simulations for the past century should really be much greater than stated (Schwartz et al., 2007; Kerr, 2007), since, in general, models with low/high sensitivity to greenhouse warming used weaker/stronger aerosol cooling to obtain the same temperature response (Kiehl, 2007). Had the situation been reversed and the low/high sensitivity models used strong/weak aerosol forcing, there would have been a greater divergence in model simulations of the past century.

Therefore, the fact that a model has accurately reproduced the global temperature change in the past does not imply that its future forecast is reliable. This state of affairs will remain until a

1 firmer estimate of radiative forcing (RF) by aerosols, in addition to that by greenhouse gases, is  
2 available.

3 Two different approaches are used to assess the aerosol effect on climate. “Forward modeling”  
4 studies incorporate different aerosol types and attempt to explicitly calculate the aerosol RF.  
5 From this approach, IPCC (2007) concluded that the best estimate of the global aerosol direct RF  
6 (compared with preindustrial times) is  $-0.5$  ( $-0.9$  to  $-0.1$ )  $\text{W m}^{-2}$  (see Figure 1.3, Chapter 1). The  
7 RF due to the cloud albedo or brightness effect (also referred to as first indirect or Twomey  
8 effect) is estimated to be  $-0.7$  ( $-1.8$  to  $-0.3$ )  $\text{W m}^{-2}$ . No estimate was specified for the effect  
9 associated with cloud lifetime. The total negative RF due to aerosols according to IPCC (2007)  
10 estimates (see Figure 1.3 in Chapter 1) is then  $-1.3$  ( $-2.2$  to  $-0.5$ )  $\text{W m}^{-2}$ . In comparison, the  
11 positive radiative forcing (RF) from greenhouse gases (including tropospheric ozone) is  
12 estimated to be  $+2.9 \pm 0.3$   $\text{W m}^{-2}$ ; hence tropospheric aerosols reduce the influence from  
13 greenhouse gases by about 45% (15-85%). This approach however inherits large uncertainties in  
14 aerosol amount, composition, and physical and optical properties in modeling of atmospheric  
15 aerosols. The consequences of these uncertainties are discussed in the next section.

16 The other method of calculating aerosol forcing is called the “inverse approach” – it is assumed  
17 that the observed climate change is primarily the result of the known climate forcing  
18 contributions. If one further assumes a particular climate sensitivity (or a range of sensitivities),  
19 one can determine what the total forcing had to be to produce the observed temperature change.  
20 The aerosol forcing is then deduced as a residual after subtraction of the greenhouse gas forcing  
21 along with other known forcings from the total value. Studies of this nature come up with aerosol  
22 forcing ranges of  $-0.6$  to  $-1.7$   $\text{W m}^{-2}$  (Knutti et al., 2002, 2003; IPCC AR4 Chap.9);  $-0.4$  to  $-1.6$   
23  $\text{W m}^{-2}$  (Gregory et al., 2002); and  $-0.4$  to  $-1.4$   $\text{W m}^{-2}$  (Stott et al., 2006). This approach however  
24 provides a bracket of the possible range of aerosol forcing without the assessment of current  
25 knowledge of the complexity of atmospheric aerosols.

26 This chapter reviews the current state of aerosol RF in the global models and assesses the  
27 uncertainties in these calculations. First representation of aerosols in the forward global  
28 chemistry and transport models and the diversity of the model simulated aerosol fields are  
29 discussed; then calculation of the aerosol direct and indirect effects in the climate models is  
30 reviewed; finally the impacts of aerosols on climate model simulations and their implications are  
31 assessed.

## 32 **3.2. Modeling of Atmospheric Aerosols**

33 The global aerosol modeling capability has developed rapidly in the past decade. In the late  
34 1990s, there were only a few global models that were able to simulate one or two aerosol  
35 components, but now there are a few dozen global models that simulate a comprehensive suite of  
36 aerosols in the atmosphere. As introduced in Chapter 1, aerosols consist of a variety of species  
37 including dust, sea salt, sulfate, nitrate, and carbonaceous aerosols (black and organic carbon)  
38 produced from natural and man-made sources with a wide range of physical and optical  
39 properties. Because of the complexity of the processes and composition and highly  
40 inhomogeneous distributions of aerosols, accurately modeling atmospheric aerosols and their  
41 effects remain a challenge. Models have to take into account not only the aerosol and precursor  
42 emissions, but also the chemical transformation, transport, and removal processes (e.g. dry and  
43 wet depositions) to simulate the aerosol mass concentrations. Furthermore, aerosol particle size

1 can grow in the atmosphere because the ambient water vapor can condense on the aerosol  
2 particles. This “swelling” process, called hygroscopic growth, is most commonly parameterized  
3 in the models as a function of relative humidity.

#### 4 **3.2.1. Estimates of Emissions**

5 Aerosols have various sources from natural and anthropogenic processes. Natural emissions  
6 include wind-blown mineral dust, aerosol and precursor gases from volcanic eruptions, natural  
7 wild fires, vegetation, and oceans. Anthropogenic sources include emissions from fossil fuel and  
8 biofuel combustion, industrial processes, agriculture practices, and human-induced biomass  
9 burning.

10 Following earlier attempts to quantify man-made primary emissions of aerosols (Turco et al.,  
11 1983; Penner et al., 1993) systematic work was undertaken in the late 1990s to calculate  
12 emissions of black carbon (BC) and organic carbon (OC), using fuel-use data and measured  
13 emission factors (Liousse et al., 1996; Cooke and Wilson, 1996; Cooke et al., 1999). The work  
14 was extended in greater detail and with improved attention to source-specific emission factors in  
15 Bond et al. (2004), which provides global inventories of BC and OC for the year 1996, with  
16 regional and source-category discrimination that includes contributions from industrial,  
17 transportation, residential solid-fuel combustion, vegetation and open biomass burning (forest  
18 fires, agricultural waste burning, etc.), and diesel vehicles.

19 Emissions from natural sources—which include wind-blown mineral dust, wildfires, sea salt, and  
20 volcanic eruptions—are less well quantified, mainly because of the difficulties of measuring  
21 emission rates in the field and the unpredictable nature of the events. Often, emissions must be  
22 inferred from ambient observations at some distance from the actual source. As an example, it  
23 was concluded (Lewis and Schwartz, 2004) that available information on size-dependent sea salt  
24 production rates could only provide order-of-magnitude estimates. The natural emissions in  
25 general can vary dramatically over space and time.

26 Aerosols can be produced from trace gases in the atmospheric via chemical reactions, and those  
27 aerosols are called *secondary* aerosols, as distinct from *primary* aerosols that are directly emitted  
28 to the atmosphere as aerosol particles. For example, most sulfate and nitrate aerosols are  
29 secondary aerosols that are formed from their precursor gases, sulfur dioxide (SO<sub>2</sub>) and nitrogen  
30 oxides (NO and NO<sub>2</sub>, collectively called NO<sub>x</sub>), respectively. Those sources have been studied for  
31 many years and are relatively well known. By contrast, the sources of secondary organic aerosols  
32 (SOA) are poorly understood, including emissions of their precursor gases (called volatile  
33 organic compounds, VOC) from both natural and anthropogenic sources and the atmospheric  
34 production processes.

35 Globally, sea salt and mineral dust dominate the total aerosol mass emissions because of the  
36 large source areas and/or large particle sizes. However, sea salt and dust also have shorter  
37 atmospheric lifetimes because of their large particle size, and are radiatively less active than  
38 aerosols with small particle size, such as sulfate, nitrate, BC, and particulate organic matter  
39 (POM, which includes both carbon and non-carbon mass in the organic aerosol, see Glossary),  
40 most of which are anthropogenic in origin.

41 Because the anthropogenic aerosol RF is usually evaluated (e.g., by the IPCC) as the  
42 anthropogenic perturbation since the pre-industrial period, it is necessary to estimate the

1 historical emission trends, especially the emissions in the pre-industrial era. Compared to  
 2 estimates of present-day emissions, estimates of historical emission have much larger  
 3 uncertainties. Information for past years on the source types and strengths and even locations are  
 4 difficult to obtain, so historical inventories from pre-industrial times to the present have to be  
 5 based on limited knowledge and data. Several studies on historical emission inventories of BC  
 6 and OC (e.g., Novakov et al., 2003; Ito and Penner 2005; Bond et al., 2007; Fernandes et al.,  
 7 2007; Junker and Liousse, 2008), SO<sub>2</sub> (Stern, 2005), and various species (van Aardenne et al.,  
 8 2001; Dentener et al., 2006) are available in the literature; there are some similarities and some  
 9 differences among them, but the emission estimates for early times do not have the rigor of the  
 10 studies for present-day emissions. One major conclusion from all these studies is that the growth  
 11 of primary aerosol emissions in the 20th century was not nearly as rapid as the growth in CO<sub>2</sub>  
 12 emissions. This is because in the late 19th and early 20th centuries, particle emissions such as  
 13 BC and POM were relatively high due to the heavy use of biofuels and the lack of particulate  
 14 controls on coal-burning facilities; however, as economic development continued, traditional  
 15 biofuel use remained fairly constant and particulate emissions from coal burning were reduced  
 16 by the application of technological controls (Bond et al., 2007). Thus, particle emissions in the  
 17 20th century did not grow as fast as CO<sub>2</sub> emissions, as the latter are roughly proportional to total  
 18 fuel use—oil and gas included. Another challenge is estimating historical biomass burning  
 19 emissions. A recent study suggested about a 40% increase in carbon emissions from biomass  
 20 burning from the beginning to the end of last century (Mouillot et al., 2006), but it is difficult to  
 21 verify.

22 As an example, **Table 3.1** shows estimated  
 23 anthropogenic emissions of sulfur, BC and POM  
 24 in the present day (year 2000) and pre-industrial  
 25 time (1750) compiled by Dentener et al., 2006.  
 26 These estimates have been used in the Aerosol  
 27 Comparisons between Observations and Models  
 28 (AeroCom) project (Experiment B, which uses  
 29 the year 2000 emission; and Experiment PRE,  
 30 which uses pre-industrial emissions), for  
 31 simulating atmospheric aerosols and  
 32 anthropogenic aerosol RF. The AeroCom results  
 33 are discussed in Sections 3.2.2 and 3.3.

34 Projections of aerosol emissions into the future  
 35 have been made, for example, in support of the  
 36 IPCC Third Assessment Report (TAR) (IPCC,  
 37 2001). More recent forecasts of future BC and  
 38 OC emissions based on future energy and fuel  
 39 scenarios take care to incorporate the likely  
 40 future effects of new technology deployment and  
 41 environmental regulation (e.g., Streets et al.,  
 42 2004; Rao et al., 2005). The expectation is that  
 43 global emissions of carbonaceous aerosols (BC  
 44 and OC) will likely remain flat or slightly  
 45 decrease out to 2050. Prospective emissions

**Table 3.1.** Anthropogenic emissions of aerosols and precursors for 2000 and 1750. Adapted from Dentener et al., 2006.

Source	Species*	Emission <sup>#</sup> 2000 (Tg/yr)	Emission 1750 (Tg/yr)
Biomass burning	BC	3.1	1.03
	POM	34.7	12.8
	S	4.1	1.46
Biofuel	BC	1.6	0.39
	POM	9.1	1.56
	S	9.6	0.12
Fossil fuel	BC	3.0	
	POM	3.2	
	S	98.9	

<sup>#</sup>Data source for 2000 emission: biomass burning – Global Fire Emission Dataset (GFED); biofuel BC and POM – Speciated Pollutant Emission Wizard (SPEW); biofuel sulfur – International Institute for Applied System Analysis (IIASA); fossil fuel BC and POM – SPEW; fossil fuel sulfur – Emission Database for Global Atmospheric Research (EDGAR) and IIASA. Fossil fuel emission of sulfur (S) is the sum of emission from industry, power plants, and transportation listed in Dentener et al., 2006.

\*S=sulfur, including SO<sub>2</sub> and particulate sulfate. Most emitted as SO<sub>2</sub>, and 2.5% emitted as sulfate.

1 depend strongly on assumptions about future emission controls. The effect of such emissions on  
2 future aerosol composition is discussed in Synthesis and Assessment Product (SAP) 3.2.

### 3 **3.2.2. Aerosol Mass Loading and Optical Depth**

4 In the global models, aerosols are usually simulated in the successive steps of sources (emission  
5 and chemical formation), transport (from source location to other area), and removal processes  
6 (dry deposition, in which particles fall onto the surface, and wet deposition by rain) that control  
7 the aerosol lifetime. Collectively, emission, transport, and removal determine the amount (mass)  
8 of aerosols in the atmosphere.

9 Aerosol optical depth (AOD), which is a measure of solar or thermal radiation being attenuated  
10 by aerosol particles via scattering or absorption, can be related to the atmospheric aerosol mass  
11 loading as follows:

$$12 \quad AOD = MEE \cdot M \quad (3.1)$$

13 where  $M$  is the aerosol mass loading per unit area ( $\text{g m}^{-2}$ ),  $MEE$  is the mass extinction efficiency  
14 or specific extinction in unit of  $\text{m}^2 \text{g}^{-1}$ , which is

$$15 \quad MEE = \frac{3Q_{ext}}{4\pi\rho r_{eff}} \cdot f \quad (3.2)$$

16 where  $Q_{ext}$  is the extinction coefficient (a function of particle size distribution and refractive  
17 index),  $r_{eff}$  is the aerosol particle effective radius,  $\rho$  is the aerosol particle density, and  $f$  is the  
18 ratio of ambient aerosol mass (wet) to dry aerosol mass  $M$ . Here,  $M$  is the result from model-  
19 simulated atmospheric processes and  $MEE$  embodies the aerosol physical (including  
20 microphysical) and optical properties. Since  $Q_{ext}$  varies with radiation wavelength, so do  $MEE$   
21 and AOD. AOD is the quantity that is most commonly obtained from remote sensing  
22 measurements and is frequently used for model evaluation (see Chapter 2). AOD is also a key  
23 parameter determining aerosol radiative effects.

24 Here the results from the recent multiple-global-model studies by the AeroCom project are  
25 summarized, as they represent the current assessment of model-simulated atmospheric aerosol  
26 loading, optical properties, and RF for the present-day. AeroCom aims to document differences  
27 in global aerosol models and compare the model output to observations. Sixteen global models  
28 participated in the AeroCom Experiment A, for which every model used their own configuration,  
29 including their own choice of estimating emissions (Kinne et al., 2006; Textor et al., 2006). Five  
30 major aerosol types: sulfate, BC, POM, dust, and sea salt, were included in the experiments,  
31 although some models had additional aerosol species. Of those major aerosol types, dust and sea-  
32 salt are predominantly natural in origin, whereas sulfate, BC, and POM have major  
33 anthropogenic sources.

34 **Table 3.2** summarizes the model results from the AeroCom-A for several key parameters:  
35 Sources (emission and chemical transformation), mass loading, lifetime, removal rates,  $MEE$  and  
36 AOD at a commonly used, mid-visible, wavelength of 550 nanometer (nm). These are the  
37 globally averaged values for the year 2000. Major features and conclusions are:  
38

- 1 • Globally, aerosol source (in mass) is dominated by sea salt, followed by dust, sulfate,  
2 particulate organic matter, and black carbon. Over the non-desert land area, human  
3 activity is the major source of sulfate, black carbon, and organic aerosols.
- 4 • Aerosols are removed from the atmosphere by wet and dry deposition. Although sea salt  
5 dominates the emissions, it is quickly removed from the atmosphere because of its large  
6 particle size and near-surface distributions, thus having the shortest lifetime. The median  
7 lifetime of sea salt from the AeroCom-A models is less than half a day, whereas dust and  
8 sulfate have similar lifetimes of 4 days and BC and POM 6-7 days.
- 9 • Globally, small-particle-sized sulfate, BC, and POM make up a little over 10% of total  
10 aerosol mass in the atmosphere. However, they are mainly from anthropogenic activity,  
11 so the highest concentrations are in the most populated regions, where their effects on  
12 climate and air quality are major concerns.
- 13 • Sulfate and BC have their highest MEE at mid-visible wavelengths, whereas dust is  
14 lowest among the aerosol types modeled. That means for the same amount of aerosol  
15 mass, sulfate and BC are more effective at attenuating (scattering or absorbing) solar  
16 radiation than dust. This is why the sulfate AOD is about the same as dust AOD even  
17 though the atmospheric amount of sulfate mass is 10 times less than that of the dust.
- 18 • There are large differences, or diversities, among the models for all the parameters listed  
19 in Table 3.2. The largest model diversity, shown as the % standard deviation from the all-  
20 model-mean and the range (minimum and maximum values) in Table 3.2, is in sea salt  
21 emission and removal; this is mainly associated with the differences in particle size range  
22 and source parameterizations in each model. The diversity of sea salt atmospheric loading  
23 however is much smaller than that of sources or sinks, because the largest particles have  
24 the shortest lifetimes even though they comprise the largest fraction of emitted and  
25 deposited mass.
- 26 • Among the key parameters compared in Table 3.2, the models agree best for simulated  
27 total AOD – the % of standard deviation from the model mean is 18%, with the extreme  
28 values just a factor of 2 apart. The median value of the multi-model simulated global  
29 annual mean total AOD, 0.127, is also in agreement with the global mean values from  
30 recent satellite measurements. However, despite the general agreement in total AOD,  
31 there are significant diversities at the individual component level for aerosol optical  
32 thickness, mass loading, and mass extinction efficiency. This indicates that uncertainties  
33 in assessing aerosol climate forcing are still large, and they depend not only on total AOD  
34 but also on aerosol absorption and scattering direction (see Glossary), both of which are  
35 determined by aerosol physical and optical properties. In addition, even with large  
36 differences in mass loading and MEE among different models, these terms could  
37 compensate for each other (eq. 3.1) to produce similar AOD. This is illustrated in **Figure**  
38 **3.1**. For example, model LO and LS have quite different mass loading (44 and 74 mg m<sup>-2</sup>,  
39 respectively), especially for dust and sea salt amount, but they produce nearly identical  
40 total AOD (0.127 and 0.128, respectively).
- 41 • Because of the large spatial and temporal variations of aerosol distributions, regional and  
42 seasonal diversities are even larger than the diversity for global annual means.

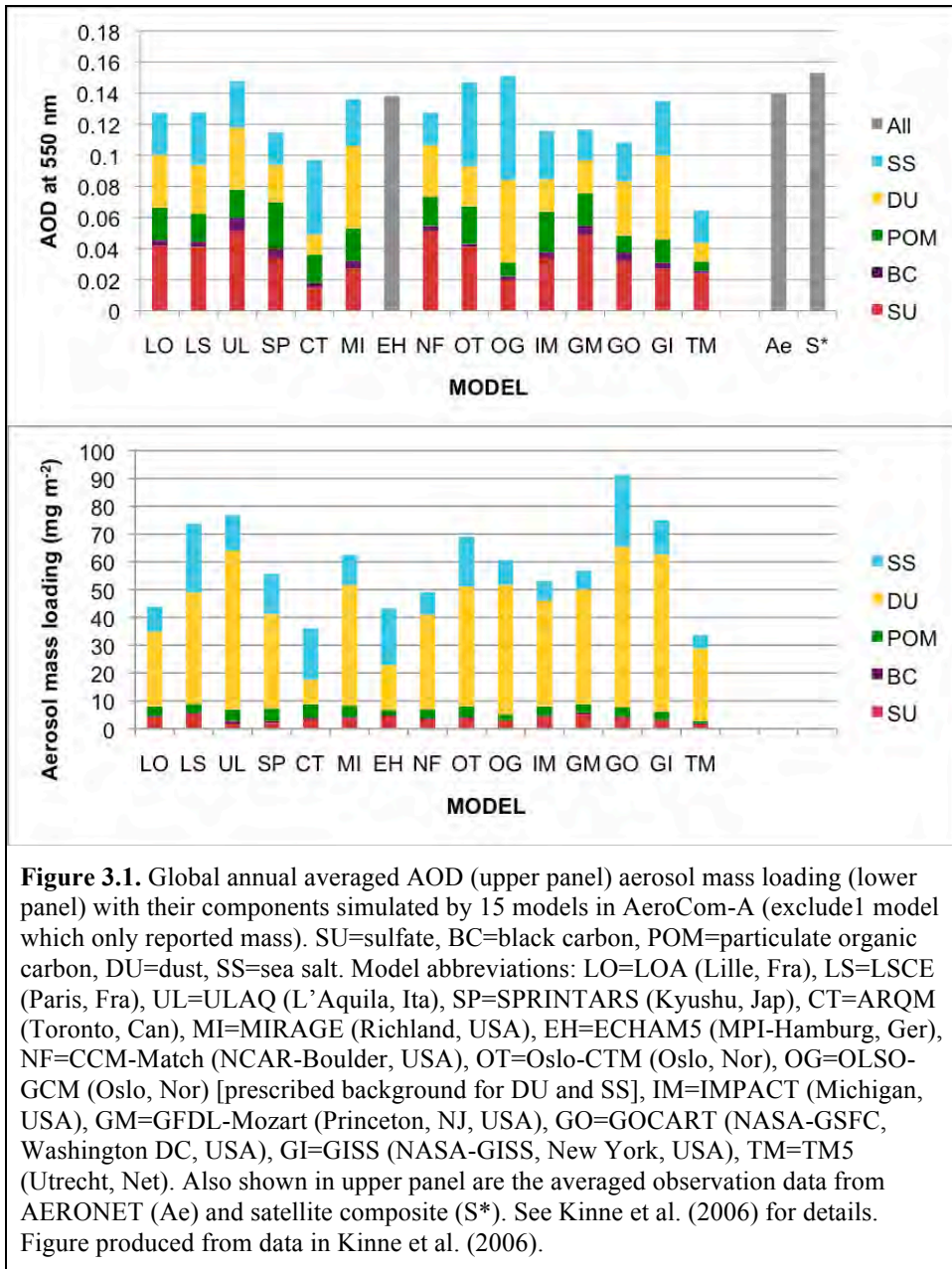
**Table 3.2.** Summary of statistics of AeroCom Experiment A results from 16 global models. Data from Textor et al. (2006) and Kinne et al. (2006), and AeroCom website (<http://nansen.ipsl.jussieu.fr/AEROCOM/data.html>).

	Mean	Median	Range	Stddev /mean*
<b>Sources (Tg yr<sup>-1</sup>):</b>				
Sulfate	179	186	98 – 232	22%
Black carbon	11.9	11.3	7.8 – 19.4	23%
Organic matter	96.6	96.0	53 – 138	26%
Dust	1840	1640	672 – 4040	49%
Sea salt	16600	6280	2180 – 121000	199%
<b>Removal rate (day<sup>-1</sup>):</b>				
Sulfate	0.25	0.24	0.19 – 0.39	18%
Black carbon	0.15	0.15	0.066 – 0.19	21%
Organic matter	0.16	0.16	0.09 – 0.23	24%
Dust	0.31	0.25	0.14 – 0.79	62%
Sea salt	5.07	2.50	0.95 – 35.0	188%
<b>Lifetime (day):</b>				
Sulfate	4.12	4.13	2.6 – 5.4	18%
Black carbon	7.12	6.54	5.3 – 15	33%
Organic matter	6.54	6.16	4.3 – 11	27%
Dust	4.14	4.04	1.3 – 7.0	43%
Sea salt	0.48	0.41	0.03 – 1.1	58%
<b>Mass loading (Tg):</b>				
Sulfate	1.99	1.98	0.92 – 2.70	25%
Black carbon	0.24	0.21	0.046 – 0.51	42%
Organic matter	1.70	1.76	0.46 – 2.56	27%
Dust	19.2	20.5	4.5 – 29.5	40%
Sea salt	7.52	6.37	2.5 – 13.2	54%
<b>MEE at 550 nm (m<sup>2</sup> g<sup>-1</sup>):</b>				
Sulfate	11.3	9.5	4.2 – 28.3	56%
Black carbon	9.4	9.2	5.3 – 18.9	36%
Organic matter	5.7	5.7	3.7 – 9.1	26%
Dust	0.99	0.95	0.46 – 2.05	45%
Sea salt	3.0	3.1	0.97 – 7.5	55%
<b>AOD at 550 nm:</b>				
Sulfate	0.035	0.034	0.015 – 0.051	33%
Black carbon	0.004	0.004	0.002 – 0.009	46%
Organic matter	0.018	0.019	0.006 – 0.030	36%
Dust	0.032	0.033	0.012 – 0.054	44%
Sea salt	0.033	0.030	0.02 – 0.067	42%
Total AOT at 550 nm	0.124	0.127	0.065 – 0.151	18%
*Stddev/mean was used as the term “diversity” in Textor et al., 2006.				

1  
2 To further isolate the impact of the differences in emissions on the diversity of simulated aerosol  
3 mass loading, identical emissions for aerosols and their precursor were used in the AeroCom  
4 Experiment B exercise in which 12 of the 16 AeroCom-A models participated (Textor et al.,  
5 2007). The comparison of the results and diversity between AeroCom-A and -B for the same  
6 models showed that using harmonized emissions does not significantly reduce model diversity  
7 for the simulated global mass and AOD fields, indicating that the differences in atmospheric  
8 processes, such as transport, removal, chemistry, and aerosol microphysics, play more important  
9 roles than emission in creating diversity among the models. This outcome is somewhat different



1 from another recent study, in which the differences in calculated clear-sky aerosol RF between  
 2 two models (a regional model STEM and a global model MOZART) were attributed mostly to  
 3 the differences in emissions (Bates et al., 2006), although the conclusion was based on only two  
 4 model simulations for a few focused regions. It is highly recommended from the outcome of  
 5 AeroCom-A and -B that, although more detailed evaluation for each individual process is  
 6 needed, multi-model ensemble results, e.g., median values of multi-model output variables,  
 7 should be used to estimate aerosol RF, due to their greater robustness, relative to individual  
 8 models, when compared to observations (Textor et al., 2006, 2007; Schulz et al., 2006).



### 3.3. Calculating Aerosol Direct Radiative Forcing

The three parameters that define the aerosol direct RF are the AOD, the single scattering albedo (SSA), and the asymmetry factor ( $g$ ), all of which are wavelength dependent. AOD is indicative of how much aerosol exists in the column, SSA is the fraction of radiation being scattered versus the total attenuation (scattered and absorbed), and the  $g$  relates to the direction of scattering that is related to the size of the particles (see Chapter 1). An indication of the particle size is provided by another parameter, the Ångström exponent ( $\text{Å}$ ), which is a measure of differences of AOD at different wavelengths. For typical tropospheric aerosols,  $\text{Å}$  tends to be inversely dependent on particle size; larger values of  $\text{Å}$  are generally associated with smaller aerosols particles. These parameters are further related; for example, for a given composition, the ability of a particle to scatter radiation decreases more rapidly with decreasing size than does its ability to absorb, so at a given wavelength varying  $\text{Å}$  can change SSA. Note that AOD, SSA,  $g$ ,  $\text{Å}$ , and all the other parameters in eq. 3.1 and 3.2 vary with space and time due to variations of both aerosol composition and relative humidity, which influence these characteristics.

In the recent AeroCom project, aerosol direct RF for the solar spectral wavelengths (or shortwave) was assessed based on the 9 models that participated in both Experiment B and PRE in which identical, prescribed emissions for present (year 2000) and pre-industrial time (year 1750) listed in Table 3.1 were used across the models (Schulz et al., 2006). The anthropogenic direct RF was obtained by subtracting AeroCom-PRE from AeroCom-B simulated results. Because dust and sea salt are predominantly from natural sources, they were not included in the anthropogenic RF assessment although the land use practice can contribute to dust emissions as “anthropogenic”. Other aerosols that were not considered in the AeroCom forcing assessment were natural sulfate (e.g. from volcanoes or ocean) and POM (e.g. from biogenic hydrocarbon oxidation), as well as nitrate. The aerosol direct forcing in the AeroCom assessment thus comprises three major anthropogenic aerosol components sulfate, BC, and POM.

The IPCC AR4 (IPCC, 2007) assessed anthropogenic aerosol RF based on the model results published after the IPCC TAR in 2001, including those from the AeroCom study discussed above. These results (adopted from IPCC AR4) are shown in **Table 3.3** for sulfate and **Table 3.4** for carbonaceous aerosols (BC and POM), respectively. All values listed in Table 3.3 and 3.4 refer to anthropogenic perturbation, i.e. excluding the natural fraction of these aerosols. In addition to the mass burden, MEE, and AOD, Table 3.3 and 3.4 also list the “normalized forcing”, also known as “forcing efficiency”, one for the forcing per unit AOD, and the other the forcing per gram of aerosol mass (dry). For some models, aerosols are externally mixed, that is, each aerosol particle contains only one aerosol type such as sulfate, whereas other models allow aerosols to mix internally to different degrees, that is, each aerosol particle can have more than one component, such as black carbon coated with sulfate. For models with internal mixing of aerosols, the component values for AOD, MEE, and forcing were extracted (Schulz et al., 2006).

Considerable variation exists among these models for all quantities in Table 3.3 and 3.4. The RF for all the components varies by a factor of 6 or more: Sulfate from 0.16 to 0.96  $\text{W m}^{-2}$ , POM from -0.06 to -0.34  $\text{W m}^{-2}$ , and BC from +0.08 to +0.61  $\text{W m}^{-2}$ , with the standard deviation in the range of 30 to 40% of the ensemble mean. It should be noted that although BC has the lowest mass loading and AOD, it is the only aerosol species that absorbs strongly, thus causing positive

1 forcing to warm the  
 2 atmosphere, in contrast to  
 3 other aerosols that impose  
 4 negative forcing that cools  
 5 the atmosphere. As a result,  
 6 the net anthropogenic aerosol  
 7 forcing as a whole becomes  
 8 more negative. The global  
 9 average anthropogenic  
 10 aerosol direct RF at the top  
 11 of the atmosphere (TOA)  
 12 from the models, together  
 13 with observation-based  
 14 estimates (see Chapter 2), is  
 15 presented in **Figure 3.2**. Note  
 16 the wide range for forcing in  
 17 Figure 3.2. The comparison  
 18 with observation-based  
 19 estimates shows that the  
 20 model estimated forcing is in  
 21 general lower, partially  
 22 because the forcing value  
 23 from the model is the  
 24 difference between present-  
 25 day and pre-industrial time,  
 26 whereas the observation-  
 27 derived quantity is the  
 28 difference between an  
 29 atmosphere with and without  
 30 anthropogenic aerosols, so  
 31 the “background” value that  
 32 is subtracted from the total  
 33 forcing is higher in the  
 34 models.

**Table 3.3.** Sulfate mass loading, AOT at 550 nm, shortwave radiative forcing at the top of the atmosphere, and normalized forcing with respect to AOT and mass. All values refer to anthropogenic perturbation. Adapted from IPCC AR4 (2007) and Schulz et al. (2006).

Model	Mass load (mg m <sup>-2</sup> )	MEE (m <sup>2</sup> g <sup>-1</sup> )	AOD at 0.55 μm	TOA Forcing (W m <sup>-2</sup> )	Forcing/AOD (W m <sup>-2</sup> )	Forcing/mass (W g <sup>-1</sup> )
<b>Published since IPCC 2001</b>						
A CCM3	2.23			-0.56		-251
B GEOSCHEM	1.53	11.8	0.018	-0.33	-18	-216
C GISS	3.30	6.7	0.022	-0.65	-30	-197
D GISS	3.27			-0.96		-294
E GISS*	2.12			-0.57		-269
F SPRINTARS	1.55	9.7	0.015	-0.21		-135
G LMD	2.76			-0.42		-152
H LOA	3.03	9.9	0.03	-0.41	-14	-135
I GATORG	3.06			-0.32		-105
J PNNL	5.50	7.6	0.042	-0.44	-10	-80
K UIO-CTM	1.79	10.6	0.019	-0.37	-19	-207
L UIO-GCM	2.28			-0.29		-127
<b>AeroCom: Identical emissions used for year 2000 and 1750</b>						
M UMI	2.64	7.6	0.02	-0.58	-29	-220
N UIO-CTM	1.70	11.2	0.019	-0.36	-19	-212
O LOA	3.64	9.6	0.035	-0.49	-14	-135
P LSCE	3.01	7.6	0.023	-0.42	-18	-140
Q ECHAM5-HAM	2.47	6.5	0.016	-0.46	-29	-186
R GISS**	1.34	4.5	0.006	-0.19	-32	-142
S UIO-GCM	1.72	7.0	0.012	-0.25	-21	-145
T SPRINTARS	1.19	10.9	0.013	-0.16	-12	-134
U ULAQ	1.62	12.3	0.02	-0.22	-11	-136
<b>Average A-L</b>	<b>2.70</b>	<b>9.4</b>	<b>0.024</b>	<b>-0.46</b>	<b>-18</b>	<b>-181</b>
<b>Average M-U</b>	<b>2.15</b>	<b>8.6</b>	<b>0.018</b>	<b>-0.35</b>	<b>-21</b>	<b>-161</b>
<b>Minimum A-U</b>	<b>1.19</b>	<b>4.5</b>	<b>0.006</b>	<b>-0.96</b>	<b>-32</b>	<b>-294</b>
<b>Maximum A-U</b>	<b>5.50</b>	<b>12.3</b>	<b>0.042</b>	<b>-0.16</b>	<b>-10</b>	<b>-80</b>
<b>Std dev A-L</b>	<b>1.09</b>	<b>1.9</b>	<b>0.010</b>	<b>0.202</b>	<b>7</b>	<b>68</b>
<b>Std dev M-U</b>	<b>0.83</b>	<b>2.6</b>	<b>0.008</b>	<b>0.149</b>	<b>8</b>	<b>35</b>
<b>%Stddev/avg A-L</b>	<b>40%</b>	<b>20%</b>	<b>41%</b>	<b>44%</b>	<b>38%</b>	<b>38%</b>
<b>%Stddev/avg M-U</b>	<b>39%</b>	<b>30%</b>	<b>45%</b>	<b>43%</b>	<b>37%</b>	<b>22%</b>
Model abbreviations: CCM3=Community Climate Model; GEOSCHEM=Goddard Earth Observing System-Chemistry; GISS=Goddard Institute for Space Studies; SPRINTARS=Spectral Radiation-Transport Model for Aerosol Species; LMD=Laboratoire de Meteorologie Dynamique; LOA=Laboratoire d'Optique Atmospherique; GATORG=Gas, Aerosol Transport and General circulation model; PNNL=Pacific Northwest National Laboratory; UIO-CTM=Univeristy of Oslo CTM; UIO-GCM=University of Oslo GCM; UMI=University of Michigan; LSCE=Laboratoire des Sciences du Climat et de l'Enviornment; ECHAMS5-HAM=European Centre Hamburg with Hamburg Aerosol Module; ULAQ=University of IL'Aquila.						

**Table 3.4.** Particulate organic matter (POM) and black carbon (BC) mass loading, AOD at 550 nm, shortwave radiative forcing at the top of the atmosphere, and normalized forcing with respect to AOD and mass. All values refer to anthropogenic perturbation. Based on IPCC AR4 (2007) and Schulz et al. (2006).

MODEL	POM						BC					
	Mass load (mg m <sup>-2</sup> )	Mass ext. eff. (m <sup>2</sup> g <sup>-1</sup> )	AOD at 550 nm	TOA Forcing (W m <sup>-2</sup> )	Forcing/AOD (W m <sup>-2</sup> )	Forcing/mass (W g <sup>-1</sup> )	Mass load (mg m <sup>-2</sup> )	Mass ext. eff. (m <sup>2</sup> g <sup>-1</sup> )	AOD at 550 nm x1000	TOA Forcing (W m <sup>-2</sup> )	Forcing/AOD (W m <sup>-2</sup> )	Forcing/mass (W g <sup>-1</sup> )
<b>Published since IPCC 2001</b>												
A SPRINTARS				-0.24		-107				0.36		
B LOA	2.33	6.9	0.016	-0.25	-16	-140	0.37			0.55		
C GISS	1.86	9.1	0.017	-0.26	-15	-161	0.29			0.61		
D GISS	1.86	8.1	0.015	-0.30	-20	-75	0.29			0.35		
E GISS*	2.39			-0.18		-92	0.39			0.50		
F GISS	2.49			-0.23		-101	0.43			0.53		
G SPRINTARS	2.67	10.9	0.029	-0.27	-9	-23	0.53			0.42		
H GATORG	2.56			-0.06		-112	0.39			0.55		
I MOZGN	3.03	5.9	0.018	-0.34	-19							
J CCM							0.33			0.34		
K UIO-GCM							0.30			0.19		
<b>AeroCom: Identical emissions for year 2000 &amp; 1750</b>												
L UMI	1.16	5.2	0.0060	-0.23	-38	-198	0.19	6.8	1.29	0.25	194	1316
M UIO-CTM	1.12	5.2	0.0058	-0.16	-28	-143	0.19	7.1	1.34	0.22	164	1158
N LOA	1.41	6.0	0.0085	-0.16	-19	-113	0.25	7.9	1.98	0.32	162	1280
O LSCE	1.50	5.3	0.0079	-0.17	-22	-113	0.25	4.4	1.11	0.30	270	1200
P ECHAM5-HAM	1.00	7.7	0.0077	-0.10	-13	-100	0.16	7.7	1.23	0.20	163	1250
Q GISS**	1.22	4.9	0.0060	-0.14	-23	-115	0.24	7.6	1.83	0.22	120	917
R UIO-GCM	0.88	5.2	0.0046	-0.06	-13	-68	0.19	10.3	1.95	0.36	185	1895
S SPRINTARS	1.84	10.9	0.0200	-0.10	-5	-54	0.37	9.5	3.50	0.32	91	865
T ULAQ	1.71	4.4	0.0075	-0.09	-12	-53	0.38	7.6	2.90	0.08	28	211
<b>Average A-K</b>	<b>2.40</b>	<b>8.2</b>	<b>0.019</b>	<b>-0.24</b>	<b>-16</b>	<b>-102</b>	<b>0.37</b>	<b>--</b>	<b>--</b>	<b>0.44</b>	<b>--</b>	<b>1242</b>
<b>Average L-T</b>	<b>1.32</b>	<b>6.1</b>	<b>0.008</b>	<b>-0.13</b>	<b>-19</b>	<b>-106</b>	<b>0.25</b>	<b>7.7</b>	<b>1.90</b>	<b>0.25</b>	<b>153</b>	<b>1121</b>
<b>Minimum A-T</b>	<b>0.88</b>	<b>4.4</b>	<b>0.005</b>	<b>-0.34</b>	<b>-38</b>	<b>-198</b>	<b>0.16</b>	<b>4.4</b>	<b>1.11</b>	<b>0.08</b>	<b>28</b>	<b>211</b>
<b>Maximum A-T</b>	<b>3.03</b>	<b>10.9</b>	<b>0.029</b>	<b>-0.06</b>	<b>-5</b>	<b>-23</b>	<b>0.53</b>	<b>10.3</b>	<b>3.50</b>	<b>0.61</b>	<b>270</b>	<b>2103</b>
<b>Std dev A-K</b>	<b>0.39</b>	<b>1.7</b>	<b>0.006</b>	<b>0.09</b>	<b>4</b>	<b>41</b>	<b>0.08</b>	<b>--</b>	<b>--</b>	<b>0.06</b>	<b>--</b>	<b>384</b>
<b>Std dev L-T</b>	<b>0.32</b>	<b>2.0</b>	<b>0.005</b>	<b>0.05</b>	<b>10</b>	<b>46</b>	<b>0.08</b>	<b>1.6</b>	<b>0.82</b>	<b>0.09</b>	<b>68</b>	<b>450</b>
<b>%Stddev/avg A-K</b>	<b>16%</b>	<b>21%</b>	<b>30%</b>	<b>36%</b>	<b>26%</b>	<b>41%</b>	<b>22%</b>	<b>--</b>	<b>--</b>	<b>23%</b>	<b>--</b>	<b>31%</b>
<b>%Stddev/avg L-T</b>	<b>25%</b>	<b>33%</b>	<b>56%</b>	<b>39%</b>	<b>52%</b>	<b>43%</b>	<b>32%</b>	<b>21%</b>	<b>43%</b>	<b>34%</b>	<b>45%</b>	<b>40%</b>

1  
2 The discussion so far has dealt with global average values. The geographic distributions of multi-  
3 model aerosol direct RF has been evaluated among the AeroCom models, which are shown in  
4 **Figure 3.3** for total and anthropogenic AOD at 550 nm and anthropogenic aerosol RF at TOA,  
5 within the atmospheric column, and at the surface. Globally, anthropogenic AOD is about 25%  
6 of total AOD (Figure 3.3a and b) but is more concentrated over polluted regions in Asia, Europe,  
7 and North America and biomass burning regions in tropical southern Africa and South America.  
8 At TOA, anthropogenic aerosol causes negative forcing over mid-latitude continents and oceans  
9 with the most negative values (-1 to -2 W m<sup>-2</sup>) over polluted regions (Figure 3.3c). Although  
10 anthropogenic aerosol has a cooling effect at the surface with surface forcing values down to -10

1  $W m^{-2}$  over China, India, and tropical Africa (Figure 3.3e), it warms the atmospheric column  
 2 with the largest effects again over the polluted and biomass burning regions. This heating effect  
 3 will change the atmospheric circulation and can affect the weather and precipitation (e.g., Kim et  
 4 al., 2006).

5 Basic conclusions from forward modeling  
 6 of aerosol direct RF are:

- 7 • The most recent estimate of all-sky shortwave aerosol direct RF at TOA  
 8 from anthropogenic sulfate, BC, and  
 9 POM (mostly from fossil fuel/biofuel  
 10 combustion and biomass burning) is -  
 11  $0.22 \pm 0.18 W m^{-2}$  averaged globally,  
 12 exerting a net cooling effect. This  
 13 value would represent the low-end of  
 14 the forcing magnitude, since some  
 15 potentially significant anthropogenic  
 16 aerosols, such as nitrate and dust from  
 17 human activities are not included  
 18 because of their highly uncertain  
 19 sources and processes. IPCC AR4 had  
 20 adjusted the total anthropogenic  
 21 aerosol direct RF to  $-0.5 \pm 0.4 W m^{-2}$  by  
 22 adding estimated anthropogenic nitrate  
 23 and dust forcing values based on  
 24 limited modeling studies and by  
 25 considering the observation-based  
 26 estimates (see Chapter 2).  
 27

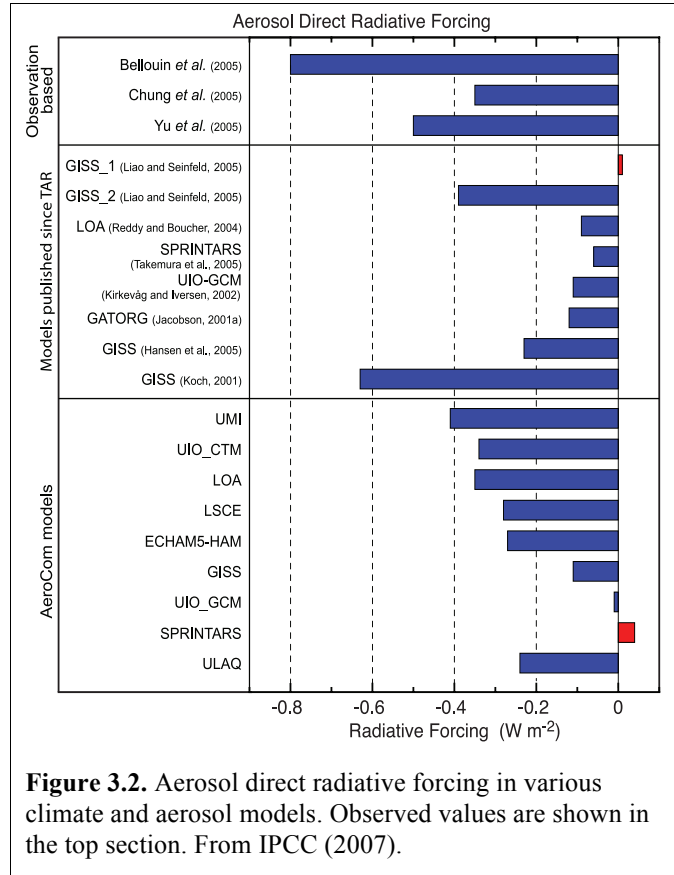


**Figure 3.2.** Aerosol direct radiative forcing in various climate and aerosol models. Observed values are shown in the top section. From IPCC (2007).

- 28 • Both sulfate and POM causes negative forcing whereas BC causes positive forcing because  
 29 of its highly absorbing nature. Although BC comprises only a small fraction of  
 30 anthropogenic aerosol mass load and AOD, its forcing efficiency (with respect to either  
 31 AOD or mass) is an order of magnitude stronger than sulfate and POM, so its positive  
 32 shortwave forcing largely offsets the negative forcing from sulfate and POM. This points  
 33 out the importance of improving the model ability to simulate each individual aerosol  
 34 components more accurately, especially black carbon. Separately, it is estimated from  
 35 recent model studies that anthropogenic sulfate, POM, and BC forcings at TOA are  $-0.4$ ,  $-$   
 36  $0.18$ ,  $+0.35 W m^{-2}$ , respectively. The anthropogenic nitrate and dust forcings are estimated  
 37 at  $-0.1 W m^{-2}$  for each, with uncertainties exceeds 100% (IPCC AR4, 2007).
- 38 • In contrast to long-lived greenhouse gases, anthropogenic aerosol RF exhibits significant  
 39 regional and seasonal variations. The forcing magnitude is the largest over the industrial  
 40 and biomass burning source regions, where the magnitude of the negative aerosol forcing  
 41 can be of the same magnitude or even stronger than that of positive greenhouse gas forcing.
- 42 • There is a large spread of model-calculated aerosol RF even in the global annual averaged  
 43 values. The AeroCom study shows that the model diversity at some locations (mostly East

1 Asia and African biomass burning regions) can reach  $\pm 3 \text{ W m}^{-2}$ , which is an order of  
 2 magnitude above the global averaged forcing value of  $-0.22 \text{ W m}^{-2}$ . The large diversity  
 3 reflects the low level of current understanding of aerosol radiative forcing, which is  
 4 compounded by uncertainties in emissions, transport, transformation, removal, particle  
 5 size, and optical and microphysical (including hygroscopic) properties.

6 • In spite of the relatively small value of total anthropogenic aerosol forcing at TOA, the  
 7 surface forcing and atmospheric column forcing values are considerably larger but opposite  
 8 in sign:  $-1$  to  $-2 \text{ W m}^{-2}$  at the surface and  $+0.8$  to  $+2 \text{ W m}^{-2}$  in the atmosphere.  
 9 Anthropogenic aerosols thus cool the surface but heat the atmosphere, on average.  
 10 Regionally, the atmospheric heating can reach annually averaged values exceeding  $5 \text{ W m}^{-2}$   
 11 (Figure 3.3d). These regional effects and the negative surface forcing are expected to exert  
 12 an important effect on climate through alteration of the hydrological cycle.

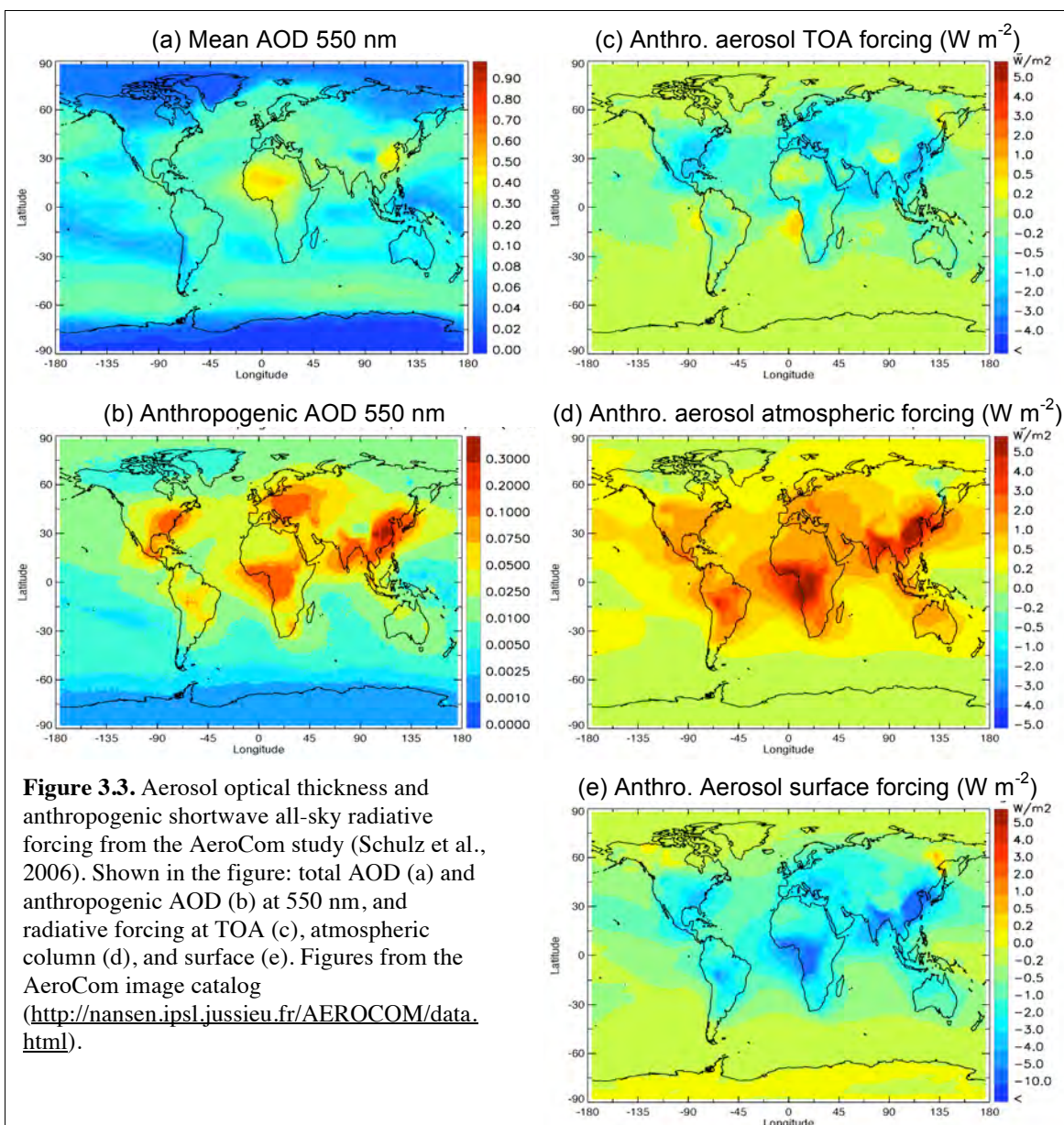


**Figure 3.3.** Aerosol optical thickness and anthropogenic shortwave all-sky radiative forcing from the AeroCom study (Schulz et al., 2006). Shown in the figure: total AOD (a) and anthropogenic AOD (b) at 550 nm, and radiative forcing at TOA (c), atmospheric column (d), and surface (e). Figures from the AeroCom image catalog (<http://nansen.ipsl.jussieu.fr/AEROCOM/data.html>).

## 3.4. Calculating Aerosol Indirect Forcing

### 3.4.1. Aerosol Effects on Clouds

A subset of the aerosol particles can act as cloud condensation nuclei (CCN) and/or ice nuclei (IN). Increases in aerosol particle concentrations, therefore, may increase the ambient concentrations of CCN and IN, affecting cloud properties. For a fixed cloud liquid water content, a CCN increase will lead to more cloud droplets so that the cloud droplet size will decrease. That effect leads to brighter clouds, the enhanced albedo then being referred to as the “cloud albedo effect” (Twomey, 1977), also known as the first indirect effect. If the droplet size is smaller, it may take longer to rainout, leading to an increase in cloud lifetime, hence the “cloud lifetime” effect (Albrecht, 1989), also called the second indirect effect. Approximately one-third of the models used for the IPCC 20th century climate change simulations incorporated an aerosol indirect effect, generally (though not exclusively) considered only with sulfates.

Shown in **Figure 3.4** are results from published model studies indicating the different RF values from the cloud albedo effect. The cloud albedo effect ranges from  $-0.22$  to  $-1.85 \text{ W m}^{-2}$ ; the lowest estimates are from simulations that constrained representation of aerosol effects on clouds with satellite measurements of drop size vs. aerosol index. In view of the difficulty of quantifying this effect remotely (discussed later), it is not clear whether this constraint provides an improved estimate. The estimate in the IPCC AR4 ranges from  $+0.4$  to  $-1.1 \text{ W m}^{-2}$ , with a “best-guess” estimate of  $-0.7 \text{ W m}^{-2}$ .

The representation of cloud effects in GCMs is considered below. However, it is becoming increasingly clear from studies based on high resolution simulations of aerosol-cloud interactions that there is a great deal of complexity that is unresolved in climate models. This point is examined again in section 3.4.4.

Most models did not incorporate the “cloud lifetime effect”. Hansen et al. (2005) compared this latter influence (in the form of time-averaged cloud area or cloud cover increase) with the cloud albedo effect. In contrast to the discussion in IPCC (2007), they argue

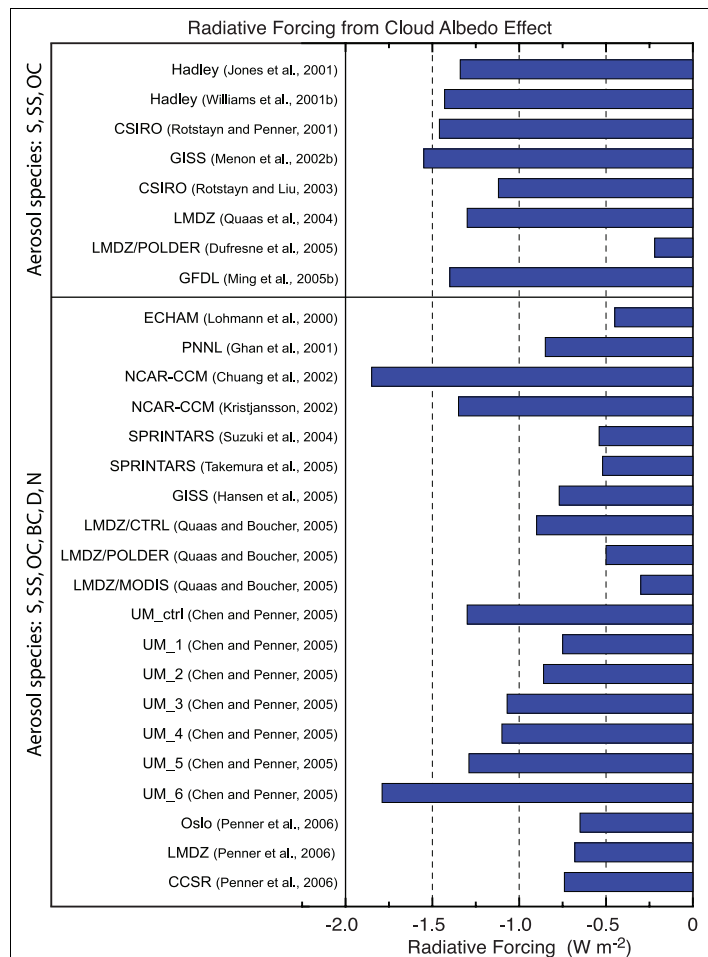
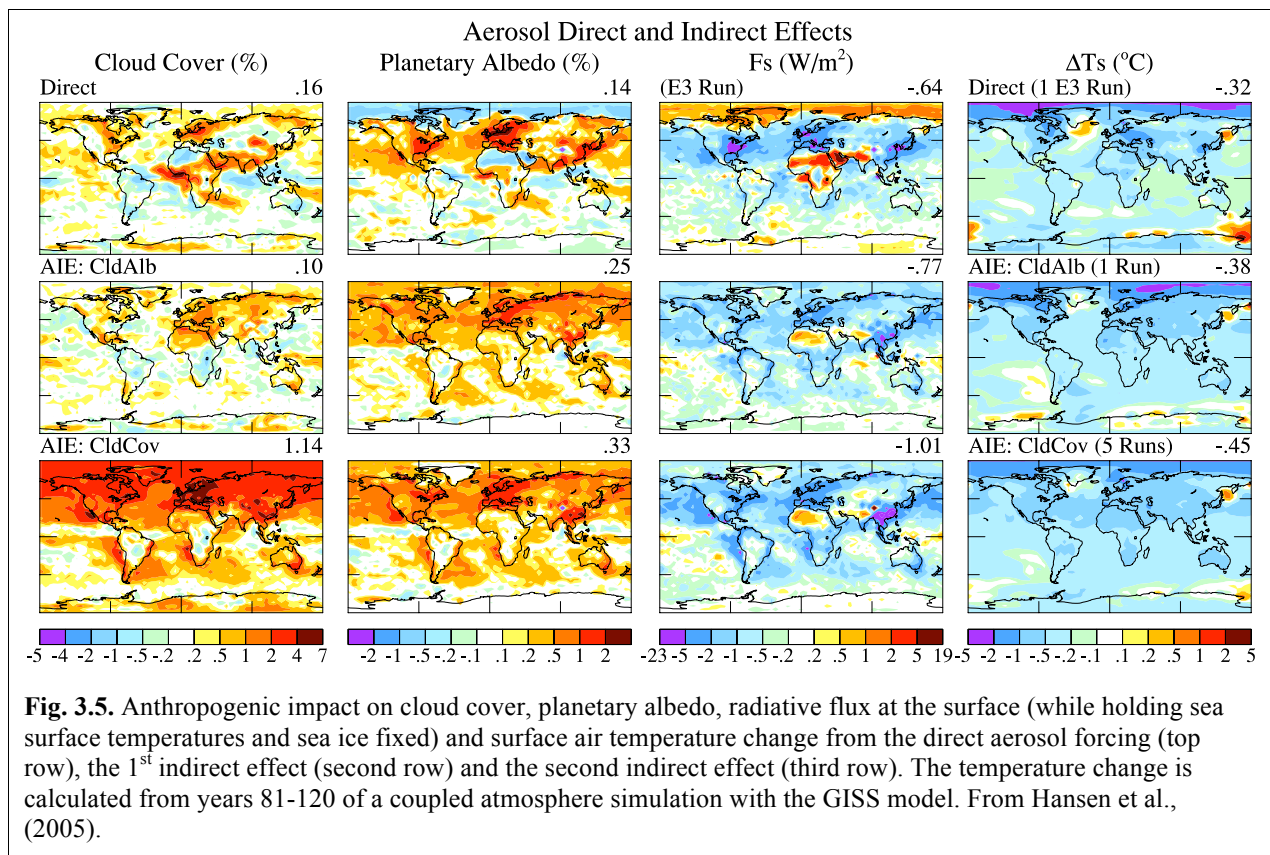


**Fig. 3.4.** Radiative forcing from the cloud albedo effect (1<sup>st</sup> aerosol indirect effect) in the global climate models used in IPCC 2007 (IPCC Fig. 2.14). For additional model designations and references, see IPCC 2007, chapter 2. Species included in the lower part of the panel include sulfate, sea salt, organic and black carbon, dust and nitrates; in the top panel only sulfate, sea salt and organic carbon.

1 that the cloud cover effect is more likely to be the dominant one, as suggested both by cloud-  
 2 resolving model studies (Ackerman et al., 2004) and satellite observations (Kaufman et al.,  
 3 2005c). The cloud albedo effect may be partly offset by reduced cloud thickness accompanying  
 4 aerosol pollutants, producing a meteorological (cloud) rather than aerosol effect (see the  
 5 discussion in Lohmann and Feichter, 2005). (The distinction between meteorological feedback  
 6 and aerosol forcing can become quite opaque; as noted earlier, the term feedback is restricted  
 7 here to those processes that are responding to a change in temperature.) Nevertheless, both  
 8 aerosol indirect effects were utilized in the GISS model, with the second indirect effect  
 9 calculated by relating cloud cover to the aerosol number concentration, which in turn is a  
 10 function of sulfate, nitrate, black carbon and organic carbon concentration. Only the low altitude  
 11 cloud influence was modeled, principally because there are greater aerosol concentrations at low  
 12 levels, and because low clouds currently exert greater cloud RF. The aerosol influence on high  
 13 altitude clouds, associated with IN changes, is a relatively unexplored area for models and as  
 14 well for process-level understanding.

15 Hansen et al. (2005) used coefficients to normalize the cooling from aerosol indirect effects to  
 16 between  $-0.75$  and  $-1 \text{ W m}^{-2}$ , based on comparisons of modeled and observed changes in the  
 17 diurnal temperature range as well as some satellite observations. The response of the GISS  
 18 model to the direct and two indirect effects is shown in **Figure 3.5**. As parameterized, the cloud  
 19 lifetime effect produced somewhat greater negative RF (cooling), but this was the result of the  
 20 coefficients chosen. Geographically, it appears that the “cloud cover” effect produced slightly  
 21 more cooling in the Southern Hemisphere than did the “cloud albedo” response, with the reverse  
 22 being true in the Northern Hemisphere (differences on the order of a few tenths  $^{\circ}\text{C}$ ).





### 3.4.2. Model Experiments

There are many different factors that can explain the large divergence of indirect effects in models (Fig. 3.4). To explore this in more depth, Penner et al. (2006) used three general circulation models to analyze the differences between models for the first indirect effect, as well as a combined first plus second indirect effect. The models all had different cloud and/or convection parameterizations.

In the first experiment, the monthly average aerosol mass and size distribution of, effectively, sulfate aerosol were prescribed, and all models followed the same prescription for parameterizing the cloud droplet number concentration (CDNC) as a function of aerosol concentration. In that sense, the only difference among the models was their separate cloud formation and radiation schemes. The different models all produced similar droplet effective radii, and therefore shortwave cloud forcing, and change in net outgoing whole sky radiation between pre-industrial times and the present. Hence the first indirect effect was not a strong function of the cloud or radiation scheme. The results for this and the following experiments are presented in **Figure 3.6**, where the experimental results are shown sequentially from left to right for the whole sky effect, and in **Table 3.5** for the clear-sky and cloud forcing response as well.

The change in cloud forcing is the difference between whole sky and clear sky outgoing radiation in the present day minus pre-industrial simulation. The large differences seen between experiments 5 and 6 are due to the inclusion of the clear sky component of aerosol scattering and absorption (the direct effect) in experiment 6.

In the second experiment, the aerosol mass and size distribution were again prescribed, but now each model used its own formulation for relating aerosols to droplets. In this case one of the models produced larger effective radii and therefore a much smaller first indirect aerosol effect (Figure 3.6, Table 3.5). However, even in the two models where the effective radius change and net global forcing were similar, the spatial patterns of cloud forcing differ, especially over the biomass burning regions of Africa and South America.

The third experiment allowed the models to relate the change in droplet size to change in precipitation efficiency (i.e., they were now also allowing the second indirect effect - smaller

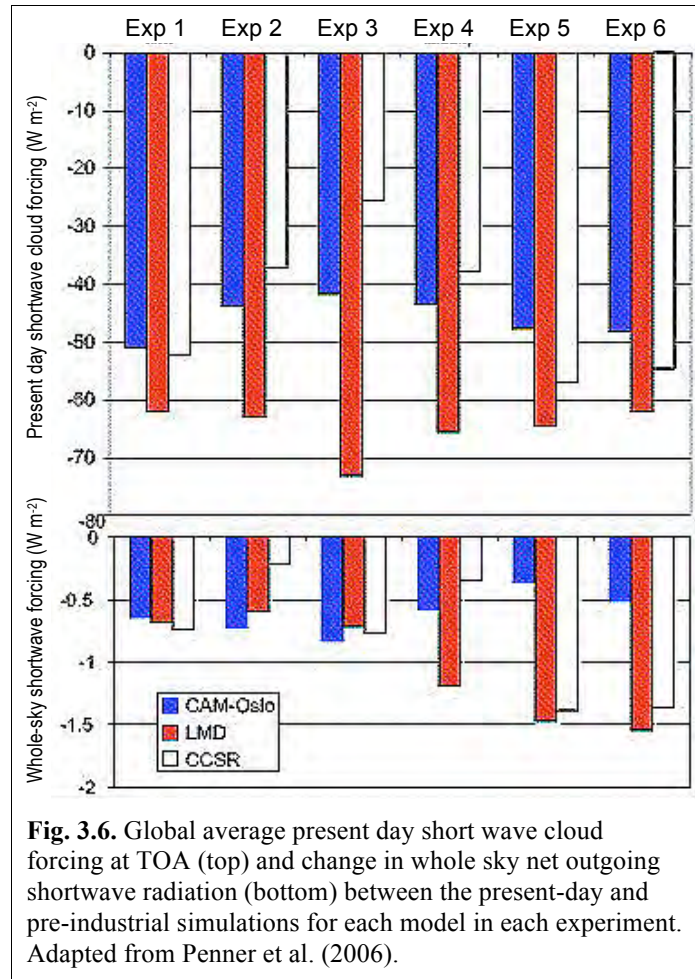


**Fig. 3.6.** Global average present day short wave cloud forcing at TOA (top) and change in whole sky net outgoing shortwave radiation (bottom) between the present-day and pre-industrial simulations for each model in each experiment. Adapted from Penner et al. (2006).

1 droplets being less efficient rain producers – as well as the first). The models utilized the same  
 2 relationship for autoconversion of cloud droplets to precipitation. Changing the precipitation  
 3 efficiency results in all models producing an increase in cloud liquid water path, although the  
 4 effect on cloud fraction was smaller than in the previous experiments. The net result was to  
 5 increase the negative radiative forcing in all three models, albeit with different magnitudes: for  
 6 two of the models the net impact on outgoing shortwave radiative increased by about 20%,  
 7 whereas in the third model (which had the much smaller first indirect effect), it was magnified by  
 8 a factor of three.

9 In the fourth experiment, the  
 10 models were now each allowed  
 11 to use their own formulation to  
 12 relate aerosols to precipitation  
 13 efficiency. This introduced some  
 14 additional changes in the whole  
 15 sky shortwave forcing (Figure  
 16 3.6).

17 In the fifth experiment, models  
 18 were allowed to produce their  
 19 own aerosol concentrations, but  
 20 were given common sources.  
 21 This produced the largest  
 22 changes in the RF in several of  
 23 the models. Within any one  
 24 model, therefore, the change in  
 25 aerosol concentration has the  
 26 largest effect on droplet  
 27 concentrations and effective  
 28 radii. This experiment too  
 29 resulted in large changes in RF.

30 In the last experiment, the aerosol direct effect was included, based on the full range of aerosols  
 31 used in each model. While the impact on the whole-sky forcing was not large, the addition of  
 32 aerosol scattering and absorption primarily affected the change in clear sky radiation (Table 3.5).

33 The results of this study emphasize that in addition to questions concerning cloud physics, the  
 34 differences in aerosol concentrations among the models play a strong role in inducing differences  
 35 in the indirect effect(s), as well as the direct one.

36 Observational constraints on climate model simulations of the indirect effect with satellite data  
 37 (e.g. MODIS) have been performed previously in a number of studies (e.g. Storelvmo et al.  
 38 2006, Lohmann et al. 2006, Quaas et al. 2006, Menon et al. 2008). These have been somewhat  
 39 limited since the satellite retrieved data used do not have the vertical profiles needed to resolve  
 40 aerosol and cloud fields (e.g. cloud droplet number and liquid water content); the temporal  
 41 resolution of simultaneous aerosol and cloud product retrievals are usually not available at a  
 42 frequency of more than one a day; and higher level clouds often obscure low clouds and  
 43 aerosols. Thus, the indirect effect, especially the second indirect effect, remains, to a large extent,

**Table 3.5.** Differences ( $Wm^{-2}$ ) in present day and pre-industrial outgoing solar radiation in the different experiments. Adapted from Penner et al. (2006).

MODEL	EXP 1	EXP 2	EXP 3	EXP 4	EXP 5	EXP 6
<b>Whole-sky</b>						
CAM-Oslo	-0.648	-0.726	-0.833	-0.580	-0.365	-0.518
LMD-Z	-0.682	-0.597	-0.722	-1.194	-1.479	-1.553
CCSR	-0.739	-0.218	-0.733	-0.350	-1.386	-1.386
<b>Clear-sky</b>						
CAM-Oslo	-0.063	-0.066	-0.026	0.014	-0.054	-0.575
LMD-Z	-0.054	0.019	0.030	-0.066	-0.126	-1.034
CCSR	0.018	-0.007	-0.045	-0.008	0.018	-1.160
<b>Cloud-forcing</b>						
CAM-Oslo	-0.548	-0.660	-0.807	-0.595	-0.311	0.056
LMD-Z	-0.628	-0.616	-0.752	-1.128	-1.353	-0.518
CCSR	-0.757	-0.212	-0.728	-0.345	-1.404	-0.200
EXP1: tests cloud formation and radiation schemes EXP2: tests formulation for relating aerosols to droplets EXP3: tests inclusion of droplet size influence on precipitation efficiency EXP4: tests formulation of droplet size influence on precipitation efficiency EXP5: tests model aerosol formulation from common sources EXP6: added the direct aerosol effect						

1 unconstrained by satellite observations. However, improved measurements of aerosol vertical  
2 distribution from the newer generation of sensors on the A-train platform may provide a better  
3 understanding of changes to cloud properties from aerosols. Simulating the top-of-atmosphere  
4 reflectance for comparison to satellite measured values could be another way to compare model  
5 with observations, which would eliminate the inconsistent assumptions of aerosol optical  
6 properties and surface reflectance encountered when compared the model calculated and satellite  
7 retrieved AOD values.

### 8 **3.4.3. Additional Aerosol Influences**

9 Various observations have empirically related aerosols injected from biomass burning or  
10 industrial processes to reductions in rainfall (e.g., Warner, 1968; Eagan et al., 1974; Andreae et  
11 al., 2004; Rosenfeld, 2000). There are several potential mechanisms associated with this  
12 response.

13 In addition to the two indirect aerosol effects noted above, a process denoted as the “semi-direct”  
14 effect involves the absorption of solar radiation by aerosols such as black carbon and dust. The  
15 absorption increases the temperature, thus lowering the relative humidity and producing  
16 evaporation, hence a reduction in cloud liquid water. The impact of this process depends strongly  
17 on what the effective aerosol absorption actually is; the more absorbing the aerosol, the larger the  
18 potential positive forcing on climate (by reducing low level clouds and allowing more solar  
19 radiation to reach the surface). This effect is responsible for shifting the critical value of SSA  
20 (separating aerosol cooling from aerosol warming) from 0.86 with fixed clouds to 0.91 with  
21 varying clouds (Hansen et al., 1997). Reduction in cloud cover and liquid water is one way  
22 aerosols could reduce rainfall.

23 More generally, aerosols can alter the location of solar radiation absorption within the system,  
24 and this aspect alone can alter climate and precipitation even without producing any change in  
25 net radiation at the top of the atmosphere (the usual metric for climate impact). By decreasing  
26 solar absorption at the surface, aerosols (from both the direct and indirect effects) reduce the  
27 energy available for evapotranspiration, potentially resulting in a decrease in precipitation. This  
28 effect has been suggested as the reason for the decrease in pan evaporation over the last 50 years  
29 (Roderick and Farquhar, 2002). The decline in solar radiation at the surface appears to have  
30 ended in the 1990s (Wild et al., 2005), perhaps because of reduced aerosol emissions in  
31 industrial areas (Kruger and Grasl, 2002), although this issue is still not settled.

32 Energy absorption by aerosols above the boundary layer can also inhibit precipitation by  
33 warming the air at altitude relative to the surface, i.e., increasing atmospheric stability. The  
34 increased stability can then inhibit convection, affecting both rainfall and atmospheric circulation  
35 (Ramanathan et al., 2001a; Chung and Zhang, 2004). To the extent that aerosols decrease droplet  
36 size and reduce precipitation efficiency, this effect by itself could result in lowered rainfall  
37 values locally.

38 In their latest simulations, Hansen et al. (2007) did find that the indirect aerosol effect reduced  
39 tropical precipitation; however, the effect is similar regardless of which of the two indirect  
40 effects is used, and also similar to the direct effect. So it is likely that the reduction of tropical  
41 precipitation is because of aerosol induced cooling at the surface and the consequent reduced

1 evapotranspiration. Similar conclusions were reached by Yu et al. (2002) and Feingold et al.  
2 (2005). In this case, the effect is a feedback and not a forcing.

3 The local precipitation change, through its impacts on dynamics and soil moisture, can have  
4 large positive feedbacks. Harvey (2004) concluded from assessing the response to aerosols in 8  
5 coupled models that the aerosol impact on precipitation was larger than on temperature. He also  
6 found that the precipitation impact differed substantially among the models, with little  
7 correlation among them.

8 Recent GCM simulations have further examined the aerosol effects on hydrological cycle.  
9 Ramanathan et al. (2005) showed from fully coupled ocean–atmosphere GCM experiments that  
10 the “solar dimming” effect at the surface, i.e., the reduction of solar radiation reaching the  
11 surface, due to the inclusion of absorbing aerosol forcing causes a reduction in surface  
12 evaporation, a decrease in meridional sea surface temperature (SST) gradient and an increase in  
13 atmospheric stability, and a reduction in rainfall over South Asia. Lau and Kim (2006) examined  
14 the direct effects of aerosol on the monsoon water cycle variability from GCM simulations with  
15 prescribed realistic global aerosol forcing and proposed the “elevated heat pump” effect,  
16 suggesting that atmospheric heating by absorbing aerosols (dust and black carbon), through  
17 water cycle feedback, may lead to a strengthening of the South Asia monsoon. These model  
18 results are not necessarily at odds with each other, but rather illustrate the complexity of the  
19 aerosol–monsoon interactions that are associated with different mechanisms, whose relative  
20 importance in affecting the monsoon may be strongly dependent on spatial and temporal scales  
21 and the timing of the monsoon. These results may be model dependent and should be further  
22 examined.

#### 23 **3.4.4. High Resolution Modeling**

24 Largely by its nature, the representation of the interaction between aerosol and clouds in GCMs  
25 is poorly resolved. This stems in large part from the fact that GCMs do not resolve convection on  
26 their large grids (order of several hundred km), that their treatment of cloud microphysics is  
27 rather crude, and that as discussed previously, their representation of aerosol needs improvement.  
28 Superparametrization efforts (where standard cloud parameterizations in the GCM are replaced  
29 by resolving clouds in each grid column of the GCM via a cloud resolving model, e.g.,  
30 Grabowski, 2004) could lead the way for the development of more realistic cloud fields and thus  
31 improved treatments of aerosol-cloud interactions in large-scale models. However, these are just  
32 being incorporated in models that resolve both cloud and aerosols. Detailed cloud parcel models  
33 have been developed to focus on the droplet activation problem (that asks under what conditions  
34 droplets actually start forming) and questions associated with the first indirect effect. The  
35 coupling of aerosol and cloud modules to dynamical models that resolve the large turbulent  
36 eddies associated with vertical motion and clouds [large eddy simulations (LES) models, with  
37 grid sizes of ~ 100 m and domains ~ 10 km] has proven to be a powerful tool for representing the  
38 details of aerosol-cloud interactions together with feedbacks (e.g., Feingold et al. 1994; Kogan et  
39 al. 1994; Stevens et al, 1996; Feingold et al. 1999; Ackerman et al. 2004). This section explores  
40 some of the complexity in the aerosol indirect effects revealed by such studies to illustrate how  
41 difficult parameterizing these effects properly in GCMs could really be.

1 **3.4.4a. The first indirect effect**

2 The relationship between aerosol and drop concentrations (or drop sizes) is a key piece of the  
3 first indirect effect puzzle. (It should not, however, be equated to the first indirect effect which  
4 concerns itself with the resultant RF). A huge body of measurement and modeling work points to  
5 the fact that drop concentrations increase with increasing aerosol. The main unresolved questions  
6 relate to the degree of this effect, and the relative importance of aerosol size distribution,  
7 composition and updraft velocity in determining drop concentrations (for a review, see  
8 McFiggans et al., 2006). Studies indicate that the aerosol number concentration and size  
9 distribution are the most important aerosol factors. Updraft velocity (unresolved by GCMs) is  
10 particularly important under conditions of high aerosol particle number concentration.

11 Although it is likely that composition has some effect on drop number concentrations,  
12 composition is generally regarded as relatively unimportant compared to the other parameters  
13 (Fitzgerald, 1975; Feingold, 2003; Ervens et al., 2005; Dusek et al., 2006). Therefore, it has been  
14 stated that the significant complexity in aerosol composition can be modeled, for the most part,  
15 using fairly simple parameterizations that reflect the soluble and insoluble fractions (e.g., Rissler  
16 et al. 2004). However, composition cannot be simply dismissed. Furthermore, chemical  
17 interactions also cannot be overlooked. A large uncertainty remains concerning the impact of  
18 organic species on cloud droplet growth kinetics, thus cloud droplet formation. Cloud drop size  
19 is affected by wet scavenging, which depends on aerosol composition especially for freshly  
20 emitted aerosol. And future changes in composition will presumably arise due to  
21 biofuels/biomass burning and a reduction in sulfate emissions, which emphasizes the need to  
22 include composition changes in models when assessing the first indirect effect. The simple  
23 soluble/insoluble fraction model may become less applicable than is currently the case.

24 The updraft velocity, and its change as climate warms, may be the most difficult aspect to  
25 simulate in GCMs because of the small scales involved. In GCMs it is calculated in the dynamics  
26 as a grid box average, and parameterized on the small scale indirectly because it is a key part of  
27 convection and the spatial distribution of condensate, as well as droplet activation. Numerous  
28 solutions to this problem have been sought, including estimation of vertical velocity based on  
29 predicted turbulent kinetic energy from boundary layer models (Lohmann et al., 1999; Larson et  
30 al., 2001) and PDF representations of subgrid quantities, such as vertical velocity and the  
31 vertically-integrated cloud liquid water ('liquid water path', or LWP) (Pincus and Klein, 2000;  
32 Golaz et al., 2002a,b; Larson et al., 2005). Embedding cloud-resolving models within GCMs is  
33 also being actively pursued (Grabowski et al. 1999; Randall et al., 2003). Numerous other details  
34 come into play; for example, the treatment of cloud droplet activation in GCM frameworks is  
35 often based on the assumption of adiabatic conditions, which may overestimate the sensitivity of  
36 cloud to changes in CCN (Sotiropoulou et al., 2006, 2007). This points to the need for improved  
37 theoretical understanding followed by new parameterizations.

38 **3.4.4b. Other indirect effects**

39 The second indirect effect is often referred to as the "cloud lifetime effect", based on the premise  
40 that non-precipitating clouds will live longer. In GCMs the "lifetime effect" is equivalent to  
41 changing the representation of precipitation production and can be parameterized as an increase  
42 in cloud area or cloud cover (e.g., Hansen et al., 2005). The second indirect effect hypothesis  
43 states that the more numerous and smaller drops associated with aerosol perturbations, suppress  
44 collision-induced rain, and result in a longer cloud lifetime. Observational evidence for the

1 suppression of rain in warm clouds exists in the form of isolated studies (e.g. Warner, 1968) but  
2 to date there is no statistically robust proof of surface rain suppression (Levin and Cotton, 2008).  
3 Results from ship-track studies show that cloud water may increase or decrease in the tracks  
4 (Coakley and Walsh, 2002) and satellite studies suggest similar results for warm boundary layer  
5 clouds (Han et al. 2002). Ackerman et al. (2004) used LES to show that in stratocumulus, cloud  
6 water may increase or decrease in response to increasing aerosol depending on the relative  
7 humidity of the air overlaying the cloud. Wang et al. (2003) showed that all else being equal,  
8 polluted stratocumulus clouds tend to have lower water contents than clean clouds because the  
9 small droplets associated with polluted clouds evaporate more readily and induce an evaporation-  
10 entrainment feedback that dilutes the cloud. This result was confirmed by Xue and Feingold  
11 (2006) and Jiang and Feingold (2006) for shallow cumulus, where pollution particles were  
12 shown to decrease cloud fraction. Furthermore, Xue et al. (2008) suggested that there may exist  
13 two regimes: the first, a precipitating regime at low aerosol concentrations where an increase in  
14 aerosol will suppress precipitation and increase cloud cover (Albrecht, 1989); and a second, non  
15 precipitating regime where the enhanced evaporation associated with smaller drops will decrease  
16 cloud water and cloud fraction.

17 The possibility of bistable aerosol states was proposed earlier by Baker and Charlson (1990)  
18 based on consideration of aerosol sources and sinks. They used a simple numerical model to  
19 suggest that the marine boundary layer prefers two aerosol states: a clean, oceanic regime  
20 characterized by a weak aerosol source and less reflective clouds; and a polluted, continental  
21 regime characterized by more reflective clouds. On the other hand, study by Ackerman et al.  
22 (1994) did not support such a bistable system using a somewhat more sophisticated model.  
23 Further observations are needed to clarify the nature of cloud/aerosol interactions under a variety  
24 of conditions.

25 Finally, the question of possible effects of aerosol on cloud lifetime was examined by Jiang et al.  
26 (2006), who tracked hundreds of cumulus clouds generated by LES from their formative stages  
27 until they dissipated. They showed that in the model there was no effect of aerosol on cloud  
28 lifetime, and that cloud lifetime was dominated by dynamical variability.

29 It could be argued that the representation of these complex feedbacks in GCMs is not warranted  
30 until a better understanding of the processes is at hand. Moreover, until GCMs are able to  
31 represent cloud scales, it is questionable what can be obtained by adding microphysical  
32 complexity to poorly resolved clouds. A better representation of aerosol-cloud interactions in  
33 GCMs therefore depends on ability to improve representation of aerosols and clouds, and indeed  
34 the entire hydrologic cycle, as well as their interaction. This issue is discussed further in the next  
35 chapter.

## 36 **3.5. Aerosol in the Climate Models**

### 37 ***3.5.1. Aerosol in the IPCC AR4 Climate Model Simulations***

38 To assess the atmospheric and climate response to aerosol forcing, e.g., changes in surface  
39 temperature, precipitation, or atmospheric circulation, aerosols, together with greenhouse gases  
40 should be an integrated part of climate model simulation under the past, present, and future  
41 conditions. **Table 3.6** lists the forcing species that were included in 25 climate modeling groups  
42 used in the IPCC AR4 (2007) assessment. All the models included long-lived greenhouse gases,

1 most models included sulfate direct forcing, but only a fraction of those climate models  
 2 considered other aerosol types. In other words, aerosol RF was not adequately accounted for in  
 3 the climate simulations for the IPCC AR4. Put still differently, the current aerosol modeling  
 4 capability has not been fully incorporated into the climate model simulations. As pointed out in  
 5 Section 3.4, fewer than one-third of the models incorporated an aerosol indirect effect, and most  
 6 considered only sulfates.

**Table 3.6.** Forcings used in IPCC AR4 simulations of 20th century climate change. This Table is adapted from SAP 1.1 Table 5.2 (compiled using information provided by the participating modeling centers, see [http://www-pcmdi.llnl.gov/ipcc/model\\_documentation/ipcc\\_model\\_documentation.php](http://www-pcmdi.llnl.gov/ipcc/model_documentation/ipcc_model_documentation.php)) plus additional information from that website. Eleven different forcings are listed: well-mixed greenhouse gases (G), tropospheric and stratospheric ozone (O), sulfate aerosol direct (SD) and indirect effects (SI), black carbon (BC) and organic carbon aerosols (OC), mineral dust (MD), sea salt (SS), land use/land cover (LU), solar irradiance (SO), and volcanic aerosols (V). Check mark denotes inclusion of a specific forcing. As used here, “inclusion” means specification of a time-varying forcing, with changes on interannual and longer timescales.

	MODEL	COUNTRY	G	O	SD	SI	BC	OC	MD	SS	LU	SO	V
1	BCC-CM1	China	√	√	√								
2	BCCR-BCM2.0	Norway	√		√				√	√			
3	CCSM3	USA	√	√	√		√	√				√	√
4	CGCM3.1(T47)	Canada	√		√								
5	CGCM3.1(T63)	Canada	√		√								
6	CNRM-CM3	France	√	√	√		√						
7	CSIRO-Mk3.0	Australia	√		√								
8	CSIRO-Mk3.5	Australia	√		√								
9	ECHAM5/MPI-OM	Germany	√	√	√	√							
10	ECHO-G	Germany/Korea	√	√	√	√						√	√
11	FGOALS-g1.0	China	√		√								
12	GFDL-CM2.0	USA	√	√	√		√	√			√	√	√
13	GFDL-CM2.1	USA	√	√	√		√	√			√	√	√
14	GISS-AOM	USA	√		√					√			
15	GISS-EH	USA	√	√	√	√	√	√	√	√	√	√	√
16	GISS-ER	USA	√	√	√	√	√	√	√	√	√	√	√
17	INGV-SXG	Italy	√	√	√								
18	INM-CM3.0	Russia	√		√							√	
19	IPSL-CM4	France	√		√	√							
20	MIROC3.2(hires)	Japan	√	√	√		√	√	√	√	√	√	√
21	MIROC3.2(medres)	Japan	√	√	√		√	√	√	√	√	√	√
22	MRI-CGCM2.3.2	Japan	√		√							√	√
23	PCM	USA	√	√	√							√	√
24	UKMO-HadCM3	UK	√	√	√	√							
25	UKMO-HadGEM1	UK	√	√	√	√	√	√			√	√	√

7  
 8 The following discussion compares two of the IPCC AR4 climate models that include all major  
 9 forcing agencies in their climate simulation: The model from the NASA Goddard Institute for  
 10 Space Studies (GISS) and from the NOAA Geophysical Fluid Dynamics Laboratory (GFDL).

1 The purpose in presenting these comparisons is to help elucidate how modelers go about  
2 assessing their aerosol components, and the difficulties that entail. A particular concern is how  
3 aerosol forcings were obtained in the climate model experiments for IPCC AR4. Comparisons  
4 with observations have already led to some improvements that can be implemented in climate  
5 models for subsequent climate change experiments (e.g., Koch et al., 2006, for GISS model).  
6 This aspect is discussed further in chapter 4.

### 7 **3.5.1a. The GISS model**

8 There have been many different configurations of aerosol simulations in the GISS model over  
9 the years, with different emissions, physics packages, etc., as is apparent from the multiple GISS  
10 entries in the preceding figures and tables. There were also three different GISS GCM  
11 submissions to IPCC AR4, which varied in their model physics and ocean formulation. (Note  
12 that the aerosols in these three GISS versions are different from those in the AeroCom  
13 simulations described in section 3.2 and 3.3.) The GCM results discussed below all relate to the  
14 simulations known as GISS model ER (Schmidt et al., 2006, see Table 3.6).

15 Although the detailed description and model evaluation have been presented in Liu et al. (2006),  
16 below are the general characteristics of aerosols in the GISS ER:

17 *Aerosol fields:* The aerosol fields used in the GISS ER is a prescribed “climatology” which is  
18 obtained from chemistry transport model simulations with monthly averaged mass  
19 concentrations representing conditions up to 1990. Aerosol species included are sulfate, nitrate,  
20 BC, POM, dust, and sea salt. Dry size effective radii are specified for each of the aerosol types,  
21 and laboratory-measured phase functions are employed for all solar and thermal wavelengths.  
22 For hygroscopic aerosols (sulfate, nitrate, POM, and sea salt), formulas are used for the particle  
23 growth of each aerosol as a function of relative humidity, including the change in density and  
24 optical parameters. With these specifications, the AOD, single scattering albedo, and phase  
25 function of the various aerosols are calculated. While the aerosol distribution is prescribed as  
26 monthly mean values, the relative humidity component of the extinction is updated each hour.  
27 The global averaged AOD at 550 nm is about 0.15.

28 *Global distribution:* When comparing with AOD from observations by multiple satellite sensors  
29 of MODIS, MISR, POLDER, and AVHRR and surface based sunphotometer network  
30 AERONET (see chapter 2 for detailed information about data), qualitative agreement is apparent,  
31 with generally higher burdens in Northern Hemisphere summer, and seasonal variations of  
32 smoke over southern Africa and South America, as well as wind blown dust over northern  
33 African and the Persian Gulf. Aerosol optical depth in both model and observations is smaller  
34 away from land. There are, however, considerable discrepancies between the model and  
35 observations. Overall, the GISS GCM has reduced aerosol optical depths compared with the  
36 satellite data (a global, clear-sky average of about 80% compared with MODIS and MISR data),  
37 although it is in better agreement with AERONET ground-based measurements in some  
38 locations (note that the input aerosol values were calibrated with AERONET data). The model  
39 values over the Sahel in Northern Hemisphere winter and the Amazon in Southern Hemisphere  
40 winter are excessive, indicative of errors in the biomass burning distributions, at least partially  
41 associated with an older biomass burning source used (the source used here was from Liousse et  
42 al., 1996).

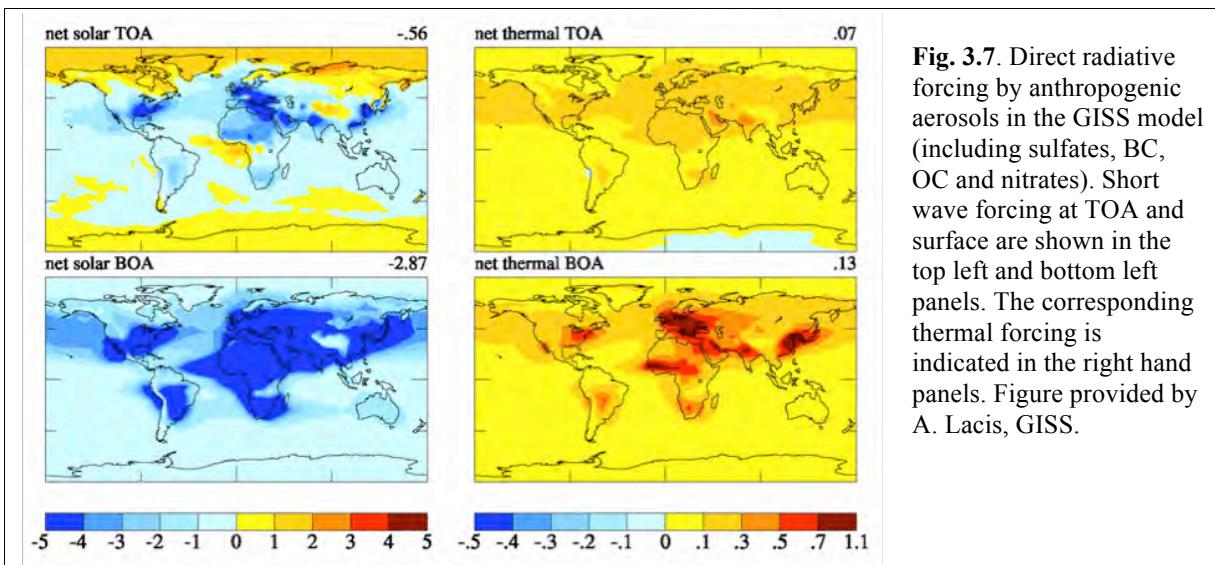


1 *Seasonal variation:* A comparison of the seasonal distribution of the global AOD between the  
2 GISS model and satellite data indicates that the model seasonal variation is in qualitative  
3 agreement with observations for many of the locations that represent major aerosol regimes,  
4 although there are noticeable differences. For example, in some locations the seasonal variations  
5 are different from or even opposite to the observations.

6 *Particle size parameter:* The Ångström exponent ( $\text{\AA}$ ), which is determined by the contrast  
7 between the AOD at two or more different wavelengths and is related to aerosol particle size  
8 (discussed in section 3.3). This parameter is important because the particle size distribution  
9 affects the efficiency of scattering of both short and long wave radiation, as discussed earlier.  $\text{\AA}$   
10 from the GISS model is biased low compared with AERONET, MODIS, and POLDER data,  
11 although there are technical differences in determining the  $\text{\AA}$ . This low bias suggests that the  
12 aerosol particle size in the GISS model is probably too large. The average effective radius in the  
13 GISS model appears to be 0.3-0.4  $\mu\text{m}$ , whereas the observational data indicates a value more in  
14 the range of 0.2-0.3  $\mu\text{m}$  (Liu et al., 2006).

15 *Single scattering albedo:* The model-calculated SSA (at 550 nm) appears to be generally higher  
16 than the AERONET data at worldwide locations (not enough absorption), but lower than  
17 AERONET data in Northern Africa, the Persian Gulf, and the Amazon (too much absorption).  
18 This discrepancy reflects the difficulties in modeling BC, which is the dominant absorbing  
19 aerosol, and aerosol sizes. Global averaged SSA at 550 nm from the GISS model is at about  
20 0.95.

21 *Aerosol direct RF:* The GISS model calculated aerosol direct shortwave RF is  $-0.56 \text{ W m}^{-2}$  at  
22 TOA and  $-2.87 \text{ W m}^{-2}$  at the surface. The TOA forcing (upper left, **Figure 3.7**) indicates that, as  
23 expected, the model has larger negative values in polluted regions and positive forcing at the  
24 highest latitudes. At the surface (lower left, Figure 3.7) GISS model values exceed  $-4 \text{ W m}^{-2}$  over  
25 large regions. Note that these results are for the model's total aerosols (anthropogenic plus  
26 natural) and thus differ from the anthropogenic aerosol effect discussed earlier (section 3.3 and  
27 Figure 3.3). Note there is also a longwave RF of aerosols (right column), although they are much  
28 weaker than the shortwave RF.



1 There are several concerns for climate change simulations related to the aerosol trend in the  
2 GISS model. One is that the aerosol fields in the GISS AR4 climate simulation (version ER) are  
3 kept fixed after 1990. In fact, the observed trend shows a reduction in tropospheric aerosol  
4 optical thickness from 1990 through the present, at least over the oceans (Mishchenko and  
5 Geogdzhayev, 2007). Hansen et al. (2007) suggested that the deficient warming in the GISS  
6 model over Eurasia post-1990 was due to the lack of this trend. Indeed, a possible conclusion  
7 from the Penner et al. (2002) study was that the GISS model overestimated the AOD  
8 (presumably associated with anthropogenic aerosols) poleward of 30°N. However, when an  
9 alternate experiment reduced the aerosol optical depths, the polar warming became excessive  
10 (Hansen et al., 2007). The other concern is that the GISS model may underestimate the organic  
11 and sea salt AOD, and overestimate the influence of black carbon aerosols in the biomass  
12 burning regions (deduced from Penner et al., 2002; Liu et al., 2006). To the extent that is true, it  
13 would indicate the GISS model underestimates the aerosol direct cooling effect in a substantial  
14 portion of the tropics, outside of biomass burning areas. Clarifying those issues requires  
15 numerous modeling experiments and various types of observations.

### 16 ***3.5.1b. The GFDL model***

17 A comprehensive description and evaluation of the GFDL aerosol simulation are given in  
18 Ginoux et al. (2006). Below are the general characteristics:

19 *Aerosol fields:* The aerosols used in the GFDL climate experiments are obtained from  
20 simulations performed with the MOZART 2 model (Model for Ozone and Related chemical  
21 Tracers) (Horowitz et al., 2003; Horowitz, 2006). The exceptions were dust, which was  
22 generated with a separate simulation of MOZART 2, using sources from Ginoux et al. (2001)  
23 and wind fields from NCEP/NCAR reanalysis data; and sea salt, whose monthly mean  
24 concentrations were obtained from a previous study by Haywood et al. (1999). It includes most  
25 of the same aerosol species as in the GISS model (although it does not include nitrates), and, as  
26 in the GISS model, relates the dry aerosol to wet aerosol optical depth via the model's relative  
27 humidity for sulfate (but not for organic carbon); for sea salt, a constant relative humidity of 80%  
28 was used. Although the parameterizations come from different sources, both models maintain a  
29 very large growth in sulfate particle size when the relative humidity exceeds 90%.

30 *Global distributions:* Overall, the GFDL global mean aerosol mass loading is within 30% of that  
31 of other studies (Chin et al., 2002; Tie et al., 2005; Reddy et al., 2005a), except for sea salt,  
32 which is 2 to 5 times smaller. However, the sulfate AOD (0.1) is 2.5 times that of other studies,  
33 whereas the organic carbon value is considerably smaller (on the order of 1/2). Both of these  
34 differences are influenced by the relationship with relative humidity. In the GFDL model, sulfate  
35 is allowed to grow up to 100% relative humidity, but organic carbon does not increase in size as  
36 relative humidity increases. Comparison of AOD with AVHRR and MODIS data for the time  
37 period 1996-2000 shows that the global mean value over the ocean (0.15) agrees with AVHRR  
38 data (0.14) but there are significant differences regionally, with the model overestimating the  
39 value in the northern mid latitude oceans and underestimating it in the southern ocean.  
40 Comparison with MODIS also shows good agreement globally (0.15), but in this case indicates  
41 large disagreements over land, with the model producing excessive AOD over industrialized  
42 countries and underestimating the effect over biomass burning regions. Overall, the global  
43 averaged AOD at 550 nm is 0.17, which is higher than the maximum values in the AeroCom-A  
44 experiments (Table 3.2) and exceeds the observed value too (Ae and S\* in Figure 3.1).

1 *Composition:* Comparison of GFDL modeled species with *in situ* data over North America,  
2 Europe, and over oceans has revealed that the sulfate is overestimated in spring and summer and  
3 underestimated in winter in many regions, including Europe and North America. Organic and  
4 black carbon aerosols are also overestimated in polluted regions by a factor of two, whereas  
5 organic carbon aerosols are elsewhere underestimated by factors of 2 to 3. Dust concentrations at  
6 the surface agree with observations to within a factor of 2 in most places where significant dust  
7 exists, although over the southwest U.S. it is a factor of 10 too large. Surface concentrations of  
8 sea salt are underestimated by more than a factor of 2. Over the oceans, the excessive sulfate  
9 AOD compensates for the low sea salt values except in the southern oceans.

10 *Size and single-scattering albedo:* No specific comparison was given for particle size or single-  
11 scattering albedo, but the excessive sulfate would likely produce too high a value of reflectivity  
12 relative to absorption except in some polluted regions where black carbon (an absorbing aerosol)  
13 is also overestimated.

14 As in the case of the GISS model, there are several concerns with the GFDL model. The good  
15 global-average agreement masks an excessive aerosol loading over the Northern Hemisphere (in  
16 particular, over the northeast U.S. and Europe) and an underestimate over biomass burning  
17 regions and the southern oceans. Several model improvements are needed, including better  
18 parameterization of hygroscopic growth at high relative humidity for sulfate and organic carbon;  
19 better sea salt simulations; correcting an error in extinction coefficients; and improved biomass  
20 burning emissions inventory (Ginoux et al., 2006).

### 21 ***3.5.1c. Comparisons between GISS and GFDL model***

22 Both GISS and GFDL models were used in the IPCC AR4 climate simulations for climate  
23 sensitivity that included aerosol forcing. It would be constructive, therefore, to compare the  
24 similarities and differences of aerosols in these two models and to understand what their impacts  
25 are in climate change simulations. **Figure 3.8** shows the percentage AOD from different aerosol  
26 components in the two models.

27 *Sulfate:* The sulfate AOD from the GISS model is within the range of that from all other models  
28 (Table 3.3), but that from the GFDL model exceeds the maximum value by a factor of 2.5. An  
29 assessment in SAP 3.2 (2008; Shindell et al., 2008b) also concludes that GFDL had excessive  
30 sulfate AOD compared with other models. The sulfate AOD from GFDL is nearly a factor of 4  
31 large than that from GISS, although the sulfate burden differs only by about 50% between the  
32 two models. Clearly, this implies a large difference in sulfate MEE between the two models.

33 *BC and POM:* Compared to observations, the GISS model appears to overestimate the influence  
34 of BC and POM in the biomass burning regions and underestimate it elsewhere, whereas the  
35 GFDL model is somewhat the reverse: it overestimates it in polluted regions, and underestimates  
36 it in biomass burning areas. The global comparison shown in Table 3.4 indicates the GISS model  
37 has values similar to those from other models, which might be the result of such compensating  
38 errors. The GISS and GFDL models have relatively similar global-average black carbon  
39 contributions, and the same appears true for POM.

40 *Sea salt:* The GISS model has a much larger sea salt contribution than does GFDL (or indeed  
41 other models).

2 *Global and regional distributions:*  
 4 Overall, the global averaged AOD is  
 6 0.15 from the GISS model and 0.17  
 8 from GFDL. However, as shown in  
 10 Figure 3.8, the contribution to this  
 12 AOD from different aerosol  
 14 components shows greater disparity.  
 16 For example, over the Southern  
 18 Ocean where the primary influence is  
 20 due to sea salt in the GISS model, but  
 22 in the GFDL it is sulfate. The lack of  
 24 satellite observations of the  
 26 component contributions and the  
 28 limited available *in situ*  
 30 measurements make the model  
 32 improvements at aerosol composition  
 34 level difficult.

36 *Climate simulations:* With such large  
 38 differences in aerosol composition  
 40 and distribution between the GISS  
 42 and GFDL models, one might expect  
 44 that the model simulated surface  
 46 temperature might be quite different.  
 48 Indeed, the GFDL model was able to  
 50 reproduce the observed temperature  
 52 change during the 20th century  
 54 without the use of an indirect aerosol  
 56 effect, whereas the GISS model  
 58 required a substantial indirect aerosol  
 60 contribution (more than half of the  
 62 total aerosol forcing; Hansen et al.,  
 64 2007). It is likely that the reason for  
 66 this difference was the excessive  
 68 direct effect in the GFDL model  
 70 caused by its overestimation of the  
 72 sulfate optical depth. The GISS  
 74 model direct aerosol effect (see  
 76 Section 3.6) is close to that derived  
 78 from observations (Chapter 2); this  
 80 suggests that for models with climate  
 82 sensitivity close to  $0.75^{\circ}\text{C}/(\text{W m}^{-2})$   
 84 (as in the GISS and GFDL models),  
 86 an indirect effect is needed.

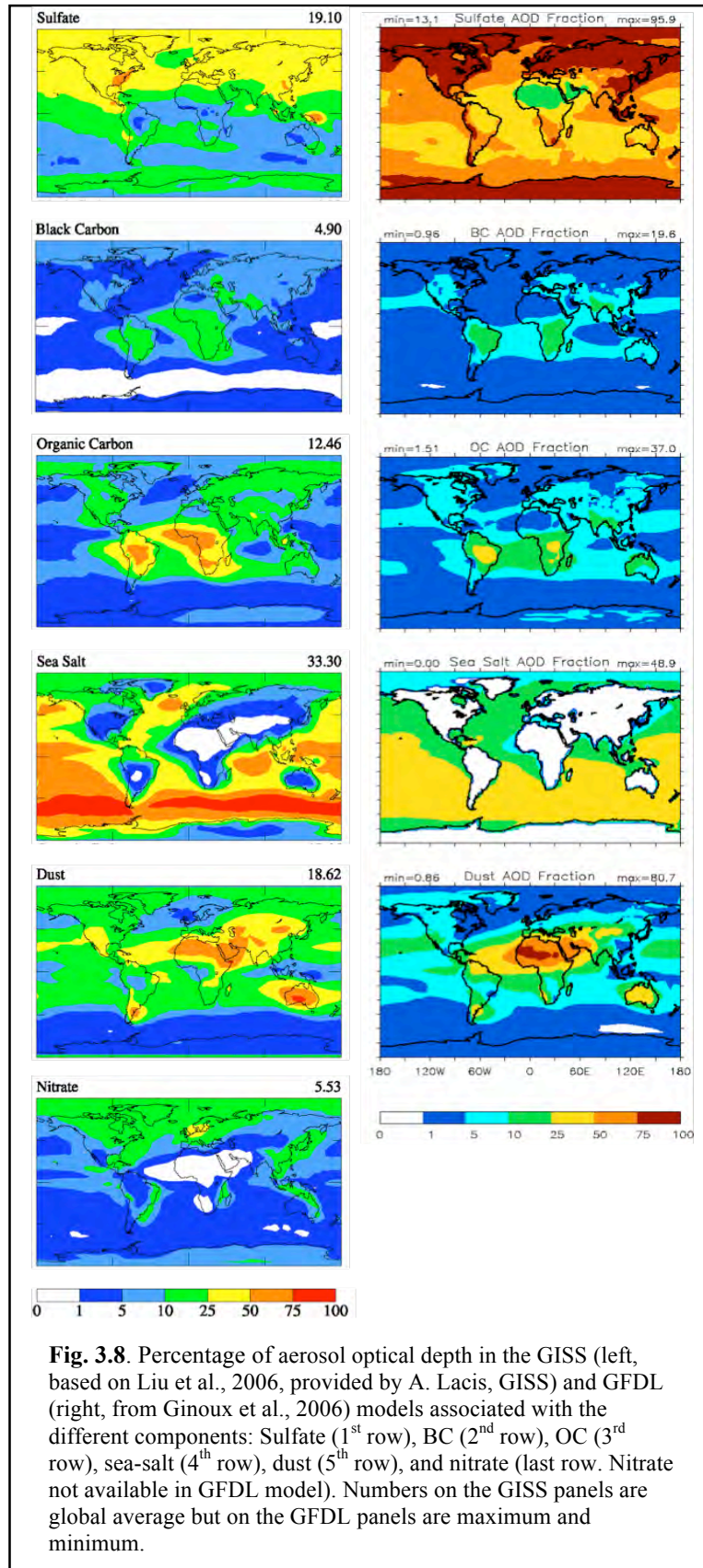


**Fig. 3.8.** Percentage of aerosol optical depth in the GISS (left, based on Liu et al., 2006, provided by A. Lacis, GISS) and GFDL (right, from Ginoux et al., 2006) models associated with the different components: Sulfate (1<sup>st</sup> row), BC (2<sup>nd</sup> row), OC (3<sup>rd</sup> row), sea-salt (4<sup>th</sup> row), dust (5<sup>th</sup> row), and nitrate (last row. Nitrate not available in GFDL model). Numbers on the GISS panels are global average but on the GFDL panels are maximum and minimum.

### 1 **3.5.2. Additional considerations**

2 *Long wave aerosol forcing:* So far only the aerosol RF in the shortwave (solar) spectrum has  
3 been discussed. Figure 3.7 (right column) shows that compared to the shortwave forcing, the  
4 values of aerosol long wave (thermal) forcing in the GISS model are on the order of 10%, with  
5 contribution coming mainly from dust aerosol. Like the shortwave forcing, these values will also  
6 be affected by the particular aerosol characteristics used in the simulation.

7 *Aerosol vertical distribution:* Vertical distribution is  
8 particularly important for absorbing aerosols, such as BC  
9 and dust in calculating the RF, particularly when  
10 longwave forcing is considered (e.g. Figure 3.7) because  
11 the energy they reradiate depends on the temperature (and  
12 hence altitude), which affects the calculated forcing  
13 values. Several model inter-comparison studies have  
14 shown that the largest difference among model simulated  
15 aerosol distributions is the vertical profile (e.g. Lohmann  
16 et al., 2001; Penner et al., 2002; Textor et al., 2006), due  
17 to the significant diversities in atmospheric processes in  
18 the models (e.g., Table 3.2). In addition, the vertical  
19 distribution also varies with space and time, as illustrated  
20 in **Figure 3.9** from the GISS ER simulations for January  
21 and July showing the most probable altitude of aerosol  
22 vertical locations. In general, aerosols in the northern  
23 hemisphere are located at lower altitudes in January than  
24 in July, and vice versa for the southern hemisphere.

25 *Mixing state:* Most climate model simulations  
26 incorporating different aerosol types have been made using external mixtures, i.e., the evaluation  
27 of the aerosols and their radiative properties are calculated separately for each aerosol type  
28 (assuming no mixing between different components within individual particles). Observations  
29 indicate that aerosols commonly consist of internally mixed particles, and these “internal  
30 mixtures” can have very different radiative impacts. For example, the GISS-1 (internal mixture)  
31 and GISS-2 (external mixture) model results shows very different magnitude and sign of aerosol  
32 forcing from slightly positive (implying slight warming) to strong negative (implying significant  
33 cooling) TOA forcing (Figure 3.2), due to changes in both radiative properties of the mixtures,  
34 and in aerosol amount. The more sophisticated aerosol mixtures from detailed microphysics  
35 calculations now being used/developed by different modeling groups may well end up producing  
36 very different direct (and indirect) forcing values.

37 *Cloudy sky vs. clear sky:* The satellite or AERONET observations are all for clear sky only  
38 because aerosol cannot be measured in the remote sensing technique when clouds are present.  
39 However, almost all the model results are for all-sky because of difficulty in extracting cloud-  
40 free scenes from the GCMs. So the AOD comparisons discussed earlier are not completely  
41 consistent. Because AOD can be significantly amplified when relative humidity is high, such as  
42 near or inside clouds, all-sky AOD values are expected to be higher than clear sky AOD values.  
43 On the other hand, the aerosol RF at TOA is significantly lower for all-sky than for clear sky  
44 conditions; the IPCC AR4 and AeroCom RF study (Schulz et al., 2006) have shown that on

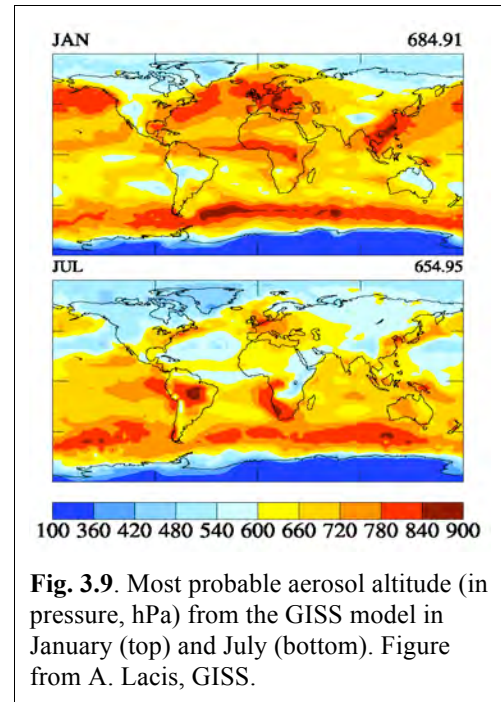


**Fig. 3.9.** Most probable aerosol altitude (in pressure, hPa) from the GISS model in January (top) and July (bottom). Figure from A. Lacis, GISS.

1 average the aerosol RF value for all-sky is about 1/3 of that for clear sky although with large  
 2 diversity (63%). These aspects illustrate the complexity of the system and the difficulty of  
 3 representing aerosol radiative influences in climate models whose cloud and aerosol distributions  
 4 are somewhat problematic. And of course aerosols in cloudy regions can affect the clouds  
 5 themselves, as discussed in Section 3.4.

## 6 **3.6. Impacts of Aerosols on Climate Model Simulations**

### 7 **3.6.1. Surface Temperature Change**

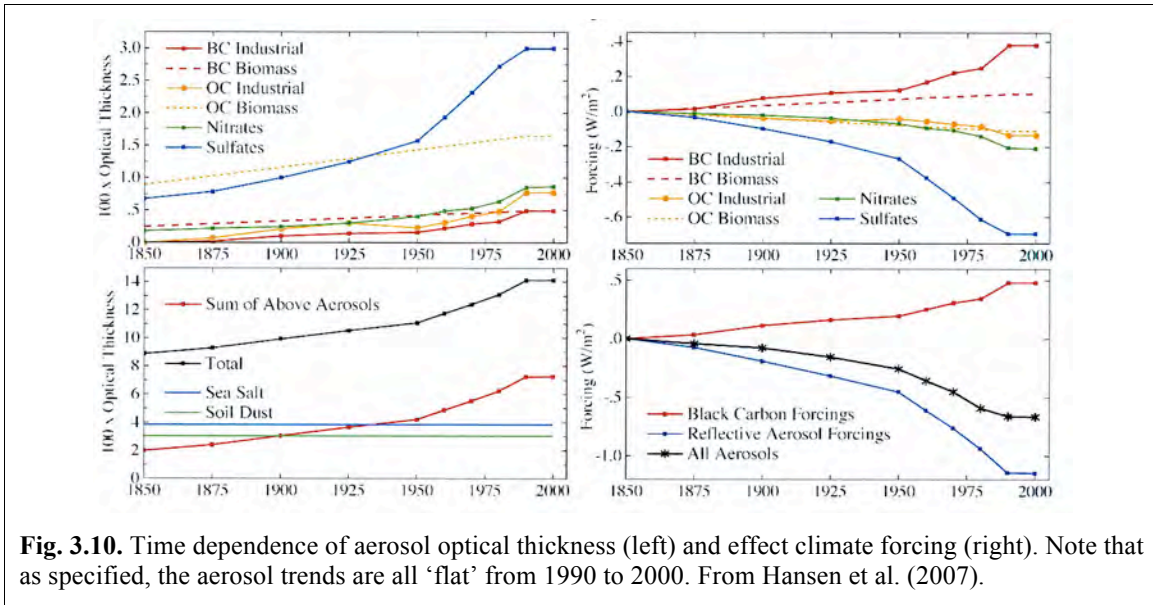
8 It was noted in the introduction that aerosol cooling is essential in order for models to produce  
 9 the observed global temperature rise over the last century, at least models with climate  
 10 sensitivities in the range of 3°C for doubled CO<sub>2</sub> (or ~0.75°C/Wm<sup>-2</sup>). The implications of this are  
 11 discussed here in somewhat more detail.

12 Hansen et al. (2007) show that in the GISS model, well-mixed greenhouse gases produce a  
 13 warming of close to 1°C between 1880 and the present (**Table 3.7**). The direct effect of  
 14 tropospheric aerosols as calculated in that model produces cooling of close to -0.3°C between  
 15 those same years, while the indirect effect (represented in that study as cloud cover change)  
 16 produces an additional cooling of similar magnitude (note that the general model result quoted in  
 17 IPCC AR4 is that the indirect RF is twice that of the direct effect).

18 The time dependence of the total aerosol forcing used as well as the individual species  
 19 components is shown in **Figure 3.10**. The resultant warming, 0.53 (±0.04) °C including these  
 20 and other forcings (Table 3.7), is less than the observed value of 0.6-0.7°C from 1880-2003.  
 21 Hansen et al. (2007) further show that a reduction in sulfate optical thickness and the direct  
 22 aerosol effect by 50%, which also reduced the aerosol indirect effect by 18%, produces a  
 23 negative aerosol forcing from 1880 to 2003 of -0.91 W m<sup>-2</sup> (down from -1.37 W m<sup>-2</sup> with this  
 24 revised forcing). The model now warms 0.75°C over that time. Hansen et al. (2007) defend this  
 25 change by noting that sulfate aerosol removal over North America and western Europe during  
 26 the 1990s led to a cleaner atmosphere. Note that the comparisons shown in the previous section  
 27 suggest that the GISS model already underestimates aerosol optical depths; it is thus trends that  
 28 are the issue here.

**Table 3.7.** Climate forcings (1880-2003) used to drive GISS climate simulations, along with the surface air temperature changes obtained for several periods. Instantaneous (Fi), adjusted (Fa), fixed SST (Fs) and effective (Fe) forcings are defined in Hansen et al. 2005. From Hansen et al., 2007.

Forcing agent	Forcing W m <sup>-2</sup> (1880 – 2003)				ΔT surface °C (year to 2003)			
	Fi	Fa	Fs	Fe	1880	1900	1950	1979
Well-mixed GHGs	2.62	2.50	2.65	2.72	0.96	0.93	0.74	0.43
Stratospheric H <sub>2</sub> O	-	-	0.06	0.05	0.03	0.01	0.05	0.00
Ozone	0.44	0.28	0.26	0.23	0.08	0.05	0.00	-0.01
Land Use	-	-	-0.09	-0.09	-0.05	-0.07	-0.04	-0.02
Snow albedo	0.05	0.05	0.14	0.14	0.03	0.00	0.02	-0.01
Solar Irradiance	0.23	0.24	0.23	0.22	0.07	0.07	0.01	0.02
Stratospheric aerosols	0.00	0.00	0.00	0.00	-0.08	-0.03	-0.06	0.04
Trop. aerosol direct forcing	-0.41	-0.38	-0.52	-0.60	-0.28	-0.23	-0.18	-0.10
Trop. aerosol indirect forcing	-	-	-0.87	-0.77	-0.27	-0.29	-0.14	-0.05
<b>Sum of above</b>	-	-	<b>1.86</b>	<b>1.90</b>	<b>0.49</b>	<b>0.44</b>	<b>0.40</b>	<b>0.30</b>
<b>All forcings at once</b>	-	-	<b>1.77</b>	<b>1.75</b>	<b>0.53</b>	<b>0.61</b>	<b>0.44</b>	<b>0.29</b>



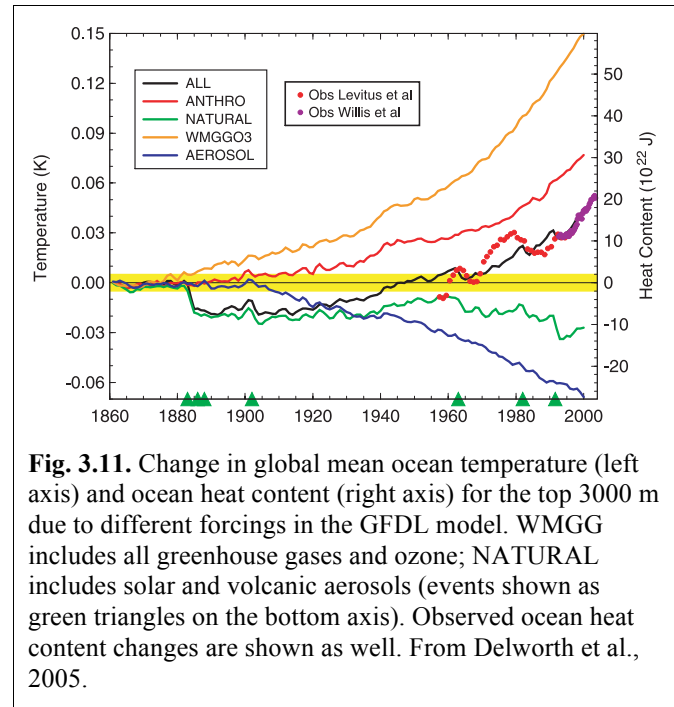
2 The magnitude of the indirect effect used by Hansen et al. (2005) is roughly calibrated to  
 3 reproduce the observed change in diurnal temperature cycle and is consistent with some satellite  
 4 observations. However, as Anderson et al., (2003) note, the forward calculation of aerosol  
 5 negative forcing covers a much larger range than is normally used in GCMs; the values chosen,  
 6 as in this case, are consistent with the inverse reasoning estimates of what is needed to produce  
 7 the observed warming, and hence generally consistent with current model climate sensitivities.  
 8 The authors justify this approach by claiming that paleoclimate data indicate a climate sensitivity  
 9 of close to  $0.75^{\circ}(\pm 0.25) \text{ }^{\circ}\text{C}/\text{Wm}^{-2}$ , and therefore something close to this magnitude of negative  
 10 forcing is reasonable. Even this stated range leaves significant uncertainty in climate sensitivity  
 11 and the magnitude of the aerosol negative forcing. Furthermore, IPCC (2007) concluded that  
 12 paleoclimate data are not capable of narrowing the range of climate sensitivity, nominally 0.375  
 13 to  $1.13 \text{ }^{\circ}\text{C}/\text{Wm}^{-2}$ , because of uncertainties in paleoclimate forcing and response; so from this  
 14 perspective the total aerosol forcing is even less constrained than the GISS estimate. Hansen et  
 15 al. (2007) acknowledge that “an equally good match to observations probably could be obtained  
 16 from a model with larger sensitivity and smaller net forcing, or a model with smaller sensitivity  
 17 and larger forcing”.

18 The GFDL model results for global mean ocean temperature change (down to 3 km depth) for  
 19 the time period 1860 to 2000 is shown in **Figure 3.11**, along with the different contributing  
 20 factors (Delworth et al., 2005). This is the same GFDL model whose aerosol distribution was  
 21 discussed previously. The aerosol forcing produces a cooling on the order of 50% that of  
 22 greenhouse warming (generally similar to that calculated by the GISS model, Table 3.7). Note  
 23 that this was achieved without any aerosol indirect effect.

24 The general model response noted by IPCC, as discussed in the introduction, was that the total  
 25 aerosol forcing of  $-1.3 \text{ W m}^{-2}$  reduced the greenhouse forcing of near  $3 \text{ W m}^{-2}$  by about 45%, in  
 26 the neighborhood of the GFDL and GISS forcings. Since the average model sensitivity was close  
 27 to  $0.75 \text{ }^{\circ}\text{C}/\text{Wm}^{-2}$ , similar to the sensitivities of these models, the necessary negative forcing is

1 therefore similar. The agreement cannot therefore be used to validate the actual aerosol effect  
2 until climate sensitivity itself is better known.

3 Is there some way to distinguish between  
4 greenhouse gas and aerosol forcing that  
5 would allow the observational record to  
6 indicate how much of each was really  
7 occurring? This question of attribution has  
8 been the subject of numerous papers, and  
9 the full scope of the discussion is beyond the  
10 range of this report. It might be briefly noted  
11 that Zhang et al. (2006) using results from  
12 several climate models and including both  
13 spatial and temporal patterns, found that the  
14 climate responses to greenhouse gases and  
15 sulfate aerosols are correlated, and  
16 separation is possible only occasionally,  
17 especially at global scales. This conclusion  
18 appears to be both model and method-  
19 dependent: using time-space distinctions as  
20 opposed to trend detection may work  
21 differently in different models (Gillett et al.,  
22 2002a). Using multiple models helps  
23 primarily by providing larger-ensemble sizes for statistics (Gillett et al., 2002b). However, even  
24 separating between the effects of different aerosol types is difficult. Jones et al. (2005) concluded  
25 that currently the pattern of temperature change due to black carbon is indistinguishable from the  
26 sulfate aerosol pattern. In contrast, Hansen et al. (2005) found that absorbing aerosols produce a  
27 different global response than other forcings, and so may be distinguishable. Overall, the  
28 similarity in response to all these very different forcings is undoubtedly due to the importance of  
29 climate feedbacks in amplifying the forcing, whatever its nature.



30 Distinctions in the climate response do appear to arise in the vertical, where absorbing aerosols  
31 produce warming that is exhibited throughout the troposphere and into the stratosphere, whereas  
32 reflective aerosols cool the troposphere but warm the stratosphere (Hansen et al., 2005; IPCC,  
33 2007). Delworth et al. (2005) noted that in the ocean, the cooling effect of aerosols extended to  
34 greater depths, due to the thermal instability associated with cooling the ocean surface. Hence the  
35 temperature response at levels both above and below the surface may provide an additional  
36 constraint on the magnitudes of each of these forcings, as may the difference between Northern  
37 and Southern Hemisphere changes (IPCC, 2007 Chapter 9). The profile of atmospheric  
38 temperature response will be useful to the extent that the vertical profile of aerosol absorption, an  
39 important parameter to measure, is known.

### 40 **3.6.2. Implications for Climate Model Simulations**

41 The comparisons in Sections 3.2 and 3.3 suggest that there are large differences in model  
42 calculated aerosol distributions, mainly because of the large uncertainties in modeling the aerosol  
43 atmospheric processes in addition to the uncertainties in emissions. The fact that the total optical  
44 depth is in better agreement between models than the individual components means that even



1 with similar optical depths, the aerosol direct forcing effect can be quite different, as shown in  
2 the AeroCom studies. Because the diversity among models and discrepancy between models and  
3 observations are much larger at the regional level than in global average, the assessment of  
4 climate response (e.g. surface temperature change) to aerosol forcing would be more accurate for  
5 global average than for regional or hemispheric differentiation. However, since aerosol forcing is  
6 much more pronounced on regional than on global scales because of the highly variable aerosol  
7 distributions, it is insufficient or even misleading to just get the global average right.

8 The indirect effect is strongly influenced by the aerosol concentrations, size, type, mixing state,  
9 microphysical processes, and vertical profile. As shown in previous sections, very large  
10 differences exist in those quantities even among the models having similar AOD. Moreover,  
11 modeling aerosol indirect forcing presents more challenges than direct forcing because there is  
12 so far no rigorous observational data, especially on a global scale, that one can use to test the  
13 model simulations. As seen in the comparisons of the GISS and GFDL model climate  
14 simulations for IPCC AR4, aerosol indirect forcing was so poorly constrained that it was  
15 completely ignored by one model (GFDL) but used by another (GISS) at a magnitude that is  
16 more than half of the direct forcing, in order to reproduce the observed surface temperature  
17 trends. A majority of the climate models used in IPCC AR4 do not consider indirect effects; the  
18 ones that did were mostly limited to highly simplified sulfate indirect effects (Table 3.6).  
19 Improvements must be made to at least the degree that the aerosol indirect forcing can no longer  
20 be used to mask the deficiencies in estimating the climate response to greenhouse gas and  
21 aerosol direct RF.

### 22 **3.7. Outstanding Issues**

23 Clearly there are still large gaps in assessing the aerosol impacts on climate through modeling.  
24 Major outstanding issues and prospects of improving model simulations are discussed below.

25 *Aerosol composition:* Many global models are now able to simulate major aerosol types such as  
26 sulfate, black carbon, and POM, dust, and sea salt, but only a small fraction of these models  
27 simulate nitrate aerosols or consider anthropogenic secondary organic aerosols. And it is difficult  
28 to quantify the dust emission from human activities. As a result, the IPCC AR4 estimation of the  
29 nitrate and anthropogenic dust TOA forcing was left with very large uncertainty. The next  
30 generation of global models should therefore have a more comprehensive suite of aerosol  
31 compositions with better-constrained anthropogenic sources.

32 *Aerosol absorption:* One of the most critical parameters in aerosol direct RF and aerosol impact  
33 on hydrological cycles is the aerosol absorption. Most of the absorption is from BC despite its  
34 small contribution to total aerosol load and AOD; dust too absorbs in both the short and long-  
35 wave spectral ranges, whereas POM absorbs in the UV to visible. The aerosol absorption or  
36 SSA, will have to be much better represented in the models through improving the estimates of  
37 carbonaceous and dust aerosol sources, their atmospheric distributions, and optical properties.

38 *Aerosol indirect effects:* The activation of aerosol particles into CCN depends not only on  
39 particle size but chemical composition, with the relative importance of size and composition  
40 unclear. In current aerosol-climate modeling, aerosol size distribution is generally prescribed and  
41 simulations of aerosol composition have large uncertainties. Therefore the model estimated  
42 “albedo effect” has large uncertainties. How aerosol would influence cloud lifetime/cover is still  
43 in debate. The influence of aerosols on other aspects of the climate system, such as precipitation,

1 is even more uncertain, as are the physical processes involved. Processes that determine aerosol  
2 size distributions, hygroscopic growth, mixing state, as well as CCN concentrations, however,  
3 are inadequately represented in most of the global models. It will also be difficult to improve the  
4 estimate of indirect effects until the models can produce more realistic cloud characteristics.

5 *Aerosol impacts on surface radiation and atmospheric heating:* Although these effects are well  
6 acknowledged to play roles in modulating atmospheric circulation and water cycle, few coherent  
7 or comprehensive modeling studies have focused on them, as compared to the efforts that have  
8 gone to assessing aerosol RF at TOA. They have not yet been addressed in the previous IPCC  
9 reports. Here, of particular importance is to improve the accuracy of aerosol absorption.

10 *Long-term trends of aerosol:* To assess the aerosol effects on climate change the long-term  
11 variations of aerosol amount and composition and how they are related to the emission trends in  
12 different regions have to be specified. Simulations of historical aerosol trends can be problematic  
13 since historical emissions of aerosols have shown large uncertainties—as information is difficult  
14 to obtain on past source types, strengths, and even locations. The IPCC AR4 simulations used  
15 several alternative aerosol emission histories, especially for BC and POM aerosols.

16 *Climate modeling:* Current aerosol simulation capabilities from CTMs have not been fully  
17 implemented in most models used in IPCC AR4 climate simulations. Instead, a majority  
18 employed simplified approaches to account for aerosol effects, to the extent that aerosol  
19 representations in the GCMs, and the resulting forcing estimates, are inadequate. The  
20 oversimplification occurs in part because the modeling complexity and computing resource  
21 would be significantly increased if the full suite of aerosols were fully coupled in the climate  
22 models.

23 *Observational constraints:* Model improvement has been hindered by a lack of comprehensive  
24 datasets that could provide multiple constraints for the key parameters simulated in the model.  
25 The extensive AOD coverage from satellite observations and AERONET measurements has  
26 helped a great deal in validating model-simulated AOD over the past decade, but further progress  
27 has been slow. Large model diversities in aerosol composition, size, vertical distribution, and  
28 mixing state are difficult to constrain, because of lack of reliable measurements with adequate  
29 spatial and temporal coverage (see Chapter 2).

30 *Aerosol radiative forcing:* Because of the large spatial and temporal differences in aerosol  
31 sources, types, emission trends, compositions, and atmospheric concentrations, anthropogenic  
32 aerosol RF has profound regional and seasonal variations. So it is an insufficient measure of  
33 aerosol RF scientific understanding, however useful, for models (or observation-derived  
34 products) to converge only on globally and annually averaged TOA RF values and accuracy.  
35 More emphasis should be placed on regional and seasonal comparisons, and on climate effects in  
36 addition to direct RF at TOA.

### 37 **3.8 Conclusions**

38 From forward modeling studies, as discussed in the IPCC (2007), the direct effect of aerosols  
39 since pre-industrial times has resulted in a negative RF of about  $-0.5 \pm 0.4 \text{ W m}^{-2}$ . The RF due to  
40 cloud albedo or brightness effect is estimated to be  $-0.7$  ( $-1.8$  to  $-0.3$ )  $\text{W m}^{-2}$ . Forcing of similar  
41 magnitude has been used in some modeling studies for the effect associated with cloud lifetime,  
42 in lieu of the cloud brightness influence. The total negative RF due to aerosols according to  
43 IPCC (2007) estimates is therefore  $-1.3$  ( $-2.2$  to  $-0.5$ )  $\text{W m}^{-2}$ . With the inverse approach, in which

1 aerosols provide forcing necessary to produce the observed temperature change, values range  
2 from -1.7 to -0.4 Wm<sup>-2</sup> (IPCC, 2007). These results represent a substantial advance over previous  
3 assessments (e.g., IPCC TAR), as the forward model estimated and inverse approach required  
4 aerosol TOA forcing values are converging. However, large uncertainty ranges preclude using  
5 the forcing and temperature records to more accurately determine climate sensitivity.

6 There are now a few dozen models that simulate a comprehensive suite of aerosols. This is done  
7 primarily in the CTMs. Model inter-comparison studies have shown that models have merged at  
8 matching the global annual averaged AOD observed by satellite instruments, but they differ  
9 greatly in the relative amount of individual components, in vertical distributions, and in optical  
10 properties. Because of the great spatial and temporal variations of aerosol distributions, regional  
11 and seasonal diversities are much larger than that of the global annual mean. Different emissions  
12 and differences in atmospheric processes, such as transport, removal, chemistry, and aerosol  
13 microphysics, are chiefly responsible for the spread among the models. The varying component  
14 contributions then lead to differences in aerosol direct RF, as aerosol scattering and absorption  
15 properties depend on aerosol size and type. They also impact the calculated indirect RF, whose  
16 variations are further amplified by the wide range of cloud and convective parameterizations in  
17 models. Currently, the largest aerosol RF uncertainties are associated with the aerosol indirect  
18 effect.

19 Most climate models used for the IPCC AR4 simulations employed simplified approaches, with  
20 aerosols specified from stand-alone CTM simulations. Despite the uncertainties in aerosol RF  
21 and widely varying model climate sensitivity, the IPCC AR4 models were generally able to  
22 reproduce the observed temperature record for the past century. This is because models with  
23 lower/higher climate sensitivity generally used less/more negative aerosol forcing to offset the  
24 greenhouse gas warming. An equally good match to observed surface temperature change in the  
25 past could be obtained from a model with larger climate sensitivity and smaller net forcing, or a  
26 model with smaller sensitivity and larger forcing (Hansen et al., 2007). Obviously, both  
27 greenhouse gases and aerosol effects have to be much better quantified in future assessments.

28 Progress in better quantifying aerosol impacts on climate can be made only when the capabilities  
29 of both aerosol observations and models are improved. The primary concerns and issues  
30 discussed in this chapter include:

- 31 • Better representation of aerosol composition and absorption in the global models
- 32 • Improved theoretical understanding of subgrid-scale processes crucial to aerosol-cloud  
33 interactions and lifetime
- 34 • Improved aerosol microphysics and cloud parameterizations
- 35 • Better understanding of aerosol effects on surface radiation and hydrological cycles
- 36 • More focused analysis on regional and seasonal variations of aerosols
- 37 • More reliable simulations of aerosol historic long-term trends
- 38 • More sophisticated climate model simulations with coupled aerosol and cloud processes
- 39 • Enhanced satellite observations of aerosol type, SSA, vertical distributions, and aerosol  
40 radiative effect at TOA; more coordinated field experiments to provide constraints on  
41 aerosol chemical, physical, and optical properties.

42 A discussion of the “way forward” toward better constraints on aerosol radiative forcing, and  
43 hence climate sensitivity, is provided in the next chapter.

44

# CHAPTER 4

## The Way Forward

**Authors:** David Rind, NASA GISS; Ralph A. Kahn, NASA GSFC; Mian Chin, NASA GSFC; Stephen E. Schwartz, DOE BNL; Lorraine A. Remer, NASA GSFC; Graham Feingold, NOAA ESRL; Hongbin Yu, NASA GSFC; Patricia Quinn, NOAA PMEL; Rangasayi Halthore, NASA HQ/NRL

### 4.1. Major Research Needs

This review has emphasized that despite the increase in understanding aerosol forcing of the climate system, many important uncertainties remain. By way of perspective, that concerted effort has been directed toward this issue only for about the past 20 years. In view of the variety of aerosol types and emissions, uncertain microphysical properties, great temporal and spatial variability, and the added complexity of aerosol-cloud interactions, it is easy to understand why much more work is required to define anthropogenic aerosol forcing with confidence comparable to that for other climate forcing agents.

When comparing surface temperature changes calculated by climate models with those observed, the IPCC AR4 noted "broad consistency" between the modeled and observed temperature record over the industrial period. However, understanding of the degree to which anthropogenic aerosols offset the better-established greenhouse gas forcing is still inadequate. This limits confidence in the predicted magnitude of climate response to future changes in greenhouse gases and aerosols.

This chapter briefly summarizes the major research needs that have been highlighted in previous chapters, recognizing that achieving them will not necessarily be easy or straightforward. Although some important accomplishments will likely be possible in the next decade, others may, realistically, take considerably longer. Several important points should be kept in mind:

- 1. The uncertainty in assessing total anthropogenic greenhouse gas and aerosol impacts on climate must be much reduced from its current level to allow meaningful predictions of future climate.** Using statistical methods, IPCC AR4 concluded that the present-day global-average anthropogenic RF is  $2.9 \pm 0.3 \text{ W m}^{-2}$  for long-lived greenhouse gases plus ozone,  $-1.3$  ( $-2.2$  to  $-0.5$ )  $\text{W m}^{-2}$  for aerosol direct plus aerosol-cloud-albedo, and  $+1.6$  ( $0.6$  to  $2.4$ )  $\text{W m}^{-2}$  for total anthropogenic forcing (Figure 1.3 in Chapter 1). As shown in Chapter 1, the current estimate of total anthropogenic RF yields the transient climate sensitivity range of  $0.3 - 1.1^\circ\text{C}/(\text{W m}^{-2})$ . This translates to a possible surface temperature increase from  $1.2^\circ\text{C}$  to  $4.4^\circ\text{C}$  at the time of (equivalent) doubled  $\text{CO}_2$  forcing, which will likely occur toward the latter part of this century. Such a range is too wide to meaningfully predict the climate response to increased greenhouse gases.

The large uncertainty in total anthropogenic forcing arises primarily from current uncertainty in the current understanding of aerosol RF, as illustrated in Figure 1.3. One

1 objective should be to reduce the uncertainty in global average RF by anthropogenic  
2 aerosols over the industrial period to  $\pm 0.3 \text{ W m}^{-2}$ , equal to the current uncertainty in RF  
3 by anthropogenic greenhouse gases over this period. Then, taking the total anthropogenic  
4 forcing taken as the IPCC central value,  $1.6 \text{ W m}^{-2}$ , the range in transient climate  
5 sensitivity would be reduced to  $0.37 - 0.54^\circ\text{C}/(\text{W m}^{-2})$ , and the corresponding increase in  
6 global mean surface temperature change at the time of doubled  $\text{CO}_2$  forcing would be  
7 between  $1.5^\circ\text{C}$  and  $2.2^\circ\text{C}$ . This range is small enough to make more meaningful global  
8 predictions pertinent to planning for mitigation and adaptation.

9 **2. Evaluation of aerosol effects on climate must take into account high spatial and**  
10 **temporal variation of aerosol amounts and properties.** Determining the global mean  
11 aerosol TOA RF is necessary but far from sufficient, because of the large spatial and  
12 temporal variation of aerosol distributions and composition that is in contrast to the much  
13 more uniformly distributed longer-lived greenhouse gases such as  $\text{CO}_2$  and methane.  
14 Therefore, aerosol RF at local to regional scales could be much stronger than its global  
15 average.

16 **3. Understanding of the aerosol effects on global water cycle should be much**  
17 **advanced.** Besides the radiative forcing, aerosols have other important climate effects.  
18 They heat the atmosphere and cool the surface, thus affecting atmospheric circulations  
19 and water cycle. The level of scientific understanding of these effects is much lower than  
20 that for aerosol direct RF; it requires concerted research effort to move forward.

21 The approach taken for assessing aerosol forcing of the climate system includes both  
22 measurement and modeling components. As discussed in Chapters 2 and 3, improved  
23 observations, with some assistance from models, are already helping produce measurement-  
24 based estimates of the current aerosol direct effect on climate. Global models are now  
25 converging on key parameters such as AOD, and thanks to satellite and other atmospheric  
26 measurements, are moving toward better assessments of present-day aerosol RF. However, given  
27 the relatively short history of satellite observations and the nature of future climate prediction,  
28 the assessment of anthropogenic aerosol climate impact for past and future times will inevitably  
29 depend on models. Models are also required to apportion observed aerosols between natural and  
30 anthropogenic sources. Therefore, improving model predictions of aerosol climate forcing is the  
31 key to progress. To do so, it is essential to advance the current measurement capabilities that will  
32 allow much better validation of the models and fundamental improvement of model components.

33 The accuracy of regional to global-scale AOD measured by satellites is currently poorer than  
34 needed to substantially reduce uncertainty in direct radiative forcing by aerosols, but the required  
35 capability is within reach, based on the accuracy of current local surface-based measurement  
36 techniques. Problems remain in converting total aerosol forcing to forcing by anthropogenic  
37 aerosols. The accuracy of aerosol vertical distributions as measured by Lidar from space is  
38 approaching that required to be useful for evaluating chemical transport models, and is within  
39 reach of that required to reduce uncertainties in aerosol direct radiative forcing.

40 Measurement accuracy for remotely sensed aerosol optical and physical properties (e.g., SSA, g,  
41 size) is poorer than needed to significantly reduce uncertainty in aerosol direct radiative forcing  
42 and to effect satisfactory translation between AOD retrieved from radiation-based remote-  
43 sensing measurements and AOD calculated from CTMs based on aerosol mass concentrations

1 (the fundamental quantities tracked in the model) and optical properties. Combinations of  
2 remote-sensing and targeted *in situ* measurement with modeling are required for near-term  
3 progress in this area.

4 Measurements for aerosol indirect effect remain a major challenge. Sensitivity of remote-sensing  
5 measurement to particle size, composition, concentration, vertical distribution, and horizontal  
6 distribution in the vicinity of clouds is poor. Combinations of detailed *in situ* and laboratory  
7 measurements and cloud-resolved modeling, along with spatial extrapolation using remote-  
8 sensing measurements and larger-scale modeling, are required for near-term progress in this area.

9 The next sections address the priorities and recommend approach to moving forward.

## 10 **4.2. Priorities**

### 11 **4.2.1. Measurements**

12 ***Maintain current and enhance the future satellite aerosol monitoring capabilities.*** Satellites  
13 have been providing global aerosol observations since the late 1970s, with much improved  
14 accuracy measurements since late 1990s, but some of them, such as the NASA EOS satellites  
15 (Terra, Aqua, Aura), are reaching or exceeding their design lives. Timely follow-on missions to  
16 at least maintain these capabilities are important. Assessment of aerosol climate impacts requires  
17 a long-term data record having consistent accuracy and high quality, suitable for detecting  
18 changes in aerosol amount and type over decadal time scales. Future satellite sensors should  
19 have the capability of acquiring information on aerosol size distribution, absorption, vertical  
20 distribution, and type with sufficiently high accuracy and adequate spatial coverage and  
21 resolution to permit quantification of forcing to required accuracy. The separation of  
22 anthropogenic from natural aerosols, perhaps based on size and shape, is essential for assessing  
23 human impacts. A brief summary of current capabilities and future needs of major aerosol  
24 measurement requirements from space is provided in **Table 4.1**. (More detailed discussion is in  
25 Chapter 2.)

26 ***Maintain, enhance, and expand the surface observation networks.*** Long-term surface-based  
27 networks such as the NASA AERONET network, the NOAA ESRL and the DOE ARM sites  
28 have for several decades been providing essential information on aerosol properties that is vital  
29 for satellite validation, model evaluation, and climate change assessment from trend analysis.  
30 Observation should be enhanced with additional, routine measurements of size-resolved  
31 composition, more lidar profiling of vertical features, and improved measurements of aerosol  
32 absorption with state-of-art techniques. This, along with climate-quality data records constructed  
33 from satellites, would help establish connections between aerosol trends and the observed trends  
34 in radiation (e.g., dimming or brightening).

35 ***Execute a continuing series of coordinated field campaigns.*** These would aim to: (1) broaden  
36 the database of detailed particle optical, physical, and chemical (including cloud-nucleating)  
37 properties for major aerosol types, (2) refine and validate satellite and surface-based remote-  
38 sensing retrieval algorithms, (3) make comprehensive, coordinated, multi-platform  
39 measurements characterizing aerosols, radiation fields, cloud properties and related aerosol-  
40 cloud interactions, to serve as testbeds for modeling experiments at several scales, and (4)  
41 deepen the links between aerosol (and cloud) measuring and modeling communities. New and

1 improved instrument capabilities will be needed to provide more accurate measurements of  
 2 aerosol absorption and scattering properties across the solar spectrum.

**Table 4.1.** Summary of current status and future needs of major aerosol measurements from space for characterization of tropospheric aerosol and determination of aerosol climate forcing.

Satellite instrument	Time Period	AOD	Size or Shape <sup>1</sup>	Absorption <sup>2</sup>	Vertical Profile	Global Coverage
<b>Historic / Current:</b>						
AVHRR	Since 1981	✓	✓			Ocean only
TOMS	1979 – 2001	✓		✓		✓
POLDER	Since 1997	✓	✓			✓
MODIS	Since 2000	✓	✓			✓
MISR	Since 2000	✓	✓	✓		✓
OMI	Since 2004	✓		✓		✓
GLAS	Since 2003 <sup>3</sup>		✓		✓	
CALIOP	Since 2006		✓		✓	
<b>Scheduled to Launch:</b>						
VIIRS (on NPP/NPOESS)	2009 –	✓				✓
OMPS (on NPP)	2009 –	✓		✓		✓
APS (on Glory)	2009 –	✓	✓	✓		
HSRL (on EarthCARE)	2013 –				✓	
<b>Future Needs:</b>						
Next generation instruments (polarimeter, lidar, etc.) with much improved detection accuracy and coverage for AOD and absorption, enhanced capability for measuring vertical profiles, aerosol types and properties, augmented capacity with measurements of aerosol, clouds, and precipitation.						
<sup>1</sup> Size is inferred from the spectral variation of AOD, expressed as the Ångström exponent.						
<sup>2</sup> Determination of absorption from MISR is conditional and not always available.						
<sup>3</sup> Aerosol detection by GLAS is limited to only a few months each year because of laser power problems.						

3  
 4 **Measure aerosol, clouds, and precipitation variables jointly.** Measurements of aerosol  
 5 properties must go hand in hand with measurements of cloud properties, and also with  
 6 measurements of precipitation and meteorological variables, whether this will be from aircraft,  
 7 ground-based remote sensing or satellite. Assessing aerosol effects on climate has focused on the  
 8 interactions of aerosol with Earth’s radiation balance (i.e., radiative forcing), but in the near  
 9 future, focus will shift to include aerosol effects on precipitation patterns, atmospheric  
 10 circulation, and weather.

11 **Fully exploit the existing information in satellite observations of AOD and particle type.** An  
 12 immense amount of data has been collected. Table 4.1 lists the most widely used aerosol  
 13 property data sets retrieved from satellite sensors. A synthesis of data from multiple sensors  
 14 would in many cases be a more effective resource for aerosol characterizing than data from  
 15 individual sensors alone. However, techniques for achieving such synthesis are still in their  
 16 infancy, and multi-sensor products have only begun to be developed. The full information  
 17 content of existing data, even with individual sensors, has not been realized. There is a need to:

1 (1) refine retrieval algorithms and extract greater information about aerosols from the joint data  
2 sets, (2) quantify data quality, (3) generate uniform (and as appropriate, merged), climate-quality  
3 data records, and to apply them to: (4) initialize, constrain, and validate models, (5) conduct  
4 detailed process studies, and (6) perform statistical trend analysis.

5 **Measure aerosol properties in the laboratory.** Laboratory studies are essential to determine  
6 chemical transformation rates for aerosol particle formation. They can also provide information,  
7 in a controlled environment, for particle hygroscopic growth, light scattering and absorption  
8 properties, and particle activation for aerosols of specific, known composition. Such  
9 measurements will allow development of suitable mixing rules and evaluation of the  
10 parameterizations that rely on such mixing rules.

11 **Improve measurement-based techniques for distinguishing anthropogenic from natural**  
12 **aerosols.** Current satellite-based estimates of anthropogenic aerosol fraction rely on retrievals of  
13 aerosol type. These estimates suffer from limited information content of the data under many  
14 circumstances. More needs to be done to combine satellite aerosol type and vertical distribution  
15 retrievals with supporting information from: (1) back-trajectory and inverse modeling, (2) at  
16 least qualitative time-series of plume evolution from geosynchronous satellite imaging, and (3)  
17 surface monitoring and particularly targeted aircraft *in situ* measurements. Different definitions  
18 of “anthropogenic” aerosols will require reconciliation. The anthropogenic fraction of today’s  
19 aerosol, estimated from current measurements, will not produce the same aerosol radiative  
20 forcing defined as the perturbation of the total aerosol from pre-industrial times. Consistently  
21 defined perturbation states are required before measurement-based and model-based aerosol  
22 radiative forcing estimates can be meaningfully compared.

#### 23 **4.2.2. Modeling**

24 **Improve model simulations of aerosols and their direct radiative forcing.** Spatial and temporal  
25 distributions of aerosol mass concentrations are affected primarily by sources, removal  
26 mechanisms, atmospheric transport, and chemical transformations; calculations of aerosol direct  
27 RF require additional information about on the aerosol optical properties. Coordinated studies  
28 are needed to understand the importance of individual processes, especially vertical mixing and  
29 removal by convection/precipitation. Observational strategies must be developed to constrain  
30 and validate the key parameters describing: (a) aerosol composition, (b) mass concentration, (c)  
31 vertical distribution, (d) size distribution, (e) hygroscopic growth, (f) aerosol absorption, (g)  
32 asymmetry parameter and (h) aerosol optical depth. As many models now include major aerosol  
33 types including sulfate, BC, primary POM, dust, and sea salt, progress is needed on simulating  
34 nitrate and secondary organic aerosols. In addition, aerosol microphysical processes should be  
35 much better represented in the models. In practice, improving the capability of aerosol  
36 composition modeling will require improved remote sensing and *in situ* observations to  
37 discriminate among aerosol components. Improvement in modeling radiative forcing could be  
38 aided by data assimilation methods, in which the observed aerosol distributions that are input to  
39 the model, and the modeled short-term response, could be compared directly with RF  
40 observations.

41 **Advance the capability for modeling aerosol-cloud interaction.** The interaction between  
42 aerosols and clouds is probably the biggest uncertainty of all climate forcing/feedback processes.  
43 The processes involved are complex, and accurate simulation will require sub-grid calculations



1 or improved aerosol and cloud parameterizations on global-model scales. Among the key  
2 elements required are: (a) cloud nucleating properties for different aerosol types and size  
3 distributions, (b) CCN concentrations as functions of supersaturation and any kinetic influences,  
4 (c) algorithms to simulate aerosol influences on cloud brightness, that include cloud fraction,  
5 cloud liquid water content, and precipitation efficiency, and (d) cloud drop concentration for  
6 known (measured) updraft, humidity, and temperature conditions. Improved aerosol-cloud  
7 interaction modeling must be built upon more realistic simulation of clouds and cloud process in  
8 GCMs. Cloud-resolving models offer one approach to tackling these questions, aided by the  
9 continual improvement in computing capability that makes possible simulations at the higher  
10 resolutions appropriate to these processes. Realizing the latter approach, however, may be a  
11 long-term goal.

12 ***Simulate climate change with coupled aerosol-climate system models.*** Coupling aerosol  
13 processes in the GCMs would represent a major step in climate simulation beyond the IPCC  
14 AR4. This would enable aerosols to interact with the meteorological variables such as clouds and  
15 precipitation. Climate change simulations need to be run for hundreds of years with coupled  
16 atmosphere-ocean models. Inclusion of aerosol physics and chemistry, and increasing the model  
17 resolution, will put large demands on computing power and resources. Some simplification may  
18 be necessary, especially considering that other required model improvements, such as finer  
19 resolution and carbon cycle models, also increase computing time. The near-term step is to  
20 include simple representations of aerosols directly in climate models, incorporating the major  
21 aerosol types, basic chemistry, and parameterized cloud droplet activation schemes. Such models  
22 exist today, and are ready to be applied to long-term simulations, making it possible to calculate  
23 first-order aerosol climate feedbacks. The next generation of models will include aerosol  
24 processes that allow for more realistic interactions, such as aerosol and cloud microphysical  
25 processes; however, the complexity included should be commensurate with that for other  
26 relevant portions of the simulation, such as clouds and convection. Fully coupled aerosol-  
27 chemistry-physics-climate models will likely be a model-development focus for at least the next  
28 decade. This should eventually lead to increasingly sophisticated model simulations of aerosol  
29 effects on climate, and better assessments of climate sensitivity.

### 30 **4.2.3. Emissions**

31 ***Develop and evaluate emissions inventories of aerosol particles and precursor gases.*** A  
32 systematic determination of emissions of primary particles and of aerosol precursor gases is  
33 needed as input to modeling the geographical and temporal distribution of the amount and  
34 radiative forcing of aerosols. The required description of emissions includes the location, timing,  
35 activity, and amount. For particles the emissions should be characterized by size distributed  
36 composition, not simply just by mass emissions because of the effects of these properties on  
37 direct and indirect forcings. Natural emissions from biogenic and volcanic sources should be  
38 systematically assessed. Satellite fire data are now being used to help constrain biomass-burning  
39 emissions, which include new information on aerosol injection height. Dust emission from  
40 human activities, such as from farming practices and land-use changes, likewise needs to be  
41 quantified. Characterization of aerosol trends and radiative forcing also requires historical  
42 emission data. For assessing anthropogenic impacts on future climate, projections of future  
43 anthropogenic fuel use and changes in wildfire, desert dust, biogenic, and other sources are  
44 needed, and methods used to obtain them carefully evaluated and possibly refined. Some such  
45 efforts are being pursued in conjunction with the IPCC.

### 1 **4.3. Concluding Remarks**

2 Narrowing the gap between the current understanding of long-lived greenhouse gas and that of  
3 anthropogenic aerosol contributions to RF will require progress in all aspects of aerosol-climate  
4 science. Development of new space-based, field, and laboratory instruments will be needed, and  
5 in parallel, more realistic simulations of aerosol, cloud, and atmospheric processes must be  
6 incorporated into models. Most importantly, greater synergy among different types of  
7 measurements, different types of models, and especially between measurements and models, is  
8 critical. Aerosol-climate science must expand to encompass not only radiative effects on climate,  
9 but also aerosol effects on cloud processes, precipitation, and weather. New initiatives will strive  
10 to more effectively include experimentalists, remote sensing scientists and modelers as equal  
11 partners, and the traditionally defined communities of aerosol scientists, cloud scientists,  
12 radiation scientists increasingly will find common ground in addressing the challenges ahead.

13

# References

- 1  
2  
3 **Abdou, W.**, D. Diner, J. Martonchik, C. Bruegge, R. Kahn, B. Gaitley, and K. Crean, 2005: Comparison  
4 of coincident MISR and MODIS aerosol optical depths over land and ocean scenes containing  
5 AERONET sites. *J. Geophys. Res.* **110**: D10S07, doi:10.1029/2004JD004693.
- 6 **Ackerman, A.S.**, Toon, O. B., and P. V. Hobbs, 1994: Reassessing the dependence of cloud condensation  
7 nucleus concentration on formation rate. *Nature* **367**: 445 – 447, doi:10.1038/367445a0.
- 8 **Ackerman, A.**, O. Toon, D. Stevens, A. Heymsfield, V. Ramanathan, and E. Welton, 2000: Reduction of  
9 tropical cloudiness by soot. *Science* **288**:1042-1047.
- 10 **Ackerman, A. S.**, M. P. Kirkpatrick, D. E. Stevens and O. B. Toon, 2004: The impact of humidity above  
11 stratiform clouds on indirect aerosol climate forcing. *Nature* **432**:1014-1017.
- 12 **Ackerman, T.**, and G. Stokes, 2003: The Atmospheric Radiation Measurement Program. *Physics Today*  
13 **56**:38-44.
- 14 **Albrecht, B.**, 1989: Aerosols, cloud microphysics, and fractional cloudiness. *Science* **245**:1227-1230.
- 15 **Alpert, P.**, P. Kishcha, Y. Kaufman, and R. Schwarzbard, 2005: Global dimming or local dimming?  
16 Effect of urbanization on sunlight availability. *Geophys. Res. Lett.* **32**:L17802, doi:  
17 10.1029/GL023320.
- 18 **Anderson, T.**, R. Charlson, S. Schwartz, R. Knutti, O. Boucher, H. Rodhe, and J. Heintzenberg, 2003:  
19 Climate forcing by aerosols - A hazy picture. *Science* **300**:1103-1104.
- 20 **Anderson, T.**, R. Charlson, N. Bellouin, O. Boucher, M. Chin, S. Christopher, J. Haywood, Y. Kaufman,  
21 S. Kinne, J. Ogren, L. Remer, T. Takemura, D. Tanré, O. Torres, C. Trepte, B. Wielicki, D. Winker,  
22 and H. Yu, 2005a: An "A-Train" strategy for quantifying direct aerosol forcing of climate. *Bull. Am.*  
23 *Met. Soc.* **86**:1795-1809.
- 24 **Anderson, T.**, Y. Wu, D. Chu, B. Schmid, J. Redemann, and O. Dubovik, 2005b: Testing the MODIS  
25 satellite retrieval of aerosol fine-mode fraction. *J. Geophys. Res.* **110**: D18204,  
26 doi:10.1029/2005JD005978.
- 27 **Andreae, M. O.**, D. Rosenfeld, P. Artaxo, A. A. Costa, G. P. Frank, K. M. Longo and M. A. F. Silvas-  
28 Dias, 2004: Smoking rain clouds over the amazon. *Science* **303**:1337-1342.
- 29 **Andrews, E.**, P. J. Sheridan, J. A. Ogren, R. Ferrare, 2004: In situ aerosol profiles over the Southern  
30 Great Plains cloud and radiation test bed site: 1. Aerosol optical properties. *J. Geophys. Res.* **109**:  
31 D06208, doi:10.1029/2003JD004025.
- 32 **Ansmann, A.**, U. Wandinger, A. Wiedensohler, and U. Leiterer, 2002: Lindenberg Aerosol  
33 Characterization Experiment 1998 (LACE 98): Overview, *J. Geophys. Res.* **107**:8129,  
34 doi:10.1029/2000JD000233.
- 35 **Arnott, W.**, H. Moosmuller, and C. Rogers, 1997: Photoacoustic spectrometer for measuring light  
36 absorption by aerosol: instrument description. *Atmos. Environ.* **33**:2845-2852.
- 37 **Atwater, M.**, 1970: Planetary albedo changes due to aerosols. *Science* **170(3953)**:64-66.
- 38 **Augustine, J.A.**, G.B. Hodges, E.G. Dutton, J.J. Michalsky, and C.R. Cornwall, 2008: An aerosol optical  
39 depth climatology for NOAA's national surface radiation budget network (SURFRAD). *J. Geophys.*  
40 *Res.* **113**:D11204, doi:10.1029/2007JD009504.

- 1 **Baker**, M. B., and R.J. Charlson, 1990: Bistability of CCN concentrations and thermodynamics in the  
2 cloud-topped boundary layer. *Nature* **345**:142-145.
- 3 **Balkanski**, Y., M. Schulz, T. Claquin, and S. Guibert, 2007: Reevaluation of mineral aerosol radiative  
4 forcings suggests a better agreement with satellite and AERONET data. *Atmos. Chem. Phys.* **7**:81-95.
- 5 **Bates**, T., B. Huebert, J. Gras, F. Griffiths, and P. Durkee (1998): The International Global Atmospheric  
6 Chemistry (IGAC) Project's First Aerosol Characterization Experiment (ACE-1) - Overview. *J.*  
7 *Geophys. Res.* **103**:16297-16318.
- 8 **Bates**, T.S., P.K. Quinn, D.J. Coffman, J.E. Johnson, T.L. Miller, D.S. Covert, A. Wiedensohler, S.  
9 Leinert, A. Nowak, and C. Neusüb, 2001: Regional physical and chemical properties of the marine  
10 boundary layer aerosol across the Atlantic during Aerosols99: An overview. *J. Geophys. Res.*  
11 **106**:20767-20782.
- 12 **Bates** T., P. Quinn, D. Coffman, D. Covert, T. Miller, J. Johnson, G. Carmichael, S. uazzotti, D.  
13 Sodeman, K. Prather, M. Rivera, L. Russell, and J. Merrill, 2004: Marine boundary layer dust and  
14 pollution transport associated with the passage of a frontal system over eastern Asia. *J. Geophys. Res.*  
15 **109**:doi:10.1029/2003JD004094.
- 16 **Bates** T., et al., 2006: Aerosol direct radiative effects over the northwestern Atlantic, northwestern  
17 Pacific, and North Indian Oceans: estimates based on in-situ chemical and optical measurements and  
18 chemical transport modeling. *Atmos. Cehm. Phys.* **6**:1657-1732.
- 19 **Baynard**, T., E.R. Lovejoy, A. Pettersson, S.S. Brown, D. Lack, H. Osthoff, P. Massoli, S. Ciciora, W.P.  
20 Dube, and A.R. Ravishankara, 2007: Design and application of a pulsed cavity ring-down aerosol  
21 extinction spectrometer for field measurements. *Aerosol. Sci. Technol.* **41**:447-462.
- 22 **Bellouin**, N., O. Boucher, D. Tanré, and O. Dubovik, 2003: Aerosol absorption over the clear-sky oceans  
23 deduced from POLDER-1 and AERONET observations. *Geophys. Res. Lett.* **30**:1748,  
24 doi:10.1029/2003GL017121.
- 25 **Bellouin**, N., O. Boucher, J. Haywood, and M. Reddy, 2005: Global estimates of aerosol direct radiative  
26 forcing from satellite measurements. *Nature* **438**:1138-1140, doi:10.1038/nature04348.
- 27 **Bellouin**, N., A. Jones, J. Haywood, and S.A. Christopher, 2008: Updated estimate of aerosol  
28 direct radiative forcing from satellite observations and comparison against the Hadley Centre  
29 climate model. *J. Geophys. Res.* **113**:D10205, doi:10.1029/2007JD009385.
- 30 **Bond**, T.C., D.G. Streets, K.F. Yarber, S.M. Nelson, J.-H. Woo, and Z. Klimont, 2004: A technology-  
31 based global inventory of black and organic carbon emissions from combustion. *J. Geophys. Res.*  
32 **109**:D14203, doi:10.1029/2003JD003697.
- 33 **Bond**, T.C., E. Bhardwaj, R. Dong, R. Jogani, S. Jung, C. Roden, D.G. Streets, and N.M. Trautmann,  
34 2007: Historical emissions of black and organic carbon aerosol from energy-related combustion, 1850-  
35 2000. *Global Biogeochem. Cycles* **21**:GB2018, doi:10.1029/2006GB002840.
- 36 **Boucher**, O., and D. Tanré, 2000: Estimation of the aerosol perturbation to the Earth's radiative budget  
37 over oceans using POLDER satellite aerosol retrievals. *Geophys. Res. Lett.* **27**:1103-1106.
- 38 **Brenguier**, J. L., P. Y. Chuang, Y. Fouquart, D. W. Johnson, F. Parol, H. Pawlowska, J. Pelon, L.  
39 Schuller, F. Schroder, and J. Snider, 2000: An overview of the ACE-2 CLOUDYCOLUMN closure  
40 experiment. *Tellus* **52B**: 815-827.
- 41 **Carmichael**, G., G. Calori, H. Hayami, I. Uno, S. Cho, M. Engardt, S. Kim, Y. Ichikawa, Y. Ikeda, J.  
42 Woo, H. Ueda and M. Amann, 2002: The Mics-Asia study: Model intercomparison of long-range  
43 transport and sulfur deposition in East Asia. *Atmos. Environ.* **36**:175-199.

- 1 **Carmichael, G.**, Y. Tang, G. Kurata, I. Uno, D. Streets, N. Thongboonchoo, J. Woo, S. Guttikunda, A.  
2 White, T. Wang, D. Blake, E. Atlas, A. Fried, B. Potter, M. Avery, G. Sachse, S. Sandholm, Y. Kondo,  
3 R. Talbot, A. Bandy, D. Thornton and A. Clarke, 2003: Evaluating regional emission estimates using the  
4 TRACE-P observations. *J. Geophys. Res.* **108**:8810, doi:10.1029/2002JD003116.
- 5 **Carrico, C.** et al., 2005: Hygroscopic growth behavior of a carbon-dominated aerosol in Yosemite  
6 National Park. *Atmos. Environ.* **39**:1393–1404.
- 7 **Chand, D.**, T. Anderson, R. Wood, R. J. Charlson, Y. Hu, Z. Liu, and M. Vaughan, 2008: Quantifying  
8 above-cloud aerosol using spaceborne lidar for improved understanding of cloudy-sky direct climate  
9 forcing. *J. Geophys. Res.* **113**:D13206, doi:10.1029/2007JD009433.
- 10 **Charlson, R.** and M. Pilat, 1969: Climate: The influence of aerosols. *J. Appl. Meteorol.* **8**:1001-1002.
- 11 **Charlson, R.**, J. Langner, and H. Rodhe, 1990: Sulfate aerosol and climate. *Nature* **348**:22.
- 12 **Charlson, R.**, J. Langner, H. Rodhe, C. Leovy, and S. Warren, 1991: Perturbation of the Northern  
13 Hemisphere radiative balance by backscattering from anthropogenic sulfate aerosols. *Tellus* **43AB**:152-  
14 163.
- 15 **Charlson, R.**, S. Schwartz, J. Hales, R. Cess, R. J. Coakley, Jr., J. Hansen, and D. Hofmann, 1992:  
16 Climate forcing by anthropogenic aerosols. *Science* **255**:423-430.
- 17 **Chen, W-T.**, R. Kahn, D. Nelson, K. Yau, and J. Seinfeld, 2008: Sensitivity of multi-angle imaging to  
18 optical and microphysical properties of biomass burning aerosols. *J. Geophys. Res.* **113**:D10203,  
19 doi:10.1029/2007JD009414.
- 20 **Chin, M.**, P. Ginoux, S. Kinne, O. Torres, B. Holben, B. Duncan, R. Martin, J. Logan, A. Higurashi, and  
21 T. Nakajima, 2002: Tropospheric aerosol optical thickness from the GOCART model and comparisons  
22 with satellite and sun photometer measurements. *J. Atmos., Sci.* **59**:461-483.
- 23 **Chou, M.**, P. Chan, and M. Wang, 2002: Aerosol radiative forcing derived from SeaWiFS-retrieved  
24 aerosol optical properties. *J. Atmos. Sci.* **59**:748-757.
- 25 **Christopher, S.**, and J. Zhang, 2002: Daytime variation of shortwave direct radiative forcing of biomass  
26 burning aerosols from GEOS-8 imager. *J. Atmos. Sci.* **59**:681-691
- 27 **Christopher, S.**, J. Zhang, Y. Kaufman, and L. Remer, 2006: Satellite-based assessment of top of  
28 atmosphere anthropogenic aerosol radiative forcing over cloud-free oceans. *Geophys. Res. Lett.*  
29 **33**:L15816.
- 30 **Christopher, A.**, and T. Jones, 2008: Short-wave aerosol radiative efficiency over the global oceans  
31 derived from satellite data. *Tellus (B)* **60(4)**:636-640.
- 32 **Chu, D.**, Y. Kaufman, C. Ichoku, L. Remer, D. Tanré, and B. Holben, 2002: Validation of MODIS  
33 aerosol optical depth retrieval over land. *Geophys. Res. Lett.* **29**:8007, doi:10.1029/2001/GL013205.
- 34 **Chung, C.**, V. Ramanathan, D. Kim, and I. Podgomy, 2005: Global anthropogenic aerosol direct forcing  
35 derived from satellite and ground-based observations. *J. Geophys. Res.* **110**:D24207,  
36 doi:10.1029/2005JD006356.
- 37 **Chung, C. E.** and G. Zhang, 2004: Impact of absorbing aerosol on precipitation. *J. Geophys. Res.*  
38 **109**:doi:10.1029/2004JD004726.
- 39 **Clarke, A.D.**, J.N. Porter, F.P.J. Valero, and P. Pilewskie, 1996: Vertical profiles, aerosol microphysics,  
40 and optical closure during the Atlantic Stratocumulus Transition Experiment: Measured and modeled  
41 column optical properties. *J. Geophys. Res.* **101**:4443-4453.
- 42 **Coakley, J. Jr.**, R. Cess, and F. Yurevich, 1983: The effect of tropospheric aerosols on the earth's  
43 radiation budget: A parameterization for climate models. *J. Atmos. Sci.* **40**:116-138.

- 1 **Coakley, J. A. Jr. and C. D. Walsh, 2002:** Limits to the aerosol indirect radiative effect derived from  
2 observations of ship tracks. *J. Atmos. Sci.* **59**:668-680
- 3 **Collins, D.R., H.H. Jonsson, J.H. Seinfeld, R.C. Flagan, S. Gassó, D.A. Hegg, P.B. Russell, B. Schmid,**  
4 **J.M. Livingston, E. Öström, K.J. Noone, L.M. Russell, and J.P. Putaud, 2000:** In Situ aerosol size  
5 distributions and clear column radiative closure during ACE-2. *Tellus* **52B**:498-525.
- 6 **Collins, W., P. Rasch, B. Eaton, B. Khattatov, J. Lamarque, and C. Zender, 2001:** Simulating aerosols  
7 using a chemical transport model with assimilation of satellite aerosol retrievals: Methodology for  
8 INDOEX. *J. Geophys. Res.* **106**:7313—7336.
- 9 **Conant, W. C., T. M. VanReken, T. A. Rissman, V. Varutbangkul, H. H. Jonsson, A. Nenes, J. L.**  
10 **Jimenez, A. E. Delia, R. Bahreini, G. C. Roberts, R. C. Flagan, J. H. Seinfeld, 2004:** Aerosol, cloud  
11 drop concentration closure in warm cumulus. *J. Geophys. Res.* **109**:D13204,  
12 doi:10.1029/2003JD004324
- 13 **Cooke, W.F., and J.J.N. Wilson, 1996:** A global black carbon aerosol model. *J. Geophys. Res.*,  
14 **101**:19395-19409.
- 15 **Cooke, W.F., C. Liousse, H. Cachier, and J. Feichter, 1999:** Construction of a 1° × 1° fossil fuel emission  
16 data set for carbonaceous aerosol and implementation and radiative impact in the ECHAM4 model. *J.*  
17 *Geophys. Res.* **104**:22137-22162.
- 18 **Costa, M., A. Silva, and V. Levizzani, 2004a:** Aerosol characterization and direct radiative forcing  
19 assessment over the ocean. Part I: Methodology and sensitivity analysis. *J. Appl. Meteorol.* **43**:1799-  
20 1817.
- 21 **Costa, M., A. Silva AM, and V. Levizzani, 2004b:** Aerosol characterization and direct radiative forcing  
22 assessment over the ocean. Part II: Application to test cases and validation. *J. Appl. Meteorol.* **43**:1818-  
23 1833.
- 24 **de Gouw, J., et al., 2005:** Budget of organic carbon in a polluted atmosphere: Results from the New  
25 England Air Quality Study in 2002. *J. Geophys. Res.* **110**:D16305, doi:10.1029/2004JD005623.
- 26 **Delene, D. and J. Ogren, 2002:** Variability of aerosol optical properties at four North American surface  
27 monitoring sites. *J. Atmos. Sci.* **59**:1135-1150.
- 28 **Delworth, T. L., V. Ramaswamy and G. L. Stenchikov, 2005:** The impact of aerosols on simulated ocean  
29 temperature and heat content in the 20<sup>th</sup> century. *Geophys. Res. Lett.* **32**:doi:10.1029/2005GL024457.
- 30 **Dentener, F., S. Kinne, T. Bond, O. Boucher, J. Cofala, S. Generoso, P. Ginoux, S. Gong, J.J.**  
31 **Hoelzemann, A. Ito, L. Marelli, J.E. Penner, J.-P. Putaud, C. Textor, M. Schulz, G.R. van der Werf,**  
32 **and J. Wilson, 2006:** Emissions of primary aerosol and precursor gases in the years 2000 and 1750  
33 prescribed data-sets for AeroCom. *Atmos. Chem. Phys.* **6**:4321-4344.
- 34 **Deuzé, J., F. Bréon, C. Devaux, P. Goloub, M. Herman, B. Lafrance, F. Maignan, A. Marchand, F. Nadal,**  
35 **G. Perry, and D. Tanré, 2001:** Remote sensing of aerosols over land surfaces from POLDER-ADEOS-1  
36 polarized measurements. *J. Geophys. Res.* **106**:4913-4926.
- 37 **Diner, D., J. Beckert, T. Reilly, et al., 1998:** Multiangle Imaging Spectroradiometer (MISR) description  
38 and experiment overview. *IEEE Trans. Geosci. Remote. Sens.* **36**:1072-1087.
- 39 **Diner, D., J. Beckert, G. Bothwell and J. Rodriguez, 2002:** Performance of the MISR instrument during  
40 its first 20 months in Earth orbit. *IEEE Trans. Geosci. Remote Sens.* **40**:1449-1466.
- 41 **Diner, D., T. Ackerman, T. Anderson, et al., 2004:** Progressive Aerosol Retrieval and Assimilation  
42 Global Observing Network (PARAGON): An integrated approach for characterizing aerosol climatic  
43 and environmental interactions. *Bull. Amer. Meteor. Soc.* **85**:1491-1501.

- 1 **Doherty**, S.J., P. Quinn, A. Jefferson, C. Carrico, T.L. Anderson, and D. Hegg, 2005: A comparison and  
2 summary of aerosol optical properties as observed in-situ from aircraft, ship and land during ACE-  
3 Asia. *J. Geophys. Res.* **110**:D04201, doi: 10.1029/2004JD004964.
- 4 **Dubovik**, O., A. Smirnov, B. Holben, M. King, Y. Kaufman, and Slutsker, 2000: Accuracy assessments  
5 of aerosol optical properties retrieved from AERONET sun and sky radiance measurements. *J.*  
6 *Geophys. Res.* **105**:9791-9806.
- 7 **Dubovik**, O., and M. King, 2000: A flexible inversion algorithm for retrieval of aerosol optical properties  
8 from Sun and sky radiance measurements. *J. Geophys. Res.*, **105**:20673-20696.
- 9 **Dubovik**, O., B. Holben, T. Eck, A. Smirnov, Y. Kaufman, M. King, D. Tanré, and I. Slutsker, 2002:  
10 Variability of absorption and optical properties of key aerosol types observed in worldwide locations. *J.*  
11 *Atmos. Sci.* **59**:590-608.
- 12 **Dubovik**, O., T. Lapyonok, Y. Kaufman, M. Chin, P. Ginoux, and A. Sinyuk, 2007: Retrieving global  
13 sources of aerosols from MODIS observations by inverting GOCART model, *Atmos. Chem.*  
14 *Phys. Discuss.* **7**:3629-3718.
- 15 **Dusek**, U., G. P. Frank, L. Hildebrandt, J. Curtius, S. Walter, D. Chand, F. Drewnick, S. Hings, D. Jung,  
16 S. Borrmann, and M. O. Andreae, 2006: Size matters more than chemistry in controlling which aerosol  
17 particles can nucleate cloud droplets. *Science* **312**:1375-1378.
- 18 **Eagan**, R.C., P. V. Hobbs and L. F. Radke, 1974: Measurements of cloud condensation nuclei and cloud  
19 droplet size distributions in the vicinity of forest fires. *J. Appl. Meteor.* **13**:553-557.
- 20 **Eck**, T., B. Holben, J. Reid, O. Dubovik, A. Smirnov, N. O'Neill, I. Slutsker, and S. Kinne, 1999:  
21 Wavelength dependence of the optical depth of biomass burning, urban and desert dust aerosols. *J.*  
22 *Geophys. Res.* **104**:31333-31350.
- 23 **Eck**, T., et al., 2008: Spatial and temporal variability of column-integrated aerosol optical properties in  
24 the southern Arabian Gulf and United Arab Emirates in summer. *J. Geophys. Res.* **113**:D01204,  
25 doi:10.1029/2007JD008944.
- 26 **Ervens**, B., G. Feingold, and S. M. Kreidenweis, 2005: The influence of water-soluble organic carbon on  
27 cloud drop number concentration. *J. Geophys. Res.* **110**:D18211, doi:10.1029/2004JD005634.
- 28 **Fehsenfeld**, F., et al., 2006: International Consortium for Atmospheric Research on Transport and  
29 Transformation (ICARTT): North America to Europe—Overview of the 2004 summer field study. *J.*  
30 *Geophys. Res.* **111**:D23S01, doi:10.1029/2006JD007829.
- 31 **Feingold**, G., B. Stevens, W.R. Cotton, and R.L. Walko, 1994: An explicit microphysics/LES model  
32 designed to simulate the Twomey Effect. *Atmospheric Research* **33**:207-233.
- 33 **Feingold**, G., W. R. Cotton, S. M. Kreidenweis, and J. T. Davis, 1999: The impact of giant cloud  
34 condensation nuclei on drizzle formation in stratocumulus: Implications for cloud radiative properties.  
35 *J. Atmos. Sci.*, **56**: 4100-4117.
- 36 **Feingold**, G., Remer, L. A., Ramaprasad, J. and Kaufman, Y. J., 2001: Analysis of smoke impact on  
37 clouds in Brazilian biomass burning regions: An extension of Twomey's approach. *J. Geophys. Res.*  
38 **106**:22907-22922.
- 39 **Feingold**, G. W. Eberhard, D. Veron, and M. Previdi, 2003: First measurements of the Twomey aerosol  
40 indirect effect using ground-based remote sensors. *Geophys. Res. Lett.* **30**:1287,  
41 doi:10.1029/2002GL016633.
- 42 **Feingold**, G., 2003: Modeling of the first indirect effect: Analysis of measurement requirements.  
43 *Geophys. Res. Lett.* **30**: 1997, doi:10.1029/2003GL017967.

- 1 **Feingold, G.**, H. Jiang, and J. Harrington, 2005: On smoke suppression of clouds in Amazonia. *Geophys.*  
2 *Res. Lett.* **32**:L02804, doi:10.1029/2004GL021369.
- 3 **Feingold, G.**, R. Furrer, P. Pilewskie, L. A. Remer, Q. Min, H. Jonsson, 2006: Aerosol indirect effect  
4 studies at Southern Great Plains during the May 2003 Intensive Operations Period. *J. Geophys. Res.*  
5 **111**: D05S14, doi:10.1029/2004JD005648.
- 6 **Fernandes, S.D.**, N.M. Trautmann, D.G. Streets, C.A. Roden, and T.C. Bond, 2007: Global biofuel use,  
7 1850-2000. *Global Biogeochem. Cycles* **21**:GB2019, doi:10.1029/2006GB002836.
- 8 **Ferrare, R.**, G. Feingold, S. Ghan, J. Ogren, B. Schmid, S.E. Schwartz, and P. Sheridan, 2006: Preface to  
9 special section: Atmospheric Radiation Measurement Program May 2003 Intensive Operations Period  
10 examining aerosol properties and radiative influences. *J. Geophys. Res.* **111**:D05S01,  
11 doi:10.1029/2005JD006908.
- 12 **Fiebig, M.**, and J.A. Ogren, 2006: Retrieval and climatology of the aerosol asymmetry parameter in the  
13 NOAA aerosol monitoring network. *J. Geophys. Res.* **111**:D21204, doi:10.1029/2005JD006545.
- 14 **Fishman, J.**, J.M. Hoell, R.D. Bendura, R.J. McNeal, and V. Kirchhoff, 1996: NASA GTE TRACE A  
15 experiment (Septemner-October 2002): Overview. *J. Geophys. Res.* **101**:23865-23880.
- 16 **Fitzgerald, J. W.**, 1975: Approximation formulas for the equilibrium size of an aerosol particle as a  
17 function of its dry size and composition and the ambient relative humidity. *J. Appl. Meteor.* **14**:1044-  
18 1049.
- 19 **Fraser, R.** and Y. Kaufman, 1985: The relative importance of aerosol scattering and absorption in  
20 Remote Sensing. *Transactions on Geoscience and Remote Sensing*, GE-**23**:625-633.
- 21 **Garrett, T.**, C. Zhao, X. Dong, G. Mace, and P. Hobbs, 2004: Effects of varying aerosol regimes on low-  
22 level Arctic stratus. *Geophys. Res. Lett.* **31**:L17105, doi:10.1029/2004GL019928.
- 23 **Garrett, T.**, and C. Zhao, 2006: Increased Arctic cloud longwave emissivity associated with pollution  
24 from mid-latitudes. *Nature* **440**:787-789.
- 25 **Geogdzhayev, I.**, M. Mishchenko, W. Rossow, B. Cairns, B., and A. Lacis, 2002: Global two-channel  
26 AVHRR retrievals of aerosol properties over the ocean for the period of NOAA-9 observations and  
27 preliminary retrievals using NOAA-7 and NOAA-11 data. *J. Atmos. Sci.*, **59**:262--278.
- 28 **Ghan, S.**, and S.E. Schwartz, 2007: Aerosol properties and processes. *Bull. Amer. Meteor. Soc.*, **88**:1059-  
29 1083.
- 30 **Gillett, N.P.**, et al., 2002a: Reconciling two approaches to the detection of anthropogenic influence on  
31 climate. *J. Clim.* **15**:326–329.
- 32 **Gillett, N.P.**, et al., 2002b: Detecting anthropogenic influence with a multimodel ensemble. *Geophys.*  
33 *Res. Lett.* **29**:doi:10.1029/2002GL015836.
- 34 **Ginoux, P.**, M. Chin, I. Tegen, J. M. Prospero, B. Holben, O. Dubovik and S.-J. Lin, 2001: Sources and  
35 distributions of dust aerosols simulated with the GOCART model. *J. Geophys. Res.* **20**:20255-20273.
- 36 **Ginoux, P.**, L. W. Horowitz, V. Ramaswamy, I. V. Geogdzhayev, B. N. Holben, G. Stenchikov and X.  
37 tie, 2006: Evaluation of aerosol distribution and optical depth in the Geophysical Fluid Dynamics  
38 Laboratory coupled model CM2.1 for present climate. *J. Geophys. Res.*  
39 **111**:doi:10.1029/2005JD006707.
- 40 **Golaz, J-C.**, V. E. Larson, and W. R. Cotton, 2002a: A PDF-based model for boundary layer clouds. Part  
41 I: Method and model description. *J. Atmos. Sci.* **59**:3540-3551.
- 42 **Golaz, J-C.**, V. E. Larson, and W. R. Cotton, 2002b: A PDF-based model for boundary layer clouds. Part  
43 II: Model results. *J. Atmos. Sci.* **59**:3552-3571.



- 1 **Grabowski, W.W.**, 2004: An improved framework for superparameterization. *J. Atmos. Sci.* **61**:1940-52.
- 2 **Grabowski, W.W.**, X. Wu, and M.W. Moncrieff, 1999: Cloud resolving modeling of tropical cloud  
3 systems during Phase III of GATE. Part III: Effects of cloud microphysics. *J. Atmos. Sci.* **56**:2384-  
4 2402.
- 5 **Gregory, J.M.**, et al., 2002: An observationally based estimate of the climate sensitivity. *J. Clim.*  
6 **15**:3117–3121.
- 7 **Gunn, R.** and B. B. Phillips. 1957: An experimental investigation of the effect of air pollution on the  
8 initiation of rain. *J. Meteor.* **14**: 272-280.
- 9 **Han, Q.**, W. B. Rossow, J. Chou, and R. M. Welch, 1998: Global survey of the relationship of cloud  
10 albedo and liquid water path with droplet size using ISCCP. *J. Clim.* **11**, 1516– 1528.
- 11 **Han, Q.**, W.B. Rossow, J. Zeng, and R. Welch, 2002: Three different behaviors of liquid water path of  
12 water clouds in aerosol-cloud interactions. *J. Atmos. Sci.* **59**: 726-735.
- 13 **Hansen, J.**, M. Sato, and R. Ruedy, 1997: Radiative forcing and climate response. *J. Geophys. Res.*  
14 **102**:6831-6864.
- 15 **Hansen, J.**, et al., 2005: Efficacy of climate forcings. *J. Geophys. Res.* **110**:doi:10.1029/2005JD005776,  
16 45pp.
- 17 **Hansen, J.** et al., 2007: Climate simulations for 1880-2003 with GISS model E. *Clim. Dyn.* **29**:661-696.
- 18 **Harrison, L.**, J. Michalsky, and J. Berndt, 1994: Automated multifilter rotating shadowband radiometer:  
19 An instrument for optical depth and radiation measurements. *Applied Optics* **33**:5118-5125.
- 20 **Harvey, L.D.D.**, 2004: Characterizing the annual-mean climatic effect of anthropogenic CO<sub>2</sub> and aerosol  
21 emissions in eight coupled atmosphere-ocean GCMs. *Clim. Dyn.* **23**:569–599.
- 22 **Haywood, J. M.**, V. Ramanammy, and B. J. Soden, 1999: Tropospheric aerosol climate forcing in clear-  
23 sky satellite observations over the oceans. *Science* **283**(5406):1299-1303.
- 24 **Haywood, J.**, and O. Boucher, 2000: Estimates of the direct and indirect radiative forcing due to  
25 tropospheric aerosols: A review. *Rev. Geophys.* **38**:513-543.
- 26 **Haywood, J.**, P. Francis, S. Osborne, M. Glew, N. Loeb, E. Highwood, D. Tanré, E. Myhre, P. Formenti,  
27 and E. Hirst, 2003: Radiative properties and direct radiative effect of Saharan dust measured by the C-  
28 130 aircraft during SHADE: 1.Solar spectrum. *J. Geophys. Res.* **108**:8577, doi:10.1029/2002JD002687.
- 29 **Haywood, J.**, and M. Schulz, 2007: Causes of the reduction in uncertainty in the anthropogenic radiative  
30 forcing of climate between IPCC (2001) and IPCC (2007). *Geophys. Res. Lett.* **34**:L20701,  
31 doi:10.1029/2007GL030749.
- 32 **Haywood, J.**, et al., 2008: Overview of the Dust and Biomass burning Experiment and African Monsoon  
33 Multidisciplinary Analysis Special Observing Period-0. *J. Geophys. Res.* **113**: D00C17,  
34 doi:10.1029/2008JD010077.
- 35 **Heald, C. L.**, D. J. Jacob, R. J. Park, L. M. Russell, B. J. Huebert, J. H. Seinfeld, H. Liao, and R. J.  
36 Weber, 2005: A large organic aerosol source in the free troposphere missing from current models.  
37 *Geophys. Res. Lett.* **32**:L18809, doi:10.1029/2005GL023831.
- 38 **Heintzenberg, J.**, et al., 2009: The SAMUM-1 experiment over Southern Morocco: Overview and  
39 introduction. *Tellus* **61B**, in press.
- 40 **Henze, D. K.** and J.H. Seinfeld, 2006: Global secondary organic aerosol from isoprene oxidation.  
41 *Geophys. Res. Lett.* **33**:L09812, doi:10.1029/2006GL025976.

- 1 **Herman, J.**, P. Bhartia, O. Torres, C. Hsu, C. Seftor, and E. Celarier, 1997: Global distribution of UV-  
2 absorbing aerosols from Nimbus-7/TOMS data. *J. Geophys. Res.* **102**:16911--16922.
- 3 **Hoell, J.M.**, D.D. Davis, S.C. Liu, R. Newell, M. Shipham, H. Akimoto, R.J. McNeal, R.J. Bemdura, and  
4 J.W. Drewry, 1996: Pacific Exploratory Mission-West A (PEM-WEST A): September-October, 1991.  
5 *J. Geophys. Res.* **101**:1641-1653.
- 6 **Hoell, J.M.**, D.D. Davis, S.C. Liu, R. Newell, M. Shipham, H. Akimoto, R.J. McNeal, R.J. Bemdura, and  
7 J.W. Drewry, 1997: The Pacific Exploratory Mission-West Phase B: February-March, 1994. *J.*  
8 *Geophys. Res.* **102**:28223--28239.
- 9 **Hoff, R.** et al., 2002: Regional East Atmospheric Lidar Mesonet: REALM, in *Lidar Remote Sensing in*  
10 *Atmospheric and Earth Sciences*, edited by L. Bissonette, G. Roy, and G. Vallée, pp. 281-284, Def.  
11 R&D Can. Valcartier, Val-Bélair, Que.
- 12 **Hoff, R.**, J. Engel-Cox, N. Krotkov, S. Palm, R. Rogers, K. McCann, L. Sparling, N. Jordan, O. Torres,  
13 and J. Spinhirne, 2004: Long-range transport observations of two large forest fire plumes to the  
14 northeastern U.S., in 22<sup>nd</sup> *International Laser Radar Conference, ESA Spec. Publ., SP-561*:683-686.
- 15 **Holben, B.**, T. Eck, I. Slutsker, et al., 1998: AERONET - A federated instrument network and data  
16 archive for aerosol characterization. *Remote Sens. Environ.* **66**:1-16.
- 17 **Holben, B.**, D. Tanré, A. Smirnov, et al., 2001: An emerging ground-based aerosol climatology: aerosol  
18 optical depth from AERONET. *J. Geophys. Res.* **106**:12067-12098.
- 19 **Horowitz, L. W.**, et al., 2003: A global simulation of tropospheric ozone and related tracers: Description  
20 and evaluation of MOZART, version 2. *J. Geophys. Res.* **108**:4784, doi:10.1029/2002JD002853.
- 21 **Horowitz, L.**, 2006: Past, present, and future concentrations of tropospheric ozone and aerosols:  
22 Methodology, ozone evaluation, and sensitivity to aerosol wet removal. *J. Geophys. Res.* **111**:D22211,  
23 doi:10.1029/2005JD006937.
- 24 **Hoyt, D.**, and C. Frohlich, 1983: Atmospheric transmission at Davos, Switzerland 1909-1979. *Climatic*  
25 *Change* **5**:61-71.
- 26 **Hsu, N.**, S. Tsay, M. King, and J. Herman, 2004: Aerosol properties over bright-reflecting source regions.  
27 *IEEE Trans. Geosci. Remote Sens.* **42**:557-569.
- 28 **Huebert, B.**, T. Bates, P. Russell, G. Shi, Y. Kim, K. Kawamura, G. Carmichael, and T. Nakajima, 2003:  
29 An overview of ACE-Asia: strategies for quantifying the relationships between Asian aerosols and  
30 their climatic impacts. *J. Geophys. Res.* **108**:8633, doi:10.1029/2003JD003550.
- 31 **Huneus, N.**, and O. Boucher, 2007: One-dimensional variational retrieval of aerosol extinction  
32 coefficient from synthetic LIDAR and radiometric measurements. *J. Geophys. Res.* **112**:D14303,  
33 doi:10.1029/2006JD007625.
- 34 **Husar, R.**, J. Prospero, and L. Stowe, 1997: Characterization of tropospheric aerosols over the oceans  
35 with the NOAA advanced very high resolution radiometer optical thickness operational product. *J.*  
36 *Geophys. Res.* **102**:16889-16909.
- 37 **IPCC**, 1992: *Climate Change 1992: The Supplementary Report to the IPCC Scientific Assessment*. J. T.  
38 Houghton, B. A. Callander and S. K. Varney (eds). Cambridge University Press, Cambridge, UK, 198  
39 pp.
- 40 **IPCC** (Intergovernmental Panel on Climate Change), 1995: Radiative forcing of climate change and an  
41 evaluation of the IPCC IS92 emission scenarios, in *Climate Change 1994*, Cambridge Univ. Press, New  
42 York, Cambridge University Press, 1995.

- 1 **IPCC** (Intergovernmental Panel on Climate Change), 1996: Radiative forcing of climate change, in  
2 Climate Change 1995, Cambridge Univ. Press, New York, Cambridge University Press, 1996.
- 3 **IPCC** (Intergovernmental Panel on Climate Change), 2001: Radiative forcing of climate change, in  
4 Climate Change 2001, Cambridge Univ. Press, New York, Cambridge University Press, 2001.
- 5 **IPCC** (Intergovernmental Panel on Climate Change), 2007: Changes in Atmospheric Constituents and in  
6 Radiative forcing, in Climate Change 2007, Cambridge Univ. Press, New York, Cambridge University  
7 Press, 2007.
- 8 **Ito, A.**, and J.E. Penne, 2005: Historical estimates of carbonaceous aerosols from biomass and fossil fuel  
9 burning for the period 1870-2000. *Global Biogeochem. Cycles* **19**:GB2028,  
10 doi:10.1029/2004GB002374.
- 11 **Jacob, D.**, J. Crawford, M. Kleb, V. Connors, R.J. Bendura, J. Raper, G. Sachse, J. Gille, L. Emmons,  
12 and C. Heald, 2003: The Transport and Chemical Evolution over the Pacific (TRACE-P) aircraft  
13 mission: design, execution, and first results. *J. Geophys. Res.* **108**:9000, 10.1029/2002JD003276.
- 14 **Jayne, J. T.**, D. C. Leard, X. Zhang, P. Davidovits, K. A. Smith, C. E. Kolb, and D. R. Worsnop, 2000:  
15 Development of an aerosol mass spectrometer for size and composition analysis of submicron particles.  
16 *Aerosol Sci. Technol.* **33**:49–70
- 17 **Jeong, M.**, Z. Li, D. Chu, and S. Tsay, 2005: Quality and Compatibility Analyses of Global Aerosol  
18 Products Derived from the Advanced Very High Resolution Radiometer and Moderate Resolution  
19 Imaging Spectroradiometer. *J. Geophys. Res.* **110**:D10S09, doi:10.1029/2004JD004648.
- 20 **Jiang, H.**, and G. Feingold, 2006: Effect of aerosol on warm convective clouds: Aerosol-cloud-surface  
21 flux feedbacks in a new coupled large eddy model. *J. Geophys. Res.*, **111**: D01202,  
22 doi:10.1029/2005JD006138.
- 23 **Jiang, H.**, H. Xue, A. Teller, G. Feingold, and Z. Levin, 2006: Aerosol effects on the lifetime of shallow  
24 cumulus. *Geophys. Res. Lett.* **33**:doi: 10.1029/2006GL026024.
- 25 **Jiang, H.**, G. Feingold, H. H. Jonsson, M.-L. Lu, P. Y. Chuang, R. C. Flagan, J. H. Seinfeld, 2008:  
26 Statistical comparison of properties of simulated and observed cumulus clouds in the vicinity of  
27 Houston during the Gulf of Mexico Atmospheric Composition and Climate Study (GoMACCS). *J.*  
28 *Geophys. Res.* **113**:D13205, doi:10.1029/2007JD009304.
- 29 **Johnson, D. B.**, 1982: The role of giant and ultragiant aerosol particles in warm rain initiation. *J. Atmos.*  
30 *Sci.* **39**: 448-460.
- 31 **Jones, G.S.**, et al., 2005: Sensitivity of global scale attribution results to inclusion of climatic response to  
32 black carbon. *Geophys. Res. Lett.* **32**:L14701, doi:10.1029/2005GL023370.
- 33 **Junker, C.**, and C. Liousse, 2008: A global emission inventory of carbonaceous aerosol from historic  
34 records of fossil fuel and biofuel consumption for the period 1860-1997. *Atmos. Chem. Phys.* **8**:1195-  
35 1207.
- 36 **Kahn, R.**, P. Banerjee, D. McDonald, and D. Diner, 1998: Sensitivity of multiangle imaging to aerosol  
37 optical depth, and to pure-particle size distribution and composition over ocean. *J. Geophys. Res.*  
38 **103**:32195-32213.
- 39 **Kahn, R.**, P. Banerjee, and D. McDonald, 2001: The sensitivity of multiangle imaging to natural mixtures  
40 of aerosols over ocean. *J. Geophys. Res.* **106**:18219-18238.
- 41 **Kahn, R.**, J. Ogren, T. Ackerman, et al., 2004: Aerosol data sources and their roles within PARAGON.  
42 *Bull. Amer. Meteor. Soc.* **85**:1511-1522.

- 1 **Kahn, R., R. Gaitley, J. Martonchik, D. Diner, K. Crean, and B. Holben, 2005a:** MISR global aerosol  
2 optical depth validation based on two years of coincident AERONET observations. *J. Geophys. Res.*  
3 **110:**D10S04, doi:10.1029/2004JD004706.
- 4 **Kahn, R., W. Li, J. Martonchik, C. Bruegge, D. Diner, B. Gaitley, W. Abdou, O. Dubovik, B. Holben, A.**  
5 **Smirnov, Z. Jin, and D. Clark, 2005b:** MISR low-light-level calibration, and implications for aerosol  
6 retrieval over dark water. *J. Atmos. Sci.* **62:**1032-1052.
- 7 **Kahn, R., W. Li, C. Moroney, D. Diner, J. Martonchik, and E. Fishbein, 2007a:** Aerosol source plume  
8 physical characteristics from space-based multiangle imaging. *J. Geophys. Res.* **112:**D11205,  
9 doi:10.1029/2006JD007647.
- 10 **Kahn, R., et al., 2007b:** Satellite-derived aerosol optical depth over dark water from MISR and MODIS:  
11 Comparisons with AERONET and implications for climatological studies. *J. Geophys. Res.*  
12 **112:**D18205, doi:10.1029/2006JD008175.
- 13 **Kalashnikova, O., and R. Kahn, 2006:** Ability of multiangle remote sensing observations to identify and  
14 distinguish mineral dust types: Part 2. Sensitivity over dark water. *J. Geophys. Res.* **111:**D11207,  
15 doi:10.1029/2005JD006756.
- 16 **Kapustin, V.N., A.D. Clarke, Y. Shinozuka, S. Howell, V. Brekhovskikh, T. Nakajima, and A.**  
17 **Higurashi, 2006:** On the determination of a cloud condensation nuclei from satellite: Challenges and  
18 possibilities. *J. Geophys. Res.* **111:**D04202, doi:10.1029/2004JD005527.
- 19 **Kaufman, Y., 1987:** Satellite sensing of aerosol absorption. *J. Geophys. Res.* **92:**4307-4317.
- 20 **Kaufman, Y.J., A. Setzer, D. Ward, D. Tanre, B. N. Holben, P. Menzel, M. C. Pereira, and R.**  
21 **Rasmussen, 1992:** Biomass Burning Airborne and Spaceborne Experiment in the Amazonas (BASE-  
22 A). *J. Geophys. Res.* **97:**14581-14599.
- 23 **Kaufman, Y. J. and Nakajima, T., 1993:** Effect of Amazon smoke on cloud microphysics and albedo-  
24 Analysis from satellite imagery. *J. Applied Meteor.* **32:**729-744.
- 25 **Kaufman, Y. and R. Fraser, 1997:** The effect of smoke particles on clouds and climate forcing. *Science*  
26 **277:**1636-1639.
- 27 **Kaufman, Y., D. Tanré, L. Remer, E. Vermote, A. Chu, and B. Holben, 1997:** Operational remote  
28 sensing of tropospheric aerosol over land from EOS moderate resolution imaging spectroradiometer. *J.*  
29 *Geophys. Res.* **102:**17051-17067.
- 30 **Kaufman, Y.J., P. V. Hobbs, V. W. J. H. Kirchhoff, P. Artaxo, L. A. Remer, B. N. Holben, M. D. King,**  
31 **D. E. Ward, E. M. Prins, K. M. Longo, L. F. Mattos, C. A. Nobre, J. D. Spinhirne, Q. Ji, A. M.**  
32 **Thompson, J. F. Gleason, and S. A. Christopher, 1998:** Smoke, clouds, and radiation—Brazil (SCAR-  
33 B) experiment. *J. Geophys. Res.* **103:**31783-31808.
- 34 **Kaufman, Y., D. Tanré, and O. Boucher, 2002a:** A satellite view of aerosols in the climate system.  
35 *Nature* **419:** doi:10.1038/nature01091.
- 36 **Kaufman, Y., J. Martins, L. Remer, M. Schoeberl, and M. Yamasoe, 2002b:** Satellite retrieval of aerosol  
37 absorption over the oceans using sunglint. *Geophys. Res. Lett.* **29:** 1928, doi:10.1029/2002GL015403.
- 38 **Kaufman, Y., J. Haywood, P. Hobbs, W. Hart, R. Kleidman, and B. Schmid, 2003:** Remote sensing of  
39 vertical distributions of smoke aerosol off the coast of Africa. *Geophys. Res. Lett.* **30:**1831,  
40 doi:10.1029/2003GL017068.
- 41 **Kaufman, Y., O. Boucher, D. Tanré, M. Chin, L. Remer, and T. Takemura, 2005a:** Aerosol  
42 anthropogenic component estimated from satellite data. *Geophys. Res. Lett.* **32:** L17804,  
43 doi:10.1029/2005GL023125.

- 1 **Kaufman, Y.**, L. Remer, D. Tanré, R. Li, R. Kleidman, S. Mattoo, R. Levy, T. Eck, B. Holben, C.  
2 Ichoku, J. Martins, and I. Koren, 2005b: A critical examination of the residual cloud contamination and  
3 diurnal sampling effects on MODIS estimates of aerosol over ocean. *IEEE Trans. on Geoscience &*  
4 *Remote Sensing* **43**:2886-2897.
- 5 **Kaufman, Y. J.**, I. Koren, L. A. Remer, D. Rosenfeld and Y. Rudich, 2005c: The effect of smoke, dust,  
6 and pollution aerosol on shallow cloud development over the Atlantic Ocean. *Proc. Nat. Acad. Sci.*  
7 **102**:11207-11212.
- 8 **Kaufman, Y. J.** and Koren, I., 2006: Smoke and pollution aerosol effect on cloud cover. *Science*  
9 **313**:655-658.
- 10 **Kerr, R.**, 2007: Another global warming icon comes under attack. *Science* **317**:28.
- 11 **Kiehl, J. T.**, 2007: Twentieth century climate model response and climate sensitivity. *Geophys. Res. Lett.*  
12 **34**:doi:10.1029/2007GL031383.
- 13 **Kim, B.-G.**, S. Schwartz, M. Miller, and Q. Min, 2003: Effective radius of cloud droplets by ground-  
14 based remote sensing: Relationship to aerosol. *J. Geophys. Res.* **108**:4740, doi:10.1029/2003JD003721.
- 15 **Kim, B.-G.**, M. A. Miller, S. E. Schwartz, Y. Liu, and Q. Min, 2008: The role of adiabaticity in the  
16 aerosol first indirect effect. *J. Geophys. Res.* **113**: D05210, doi:10.1029/2007JD008961.
- 17 **Kim, M.-K.**, K.-M. Lau, M. Chin, K.-M. Kim, Y. Sud, and G. K. Walker, 2006: Atmospheric  
18 teleconnection over Eurasia induced by aerosol radiative forcing during boreal spring. *J. Climate*  
19 **19**:4700-4718.
- 20 **King, M.**, Y. Kaufman, D. Tanré, and T. Nakajima, 1999: Remote sensing of tropospheric aerosols: Past,  
21 present, and future. *Bull. Am. Meteorol. Soc.* **80**:2229-2259.
- 22 **King, M.**, S. Platnick, C. Moeller, Revercomb, and D. Chu, 2003: Remote sensing of smoke, land, and  
23 clouds from the NASA ER-2 during SAFARI 2000. *J. Geophys. Res.* **108**:8502,  
24 doi:10.1029/2002JD003207.
- 25 **Kinne, S.**, M. Schulz, C. Textor, et al., 2006: An AeroCom initial assessment -- optical properties in  
26 aerosol component modules of global models. *Atmos. Chem. Phys.* **6**:1815-1834.
- 27 **Kirchstetter, T.W.**, R.A. Harley, N.M. Kreisberg, M.R. Stolzenburg, and S.V. Hering, 1999: On-road  
28 measurement of fine particle and nitrogen oxide emissions from light- and heavy-duty motor vehicles.  
29 *Atmos. Environ.* **33**:2955-2968.
- 30 **Kristjánsson, J. E.**, Stjern, C. W., Stordal, F., Fjæraa, A. M., Myhre, G., and Jónasson, K., 2008: Cosmic  
31 rays, cloud condensation nuclei and clouds – a reassessment using MODIS data, *Atmos. Chem. Phys.* **8**:  
32 7373-7387.
- 33 **Kleinman, L.I.** et al., 2008: The time evolution of aerosol composition over the Mexico City plateau.  
34 *Atmos. Chem. Phys.* **8**:1559-1575.
- 35 **Kleidman, R.**, N. O'Neill, L. Remer, Y. Kaufman, T. Eck, D. Tanré, O. Dubovik, and B. Holben, 2005:  
36 Comparison of Moderate Resolution Imaging Spectroradiometer (MODIS) and Aerosol Robotic  
37 Network (AERONET) remote-sensing retrievals of aerosol fine mode fraction over ocean. *J. Geophys.*  
38 *Res.* **110**:D22205, doi:10.1029/2005JD005760.
- 39 **Knutti, R.**, T.F. Stocker, F. Joos, and G.-K. Plattner, 2002: Constraints on radiative forcing and future  
40 climate change from observations and climate model ensembles. *Nature* **416**:719–723.
- 41 **Knutti, R.**, T.F. Stocker, F. Joos, and G.-K. Plattner, 2003: Probabilistic climate change projections using  
42 neural networks. *Clim. Dyn.* **21**:257–272.

- 1 **Koch, D.**, and J. Hansen, 2005: Distant origins of Arctic black carbon: A Goddard Institute for Space  
2 Studies ModelE experiment. *J. Geophys. Res.* **110**: D04204, doi:10.1029/2004JD005296.
- 3 **Koch, D.**, G. Schmidt, and C. Field, 2006: Sulfur, sea salt and radionuclide aerosols in GISS ModelE. *J.*  
4 *Geophys. Res.* **111**:D06206, doi:10.1029/2004JD005550.
- 5 **Koch, D.**, T.C. Bond, D. Streets, N. Unger, G.R. van der Werf, 2007: Global impact of aerosols from  
6 particular source regions and sectors, *J. Geophys. Res.* **112**:D02205, doi:10.1029/2005JD007024.
- 7 **Kogan, Y. L.**, D. K. Lilly, Z. N. Kogan, and V. Filyushkin, 1994: The effect of CCN regeneration on the  
8 evolution of stratocumulus cloud layers. *Atmos. Res.* **33**:137- 150.
- 9 **Koren, I.**, Y. Kaufman, L. Remer, and J. Martins, 2004: Measurement of the effect of Amazon smoke on  
10 inhibition of cloud formation. *Science* **303**:1342.
- 11 **Koren, I.**, Y.J. Kaufman, D. Rosenfeld, L.A. Remer, and Y. Rudich, 2005: Aerosol invigoration and  
12 restructuring of Atlantic convective clouds. *Geophys. Res. Lett.*, **32**:doi:10.1029/2005GL023187.
- 13 **Koren, I.**, L.A. Remer, and K. Longo, 2007a: Reversal of trend of biomass burning in the Amazon.  
14 *Geophys. Res. Lett.* **34**: L20404, doi:10.1029/2007GL031530.
- 15 **Koren, I.**, L.A. Remer, Y.J. Kaufman, Y. Rudich, and J.V. Martins, 2007b: On the twilight zone between  
16 clouds and aerosols. *Geophys. Res. Lett.* **34**:L08805, doi:10.1029/2007GL029253.
- 17 **Koren, I.**, J. V. Martins, L. A. Remer, and H. Afargan, 2008: Smoke invigoration versus inhibition of  
18 clouds over the Amazon. *Science* 321:946, doi: 10.1126/science.1159185.
- 19 **Kroll, J. H.**, N.L. Ng, S.M. Murphy, R.C. Flagan, and J.H. Seinfeld, 2006: Secondary organic aerosol  
20 formation from isoprene photooxidation. *Environ. Sci. Technol.* **40**:1869–1877.
- 21 **Kruger, O.** and H. Grasl, 2002: The indirect aerosol effect over Europe. *Geophys. Res. Lett.*  
22 **29**:doi:10.1029/2001GL014081.
- 23 **Lack, D.**, E. Lovejoy, T. Baynard, A. Pettersson, and A. Ravishankara, 2006: Aerosol absorption  
24 measurements using photoacoustic spectroscopy: sensitivity, calibration, and uncertainty  
25 developments. *Aerosol. Sci. Technol.* **40**:697-708.
- 26 **Larson, V. E.**, R. Wood, P. R. Field, J.-C. Golaz, T. H. Vonder Haar, and W. R. Cotton, 2001: Small-  
27 scale and mesoscale variability of scalars in cloudy boundary layers: One-dimensional probability  
28 density functions. *J. Atmos. Sci.* **58**:1978-1996.
- 29 **Larson, V.E.**, J.-C. Golaz, H. Jiang and W.R. Cotton, 2005: Supplying local microphysics  
30 parameterizations with information about subgrid variability: Latin hypercube sampling. *J. Atmos. Sci.*  
31 **62**:4010-4026.
- 32 **Lau, K.**, M. Kim, and K. Kim, 2006: Asian summer monsoon anomalies induced by aerosol direct  
33 forcing - the role of the Tibetan Plateau. *Climate Dynamics* **36**:855-864, doi:10.1007/s00382-006-  
34 10114-z.
- 35 **Lau, K.-M.**, and K.-M. Kim, 2006: Observational relationships between aerosol and Asian monsoon  
36 rainfall, and circulation. *Geophys. Res. Lett.* **33**:L21810, doi:10.1029/2006GL027546.
- 37 **Lau, K.-M.**, K.-M. Kim, G. Walker, and Y. C. Sud, 2008: A GCM study of the possible impacts of  
38 Saharan dust heating on the water cycle and climate of the tropical Atlantic and Caribbean regions. *J.*  
39 *Climate* (submitted).
- 40 **Leahy, L.**, T. Anderson, T. Eck, and R. Bergstrom, 2007: A synthesis of single scattering albedo of  
41 biomass burning aerosol over southern Africa during SAFARI 2000. *Geophys. Res. Lett.* **34**:L12814,  
42 doi:10.1029/2007GL029697.

- 1 **Leaitch, W. R., G.A. Isaac, J.W. Strapp, C.M. Banic and H.A. Wiebe, 1992: The Relationship between**  
2 **Cloud Droplet Number Concentrations and Anthropogenic Pollution - Observations and Climatic**  
3 **Implications. *J. Geophys. Res.* **97**:2463-2474.**
- 4 **Leaitch, W. R., C. M. Banic, G. A. Isaac, M. D. Couture, P. S. K. Liu, I. Gultepe, S.-M. Li, L. Kleinman,**  
5 **J. I. MacPherson, and P. H. Daum, 1996: Physical and chemical observations in marine stratus during**  
6 **the 1993 North Atlantic Regional Experiment: Factors controlling cloud droplet number**  
7 **concentrations. *J. Geophys. Res.* **101**:29123–29135.**
- 8 **Lee, T., et al., 2006: The NPOESS VIIRS day/night visible sensor. *Bull. Amer. Meteorol. Soc.* **87**:191-**  
9 **199.**
- 10 **Lelieveld, J., H. Berresheim, S. Borrmann, S., et al., 2002: Global air pollution crossroads over the**  
11 **Mediterranean. *Science* **298**:794-799.**
- 12 **Léon, J., D. Tanré, J. Pelon, Y. Kaufman, J. Haywood, and B. Chatenet, 2003: Profiling of a Saharan dust**  
13 **outbreak based on a synergy between active and passive remote sensing. *J. Geophys. Res.* **108**:8575,**  
14 **doi:10.1029/2002JD002774.**
- 15 **Levin, Z. and W. R. Cotton, 2008: Aerosol pollution impact on precipitation: A scientific review. Report**  
16 **from the WMO/IUGG International Aerosol Precipitation Science Assessment Group (IAPSAG),**  
17 **World Meteorological Organization, Geneva, Switzerland, 482 pp.**
- 18 **Levy, R., L. Remer, and O. Dubovik, 2007a: Global aerosol optical properties and application to MODIS**  
19 **aerosol retrieval over land. *J. Geophys. Res.* **112**:D13210, doi:10.1029/2006JD007815.**
- 20 **Levy, R., L. Remer, S. Mattoo, E. Vermote, and Y. Kaufman, 2007b: Second-generation algorithm for**  
21 **retrieving aerosol properties over land from MODIS spectral reflectance. *J. Geophys. Res.***  
22 ****112**:D13211, doi:10.1029/2006JD007811.**
- 23 **Lewis, E.R. and S.E. Schwartz, 2004: *Sea Salt Aerosol Production: Mechanisms, Methods,***  
24 ***Measurements, and Models -- A Critical Review.* Geophysical Monograph Series Vol. 152, (American**  
25 **Geophysical Union, Washington, 2004), 413 pp. ISBN: 0-87590-417-3.**
- 26 **Li, R., Y. Kaufman, W. Hao, I. Salmon, and B. Gao, 2004: A technique for detecting burn scars using**  
27 **MODIS data. *IEEE Trans. on Geoscience & Remote Sensing* **42**:1300-1308.**
- 28 **Li, Z., et al., 2007: Preface to special section on East Asian studies of tropospheric aerosols: An**  
29 **international regional experiment (EAST-AIRE). *J. Geophys. Res.* **112**:D22s00,**  
30 **doi:10.1029/2007JD008853.**
- 31 **Lindesay, J. A., M.O. Andreae, J.G. Goldammer, G. Harris, H.J. Annegarn, M. Garstang, R.J. Scholes,**  
32 **and B.W. van Wilgen, 1996: International Geosphere Biosphere Programme/International Global**  
33 **Atmospheric Chemistry SAFARI-92 field experiment: Background and overview. *J. Geophys. Res.***  
34 ****101**:23521-23530.**
- 35 **Liou, K. N. and S-C. Ou, 1989: The Role of Cloud Microphysical Processes in Climate: An Assessment**  
36 **From a One-Dimensional Perspective. *J. Geophys. Res.* **94**:8599 – 8607.**
- 37 **Liousse, C., J. E. Penner, C. Chuang, J. J. Walton, H. Eddleman and H. Cachier, 1996: A three-**  
38 **dimensional model study of carbonaceous aerosols. *J. Geophys. Res.* **101**:19411-19432.**
- 39 **Liu, H., R. Pinker, and B. Holben, 2005: A global view of aerosols from merged transport models,**  
40 **satellite, and ground observations. *J. Geophys. Res.* **110**:D10S15, doi:10.1029/2004JD004695.**
- 41 **Liu, L., A. A. Lacis, B. E. Carlson, M. I. Mishchenko, and B. Cairns, 2006: Assessing Goddard Institute**  
42 **for Space Studies ModelE aerosol climatology using satellite and ground-based measurements: A**  
43 **comparison study. *J. Geophys. Res.* **111**:doi:10.1029/2006JD007334.**

- 1 **Liu, X.**, J. Penner, B. Das, D. Bergmann, J. Rodriguez, S. Strahan, M. Wang, and Y. Feng, 2007:  
2 Uncertainties in global aerosol simulations: Assessment using three meteorological data sets. *J.*  
3 *Geophys. Res.*, **112**:D11212, doi: 10.1029/2006JD008216.
- 4 **Liu, Z.**, A. Omar, M. Vaughan, J. Hair, C. Kittaka, Y. Hu, K. Powell, C. Trepte, D. Winker, C. Hostetler,  
5 R. Ferrare, and R. Pierce, 2008: CALIPSO lidar observations of the optical properties of Saharan dust:  
6 A case study of long-range transport. *J. Geophys. Res.* **113**:D07207, doi:10.1029/2007JD008878.
- 7 **Lockwood, M.**, and C. Frohlich, 2007: Recent oppositely directed trends in solar climate forcings and the  
8 global mean surface air temperature. *Proc. R. Soc. A*, 1-14, doi:10.1098/rspa.2007.1880.
- 9 **Loeb, N.**, and S. Kato, 2002: Top-of-atmosphere direct radiative effect of aerosols over the tropical  
10 oceans from the Clouds and the Earth's Radiant Energy System (CERES) satellite instrument. *J.*  
11 *Climate* **15**:1474-1484.
- 12 **Loeb, N.**, and N. Manalo-Smith, 2005: Top-of-Atmosphere direct radiative effect of aerosols over global  
13 oceans from merged CERES and MODIS observations. *J. Clim.* **18**:3506-3526.
- 14 **Loeb, N. G.**, S. Kato, K. Loukachine, and N. M. Smith, 2005: Angular distribution models for top-of-  
15 atmosphere radiative flux estimation from the Clouds and the Earth's Radiant Energy System  
16 instrument on the Terra Satellite. part I: Methodology. *J. Atmos. Oceanic Technology.* **22**:338–351.
- 17 **Lohmann, U.**, J. Feichter, C. C. Chuang, and J. E. Penner, 1999: Prediction of the number of cloud  
18 droplets in the ECHAM GCM. *J. Geophys. Res.* **104**:9169-9198.
- 19 **Lohmann, U.**, et al., 2001: Vertical distributions of sulfur species simulated by large scale atmospheric  
20 models in COSAM: Comparison with observations. *Tellus* **53B**:646-672.
- 21 **Lohmann, U.** and J. Feichter, 2005: Global indirect aerosol effects: a review. *Atmos. Chem. Phys.* **5**:715-  
22 737.
- 23 **Lohmann, U.**, I. Koren and Y.J. Kaufman, 2006: Disentangling the role of microphysical and dynamical  
24 effects in determining cloud properties over the Atlantic. *Geophys. Res. Lett.* **33**:L09802,  
25 doi:10.1029/2005GL024625.
- 26 **Lu, M.-L.**, G. Feingold, H. Jonsson, P. Chuang, H. Gates, R. C. Flagan, J. H. Seinfeld, 2008: Aerosol-  
27 cloud relationships in continental shallow cumulus. *J. Geophys. Res.* **113**:D15201,  
28 doi:10.1029/2007JD009354.
- 29 **Lubin, D.**, S. Satheesh, G. McFarquar, and A. Heymsfield, 2002: Longwave radiative forcing of Indian  
30 Ocean tropospheric aerosol. *J. Geophys. Res.* **107**:8004, doi:10.1029/2001JD001183.
- 31 **Lubin, D.** and A. Vogelmann, 2006: A climatologically significant aerosol longwave indirect effect in the  
32 Arctic. *Nature* **439**:453–456.
- 33 **Luo, Y.**, D. Lu, X. Zhou, W. Li, and Q. He, 2001: Characteristics of the spatial distribution and yearly  
34 variation of aerosol optical depth over China in last 30 years. *J. Geophys. Res.* **106**:14501,  
35 doi:10.1029/2001JD900030.
- 36 **Magi, B.**, P. Hobbs, T. Kirchstetter, T. Novakov, D. Hegg, S. Gao, J. Redemann, and B. Schmid, 2005:  
37 Aerosol properties and chemical apportionment of aerosol optical depth at locations off the United  
38 States East Coast in July and August 2001. *J. Atmos. Sci.* **62**:919-933.
- 39 **Malm, W.**, J. Sisler, D. Huffman, R. Eldred, and T. Cahill, 1994: Spatial and seasonal trends in particle  
40 concentration and optical extinction in the United States. *J. Geophys. Res.* **99**:1347-1370.
- 41 **Martins, J.**, D. Tanré, L. Remer, Y. Kaufman, S. Mattoo, and R. Levy, 2002: MODIS cloud screening for  
42 remote sensing of aerosol over oceans using spatial variability. *Geophys. Res. Lett.*  
43 **29**:10.1029/2001GL013252.



- 1 **Martonchik, J., D. Diner, R. Kahn, M. Verstraete, B. Pinty, H. Gordon, and T. Ackerman, 1998a:**  
2 Techniques for the Retrieval of aerosol properties over land and ocean using multiangle data. *IEEE*  
3 *Trans. Geosci. Remt. Sensing* **36**:1212-1227
- 4 **Martonchik, J., D. Diner, B. Pinty, M. Verstraete, R. Myneni, Y. Knjazikhin, and H. Gordon, 1998b:**  
5 Determination of land and ocean reflective, radiative, and biophysical properties using multiangle  
6 imaging. *IEEE Trans. Geosci. Remote Sens.* **36**:1266-1281.
- 7 **Martonchik, J., D. Diner, K. Crean, and M. Bull, 2002:** Regional aerosol retrieval results from MISR.  
8 *IEEE Trans. Geosci. Remote Sens.* **40**:1520-1531.
- 9 **Massie, S., O. Torres, and S. Smith, 2004:** Total ozone mapping spectrometer (TOMS) observations of  
10 increases in Asian aerosol in winter from 1979 to 2000. *J. Geophys. Res.* **109**:D18211,  
11 doi:10.1029/2004JD004620.
- 12 **Matheson, M. A., J. A. Coakley Jr., W. R. Tahnk, 2005:** Aerosol and cloud property relationships for  
13 summertime stratiform clouds in the northeastern Atlantic from Advanced Very High Resolution  
14 Radiometer observations. *J. Geophys. Res.* **110**:D24204, doi:10.1029/2005JD006165.
- 15 **Matsui, T., and R. Pielke, Sr., 2006:** Measurement-based estimation of the spatial gradient of aerosol  
16 radiative forcing. *Geophys. Res. Lett.* **33**: L11813, doi:10.1029/2006GL025974.
- 17 **Matsui, T., H. Masunaga, S. M. Kreidenweis, R. A. Pielke Sr., W.-K. Tao, M. Chin, Y. J. Kaufman,**  
18 **2006:** Satellite-based assessment of marine low cloud variability associated with aerosol, atmospheric  
19 stability, and the diurnal cycle. *J. Geophys. Res.* **111**:D17204, doi:10.1029/2005JD006097.
- 20 **Matthis, I., A. Ansmann, D. Müller, U. Wandinger, and D. Althausen, 2004:** Multiyear aerosol  
21 observations with dual-wavelength Raman lidar in the framework of EARLINET. *J. Geophys. Res.*  
22 **109**:D13203, doi:10.1029/2004JD004600.
- 23 **McComiskey, A., and G. Feingold, 2008:** Quantifying error in the radiative forcing of the first aerosol  
24 indirect effect, *Geophys. Res. Lett.*, **35**:, L02810, doi:10.1029/2007GL032667.
- 25 **McComiskey, A., S.E. Schwartz, B. Schmid, H. Guan, E.R. Lewis, P. Ricchiazzi, and J.A. Ogren, 2008a:**  
26 Direct aerosol forcing: Calculation from observables and sensitivity to inputs. *J. Geophys. Res.*  
27 **113**:D09202, doi:10.1029/2007JD009170.
- 28 **McComiskey, A, G. Feingold, A. S. Frisch, D. Turner, M. Miller, J. C. Chiu, Q. Min, and J. Ogren,**  
29 **2008b:** An assessment of aerosol-cloud interactions in marine stratus clouds based on surface remote  
30 sensing. *J. Geophys. Res.*, *submitted*.
- 31 **McCormick, R., and J. Ludwig, 1967:** Climate modification by atmospheric aerosols. *Science* **156**:1358-  
32 1359.
- 33 **McCormick, M. P., L. W. Thomason, and C. R. Trepte 1995:** Atmospheric effects of the Mt. Pinatubo  
34 eruption. *Nature* **373**: 399-404.
- 35 **McFiggans, G., P. Artaxo, U. Baltensberger, H. Coe, M.C. Facchini, G. Feingold, S. Fuzzi, M. Gysel, A.**  
36 **Laaksonen, U. Lohmann, T. F. Mentel, D. M. Murphy, C. D. O'Dowd, J. R. Snider, E. Weingartner,**  
37 **2006:** The effect of physical and chemical aerosol properties on warm cloud droplet activation. *Atmos.*  
38 *Chem. Phys.* **6**:2593-2649.
- 39 **Menon, S., A.D. Del Genio, Y. Kaufman, R. Bennartz, D. Koch, N. Loeb, and D. Orlikowski, 2008:**  
40 Analyzing signatures of aerosol-cloud interactions from satellite retrievals and the GISS GCM to  
41 constrain the aerosol indirect effect. *J. Geophys. Res.* **113**:D14S22, doi:10.1029/2007JD009442.
- 42 **Michalsky, J., J. Schlemmer, W. Berkheiser, et al., 2001:** Multiyear measurements of aerosol optical  
43 depth in the Atmospheric Radiation Measurement and Quantitative Links program. *J. Geophys. Res.*  
44 **106**:12099-12108.

- 1 **Min, Q.**, and L.C. Harrison, 1996: Cloud properties derived from surface MFRSR measurements and  
2 comparison with GEOS results at the ARM SGP site. *Geophys. Res. Lett.* **23**:1641- 1644.
- 3 **Minnis P.**, E. F. Harrison, L. L. Stowe, G. G. Gibson, F. M. Denn, D. R. Doelling. and W. L. Smith. Jr.,  
4 1993: Radiative climate forcing by the Mount Pinatubo eruption. *Science* **259**: 411-1415.
- 5 **Mishchenko, M.**, I. Geogdzhayev, B. Cairns, W. Rossow, and A. Lacis, 1999: Aerosol retrievals over the  
6 ocean by use of channels 1 and 2 AVHRR data: Sensitivity analysis and preliminary results. *Appl. Opt.*  
7 **38**:7325-7341.
- 8 **Mishchenko, M.**, et al., 2007a: Long-term satellite record reveals likely recent aerosol trend. *Science*  
9 **315**:1543.
- 10 **Mishchenko, M.**, et al., 2007b: Accurate monitoring of terrestrial aerosols and total solar irradiance. *Bull.*  
11 *Amer. Meteorol. Soc.* **88**:677-691.
- 12 **Mishchenko, M.**, and I. V. Geogdzhayev, 2007: Satellite remote sensing reveals regional tropospheric  
13 aerosol trends. *Optics Express.* **15**:7423-7438.
- 14 **Mitchell, J. Jr.**, 1971: The effect of atmospheric aerosols on climate with special reference to temperature  
15 near the Earth's surface. *J. Appl. Meteorol.* **10**:703-714.
- 16 **Molina, L. T.**, S. Madronich, J.S. Gaffney, and H.B. Singh, 2008: Overview of MILAGRO/INTEX-B  
17 Campaign. *IGACactivities, Newsletter of International Global Atmospheric Chemistry Project*, 38:2-  
18 15, April, 2008.
- 19 **Moody, E.**, M. King, S. Platnick, C. Schaaf, and F. Gao, 2005: Spatially complete global spectral surface  
20 albedos: value-added datasets derived from Terra MODIS land products. *IEEE Trans. Geosci. Remote*  
21 *Sens.* **43**:144-158.
- 22 **Mouillot, F.**, A. Narasimha, Y. Balkanski, J.-F. Lamarque, and C.B. Field, 2006: Global carbon  
23 emissions from biomass burning in the 20th century. *Geophys. Res. Lett.* **33**:L01801,  
24 doi:10.1029/2005GL024707.
- 25 **Murayama, T.**, N. Sugimoto, I. Uno, I., et al., 2001: Ground-based network observation of Asian dust  
26 events of April 1998 in East Asia. *J. Geophys. Res.* **106**:18346-18359.
- 27 **NRC (National Research Council)**, 2001: Climate Change Sciences: An analysis of some key questions,  
28 42pp., National Academy Press, Washington D.C..
- 29 **NRC (National Research Council)**, 2005: Radiative Forcing of Climate Change: Expanding the Concept  
30 and Addressing Uncertainties, National Academy Press, Washington D.C. (Available at  
31 <http://www.nap.edu/openbook/0309095069/html>).
- 32 **Nakajima, T.**, Higurashi, A., Kawamoto, K. and Penner, J. E., 2001: A possible correlation between  
33 satellite-derived cloud and aerosol microphysical parameters. *Geophys. Res. Lett.* **28**:1171-1174.
- 34 **Norris, J.**, and M. Wild, 2007: Trends in aerosol radiative effects over Europe inferred from observed  
35 cloud cover, solar “dimming”, and solar “brightening”. *J. Geophys. Res.* **112**:D08214,  
36 doi:10.1029/2006JD007794.
- 37 **Novakov, T.**, V. Ramanathan, J. Hansen, T. Kirchstetter, M. Sato, J. Sinton, and J. Sathaye, 2003: Large  
38 historical changes of fossil-fuel black carbon emissions. *Geophys. Res. Lett.* **30**:1324,  
39 doi:10.1029/2002GL016345.
- 40 **O’Dowd, C. D.**, et al. 1999: The relative importance of sea-salt and nss-sulphate aerosol to the marine  
41 CCN population: An improved multi-component aerosol-droplet parameterization. *Q. J. R. Meteorol.*  
42 *Soc.* **125**: 1295 – 1313.

- 1 **O'Neill, N.**, T. Eck, A. Smirnov, B. Holben, and S. Thulasiraman, 2003: Spectral discrimination of coarse  
2 and fine mode optical depth. *J. Geophys. Res.* **108**(D17):4559, doi:10.1029/2002JD002975.
- 3 **Patadia, F.**, P. Gupta, and S.A. Christopher, 2008: First observational estimates of global clear-sky  
4 shortwave aerosol direct radiative effect over land. *J. Geophys. Res.* **35**:L04810,  
5 doi:10.0129/2007GL032314.
- 6 **Penner, J.**, R. Dickinson, and C. O'Neill, 1992: Effects of aerosol from biomass burning on the global  
7 radiation budget. *Science* **256**:1432-1434.
- 8 **Penner, J.**, R. Charlson, J. Hales, et al., 1994: Quantifying and minimizing uncertainty of climate forcing  
9 by anthropogenic aerosols, *Bull. Amer. Meteorol. Soc.* **75**:375-400.
- 10 **Penner, J.E.**, H. Eddleman, and T. Novakov, 1993: Towards the development of a global inventory for  
11 black carbon emissions. *Atmos. Environ.* **27**:1277-1295.
- 12 **Penner, J. E.** et al., 2002: A comparison of model- and satellite-derived aerosol optical depth and  
13 reflectivity. *J. Atmos. Sci.* **59**:441-460.
- 14 **Penner, J. E.**, et al. 2006: Model intercomparison of indirect aerosol effects. *Atmos. Chem. Phys.* **6**:3391-  
15 3405.
- 16 **Pincus, R.**, and S.A. Klein, 2000: Unresolved spatial variability and microphysical process rates in large-  
17 scale models. *J. Geophys. Res.* **105**:27059-27065.
- 18 **Pinker, R.**, B. Zhang, and E. Dutton, 2005: Do satellites detect trends in surface solar radiation? *Science*  
19 **308**:850-854.
- 20 **Procopio, A. S.**, P. Artaxo, Y. J. Kaufman, L. A. Remer, J. S. Schafer, and B. N. Holben, 2004: Multiyear  
21 analysis of Amazonian biomass burning smoke radiative forcing of climate. *J. Geophys. Res.* **31**:  
22 L03108, doi: 10.1029/2003GL018646.
- 23 **Qian, Y.**, W. Wang, L Leung, and D. Kaiser, 2007: Variability of solar radiation under cloud-free skies in  
24 China: The role of aerosols. *Geophys. Res. Lett.* **34**:L12804, doi:10.1029/2006GL028800.
- 25 **Quaas, J.**, and O. Boucher, 2005: Constraining the first aerosol indirect radiative forcing in the LMDZ  
26 GCM using POLDER and MODIS satellite data. *Geophys. Res. Lett.*, **32**: L17814.
- 27 **Quaas, J.**, O. Boucher and U. Lohmann, 2006: Constraining the total aerosol indirect effect in the LMDZ  
28 GCM and ECHAM4 GCMs using MODIS satellite data. *Atmos. Chem. Phys. Disc.* **5**:9669-9690.
- 29 **Quaas, J.**, O. Boucher, N. Bellouin, and S. Kinne, 2008: Satellite-based estimate of the direct and indirect  
30 aerosol climate forcing. *J. Geophys. Res.* **113**:D05204, doi:10.1029/2007JD008962.
- 31 **Quinn, P.K.**, T. Anderson, T. Bates, R. Dlugi, J. Heintzenberg, W. Von Hoyningen-Huene, M. Kumula,  
32 P. Russel, and E. Swietlicki, 1996: Closure in tropospheric aerosol-climate research: A review and  
33 future needs for addressing aerosol direct shortwave radiative forcing. *Contrib. Atmosph. Phys.* **69**:547-  
34 577.
- 35 **Quinn, P.K.**, D. Coffman, V. Kapustin, T.S. Bates and D.S. Covert, 1998: Aerosol optical properties in  
36 the marine boundary layer during ACE 1 and the underlying chemical and physical aerosol properties.  
37 *J. Geophys. Res.* **103**:16547-16563.
- 38 **Quinn P.K.**, T. Bates, T. Miller, D. Coffman, J. Johnson, J. Harris, J. Ogren, G. Forbes, G., T. Anderson,  
39 D. Covert, and M. Rood, 2000: Surface submicron aerosol chemical composition: What fraction is not  
40 sulfate? *J. Geophys. Res.* **105**:6785-6806.
- 41 **Quinn, P.K.**, T.L. Miller, T.S. Bates, J.A. Ogren, E. Andrews, and G.E. Shaw, 2002: A three-year record  
42 of simultaneously measured aerosol chemical and optical properties at Barrow, Alaska. *J. Geophys.*  
43 *Res.* **107**(D11):doi:10.1029/2001JD001248.

- 1 **Quinn, P.K.**, and T. Bates, 2003: North American, Asian, and Indian haze: Similar regional impacts on  
2 climate? *Geophys. Res. Letts.* **30**:1555, doi:10.1029/2003GL016934.
- 3 **Quinn, P.K.**, D.J. Coffman, T.S. Bates, E.J. Welton, D.S. Covert, T.L. Miller, J.E. Johnson, S. Maria, L.  
4 Russell, R. Arimoto, C.M. Carrico, M.J. Rood, and J. Anderson, 2004: Aerosol optical properties  
5 measured aboard the Ronald H. Brown during ACE-Asia as a function of aerosol chemical composition  
6 and source region. *J. Geophys. Res.* **109**: doi:10.1029/2003JD004010.
- 7 **Quinn, P.K.** and T. Bates, 2005: Regional Aerosol Properties: Comparisons from ACE 1, ACE 2,  
8 Aerosols99, INDOEX, ACE Asia, TARFOX, and NEAQS. *J. Geophys. Res.* **110**:D14202,  
9 doi:10.1029/2004JD004755,.
- 10 **Quinn, P.K.**, et al., 2005: Impact of particulate organic matter on the relative humidity dependence of  
11 light scattering: A simplified parameterization. *Geophys. Res. Lett.*, **32**:L22809,  
12 doi:101029/2005GL024322.
- 13 **Quinn, P.K.**, G. Shaw, E. Andrews, E.G. Dutton, T. Ruoho-Airola, S.L. Gong, 2007: Arctic Haze:  
14 Current trends and knowledge gaps. *Tellus* **59B**:99–114.
- 15 **Radke, L.F.**, J.A. Coakley Jr., and M.D. King, 1989: Direct and remote sensing observations of the  
16 effects of ship tracks on clouds. *Science* **246**:1146–1149.
- 17 **Raes, F.**, T. Bates, F. McGovern, and M. van Liedekerke, 2000: The 2nd Aerosol Characterization  
18 Experiment (ACE-2): General overview and main results. *Tellus* **52B**:111–125.
- 19 **Ramanathan, V.**, P. Crutzen, J. Kiehl, and D. Rosenfeld, 2001a: Aerosols, Climate, and the Hydrological  
20 Cycle. *Science* **294**:2119-2124.
- 21 **Ramanathan, V.**, P. Crutzen, J. Lelieveld, et al., 2001b: Indian Ocean Experiment: An integrated  
22 analysis of the climate forcing and effects of the great Indo-Asian haze. *J. Geophys. Res.* **106**:28371-  
23 28398.
- 24 **Ramanathan, V.**, and P. Crutzen, 2003: Atmospheric Brown “Clouds”. *Atmos. Environ.* **37**:4033-4035.
- 25 **Ramanathan, V.**, and Coauthors, 2005: Atmospheric brown clouds: Impact on South Asian climate and  
26 hydrologic cycle. *Proc. Natl. Acad. Sci. USA* **102**:5326–5333.
- 27 **Randall, D.**, M. Khairoutdinov, A. Arakawa, and W. Grabowski, 2003: Breaking the cloud  
28 parameterization deadlock. *Bull. Amer. Meteorol. Soc.* **84**:1547-1564.
- 29 **Rao, S.**, K. Riahi, K. Kupiainen, and Z. Klimont, 2005: Long-term scenarios for black and organic carbon  
30 emissions. *Env. Sc.* **2**:205-216.
- 31 **Reddy, M.**, O. Boucher, N. Bellouin, M. Schulz, Y. Balkanski, J. Dufresne, and M. Pham, 2005a:  
32 Estimates of multi-component aerosol optical depth and direct radiative perturbation in the LMDZT  
33 general circulation model. *J. Geophys. Res.* **110**:D10S16, doi:10.1029/2004JD004757.
- 34 **Reddy, M.**, O. Boucher, Y. Balkanski, and M. Schulz, 2005b: Aerosol optical depths and direct radiative  
35 perturbations by species and source type. *Geophys. Res. Lett.* **32**: L12803, doi:10.1029/2004GL021743.
- 36 **Reid, J.**, J. Kinney, and D. Wesphal, et al., 2003: Analysis of measurements of Saharan dust by airborne  
37 and groundbased remote sensing methods during the Puerto Rico Dust Experiment (PRIDE). *J.*  
38 *Geophys. Res.* **108**:8586, doi:10.1029/2002JD002493.
- 39 **Reid, J.**, et al., 2008: An overview of UAE2 flight operations: Observations of summertime atmospheric  
40 thermodynamic and aerosol profiles of the southern Arabian Gulf. *J. Geophys. Res.* **113**:D14213,  
41 doi:10.1029/2007JD009435.
- 42 **Remer, L.**, S. Gassó, D. Hegg, Y. Kaufman, and B. Holben, 1997: Urban/industrial aerosol: ground based  
43 sun/sky radiometer and airborne in-situ measurements. *J. Geophys. Res.* **102**:16849-16859.

- 1 **Remer, L., D. Tanré, Y. Kaufman, C. Ichoku, S. Mattoo, R. Levy, D. Chu, B. Holben, O. Dubovik, A.**  
2 **Smirnov, J. Martins, R. Li, and Z. Ahman, 2002: Validation of MODIS aerosol retrieval over ocean.**  
3 ***Geophys. Res. Lett.* **29**:8008, doi:10.1029/2001/GL013204.**
- 4 **Remer, L., Y. Kaufman, D. Tanré, S. Mattoo, D. Chu, J. Martins, R. Li, C. Ichoku, R. Levy, R.**  
5 **Kleidman, T. Eck, E. Vermote, and B. Holben, 2005: The MODIS aerosol algorithm, products and**  
6 **validation. *J. Atmos. Sci.* **62**:947-973.**
- 7 **Remer, L., and Y. Kaufman, 2006: Aerosol direct radiative effect at the top of the atmosphere over cloud**  
8 **free ocean derived from four years of MODIS data. *Atmos. Chem. Phys.* **6**:237-253.**
- 9 **Remer, L., et al., 2008: An emerging aerosol climatology from the MODIS satellite sensors, *J. Geophys.***  
10 ***Res.* **113**:D14S01, doi:10.1029/2007JD009661.**
- 11 **Rissler, J., E. Swietlicki, J. Zhou, G. Roberts, M. O. Andreae, L. V. Gatti, and P. Artaxo 2004: Physical**  
12 **properties of the sub-micrometer aerosol over the Amazon rain forest during the wet-to-dry season**  
13 **transition – comparison of modeled and measured CCN concentrations. *Atmos. Chem. Phys.* **4**:2119-**  
14 **2143.**
- 15 **Robock, A., 2000: Volcanic eruptions and climate. *Rev. Geophys.* **38**(2): 191-219.**
- 16 **Robock, A., 2002: Pinatubo eruption: The climatic aftermath, *Science*, **295**: 1242-1244.**
- 17 **Roderick, M. L. and G. D. Farquhar, 2002: The cause of decreased pan evaporation over the past 50**  
18 **years. *Science* **298**:1410-1411.**
- 19 **Rosenfeld, D., and I. Lansky, 1998: Satellite-based insights into precipitation formation processes in**  
20 **continental and maritime convective clouds. *Bull. Am. Meteorol. Soc.* **79**:2457-2476.**
- 21 **Rosenfeld, D., 2000: Suppression of rain and snow by urban and industrial air pollution. *Science***  
22 ****287**:1793-1796.**
- 23 **Rosenfeld, D., 2006: Aerosols, clouds, and climate. *Science* **312**:10.1126/science.1128972.**
- 24 **Ruckstuhl, C., et al., 2008: Aerosol and cloud effects on solar brightening and recent rapid warming.**  
25 ***Geophys. Res. Lett.* **35**:L12708, doi:10.1029/2008GL034228.**
- 26 **Russell, P., S. Kinne, and R. Bergstrom, 1997: Aerosol climate effects: local radiative forcing and**  
27 **column closure experiments. *J. Geophys. Res.* **102**:9397-9407.**
- 28 **Russell, P., J. Livingston, P. Hignett, S. Kinne, J. Wong, A. Chien, R. Bergstrom, P. Durkee, and P.**  
29 **Hobbs, 1999: Aerosol-induced radiative flux changes off the United States mid-Atlantic coast:**  
30 **comparison of values calculated from sun photometer and in-situ data with those measured by airborne**  
31 **pyranometer. *J. Geophys. Res.* **104**:2289-2307.**
- 32 **SAP 3.2, 2008: Climate Projections Based on Emissions Scenarios for Long-lived and Short-lived**  
33 **Radiatively Active Gases and Aerosols. A Report by the U.S. Climate Change Science Program and the**  
34 **Subcommittee on Global Change Research, H. Levy II, D, T. Shindell, A. Gilliland, M. D.**  
35 **Schwarzkopf, L. W. Horowitz, (eds.). Department of Commerce, NOAA's National Climatic Data**  
36 **Center, Washington, D. C. USA, 100 pp.**
- 37 **Saxena, P., L. Hildemann, P. McMurry, and J. Seinfeld, 1995: Organics alter hygroscopic behavior of**  
38 **atmospheric particles. *J. Geophys. Res.* **100**:18755-18770.**
- 39 **Schmid, B., J.M. Livingston, P.B. Russell, P.A. Durkee, H.H. Jonsson, D.R. Collins, R.C. Flagan, J.H.**  
40 **Seinfeld, S. Gasso, D.A. Hegg, E. Ostrom, K.J. Noone, E.J. Welton, K.J. Voss, H.R. Gordon, P.**  
41 **Formenti, and M.O. Andreae, 2000: Clear-sky closure studies of lower tropospheric aerosol and water**  
42 **vapor during ACE-2 using airborne sunphotometer, airborne in-situ, space-borne, and ground-based**  
43 **measurements. *Tellus* **52**:568-593.**

- 1 **Schmid, B.**, R. Ferrare, C. Flynn, et al., 2006: How well do state-of-the-art techniques measuring the  
2 vertical profile of tropospheric aerosol extinction compare? *J. Geophys. Res.* **111**:  
3 doi:10.1029/2005JD005837, 2006.
- 4 **Schmidt, G. A.**, et al., 2006: Present-day atmospheric simulations using GISS Model E: Comparison to  
5 in-situ, satellite and reanalysis data. *J. Clim.* **19**:153-192.
- 6 **Schulz, M.**, C. Textor, S. Kinne, et al., 2006: Radiative forcing by aerosols as derived from the AeroCom  
7 present-day and pre-industrial simulations. *Atmos. Chem. Phys.*, **6**:5225-5246.
- 8 **Schwartz, S. E.**, R. J. Charlson and H. Rodhe, 2007: Quantifying climate change – too rosy a picture?  
9 *Nature Reports Climate Change* **2**:23-24.
- 10 **Sekiguchi, M.**, T. Nakajima, K. Suzuki, et al., A study of the direct and indirect effects of aerosols using  
11 global satellite data sets of aerosol and cloud parameters. *J. Geophys. Res.*, **108**:D22, 4699,  
12 doi:10.1029/2002JD003359, 2003
- 13 **Seinfeld, J.H.**, et al., 1996. A Plan for a Research Program on Aerosol Radiative Forcing and Climate  
14 Change. *National Research Council*. 161 pp.
- 15 **Seinfeld, J. H.**, G.R. Carmichael, R. Arimoto, et al. 2004: ACE-Asia: Regional climatic and atmospheric  
16 chemical effects of Asian dust and pollution. *Bull. Amer. Meteor. Soc.* **85**:367-380.
- 17 **Sheridan, P.**, and J. Ogren, 1999: Observations of the vertical and regional variability of aerosol optical  
18 properties over central and eastern North America. *J. Geophys. Res.* **104**:16793-16805.
- 19 **Shindell, D.T.**, M. Chin, F. Dentener, et al., 2008a: A multi-model assessment of pollution transport to  
20 the Arctic. *Atmos. Chem. Phys.* **8**:5353-5372.
- 21 **Shindell, D.T.**, H. Levy, II, M.D. Schwarzkopf, L.W. Horowitz, J.-F. Lamarque, and G. Faluvegi, 2008b:  
22 Multimodel projections of climate change from short-lived emissions due to human activities. *J.*  
23 *Geophys. Res.* **113**:D11109, doi:10.1029/2007JD009152.
- 24 **Singh, H.B.**, W.H. Brune, J.H. Crawford, F. Flocke, and D.J. Jacob, 2008: Chemistry and Transport of  
25 Pollution over the Gulf of Mexico and the Pacific: Spring 2006 INTEX-B Campaign Overview and  
26 First Results. *Atmos. Chem. Phys. Discussion*, submitted.
- 27 **Sinyuk, A.**, O. Dubovik, B. Holben, T. F. Eck, F.-M. Breon, J. Martonchik, R. A. Kahn, D. Diner, E. F.  
28 Vermote, Y. J. Kaurman, J. C. Roger, T. Lapyonok, and I. Slutsker, 2007: Simultaneous retrieval of  
29 aerosol and surface properties from a combination of AERONET and satellite data. *Remote Sens.*  
30 *Environ.* **107**:90-108, doi: 10.1016/j.rse.2006.07.022.
- 31 **Smirnov, A.**, B. Holben, T. Eck, O. Dubovik, and I. Slutsker, 2000: Cloud screening and quality control  
32 algorithms for the AERONET database. *Rem. Sens. Env.* **73**:337-349.
- 33 **Smirnov, A.**, B. Holben, T. Eck, I. Slutsker, B. Chatenet, and R. Pinker, 2002: Diurnal variability of  
34 aerosol optical depth observed at AERONET (Aerosol Robotic Network) sites. *Geophys. Res. Lett.*  
35 **29**:2115, doi:10.1029/2002GL016305.
- 36 **Smirnov, A.**, B. Holben, S. Sakerin, et al., 2006: Ship-based aerosol optical depth measurements in the  
37 Atlantic Ocean, comparison with satellite retrievals and GOCART model. *Geophys. Res. Lett.*  
38 **33**:L14817, doi: 10.1029/2006GL026051.
- 39 **Smith Jr., W.L.**, et al., 2005: EOS Terra aerosol and radiative flux validation: An overview of the  
40 Chesapeake Lighthouse and aircraft measurements from satellites (CLAMS) experiment. *J. Atmos. Sci.*  
41 **62**:903-918.
- 42 **Sokolik, I.**, D. Winker, G. Bergametti, et al., 2001: Introduction to special section: outstanding problems  
43 in quantifying the radiative impacts of mineral dust. *J. Geophys. Res.* **106**:18015-18027.

- 1 **Sotiropoulou**, R.E.P, A. Nenes, P.J. Adams, and J.H. Seinfeld, 2007: Cloud condensation nuclei  
2 prediction error from application of Kohler theory: Importance for the aerosol indirect effect.  
3 *J.Geoph.Res.* **112**:D12202, doi:10.1029/2006JD007834.
- 4 **Sotiropoulou**, R.E.P, J. Medina, and A. Nenes, 2006: CCN predictions: is theory sufficient for  
5 assessments of the indirect effect? *Geoph.Res.Lett.* **33**:L05816, doi:10.1029/2005GL025148
- 6 **Spinhirne**, J., S. Palm, W. Hart, D. Hlavka, and E. Welton, 2005: Cloud and Aerosol Measurements from  
7 the GLAS Space Borne Lidar: initial results. *Geophys. Res. Lett.* **32**:L22S03,  
8 doi:10.1029/2005GL023507.
- 9 **Squires**, P., 1958: The microstructure and colloidal stability of warm clouds. I. The relation between  
10 structure and stability. *Tellus* **10**:256-271.
- 11 **Stanhill**, G., and S. Cohen, 2001: Global dimming: a review of the evidence for a widespread and  
12 significant reduction in global radiation with discussion of its probable causes and possible agricultural  
13 consequences. *Agricul. Forest Meteorol.* **107**:255-278.
- 14 **Stephens**, G., D. Vane, R. Boain, G. Mace, K. Sassen, Z. Wang, A. Illingworth, E. O'Conner, W.  
15 Rossow, S. Durden, S. Miller, R. Austin, A. Benedetti, and C. Mitrescu, 2002: The CloudSat mission  
16 and the A-Train. *Bull. Amer. Meteo. Soc.* **83**:1771-1790.
- 17 **Stephens**, G. L. and J. M. Haynes, 2007: Near global observations of the warm rain coalescence process.  
18 *Geophys. Res. Lett.*, **34**: L20805, doi:10.1029/2007GL030259.
- 19 **Stern**, D.I., 2005: Global sulfur emissions from 1850 to 2000. *Chemosphere* **58**:163-175.
- 20 **Stevens**, B., G. Feingold, R. L. Walko and W. R. Cotton, 1996: On elements of the microphysical  
21 structure of numerically simulated non-precipitating stratocumulus. *J. Atmos. Sci.* **53**:980-1006.
- 22 **Storlevmo**, T., J.E. Kristjansson, G. Myhre, M. Johnsdud, and F. Stordal, 2006: Combined observational  
23 and modeling based study of the aerosol indirect effect. *Atmos. Chem. Phys.* **6**:3583-3601.
- 24 **Stott**, P.A., et al., 2006: Observational constraints on past attributable warming and predictions of future  
25 global warming. *J. Clim.* **19**:3055–3069.
- 26 **Strawa**, A., R. Castaneda, T. Owano, P. Baer, and B. Paldus, 2002: The measurement of aerosol optical  
27 properties using continuous wave cavity ring-down techniques. *J. Atm. Ocean. Tech.* **20**:454-465.
- 28 **Streets**, D., T. Bond, T. Lee, and C. Jang, 2004: On the future of carbonaceous aerosol emissions. *J.*  
29 *Geophys. Res.* **109**:D24212, doi:10.1029/2004JD004902.
- 30 **Streets**, D., and K. Anan, 2005: The importance of China's household sector for black carbon emissions.  
31 *Geophys. Res. Lett.* **32**:L12708, doi:10.1029/2005GL022960.
- 32 **Streets**, D., Y. Wu, and M. Chin, 2006a: Two-decadal aerosol trends as a likely explanation of the global  
33 dimming/brightening transition. *Geophys. Res. Lett.* **33**:L15806, doi:10.1029/2006GL026471.
- 34 **Streets**, D., Q. Zhang, L. Wang, K. He, J. Hao, Y. Tang, and G. Carmichael, 2006b: Revisiting China's  
35 CO emissions after TRACE-P: Synthesis of inventories, atmospheric modeling and observations *J.*  
36 *Geophys. Res.* **111**:D14306, doi:10.1029/2006JD007118.
- 37 **Svensmark**, H. and E. Friis-Christensen, 1997: Variation of cosmic ray flux and global cloud coverage -  
38 a missing link in solar-climate relationships. *J. Atmos. Sol.-Terr. Phys.*, **59**: 1225-1232.
- 39 **Takemura**, T., T. Nakajima, O. Dubovik, B. Holben, and S. Kinne, 2002: Single-scattering albedo and  
40 radiative forcing of various aerosol species with a global three-dimensional model. *J. Climate*, **15**:333-  
41 352.

- 1 **Takemura, T.**, T. Nozawa, S. Emori, T. Nakajima, and T. Nakajima, 2005: Simulation of climate  
2 response to aerosol direct and indirect effects with aerosol transport-radiation model. *J. Geophys. Res.*  
3 **110**:D02202, doi:10.1029/2004JD005029.
- 4 **Tang, Y.**, G. Carmichael, I. Uno, J. Woo, G. Kurata, B. Lefer, R. Shetter, H. Huang, B. Anderson, M.  
5 Avery, A. Clarke and D. Blake, 2003: Influences of biomass burning during the Transport and  
6 Chemical Evolution Over the Pacific (TRACE-P) experiment identified by the regional chemical  
7 transport model. *J. Geophys. Res.* **108**:8824, doi:10.1029/2002JD003110.
- 8 **Tang, Y.**, G. Carmichael, J. Seinfeld, D. Dabdub, R. Weber, B. Huebert, A. Clarke, S. Guazzotti, D.  
9 Sodeman, K. Prather, I. Uno, J. Woo, D. Streets, P. Quinn, J. Johnson, C. Song, A. Sandu, R. Talbot  
10 and J. Dibb, 2004: Three-dimensional simulations of inorganic aerosol distributions in East Asia during  
11 spring 2001. *J. Geophys. Res.* **109**:D19S23, doi:10.1029/2003JD004201.
- 12 **Tanré, D.**, Y. Kaufman, M. Herman, and S. Mattoo, 1997: Remote sensing of aerosol properties over  
13 oceans using the MODIS/EOS spectral radiances. *J. Geophys. Res.*, **102**:16971-16988.
- 14 **Tanré, D.**, J. Haywood, J. Pelon, J. Léon, B. Chatenet, P. Formenti, P. Francis, P. Goloub, E. Highwood,  
15 and G. Myhre, 2003: Measurement and modeling of the Saharan dust radiative impact: Overview of the  
16 Saharan Dust Experiment (SHADE). *J. Geophys. Res.* **108**:8574, doi:10.1029/2002JD003273.
- 17 **Textor, C.**, M. Schulz, S. Guibert, et al., 2006: Analysis and quantification of the diversities of aerosol  
18 life cycles within AEROCOM. *Atmos. Chem. Phys.* **6**:1777-1813.
- 19 **Textor, C.**, et al., 2007: The effect of harmonized emissions on aerosol properties in global models - an  
20 AeroCom experiment. *Atmos. Chem. Phys.* **7**:4489-4501.
- 21 **Tie, X.** et al., 2005: Assessment of the global impact of aerosols on tropospheric oxidants. *J. Geophys.*  
22 *Res.* **110**:doi:10.1029/2004JD005359.
- 23 **Torres, O.**, P. Bhartia, J. Herman, Z. Ahmad, and J. Gleason, 1998: Derivation of aerosol properties from  
24 satellite measurements of backscattered ultraviolet radiation: Theoretical bases. *J. Geophys. Res.*  
25 **103**:17009-17110.
- 26 **Torres, O.**, P. Bhartia, J. Herman, A. Sinyuk, P. Ginoux, and B. Holben, 2002: A long-term record of  
27 aerosol optical depth from TOMS observations and comparison to AERONET measurements. *J.*  
28 *Atmos. Sci.* **59**:398-413.
- 29 **Torres, O.**, P. Bhartia, A. Sinyuk, E. Welton, and B. Holben, 2005: Total Ozone Mapping Spectrometer  
30 measurements of aerosol absorption from space: Comparison to SAFARI 2000 ground-based  
31 observations. *J. Geophys. Res.* **110**:D10S18, doi:10.1029/2004JD004611.
- 32 **Turco, R.P.**, O.B. Toon, R.C. Whitten, J.B. Pollack, and P. Hamill, 1983: The global cycle of particulate  
33 elemental carbon: a theoretical assessment, in *Precipitation Scavenging, Dry Deposition, and*  
34 *Resuspension*, ed. H.R. Pruppacher et al., pp. 1337-1351, Elsevier Science, New York.
- 35 **Twomey, S.**, 1977: The influence of pollution on the shortwave albedo of clouds. *J. Atmos. Sci.* **34**:1149-  
36 1152.
- 37 **van Ardenne, J. A.**, F.J. Dentener, J. Olivier, J. Klein, C.G.M. Goldewijk, and J. Lelieveld, 2001: A 1° x  
38 1° resolution data set of historical anthropogenic trace gas emissions for the period 1890–1990. *Global*  
39 *Biogeochem. Cycl.* **15**:909–928.
- 40 **Veihelmann, B.**, P. F. Levelt, P. Stammes, and J. P. Veefkind, 2007: Simulation study of the aerosol  
41 information content in OMI spectral reflectance measurements. *Atmos. Chem. Phys.* **7**:3115–3127.
- 42 **Wang, J.**, S. Christopher, F. Brechtel, J. Kim, B. Schmid, J. Redemann, P. Russell, P. Quinn, and B.  
43 Holben, 2003: Geostationary satellite retrievals of aerosol optical thickness during ACE-Asia. *J.*  
44 *Geophys. Res.* **108**:8657, 10.1029/2003JD003580



- 1 **Wang, S., Q. Wang, and G. Feingold, 2003:** Turbulence, condensation and liquid water transport in  
2 numerically simulated nonprecipitating stratocumulus clouds. *J. Atmos. Sci.* **60**:262-278.
- 3 **Warner, J., and S. Twomey, 1967:** The production of cloud nuclei by cane fires and the effect on cloud  
4 droplet concentration. *J. Atmos. Sci.* **24**:704–706.
- 5 **Warner, J., 1968:** A reduction of rain associated with smoke from sugar-cane fires—An inadvertent  
6 weather modification. *J. App. Meteor.* **7**:247–251.
- 7 **Welton, E., K. Voss, P. Quinn, P. Flatau, K. Markowicz, J. Campbell, J. Spinhirne, H. Gordon, and J.**  
8 **Johnson, 2002:** Measurements of aerosol vertical profiles and optical properties during INDOEX 1999  
9 using micro-pulse lidars. *J. Geophys. Res.* **107**:8019, doi:10.1029/2000JD000038.
- 10 **Welton, E., J. Campbell, J. Spinhirne, and V. Scott, 2001:** Global monitoring of clouds and aerosols using  
11 a network of micro-pulse lidar systems, in *Lidar Remote Sensing for Industry and Environmental*  
12 *Monitoring*, U. N. Singh, T. Itabe, N. Sugimoto, (eds.), *Proc. SPIE*, **4153**:151-158.
- 13 **Wen, G., A. Marshak, and R. Cahalan, 2006:** Impact of 3D clouds on clear sky reflectance and aerosol  
14 retrieval in a biomass burning region of Brazil. *IEEE Geo. Rem. Sens. Lett.* **3**:169-172.
- 15 **Wetzel, M. A. and Stowe, L. L.:** Satellite-observed patterns in stratus microphysics, aerosol optical  
16 thickness, and shortwave radiative forcing. 1999: *J. Geophys. Res.*, **104**:31287-31299.
- 17 **Wielicki, B., B. Barkstrom, E. Harrison, R. Lee, G. Smith, and J. Cooper, 1996:** Clouds and the Earth's  
18 radiant energy system (CERES): An Earth observing system experiment. *Bull. Amer. Meteo. Soc.*  
19 **77**:853-868.
- 20 **Wild, M., H. Gilgen, A. Roesch, et al., 2005:** From dimming to brightening: Decadal changes in solar  
21 radiation at Earth's surface. *Science* **308**:847-850.
- 22 **Winker, D., R. Couch, and M. McCormick, 1996:** An overview of LITE: NASA's Lidar In-Space  
23 Technology Experiment. *Proc. IEEE* **84(2)**:164-180.
- 24 **Winker, D., J. Pelon, and M. McCormick, 2003:** The CALIPSO mission: spaceborne lidar for  
25 observation of aerosols and clouds. *Proc. SPIE* **4893**:1-11.
- 26 **Xue, H., and G. Feingold, 2006:** Large eddy simulations of trade-wind cumuli: Investigation of aerosol  
27 indirect effects. *J. Atmos. Sci.* **63**:1605-1622.
- 28 **Xue, H., G. Feingold, and B. Stevens, 2008:** Aerosol effects on clouds, precipitation, and the organization  
29 of shallow cumulus convection. *J. Atmos. Sci.* **65**:392-406.
- 30 **Yu, H., S. Liu, and R. Dickinson, 2002:** Radiative effects of aerosols on the evolution of the atmospheric  
31 boundary layer. *J. Geophys. Res.* **107**:4142, doi:10.1029/2001JD000754.
- 32 **Yu, H., R. Dickinson, M. Chin, Y. Kaufman, B. Holben, I. Geogdzhayev, and M. Mishchenko, 2003:**  
33 Annual cycle of global distributions of aerosol optical depth from integration of MODIS retrievals and  
34 GOCART model simulations. *J. Geophys. Res.* **108**:4128, doi:10.1029/2002JD002717.
- 35 **Yu, H., R. Dickinson, M. Chin, Y. Kaufman, M. Zhou, L. Zhou, Y. Tian, O. Dubovik, and B. Holben,**  
36 **2004:** The direct radiative effect of aerosols as determined from a combination of MODIS retrievals  
37 and GOCART simulations. *J. Geophys. Res.* **109**:D03206, doi:10.1029/2003JD003914.
- 38 **Yu, H., Y. Kaufman, M. Chin, G. Feingold, L. Remer, T. Anderson, Y. Balkanski, N. Bellouin, O.**  
39 **Boucher, S. Christopher, P. DeCola, R. Kahn, D. Koch, N. Loeb, M. S. Reddy, M. Schulz, T.**  
40 **Takemura, and M. Zhou, 2006:** A review of measurement-based assessments of aerosol direct radiative  
41 effect and forcing. *Atmos. Chem. Phys.* **6**:613-666.

- 1 **Yu, H., R. Fu, R. Dickinson, Y. Zhang, M. Chen, and H. Wang, 2007:** Interannual variability of smoke  
2 and warm cloud relationships in the Amazon as inferred from MODIS retrievals. *Remote Sens.*  
3 *Environ.* **111**:435-449.
- 4 **Yu, H., L.A. Remer, M. Chin, H. Bian, R. Kleidman, and T. Diehl, 2008:** A satellite-based assessment of  
5 trans-Pacific transport of pollution aerosol. *J. Geophys. Res.* **113**:D14S12, doi:10.1029/2007JD009349.
- 6 **Zhang, J., and S. Christopher, 2003:** Longwave radiative forcing of Saharan dust aerosols estimated from  
7 MODIS, MISR, and CERES observations on Terra. *Geophys. Res. Lett.* **30**:2188,  
8 doi:10.1029/2003GL018479.
- 9 **Zhang, J., S. Christopher, L. Remer, and Y. Kaufman, 2005a:** Shortwave aerosol radiative forcing over  
10 cloud-free oceans from Terra. I: Angular models for aerosols. *J. Geophys. Res.* **110**:D10S23,  
11 doi:10.1029/2004JD005008.
- 12 **Zhang, J., S. Christopher, L. Remer, and Y. Kaufman, 2005b:** Shortwave aerosol radiative forcing over  
13 cloud-free oceans from Terra. II: Seasonal and global distributions. *J. Geophys. Res.* **110**:D10S24,  
14 doi:10.1029/2004JD005009.
- 15 **Zhang, J., J. S. Reid, and B. N. Holben, 2005c:** An analysis of potential cloud artifacts in MODIS over  
16 ocean aerosol optical thickness products. *Geophys. Res. Lett.* **32**:L15803, doi:10.1029/2005GL023254.
- 17 **Zhang, J., J.S. Reid, D.L. Westphal, N.L. Baker, and E.J. Hyer, 2008:** A system for operational aerosol  
18 optical depth data assimilation over global oceans. *J. Geophys. Res.* **113**:doi:10.1029/2007JD009065.
- 19 **Zhang, Q. et al., 2007:** Ubiquity and dominance of oxygenated species in organic aerosols in  
20 anthropogenically-influenced Northern Hemisphere midlatitudes. *Geophys. Res. Lett.* **34**:L13801,  
21 doi:10.1029/2007GL029979.
- 22 **Zhang, X., F.W. Zwiers, and P.A. Stott, 2006:** Multi-model multi-signal climate change detection at  
23 regional scale. *J. Clim.* **19**:4294-4307.
- 24 **Zhang, X., F.W. Zwiers, G.C. Hegerl, F.H. Lambert, N.P. Gillett, S. Solomon, P.A. Stott, T. Nozawa,**  
25 **2006:** Detection of human influence on twentieth-century precipitation trends. *Nature*, **448**: 461-465,  
26 doi:10.1038/nature06025.
- 27 **Zhao, T. X.-P., I. Laszlo, W. Guo, A. Heidinger, C. Cao, A. Jelenak, D. Tarpley, and J. Sullivan, 2008a:**  
28 **Study of long-term trend in aerosol optical thickness observed from operational AVHRR satellite**  
29 **instrument. *J. Geophys. Res.* **113**:D07201, doi:10.1029/2007JD009061.**
- 30 **Zhao, T. X.-P., H. Yu, I. Laszlo, M. Chin, and W.C. Conant, 2008b:** Derivation of component aerosol  
31 direct radiative forcing at the top of atmosphere for clear-sky oceans. *J. Quant. Spectro. Rad. Trans.*  
32 **109**:1162-1186.
- 33 **Zhou, M., H. Yu, R. Dickinson, O. Dubovik, and B. Holben, 2005:** A normalized description of the direct  
34 effect of key aerosol types on solar radiation as estimated from AERONET aerosols and MODIS  
35 albedos. *J. Geophys. Res.* **110**:D19202, doi:10.1029/2005JD005909.

36

# Glossary

## A

**Absorption:** the process in which incident radiant energy is retained by a substance.

**Absorption coefficient:** fraction of incident radiant energy removed by **absorption** per length of travel of radiation through the substance.

**Active remote sensing:** a **remote sensing** system that transmits its own electromagnetic energy, then measures the properties of the returned radiation.

**Adiabatic equilibrium:** a vertical distribution of temperature and pressure in an atmosphere in hydrostatic equilibrium such that an air parcel displaced adiabatically will continue to possess the same temperature and pressure as its surroundings, so that no restoring force acts on a parcel displaced vertically.

**Aerosol:** a colloidal suspension of liquid or solid particles (in air).

**Aerosol asymmetry factor** (also called **asymmetry parameter**): the mean cosine of the scattering angle, found by integration over the complete scattering **phase function** of aerosol.

**Aerosol direct radiative effect:** change in radiative flux due to aerosol scattering and absorption with the presence of aerosol relative to the absence of aerosol.

**Aerosol hemispheric backscatter fraction:** the fraction of the scattered intensity that is redirected into the backward hemisphere relative to the incident light.

**Aerosol indirect effects:** processes referring to the influence of aerosol on cloud amount or radiative properties. It includes the effect of aerosols on cloud droplet size and therefore its brightness (also known as the “cloud albedo effect” or the first aerosol indirect effect); and the effect of cloud droplet size on precipitation

efficiency and possibly cloud lifetime, also known as the second aerosol indirect effect.

**Aerosol mass extinction (scattering, absorption) efficiency:** the aerosol extinction (scattering, absorption) coefficient per aerosol mass concentration, with a unit  $\text{m}^2 \text{g}^{-1}$ .

**Aerosol optical depth:** the (wavelength dependent) negative logarithm of the fraction of radiation (or light) that is extinguished (or scattered or absorbed) by aerosol particles on a vertical path, typically from the surface (or some specified altitude) to the top of the atmosphere. Alternatively and equivalently: The (dimensionless) line integral of the absorption coefficient (due to aerosol particles), or of the scattering coefficient (due to aerosol particles), or of the sum of the two (extinction coefficient due to aerosol particles), along such a vertical path. Indicative of the amount of aerosol in the column, and specifically relates to the magnitude of interaction between the aerosols and short- or longwave radiation.

**Aerosol phase function:** the angular distribution of radiation scattered by aerosol particle or by particles comprising an aerosol. In practice, the phase function is parameterized with **asymmetry factor (or asymmetry parameter) (g)**, with  $g=1$  denoting completely forward scattering and  $g=0$  denoting symmetric scattering. Another relevant parameter is the **hemispheric backscattered fraction (b)**, which can be derived from measurements made with an integrating nephelometer. The larger the particle size, the more the scattering in the forward hemisphere (i.e., larger  $g$  and smaller  $b$ ).

**Aerosol radiative forcing:** the net energy flux (down-welling minus upwelling) difference between an initial and a perturbed aerosol loading state, at a specified level in the atmosphere. (Other quantities, such as solar radiation, are assumed to be the same.) This difference is defined such that a negative aerosol forcing implies that the change in aerosols relative to the

initial state exerts a cooling influence, whereas a positive forcing would mean the change in aerosols exerts a warming influence. The aerosol radiative forcing must be qualified by specifying the initial and perturbed aerosol states for which the radiative flux difference is calculated, the altitude at which the quantity is assessed, the wavelength regime considered, the temporal averaging, the cloud conditions, and whether total or only human-induced contributions are considered (see Chapter 1, Section 1.2).

**Aerosol radiative forcing efficiency: aerosol direct radiative forcing per unit of aerosol optical depth** (usually at 550 nm). It is mainly governed by aerosol size distribution and chemical composition (determining the aerosol **single-scattering albedo** and **phase function**), surface reflectivity, and solar irradiance.

**Aerosol semi-direct effect:** the processes by which aerosols change the local temperature and moisture (e.g., by direct radiative heating and changing the heat releases from surface) and thus the local relative humidity, which leads to changes in cloud liquid water and perhaps cloud cover.

**Aerosol single-scattering albedo (SSA):** a ratio of the scattering coefficient to the extinction coefficient of an aerosol particle or of the particulate matter of an aerosol. More absorbing aerosols and smaller particles have lower SSA.

**Aerosol size distribution:** probability distribution function of the number concentration, surface area, or volume of the particles comprising an aerosol, per interval (or logarithmic interval) of radius, diameter, or volume.

**Albedo:** the ratio of reflected flux density to incident flux density, referenced to some surface; might be Earth surface, top of the atmosphere.

**Angström exponent:** negative exponent in power law representation of scattering (or extinction or absorption) coefficient of particulate matter of an aerosol with wavelength; similarly for optical depth.

**Anisotropic:** not having the same properties in all directions.

**Atmospheric boundary layer** (abbreviated **ABL**; also called planetary boundary layer - **PBL**): the bottom layer of the troposphere that is in contact with the surface of the earth. It is often turbulent and is capped by a statically stable layer of air or temperature inversion. The ABL depth (i.e., the inversion height) is variable in time and space, ranging from tens of meters in strongly statically stable situations, to several kilometers in convective conditions over deserts.

## B

**Bidirectional reflectance distribution function** (abbreviated **BRDF**): the reflected radiance from a given region as a function of both incident and viewing directions. It is equal to the reflected radiance divided by the incident irradiance from a single direction.

## C

**Clear-sky radiative forcing:** radiative forcing (of a gas or an aerosol) in the absence of clouds. Distinguished from total-sky or all-sky radiative forcing, which include both cloud-free and cloudy regions.

**Climate sensitivity:** - the change in global mean near-surface temperature per unit of **radiative forcing**; when unqualified typically refers to equilibrium sensitivity; transient sensitivity denotes time dependent change in response to a specified temporal profile.

**Cloud albedo:** the fraction of solar radiation incident at the top of cloud that is reflected by clouds in the atmosphere or some subset of the atmosphere.

**Cloud condensation nuclei (abbreviated CCN):** hygroscopic aerosol particles that can serve as seed particles of atmospheric cloud droplets, that is, particles on which water **condenses** (activates) at **supersaturations** typical of atmospheric cloud formation (fraction of one to a few percent, depending on cloud type); may be specified as function of **supersaturation**.

**Cloud resolving model:** a numerical model that resolves cloud-scale (and mesoscale) circulations in three (or sometimes two) spatial dimensions. Usually run with horizontal resolution of 5 km or less.

**Coalescence:** the merging of two or more droplets of precipitation into one

**Condensation:** in general, the physical process (phase transition) by which a vapor becomes a liquid or solid; the opposite of **evaporation**.

**Condensation nucleus** (abbreviated **CN**): an aerosol particle forming a center for **condensation** under extremely high **supersaturations** (up to 400% for water, but below that required to activate small ions).

## D

**Data assimilation:** the combining of diverse data, possibly sampled at different times and intervals and different locations, into a unified and consistent description of a physical system, such as the state of the atmosphere.

**Deliquescence:** phase transition of salt or other dry soluble substance to form saturated solution; in atmosphere, by the uptake of water vapor by an aerosol accompanying this phase transition. For a pure substance the deliquescence phase transition is characterized by a well defined value of **relative humidity** (which value is typically only weakly temperature dependent). For a mixture deliquescence may take place over a range of values of relative humidity. The deliquescence phase transition is generally marked by substantial increase in mass of condensed phase.

**Diffuse radiation:** radiation that comes from some continuous range of directions. This includes radiation that has been scattered at least once, and emission from nonpoint sources.

**Drizzle** (sometimes popularly called **mist**): small raindrops on the order of 0.1 mm to 0.5 mm diameter falling in and below clouds with weak updrafts such as low stratus or stratocumulus clouds. Unlike fog droplets, drizzle falls to the ground and is frequently accompanied by low

visibility and fog. Precipitation rate is generally less than  $0.5 \text{ mm hr}^{-1}$ .

**Dry deposition:** the process by which atmospheric gases and particles are transferred to the surface as a result of random turbulent air, impaction, and /or gravitational settling.

## E

**Earth Observing System** (abbreviated **EOS**): a major NASA initiative to develop state-of-the-art **remote sensing** instruments for global studies of the land surface, biosphere, solid earth, atmosphere, and oceans.

**Efflorescence:** phase transition from a solution at a solute concentration greater than the saturation concentration of the solute in the solvent to a solid (plus perhaps additional solution); typically occurs at **relative humidity** (water activity) below that of **deliquescence**.

**Emission:** with respect to radiation, the generation and sending out of radiant energy. The emission of radiation by natural emitters is accompanied by a loss of energy and is considered separately from the processes of **absorption** or **scattering**.

**Emission:** with respect to gases or particles, the introduction of gaseous or particulate matter into the atmosphere from Earth surface or from natural or human activity, e.g., bubble bursting of **whitecaps**, fires, and industrial processes.

**Equilibrium vapor pressure:** the pressure of a vapor in equilibrium with its condensed phase (liquid or solid).

**Evaporation** (also called **vaporization**): the physical process (phase transition) by which a liquid is transformed to the gaseous state; the opposite of **condensation**.

**External mixture** (referring to an aerosol; contrasted with **internal mixture**): an aerosol in which different particles (or in some usages, different particles in the same size range) exhibit different compositions.

**Extinction** (sometimes called **attenuation**): the process of removal of radiant energy from an

incident beam by the processes of **absorption** and/or **scattering** and consisting of the totality of this removal.

**Extinction coefficient:** fraction of incident radiant energy removed by **extinction** per length of travel of radiation through the substance.

## G

**General circulation model** (abbreviated **GCM**): a time-dependent numerical model of the entire global atmosphere or ocean or both. The acronym GCM is often applied to Global Climate Model

**Geostationary satellite:** a satellite to be placed into a circular orbit in a plane aligned with Earth's equator, and at an altitude of approximately 36000 km such that the orbital period of the satellite is exactly equal to Earth's period of rotation (approximately 24 hours). The satellite appears stationary with respect to a fixed point on the rotating Earth.

## H

**Hydrometeor:** any product of **condensation** or **sublimation** of atmosphere vapor, whether formed in free atmosphere or at the Earth's surface; also any water particles blown by the wind from the Earth's surface.

**Hydrophilic aerosol:** an aerosol (e.g., sulfate, sea salt) the particulate phase of which can take up water vapor from the surrounding air and ultimately dissolve. Contrast **hydrophobic aerosol**. Hydrophilic aerosols become larger and more scattered with increasing relative humidity of air.

**Hydrophobic aerosol:** an aerosol (e.g., mineral dust) that does not or only weakly takes up water vapor from its surroundings.

**Hygroscopicity:** the relative ability of a substance (as an aerosol) to adsorb water vapor from its surroundings and ultimately dissolve. Frequently reported as ratio of some property of particle or of particulate phase of an aerosol (e.g., diameter, mean diameter) as function of **relative humidity** to that at low relative humidity.

## I

**Ice nucleus** (abbreviated **IN**): any particle that serves as a nucleus leading to the formation of ice crystals without regard to the particular physical processes involved in the **nucleation**.

**In situ:** a method of obtaining information about properties of an object (e.g., aerosol, cloud) through direct contact with that object, as opposed to **remote sensing**.

**Internal mixture** (referring to an aerosol; contrasted with **external mixture**): an aerosol consisting of particles each of which consists of a mixture of two or more substances, for which all particles exhibit the same composition (or in some usage, the requirement of identical composition is limited to all particles in a given size range). Typically an internal mixture has a higher **absorption coefficient** than an **external mixture**.

**Irradiance** (also called **radiant flux density**): a radiometric term for the rate at which radiant energy in a radiation field is transferred across a unit area of a surface (real or imaginary) in a hemisphere of directions. In general, irradiance depends on the orientation of the surface. The radiant energy may be confined to a narrow range of frequencies (spectral or monochromatic irradiance) or integrated over a broad range of frequencies.

## L

**Lapse rate:** the decrease of an atmospheric variable (e.g., temperature) with height.

**Large eddy simulation (LES) models:** models which solve the partial differential equations governing turbulent fluid flow for large-scale motions, while the effects of the sub-grid scales are parameterized with a sub-grid scale stress term. Intermediate in computational effort between climate models which solve the Navier-Stokes equations with bulk turbulence parameterizations, and the direct numerical simulation of turbulence over both large and small scales.

**Lidar (light detection and ranging):** similar to **radar**, but using laser light instead of radio signals

**Liquid water path:** line integral of the mass concentration of the liquid water droplets in the atmosphere along a specified path, typically along the path above a point on the Earth surface to the top of the atmosphere.

**Longwave radiation:** also known as **terrestrial radiation, thermal infrared radiation.** electromagnetic radiation at wavelengths greater than 4  $\mu\text{m}$ . In practice, radiation originating by **emission** from Earth and its atmosphere, including clouds; contrasted with **shortwave radiation.**

**Low Earth orbit (LEO):** an orbit (of satellite) typically between 300 and 2000 kilometers above Earth

## M

**Multiple-scattering:** radiative transfer involving typically more than one scattering before transmission, reflection, or absorption. Multiple-scattering is the dominant effect on the transfer of solar radiation within clouds and optically thick aerosols. For scattering optical depths less than about 0.1, **single-scattering** is a useful approximation to radiative transfer in which the radiation undergoes at most one scattering event.

## N

**Nucleation:** the process of initiation of a new phase in a supercooled (for liquid) or supersaturated (for solution or vapor) environment; the initiation of a phase change of a substance to a lower thermodynamic energy state (vapor to liquid condensation, vapor to solid deposition, liquid to solid freezing).

## O

**Optical depth:** the **optical thickness** measured vertically above some given altitude. Optical depth is dimensionless and may be applied to Rayleigh scattering optical depth, aerosol **extinction** (or **scattering**, or **absorption**) optical depth.

**Optical thickness:** line integral of **extinction** (or **scattering** or **absorption**) coefficient along a path. Dimensionless.

## P

**Passive remote sensing:** a remote sensing system that relies on the **emission** (transmission) of natural levels of radiation from (through) the target.

**Phase function:** probability distribution function of the angular distribution of the intensity of radiation scattered (by a molecule, gas, particle or aerosol) relative to the direction of the incident beam.

**Polarization:** a process or state in which rays of light exhibit different properties in different directions, especially the state in which all the vibration takes place in one plane.

**Polarimeter:** instrument that measures the **polarization** of incoming light often used in the characterization of atmospheric aerosols.

**Precipitation scavenging:** removal of trace substances from the air by either rain or snow. May refer to in-cloud scavenging, uptake of trace substances into cloud water followed by **coalescence** and precipitation, or to below-cloud scavenging, uptake of material below cloud by falling **hydrometeor** and subsequent delivery to Earth surface.

**Primary,** of trace atmospheric gases or particles. Substances which are directly emitted into the atmosphere from Earth surface, vegetation or natural or human activity e.g., bubble bursting of **whitecaps**, fires, and industrial processes.

## R

**Radar (radio detection and ranging):** detects and characterize objects by transmitting pulses of radiation in microwave range and analyzing the portion of the signal that is reflected and returned to the sensor.

**Radiance:** a radiometric term for the rate at which radiant energy in a set of directions confined to a small unit solid angle around a

particular direction is transferred across unit area of a surface (real or imaginary) projected onto this direction, per unit solid angle of incident direction.

**Radiometer:** instrument that measures the intensity of radiant energy radiated by an object at a given wavelength; may or may not resolve by wavelength.

**Refractive index** (of a medium): a complex index of refraction. The real part is a measure for how much the speed of light (or other waves such as sound waves) is reduced inside the medium. The imaginary part indicates the amount of absorption loss when the electromagnetic wave propagates through the medium.

**Radiative heating:** the process by which temperature of an object (or volume of space that encompasses a gas or aerosol) increases due to an excess of absorbed radiation over emitted radiation.

**Relative humidity:** the ratio of the vapor pressure to the **saturation** vapor pressure with respect to water.

**Remote sensing:** a method of obtaining information about properties of an object (e.g., aerosol, cloud) without coming into physical contact with that object; opposed to **in situ**.

## S

**Saturation:** the condition in which the vapor pressure (of a liquid substance; for atmospheric application, water) is equal to the **equilibrium vapor pressure** of the substance over a plane surface of the pure liquid substance, sometimes similarly for ice.

**Scattering:** in a broad sense, the process by which matter is excited to radiate by an external source of electromagnetic radiation. By this definition, reflection, refraction, and even diffraction of electromagnetic waves are subsumed under scattering. Often the term scattered radiation is applied to that radiation observed in directions other than that of the source and may also be applied to acoustic and other waves.

**Scattering coefficient:** fraction of incident radiant energy removed by **scattering** per length of travel of radiation through the substance.

**Secondary**, of trace atmospheric gases or particles: formed in the atmosphere by chemical reaction, new particle formation, etc.; contrasted with **primary** substances which are directly emitted into the atmosphere.

**Secondary organic aerosols (SOA):** condensed-phase material in an aerosol formed via **condensation** of gaseous organic oxidation products of lower volatility than their precursor reactive organic gases. Such oxidation products, having a vapor pressure in excess of their **equilibrium vapor pressure**, condense onto pre-existing particles and/or homogeneously nucleate to form new particles

**Shortwave radiation:** radiation in the visible and near-visible portions of the electromagnetic spectrum (roughly 0.3 to 4.0  $\mu\text{m}$  in wavelength) which range encompasses the great majority of solar radiation and little longwave (terrestrial thermal) radiation; contrasted with **longwave (terrestrial) radiation**.

**Solar zenith angle:** angle between the vector of Sun and the zenith.

**Spectrometer:** instrument that measures light received in terms of the intensity at constituent wavelengths, used for example to determine chemical makeup, temperature profiles, and other properties of atmosphere.

**Stratosphere:** the region of the atmosphere extending from the top of the **troposphere**, at heights of roughly 10–17 km, to the base of the mesosphere, at a height of roughly 50 km.

**Sublimation:** the transition of a substance from the solid phase directly to the vapor phase, or vice versa, without passing through an intermediate liquid phase.

**Sunglint:** the portion of shortwave radiation illuminating a water surface that is specularly reflected back to atmosphere.

**Supersaturation:** the condition existing in a given portion of the atmosphere (or other space)



when the **relative humidity** is greater than 100%, that is, when it contains more water vapor than is needed to produce **saturation** with respect to a plane surface of pure water or pure ice.

**Surface albedo:** the ratio, often expressed as a percentage, of the amount of electromagnetic radiation reflected by Earth's surface to the amount incident upon it. Surface albedo is not an intrinsic property of the surface because it depends on direction of incident beam and hence whether incident radiation is direct or diffuse, cf., **bidirectional reflectance distribution function (BRDF)**. Value varies with wavelength and with the surface composition. For example, snow and ice vary from 80% to 90% and bare ground from 10% to 20%.

## T

**Troposphere:** the portion of the atmosphere from the earth's surface to the tropopause; that is, the lowest 10–20 kilometers of the atmosphere, depending on latitude and season; most weather occurs in troposphere.

**Transient climate response:** The time-dependent surface temperature response to a gradually evolving forcing.

## W

**Wet deposition:** the removal of atmospheric gases or particles through their incorporation into **hydrometeors**, which are then lost by precipitation.

**Whitecap:** a patch of white water formed subsequent to the breaking of a wave resulting from entrainment of air which results in bubbles rising to the surface and enhanced light scattering due to the large concentration of interface between air and water.

*Major reference:* Glossary of Meteorology, 2<sup>nd</sup> edition, American Meteorological Society.

# Acronyms and Symbols

A	Surface albedo (broadband)
Å	Ångström exponent
ABC	Asian Brown Cloud
ACE	Aerosol Characterization Experiment
AD-Net	Asian Dust Network
ADEOS	Advanced Earth Observation Satellite
ADM	Angular Dependence Models
AeroCom	Aerosol Comparisons between Observation and Models
AERONET	Aerosol Robotic Network
AI	Aerosol Index
AIOP	Aerosol Intensive Operative Period
AOD ( $\tau$ )	Aerosol Optical Depth
AOT	Aerosol Optical Thickness
APS	Aerosol Polarimetry Sensor
AR4	Forth Assessment Report, IPCC
ARCTAS	Arctic Research of the Composition of the Troposphere from Aircraft and Satellites
ARM	Atmospheric Radiation Measurements
AVHRR	Advanced Very High Resolution Radiometer
A-Train	Constellation of six afternoon overpass satellites
BASE-A	Biomass Burning Airborne and Spaceborne Experiment Amazon and Brazil
BC	Black Carbon
BRDF	Bidirectional Reflectance Distribution Function
CALIOP	Cloud and Aerosol Lidar with Orthogonal Polarization
CALIPSO	Cloud Aerosol Infrared Pathfinder Satellite Observations
CAPMoN	Canadian Air and Precipitation Monitoring Network
CCN	Cloud Condensation Nuclei
CCRI	Climate Change Research Initiative
CCSP	Climate Change Science Program
CDNC	Cloud Droplet Number Concentration
CERES	Clouds and the Earth's Radiant Energy System
CLAMS	Chesapeake Lighthouse and Aircraft Measurements for Satellite campaign
CTM	Chemistry and Transport Model
DABEX	Dust And Biomass-burning Experiment
DOE	Department of Energy
DRF	Direct Radiative Forcing (aerosol)
EANET	Acid Deposition Monitoring Network in East Asia
EARLINET	European Aerosol Research Lidar Network
EarthCARE	Earth Clouds, Aerosols, and Radiation Explorer
EAST-AIRE	East Asian Studies of Tropospheric Aerosols: An International Regional Experiment
EMEP	European Monitoring and Evaluation Programme
EOS	Earth Observing System
EP	Earth Pathfinder
EPA	Environmental Protection Agency
ERBE	Earth Radiation Budget Experiment

ESRL	Earth System Research Laboratory (NOAA)
$E_{\tau}$	Aerosol Forcing Efficiency (RF normalized by AOD)
FAR	IPCC First Assessment Report (1990)
FT	Free Troposphere
$g$	Particle scattering asymmetry factor
GAW	Global Atmospheric Watch
GCM	General Circulation Model, Global Climate Model
GEOS	Goddard Earth Observing System
GFDL	Geophysical Fluid Dynamics Laboratory (NOAA)
GHGs	Greenhouse Gases
GISS	Goddard Institute for Space Studies (NASA)
GLAS	Geoscience Laser Altimeter System
GMI	Global Modeling Initiative
GOCART	Goddard Chemistry Aerosol Radiation and Transport (model)
GOES	Geostationary Operational Environmental Satellite
GoMACCS	Gulf of Mexico Atmospheric Composition and Climate Study
GSFC	Goddard Space Flight Center (NASA)
HSRL	High-Spectral-Resolution Lidar
ICARTT	International Consortium for Atmospheric Research on Transport and Transformation
ICESat	Ice, Cloud, and Land Elevation Satellite
IMPROVE	Interagency Monitoring of Protected Visual Environment
INCA	Interactions between Chemistry and Aerosol (LMDz model)
INDOEX	Indian Ocean Experiment
INTEX-NA	Intercontinental Transport Experiment – North America
INTEX-B	Intercontinental Transport Experiment – Phase B
IPCC	Intergovernmental Panel on Climate Change
IR	Infrared radiation
LBA	Large-Scale Biosphere-Atmosphere Experiment in Amazon
LES	Large Eddy Simulation
LITE	Lidar In-space Technology Experiment
LMDZ	Laboratoire de Météorologie Dynamique with Zoom, France
LOA	Laboratoire d'Optique Atmosphérique, France
LOSU	Level of Scientific Understanding
LSCE	Laboratoire des Sciences du Climat et de l'Environnement, France
LWC	Liquid Water Content
LWP	Liquid Water Path
MAN	Maritime Aerosol Network
MEE	Mass Extinction Efficiency
MILAGRO	Megacity Initiative: Local and Global Research Observations
MFRSR	Multifilter Rotating Shadowband Radiometer
MINOS	Mediterranean Intensive Oxidant Study
MISR	Multi-angle Imaging SpectroRadiometer
MODIS	Moderate Resolution Imaging Spectroradiometer
MOZART	Model for Ozone and Related chemical Tracers
MPLNET	Micro Pulse Lidar Network
NASA	National Aeronautics and Space Administration
NASDA	NAtional Space Development Agency, Japan
NEAQS	New England Air Quality Study
NOAA	National Oceanography and Atmosphere Administration

NPOESS	National Polar-orbiting Operational Environmental Satellite System
NPP	NPOESS Preparatory Project
NPS	National Park Services
NRC	National Research Council
OC	Organic Carbon
OMI	Ozone Monitoring Instrument
PARASOL	Polarization and Anisotropy of Reflectance for Atmospheric Science coupled with Observations from a Lidar
PDF	Probability Distribution Function
PEM-West	Western Pacific Exploratory Mission
PM	Particulate Matter (aerosols)
PMEL	Pacific Marine Environmental Laboratory (NOAA)
POLDER	Polarization and Directionality of the Earth's Reflectance
POM	Particulate Organic Matter
PRIDE	Puerto Rico Dust Experiment
REALM	Regional East Atmospheric Lidar Mesonet
RF	Radiative Forcing, aerosol
RH	Relative Humidity
RTM	Radiative Transfer Model
SAFARI	South Africa Regional Science Experiment
SAMUM	Saharan Mineral Dust Experiment
SAP	Synthesis and Assessment Product (CCSP)
SAR	IPCC Second Assessment Report (1995)
SCAR-A	Smoke, Clouds, and Radiation – America
SCAR-B	Smoke, Clouds, and Radiation - Brazil
SeaWiFS	Sea-viewing Wide Field-of-view Sensor
SGP	Southern Great Plain, ARM site in Oklahoma
SHADE	Saharan Dust Experiment
SMOCC	Smoke, Aerosols, Clouds, Rainfall and Climate
SOA	Secondary Organic Aerosol
SPRINTARS	Spectral Radiation-Transport Model for Aerosol Species
SSA	Single-Scattering Albedo
SST	Sea Surface Temperature
STEM	Sulfate Transport and Deposition Model
SURFRAD	NOAA's national surface radiation budget network
SZA	Solar Zenith Angle
TAR	Third Assessment Report, IPCC
TARFOX	Tropospheric Aerosol Radiative Forcing Observational Experiment
TCR	Transient Climate sensitivity Range
TexAQS	Texas Air Quality Study
TOA	Top of the Atmosphere
TOMS	Total Ozone Mapping Spectrometer
TRACE-A	Transport and Chemical Evolution over the Atlantic
TRACE-P	Transport and Chemical Evolution over the Pacific
UAE <sup>2</sup>	United Arab Emirates Unified Aerosol Experiment
UMBC	University of Maryland at Baltimore County
UV	Ultraviolet radiation
VOC	Volatile Organic Compounds
WMO	World Meteorological Organization

## Contact Information

Global Change Research Information Office  
c/o Climate Change Science Program Office  
1717 Pennsylvania Avenue, NW  
Suite 250  
Washington, DC 20006  
202-223-6262 (voice)  
202-223-3065 (fax)

The Climate Change Science Program incorporates the U.S. Global Change Research Program and the Climate Change Research Initiative.  
To obtain a copy of this document, place an order at the Global Change Research Information Office (GCRI) web site:  
<http://www.gcric.org/orders>

## Climate Change Science Program and the Subcommittee on Global Change Research

**William J. Brennan**, Chair  
Department of Commerce  
National Oceanic and Atmospheric Administration  
Director, Climate Change Science Program

**Jack Kaye**, Vice Chair  
National Aeronautics and Space Administration

**Allen Dearry**  
Department of Health and Human Services

**Anna Palmisano**  
Department of Energy

**Mary Glackin**  
National Oceanic and Atmospheric Administration

**Patricia Gruber**  
Department of Defense

**William Hohenstein**  
Department of Agriculture

**Linda Lawson**  
Department of Transportation

**Mark Myers**  
U.S. Geological Survey

**Tim Killeen**  
National Science Foundation

**Patrick Neale**  
Smithsonian Institution

**Jacqueline Schafer**  
U.S. Agency for International Development

**Joel Scheraga**  
Environmental Protection Agency

**Harlan Watson**  
Department of State

### EXECUTIVE OFFICE AND OTHER LIAISONS

**Robert Marlay**  
Climate Change Technology Program

**Katharine Gebbie**  
National Institute of Standards & Technology

**Stuart Levenbach**  
Office of Management and Budget

**Margaret McCalla**  
Office of the Federal Coordinator for Meteorology

**Robert Rainey**  
Council on Environmental Quality

**Daniel Walker**  
Office of Science and Technology Policy